



**This electronic thesis or dissertation has been
downloaded from Explore Bristol Research,
<http://research-information.bristol.ac.uk>**

Author:
Jones, Vicky

Title:
**Investigating the routing and synthesis of amino acids between diet and bone collagen
via feeding experiments and applications to palaeodietary reconstruction**

General rights

The copyright of this thesis rests with the author, unless otherwise identified in the body of the thesis, and no quotation from it or information derived from it may be published without proper acknowledgement. It is permitted to use and duplicate this work only for personal and non-commercial research, study or criticism/review. You must obtain prior written consent from the author for any other use. It is not permitted to supply the whole or part of this thesis to any other person or to post the same on any website or other online location without the prior written consent of the author.

Take down policy

Some pages of this thesis may have been removed for copyright restrictions prior to it having been deposited in Explore Bristol Research. However, if you have discovered material within the thesis that you believe is unlawful e.g. breaches copyright, (either yours or that of a third party) or any other law, including but not limited to those relating to patent, trademark, confidentiality, data protection, obscenity, defamation, libel, then please contact: open-access@bristol.ac.uk and include the following information in your message:

- Your contact details
- Bibliographic details for the item, including a URL
- An outline of the nature of the complaint

On receipt of your message the Open Access team will immediately investigate your claim, make an initial judgement of the validity of the claim, and withdraw the item in question from public view.

**INVESTIGATING THE ROUTING AND SYNTHESIS OF
AMINO ACIDS BETWEEN DIET AND BONE COLLAGEN
VIA FEEDING EXPERIMENTS AND APPLICATIONS TO
PALAEODIETARY RECONSTRUCTION**

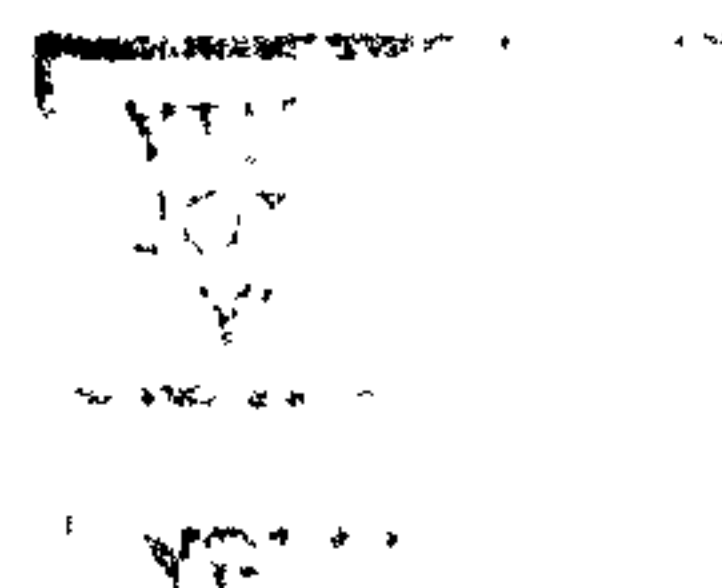
by

VICKY JONES

March 2002

A thesis submitted to the University of Bristol in accordance with the requirements
for the degree of Doctor of Philosophy in the Faculty of Science

42,386 words



Abstract

The techniques applied to measure the $\delta^{13}\text{C}$ values of individual amino acids in bone collagen were developed with authentic amino acids. It was found that after 24 and 48 h hydrolysis, the $\delta^{13}\text{C}$ values of individual amino acids as determined by GC/C/IRMS were unaffected by the procedure. The errors involved in the $\delta^{13}\text{C}$ analysis of amino acids varied from $\pm 0.7\text{‰}$ for phenylalanine to $\pm 1.5\text{‰}$ for glycine. The need for a reduction reactor in the GC/C/IRMS configuration when analysing the $\delta^{13}\text{C}$ values of amino acids was confirmed. The $\delta^{13}\text{C}$ values of commercially produced pre-derivatised TFA/methyl esters were first determined using a continuous-flow elemental analyser IRMS; the $\delta^{13}\text{C}$ values were then also determined by GC/C/IRMS. It was found that when the reduction reactor was not included in the GC/C/IRMS configuration the amino acids appeared to be more depleted in ^{13}C by up to 15‰. On inclusion of the reduction reactor, off-line and on-line $\delta^{13}\text{C}$ values were in agreement.

The $\delta^{13}\text{C}$ values were determined for individual amino acids derived from the bone collagen of rats ($n = 24$) raised on controlled diets from the Ambrose and Norr study (1993) and the diets themselves. Insights into the factors that influence the $\delta^{13}\text{C}$ values of bone collagen were gained. The $\delta^{13}\text{C}$ values of individual amino acids, in conjunction with previously measured $\delta^{13}\text{C}$ values for dietary macronutrients and bone cholesterol, collagen and apatite for the same animals, a quantitative model was constructed via the use of linear regression analysis. It was found that $\delta^{13}\text{C}_{\text{glu}}$ and $\delta^{13}\text{C}_{\text{pro}}$ values correlated highly with $\delta^{13}\text{C}_{\text{wdiet}}$ and $\delta^{13}\text{C}_{\text{protein}}$ values, respectively. It was also found that $\delta^{13}\text{C}_{\text{hyp}}$ and $\delta^{13}\text{C}_{\text{glu}}$ values correlated highly with $\delta^{13}\text{C}_{\text{coll}}$ and $\delta^{13}\text{C}_{\text{apat}}$ values, respectively. From these linear correlations models were constructed which allowed the prediction of whole diet, protein, collagen and apatite $\delta^{13}\text{C}$ values. These models improved significantly on the prediction of dietary protein $\delta^{13}\text{C}$ values when $\delta^{13}\text{C}_{\text{apat}}$ values are not available ($R^2 = 0.97$) in comparison with previous models ($R^2 = 0.70$) and allowed prediction of $\delta^{13}\text{C}_{\text{wdiet}}$ and $\delta^{13}\text{C}_{\text{energy}}$ values without the necessity for $\delta^{13}\text{C}_{\text{apat}}$ values.

The model was applied to $\delta^{13}\text{C}$ values from pigs from a controlled feeding experiment. Bone cholesterol, collagen and long- and short-term whole diet $\delta^{13}\text{C}$ values were accurately predicted. Inaccuracies in the prediction of dietary protein and energy $\delta^{13}\text{C}$ values were due to uncertainty in the measured values for these macronutrients. The model was then applied to animals from an archaeological population from Qasr Ibrim, Egypt. It was found that the $\delta^{13}\text{C}_{\text{prot}}$ values were very similar over the 2000 year timespan, but the $\delta^{13}\text{C}_{\text{wdiet}}$ values became more enriched over time indicating the introduction of C_4 foodstuffs into the animal's diets. Comparison of long- and short-term whole diet $\delta^{13}\text{C}$ values found that the short-term whole diet $\delta^{13}\text{C}$ values were consistently more depleted in ^{13}C than the long-term whole diet $\delta^{13}\text{C}$ values, possible indicating that the animals were fattened up on C_3 fodders prior to slaughter.

Acknowledgements

Firstly I would like to thank Prof. Richard Evershed for allowing me into his lab to undertake my PhD and providing me with this opportunity. Your guidance and words of wisdom were truly appreciated. Jim Carter, Andy Gledhill and Dr. Ian Bull are thanked for keeping the isotope machines running.

Thanks to all of W403 and W309. Thanks especially to Susie for giving help, advice and a lot of her time above and beyond the call of duty both during lab work and whilst writing up, and also for much chatting about anything other than work (thanks to Lorna for that as well!).

And finally a huge thank you to Paul who always arrived before me in the mornings and made using the XL and watching samples on the blowdown much more enjoyable than they had a right to be. Your advice and encouragement were invaluable to me. Thank you.

Declaration

I hereby certify that the work described herein is my own, except where otherwise stated, and has not previously been submitted for examination at this, or at any other, University. Any views expressed in the thesis are those of the author and in no way represent those of the University of Bristol.

A handwritten signature in black ink that reads "Vicky Jones". The script is cursive and fluid, with the first letter 'V' being particularly large and stylized.

Vicky Jones

TABLE OF CONTENTS

Abstract	1
Acknowledgements	2
Declaration	3
Table of contents	4
List of figures	8
List of tables	13
Preface	16
Chapter 1 Introduction	17
1.1 Palaeodietary reconstruction	18
1.2 Direct approaches	18
1.3 Stable Isotope Analysis	19
1.3.1 Carbon isotopes in terrestrial and marine environments	20
1.3.2 Nitrogen isotopes in terrestrial and marine environments	23
1.3.3 Palaeodietary reconstruction based on stable isotopes	24
1.4 Bone collagen and apatite	25
1.4.1 Development of palaeodietary indicators	26
1.4.2 Routing of dietary macronutrients	28
1.4.3 Development of models for predicting dietary $\delta^{13}\text{C}$ values	31
1.4.4 Isotopic integrity of collagen and apatite	33
1.5 Bulk stable isotope analysis	35
1.6 Compound-specific stable isotope analysis	37
1.6.1 Measurement of stable isotope ratios of individual compounds by GC/C/IRMS	39
1.7 Further Development of palaeodietary reconstruction models	41
1.8 Amino acids as palaeodietary indicators	43
1.9 Biosynthesis of amino acids	48
1.10 Aims and Objectives	54
1.10.1 Aims	54
1.10.2 Objectives	55

Chapter 2	Materials and Methods	57
2.1	Chemicals and standards	58
2.2	Sample Information	58
2.3	Preparation of modern samples	58
2.4	Preparation of archaeological samples	58
2.5	Solvent extraction of samples	59
2.6	Collagen extraction	59
2.7	Hydrolysis of rat bone and diets and archaeological collagen	59
2.8	Apatite extraction	60
2.9	Derivatisation of amino acids	60
2.10	Gas chromatography analyses (GC)	61
2.11	Gas chromatography/mass spectrometry analyses (GC/MS)	61
2.12	Stable carbon isotope analyses (IRMS and GC/C/IRMS)	61
2.13	Quantification of amino acids	62
Chapter 3	Method development of compound-specific isotope analysis of amino acids	64
3.1	Objectives	65
3.2	Introduction	66
3.3	Measuring the $\delta^{13}\text{C}$ values of amino acids using GC/C/IRMS	67
	3.3.1 Derivatisation of amino acids	67
	3.3.2 Obtaining carbon isotope data	70
3.4	Kinetic isotope effect	74
3.5	Errors	78
3.6	Poly amino acids	81
	3.6.1 Single poly amino acids (SPAAs)	82
	3.6.2 Mixed poly amino acids (MPAAs)	84
3.7	Summary	89

Chapter 4	Investigating the routing and synthesis of amino acids in bone collagen	91
4.1	Objectives	92
4.2	Influences on the $\delta^{13}\text{C}$ value of bone collagen	93
4.2.1	Essential amino acids	93
4.2.2	Non-essential amino acids	95
4.3	Other controlled feeding experiments and amino acid analyses	95
4.4	Sample description	96
4.4.1	Experimental approach	97
4.5	Results and Discussion	97
4.5.1	Amino acid composition of diet and bone collagen	97
4.5.2	$\delta^{13}\text{C}$ results for terrestrial protein diets and rats	103
4.5.3	$\delta^{13}\text{C}$ values for the amino acids of marine protein diet and rat collagen	112
4.5.4	$\delta^{13}\text{C}$ results for the diet switch experiments	121
4.6	Correlations of the isotope data	126
4.6.1	Mass balance of individual amino acid bone collagen data	126
4.6.2	Correlations between diet component and collagen amino acid $\delta^{13}\text{C}$ values	127
4.7	Summary	131
Chapter 5	Modelling the relationship between collagen amino acids and diet	132
5.1	Objectives	133
5.2	Previous models for diet reconstruction	133
5.3	Models for dietary reconstruction using amino acid $\delta^{13}\text{C}$ values	135
5.3.1	A quantitative model for predicting $\delta^{13}\text{C}$ values of dietary macronutrients and bone components from single amino acids	135
5.3.2	Combined use of bone component $\delta^{13}\text{C}$ values	141

5.3.3	Testing the models	149
5.4	Summary	156
 Chapter 6 Carbon isotope analysis of archaeological data		159
6.1	Objectives	160
6.2	Qasr Ibrim and previous work	160
6.3	Results and discussion	162
6.3.1	Results of non-isotopic analysis	162
6.3.2	Results of carbon isotopic analysis	165
6.3.3	Routing and synthesis of individual amino acids	170
6.3.4	Predicting dietary macronutrient $\delta^{13}\text{C}$ values	174
6.4	Summary	188
 Chapter 7 Summary and future work		194
7.1	Summary	195
7.1.1	Summary of aims and objectives	195
7.1.2	Summary of results and conclusions	196
7.2	Future work	200
 References		203
 Appendices		
	Appendix 1	
	Appendix 2	
	Appendix 3	
	Appendix 4	

LIST OF FIGURES

Chapter 1

1.1.	Isotopic fractionations which occur during assimilation and fixation of CO ₂ in C ₃ and C ₄ plants.	21
1.2.	Summary of the fate of dietary macronutrients	30
1.3.	Schematic of the McKinney-Nier IRMS system.	37
1.4.	Schematic of the GC/C/IRMS system.	40
1.5.	Partial traces obtained from the $\delta^{13}\text{C}$ analysis of hydrocarbons.	42
1.6.	$\delta^{13}\text{C}$ values of individual amino acids from bone collagen of pigs raised on controlled diets.	46
1.7a.	$\delta^{15}\text{N}$ values for individual amino acids from bone collagen of a lion and a lynx.	47
1.7b.	$\delta^{13}\text{C}$ values for individual amino acids from bone collagen of a lion and a lynx.	47
1.8a.	$\delta^{15}\text{N}$ values for individual amino acids from bone collagen of fossil and modern whale	48
1.8b.	$\delta^{13}\text{C}$ values for individual amino acids from bone collagen of fossil and modern whale	48
1.9.	Overview of biosynthesis of non-essential amino acids.	50
1.10.	Biosynthetic pathways of serine, glycine, alanine, glutamate and aspartate.	51
1.11.	Biosynthesis of proline and arginine.	52
1.12.	Biosynthesis of tyrosine.	53
1.13.	Chemical structures of the non-essential amino acids, 3- and 4-hydroxyproline and hydroxylysine.	53
1.14.	Prolyl hydroxylase reaction that converts proline to 3- and 4-hydroxyproline and lysine to hydroxylysine.	54

Chapter 3

3.1a.	Alanine derivatised to an acetyl isopropyl ester.	69
3.1b.	Alanine derivatised to a trifluoroacetyl isopropyl ester.	69
3.1c.	Alanine derivatised to a pivaloyl isopropyl ester.	69
3.2.	Partial gas chromatogram of authentic amino acids as TFA/IP esters.	70
3.3.	Partial GC/C/IRMS profiles of authentic amino acids derivatised to TFA/IP esters.	72
3.4a.	Effect of reduction reactor performance on $\delta^{13}\text{C}$ values of TFA methyl ester of alanine.	73
3.4b.	Effect of reduction reactor performance on $\delta^{13}\text{C}$ values of TFA methyl ester of phenylalanine.	73
3.4c.	Effect of reduction reactor performance on $\delta^{13}\text{C}$ values of TFA methyl ester of lysine.	73
3.5.	Mechanism for the trifluoroacetylation of an amino acid.	75
3.6.	Variation in the expression of the kinetic isotope effect.	77
3.7.	Comparison of the structures of TFA/IP esters of serine and leucine.	79
3.8.	GC/C/IRMS error propagation.	80
3.9a.	Compound-specific $\delta^{13}\text{C}$ values of poly alanine.	85
3.9b.	Compound-specific $\delta^{13}\text{C}$ values of poly serine.	85
3.9c.	Compound-specific $\delta^{13}\text{C}$ values of poly glutamic acid.	85
3.9d.	Compound-specific $\delta^{13}\text{C}$ values of poly ornithine.	85
3.9e.	Compound-specific $\delta^{13}\text{C}$ values of poly phenylalanine.	85
3.10.	Comparison of $\delta^{13}\text{C}$ values of MPAAs.	89

Chapter 4

4.1.	An overview of protein metabolism.	94
4.2a.	Partial gas chromatogram of individual amino acids in dietary protein.	101
4.2b.	Partial gas chromatogram of individual amino acids in rat collagen.	101
4.3a.	Relative abundances of amino acids in terrestrial protein diets.	102
4.3b.	Relative abundances of amino acids in marine protein diets	102
4.4.	Comparison of relative abundances of amino acids in rat bone collagen	

and theoretical abundances.	103
4.5a. Graph showing the $\delta^{13}\text{C}$ values of individual amino acids from diet and bone collagen for pure C_3 diet	106
4.5b. Graph showing the $\delta^{13}\text{C}$ values of individual amino acids from diet and bone collagen for pure C_4 diet.	106
4.6a. Graph showing the $\delta^{13}\text{C}$ values of individual amino acids from diet and bone collagen for C_3/C_4 diet.	108
4.6b. Graph showing the $\delta^{13}\text{C}$ values of individual amino acids from diet and bone collagen for the C_4/C_3 diet.	108
4.7a. Histogram showing the $\Delta^{13}\text{C}_{\text{collAA-dietAA}}$ values for each amino acid for pure C_3 and C_3/C_4 diet.	109
4.7b. Histogram showing the $\Delta^{13}\text{C}_{\text{collAA-dietAA}}$ values for each amino acid for pure C_4 and C_4/C_3 diet.	109
4.8. Biosynthetic pathways of serine, alanine, glutamate and aspartate.	111
4.9. Bar chart showing the $\Delta^{13}\text{C}_{\text{collAA-dietAA}}$ values for each amino acid for 20% marine protein diets.	116
4.10a. Bar chart showing the $\Delta^{13}\text{C}_{\text{collAA-dietAA}}$ values for each amino acid for marine protein/ C_3 energy diets.	119
4.10b. Bar chart showing the $\Delta^{13}\text{C}_{\text{collAA-dietAA}}$ values for each amino acid for marine protein/ C_4 energy diets.	119
4.11. Bar chart showing the $\Delta^{13}\text{C}_{\text{collAA-dietAA}}$ values for each amino acid for 20% and 70% marine protein/ $\text{C}_3 + \text{C}_4$ energy diets.	120
4.12a. Comparison of individual amino acid $\delta^{13}\text{C}$ values from bone collagen of rats from pure C_3 diet and C_3 to C_4 diet switch.	123
4.12b. Comparison of individual amino acid $\delta^{13}\text{C}$ values from bone collagen of rats from pure C_4 diet and C_4 to C_3 diet switch.	123
4.13. Percentage incorporation of isotopic signal into individual amino acids for C_3 to C_4 diet switch and C_4 to C_3 diet switch.	125
4.14. Correlation of measured bulk collagen values with estimated bulk collagen values.	127
4.15a. Correlations of bone collagen amino acids with dietary amino acids.	130
4.15b. Correlations of bone collagen amino acids with whole diet.	130

Chapter 5

5.1.	Comparison of measured and predicted bone collagen $\delta^{13}\text{C}$ values.	152
5.2.	Comparison of measured and predicted long-term whole diet $\delta^{13}\text{C}$ values.	153
5.3a.	Comparison of measured and predicted dietary protein $\delta^{13}\text{C}$ values.	154
5.3b.	Comparison of measured and predicted dietary energy $\delta^{13}\text{C}$ values.	154
5.4.	Comparison of measured and predicted dietary protein $\delta^{13}\text{C}$ values.	157

Chapter 6

6.1.	Partial gas chromatogram of individual amino acids from the bone collagen of a bovid from Qasr Ibrim.	164
6.2.	Comparison of the average relative abundances of amino acids from animal bone collagen samples with known abundances.	165
6.3.	Graph showing the $\delta^{13}\text{C}$ values of individual amino acids from ancient barley, modern barley and ancient sorghum.	169
6.4.	Graph showing the $\delta^{13}\text{C}$ values of individual amino acids from bone collagen of ovi-caprids and bovids from Qasr Ibrim.	171
6.5a.	Plot showing the $\delta^{13}\text{C}$ values of phenylalanine from bone collagen of animals from Qasr Ibrim.	172
6.5b.	Plot showing the $\delta^{13}\text{C}$ values of alanine from bone collagen of animals from Qasr Ibrim.	172
6.6a.	Comparison of measured and predicted collagen $\delta^{13}\text{C}$ values from Qasr Ibrim animal bones.	176
6.6b.	Comparison of measured and predicted apatite $\delta^{13}\text{C}$ values from Qasr Ibrim animal bones.	176
6.7a.	$\Delta^{13}\text{C}_{\text{apat-coll}}$ spacings for the ovi-caprids.	177
6.7b.	$\Delta^{13}\text{C}_{\text{apat-coll}}$ spacings for the bovids.	177
6.8a.	Predicted dietary $\delta^{13}\text{C}$ values for the ovi-caprids.	179
6.8b.	Predicted dietary $\delta^{13}\text{C}$ values for the bovids.	179
6.9a.	Comparison of $\text{C}_{16:0}$ and $\text{C}_{18:0}$ fatty acids with predicted long-term whole diet $\delta^{13}\text{C}$ values for ovi-caprids.	183

6.9b. Comparison of C _{16:0} and C _{18:0} fatty acids with predicted long-term whole diet $\delta^{13}\text{C}$ values for bovids.	183
6.10a. $\Delta^{13}\text{C}_{\text{apat-fatty acid}}$ spacings for the Qasr Ibrim samples for C _{16:0} fatty acid $\delta^{13}\text{C}$ values.	185
6.10b. $\Delta^{13}\text{C}_{\text{apat-fatty acid}}$ spacings for the Qasr Ibrim samples for C _{18:0} fatty acid $\delta^{13}\text{C}$ values.	185
6.11. Comparison of predicted short-term whole diet $\delta^{13}\text{C}$ values.	188
6.12a. Comparison of bone collagen alanine and predicted dietary energy $\delta^{13}\text{C}$ values for ovi-caprids.	191
6.12b. Comparison of bone collagen alanine and predicted dietary energy $\delta^{13}\text{C}$ values for bovids.	191
6.13a. Comparison of bone collagen phenylalanine and predicted dietary protein $\delta^{13}\text{C}$ values for ovi-caprids.	192
6.13b. Comparison of bone collagen phenylalanine and predicted dietary protein $\delta^{13}\text{C}$ values for bovids.	192

LIST OF TABLES

Chapter 1

- | | | |
|-----|---|----|
| 1.1 | Models of the fractionation between diet and bone components for herbivores and carnivores. | 32 |
| 1.2 | Models of the fractionation between diet and bone components for herbivores and carnivores. | 33 |
| 1.3 | Amino acids found in collagen. | 44 |

Chapter 2

- | | | |
|------|---|----|
| 2.1. | FID correction factors for quantifying amino acids by GC. | 63 |
|------|---|----|

Chapter 3

- | | | |
|------|--|----|
| 3.1. | Different combinations of esterification and acetylation groups used in the derivatisation of amino acids. | 68 |
| 3.2. | $\delta^{13}\text{C}$ values measured off-line for amino acid TFA/methyl esters. | 71 |
| 3.3. | Correction factors for GC/C/IRMS analyses. | 76 |
| 3.4. | Influence of the correction for added carbon on the standard deviation of $\delta^{13}\text{C}$ values for leucine and serine TFA/IP esters. | 78 |
| 3.5. | Errors associated with the GC/C/IRMS determination TFA/IP amino acids. | 81 |
| 3.6. | Expected and measured yields of amino acids recovered after hydrolysis of SPAAs. | 83 |
| 3.7. | $\delta^{13}\text{C}$ values and associated errors for the single poly amino acids. | 84 |
| 3.8. | Carbon:nitrogen ratios of the MPAAAs determined by elemental analysis and quantification and expected carbon:nitrogen ratios based on manufacturers specified amino acid compositions. | 87 |
| 3.9. | Expected and measured amounts of mixed poly amino acids recovered after 24 h hydrolysis. | 87 |

3.10. $\delta^{13}\text{C}$ values of individual amino acids comprising the mixed poly amino acids and estimated bulk values.	88
---	----

Chapter 4

4.1. Diet composition and components.	98
4.2. Diet, tissue code, sex and pair of individual animals that were analysed.	99
4.3. Relative abundances of amino acids in bone collagen of rats	100
4.4. Individual amino acid $\delta^{13}\text{C}$ values for terrestrial protein diets.	104
4.5. Individual amino acid $\delta^{13}\text{C}$ values from bone collagen of rats raised on terrestrial protein diets.	105
4.6. Bulk carbon isotope values of dietary protein and rat bone collagen.	110
4.7. Individual amino acid $\delta^{13}\text{C}$ values for marine protein diets.	113
4.8. Individual amino acid $\delta^{13}\text{C}$ values from bone collagen of rats raised on 20% marine protein diets.	114
4.9. Individual amino acid $\delta^{13}\text{C}$ values from bone collagen of rats raised on 70% marine protein diets.	115
4.10 Individual amino acid $\delta^{13}\text{C}$ values from bone collagen of rats subjected to diet switches.	121
4.11. Bulk carbon isotope values of rat bone collagen.	124
4.12. Percentage incorporation of dietary isotopic signal into bone collagen.	126
4.13. R^2 values from linear correlations of diet components and bone collagen amino acid $\delta^{13}\text{C}$ values	129

Chapter 5

5.1. R^2 values from linear correlations of diet and bone components with bone collagen amino acid $\delta^{13}\text{C}$ values.	136
5.2. Linear correlations of diet and bone component $\delta^{13}\text{C}$ values.	137
5.3 Comparison of R^2 values obtained when comparing calculated $\delta^{13}\text{C}$ values of dietary macronutrients with actual values.	140
5.4. Diet and bone components and $\Delta^{13}\text{C}$ spacings subjected to linear regression analysis.	143

5.5.	Linear correlations for calculating dietary protein $\delta^{13}\text{C}$ values from bone component $\delta^{13}\text{C}$ values where $R^2 > 0.9$.	143
5.6.	Linear correlation for calculating dietary energy $\delta^{13}\text{C}$ values from bone component $\delta^{13}\text{C}$ values where $R^2 > 0.9$.	144
5.7.	Linear correlations for calculating whole diet $\delta^{13}\text{C}$ values from bone component $\delta^{13}\text{C}$ values, where $R^2 > 0.9$.	145
5.8.	Linear correlations for calculating the $\delta^{13}\text{C}$ values of dietary macronutrients.	146
5.9.	Diet composition and bulk diet $\delta^{13}\text{C}$ values for the diets used in the Harvard pig feeding experiment.	150
5.10.	Correlations and differences between measured and predicted bone and dietary component $\delta^{13}\text{C}$ values.	151

Chapter 6

6.1	Yields of collagen and apatite obtained from animal bones from Qasr Ibrim and C:N ratio of extracted collagen.	163
6.2.	Bone collagen, apatite, $\text{C}_{16:0}$ and $\text{C}_{18:0}$ fatty acid $\delta^{13}\text{C}$ values obtained from animal bones from Qasr Ibrim.	166
6.3.	Individual amino acid $\delta^{13}\text{C}$ values obtained from animal bones from Qasr Ibrim.	167
6.4.	Predicted bone and dietary component $\delta^{13}\text{C}$ values for Qasr Ibrim animal bones.	175
6.5.	Differences between fatty acid and long-term whole diet $\delta^{13}\text{C}$ values obtained from animal bones from Qasr Ibrim.	182
6.6.	Variation in $\Delta^{13}\text{C}_{\text{apat-fatty acid}}$ spacings with respect to long- and short-term whole diet $\delta^{13}\text{C}$ values.	184
6.7.	Predicted long-term and short-term whole diet $\delta^{13}\text{C}$ values for Qasr Ibrim animal bones.	187

Preface

This thesis consists of seven chapters. Chapter 1 provides an introduction and background to the work undertaken, whilst the second chapter provides information on the materials and experimental methods used. In Chapter 3 authentic amino acids are used to investigate the effects of hydrolysis and derivatisation on the $\delta^{13}\text{C}$ values of amino acids. A rigorous investigation of the errors involved in the $\delta^{13}\text{C}$ analysis of amino acids is also presented. Chapter 4 presents the results of the compound-specific $\delta^{13}\text{C}$ analysis of individual amino acids from the bone collagen of rats raised on controlled diets. The routing and synthesis of collagenous amino acids is investigated and the rate of incorporation of the dietary isotopic signal into bone collagen is assessed. A quantitative model is developed in Chapter 5 in order to predict dietary macronutrient $\delta^{13}\text{C}$ values both from individual collagenous amino acids and in conjunction with previously measured bone cholesterol, collagen and apatite $\delta^{13}\text{C}$ values. The model is also tested using the diet and bone component $\delta^{13}\text{C}$ values from another controlled feeding experiment. In Chapter 6, the results from Chapter 4 and the model developed in Chapter 5 are applied to faunal remains from Qasr Ibrim, Egypt. Chapter 7 provides a summary of the work and suggestions for future work. References follow Chapter 7 and there are four appendices. Appendix 1 provides mass spectra for the derivatised amino acids studied in this work. Appendix 2 lists the results of the linear regression analysis of carbon isotope data from the rat feeding experiment. Appendix 3 presents the bone component $\delta^{13}\text{C}$ values provided for the pig feeding experiment and Appendix 4 lists the predicted and measured bone and dietary $\delta^{13}\text{C}$ values for the pig feeding experiment.

CHAPTER 1

INTRODUCTION

Chapter 1 Introduction

1.1 Palaeodietary reconstruction

Much effort has been devoted to the reconstruction of ancient human and animal diets, since diet influences the behaviour and ecologic interactions of ancient peoples. An animal's diet is an important factor in its evolutionary success and its impact on its environment (Fogel *et al.*, 1997). The history of this field can be separated into two categories, palaeodietary reconstruction prior to the use of stable isotope analyses and palaeodietary reconstruction with stable isotope analyses.

1.2 Direct approaches

The most direct sources of palaeodietary information are provided by preserved gut contents and faecal remains. However, these sorts of materials are rarely preserved in the fossil record, only provide information on the diet immediately prior to death, and do not include information on food that may have been fully digested. Other methods of direct investigation include the retrieval of preserved food remains from archaeological sites and also tools and pottery, which may have been used in food gathering and preparation.

Dietary information of whole populations can be obtained from research into body sizes, optimum foraging behaviour and site catchment analysis (Schwarcz and Schoeninger, 1991). The study of abrasion and wear patterns on teeth has also allowed some indirect interpretation of dietary preferences since this technique allows the discrimination between hard-object and soft-object feeding (Teaford, 1988; Teaford and Walker, 1984).

1.3 Stable Isotope Analysis

In the 1970s a new technique was introduced that allowed direct determination of the dietary preferences of ancient individuals and populations via the measurement of the ratios of stable isotopes ($^{13}\text{C}/^{12}\text{C}$ and $^{15}\text{N}/^{14}\text{N}$) in preserved tissues. Carbon occurs in three isotopic forms: ^{12}C , ^{13}C and ^{14}C and whilst ^{14}C degrades radioactively over time, ^{12}C and ^{13}C are stable isotopes with approximate natural abundances of 98.89% and 1.11%, respectively. Nitrogen exists as two stable isotopes, ^{14}N and ^{15}N , with approximate natural abundances of 99.63% and 0.37%, respectively. On average, the worldwide ratios of stable carbon and nitrogen isotopes have not varied over time; however, the ratios have been found to vary in natural materials due to the different rates at which various isotopes undergo biochemical reactions in biological processes. The differences in ratios are very small and are measured by comparison with a standard and are measured in parts per thousand or per mil (‰). The deviation (δ) of the ratio ($R = ^{13}\text{C}/^{12}\text{C}$ or $^{15}\text{N}/^{14}\text{N}$) from the standard is expressed as follows (Craig, 1957):

$$\delta X (\text{‰}) = [(R_{\text{sample}} / R_{\text{standard}}) - 1] \times 1000$$

where $X = ^{13}\text{C}$ or ^{15}N

Carbon isotope measurements are made relative to Pee Dee Belemnite (PDB). The original carbonate has now been exhausted and so secondary standards are used in its place. Nitrogen isotope measurements are made relative to the Ambient Inhalable Reservoir (AIR). Both standards are defined as having a δX value of 0‰.

As mentioned previously, the stable carbon isotope ratios of organic compounds vary due to many different reasons such as photosynthetic pathways and isotopic composition of biosynthetic precursors. It was first suggested in 1964 that the isotopic composition of animals tissues were influenced by the isotopic composition of the diet (Parker, 1964). It is now well documented that stable carbon and nitrogen isotope analyses can be used to retrieve palaeodietary

information from an individual's tissues (DeNiro and Epstein, 1978, DeNiro and Epstein, 1981).

1.3.1 Carbon isotopes in terrestrial and marine environments

The ratio of ^{13}C to ^{12}C in plant tissue is almost always lower than the ratio in atmospheric carbon dioxide, which indicates that carbon isotope discrimination occurs during the photosynthetic incorporation of CO_2 into plants (Farquhar *et al.*, 1989). There are three different types of photosynthesis, which are known as the C_3 , C_4 and CAM pathways. Plants that photosynthesise via the C_3 (or Calvin-Benson) pathway assimilate CO_2 from the air to a three carbon phosphoglycerate compound via the enzyme ribulose biphosphate carboxylase/oxygenase (RuBisCO). Plants that fall into this category include most flowering plants, trees and shrubs and grasses such as wheat and rice. Plants that photosynthesise via the C_4 (or Hatch-Slack) pathway include maize, millet and sorghum and assimilate CO_2 into the four carbon compound, oxaloacetate using the enzyme phosphoenol pyruvate carboxylase (PEPC). The final group are the Crassulacean Acid Metabolism (CAM) plants which include succulents such as the cacti. Normally the plants in this group fix CO_2 via the C_4 pathway, although under certain conditions, they are able to utilise the C_3 pathway. Figure 1.1 illustrates the isotopic discrimination that occurs during the assimilation and fixation of CO_2 in C_3 and C_4 plants. As mentioned above, C_3 plants fix CO_2 using the enzyme RuBisCO. One ribulose-1,5-bisphosphate molecule is carboxylated to form two 3-phosphoglycerate molecules and the isotope effect associated with this carboxylation is +27‰ (Gillon *et al.*, 1998). The C_4 pathway is characterised by initial fixation of CO_2 into C_4 acids via PEPC in the outer layer of photosynthetic cells. These organic acids are then transported to the inner layer of the cells (the bundle sheath) where decarboxylation and refixation by RuBisCO occurs. However, PEPC utilises the bicarbonate ion HCO_3^- , so overall fractionation by PEPC includes hydration of CO_2 as well as fractionation during carboxylation. Fractionation during carboxylation is approximately +2.2‰, but hydration of CO_2 fractionates by ca. -8‰ so that bicarbonate is enriched in ^{13}C relative to CO_2 and

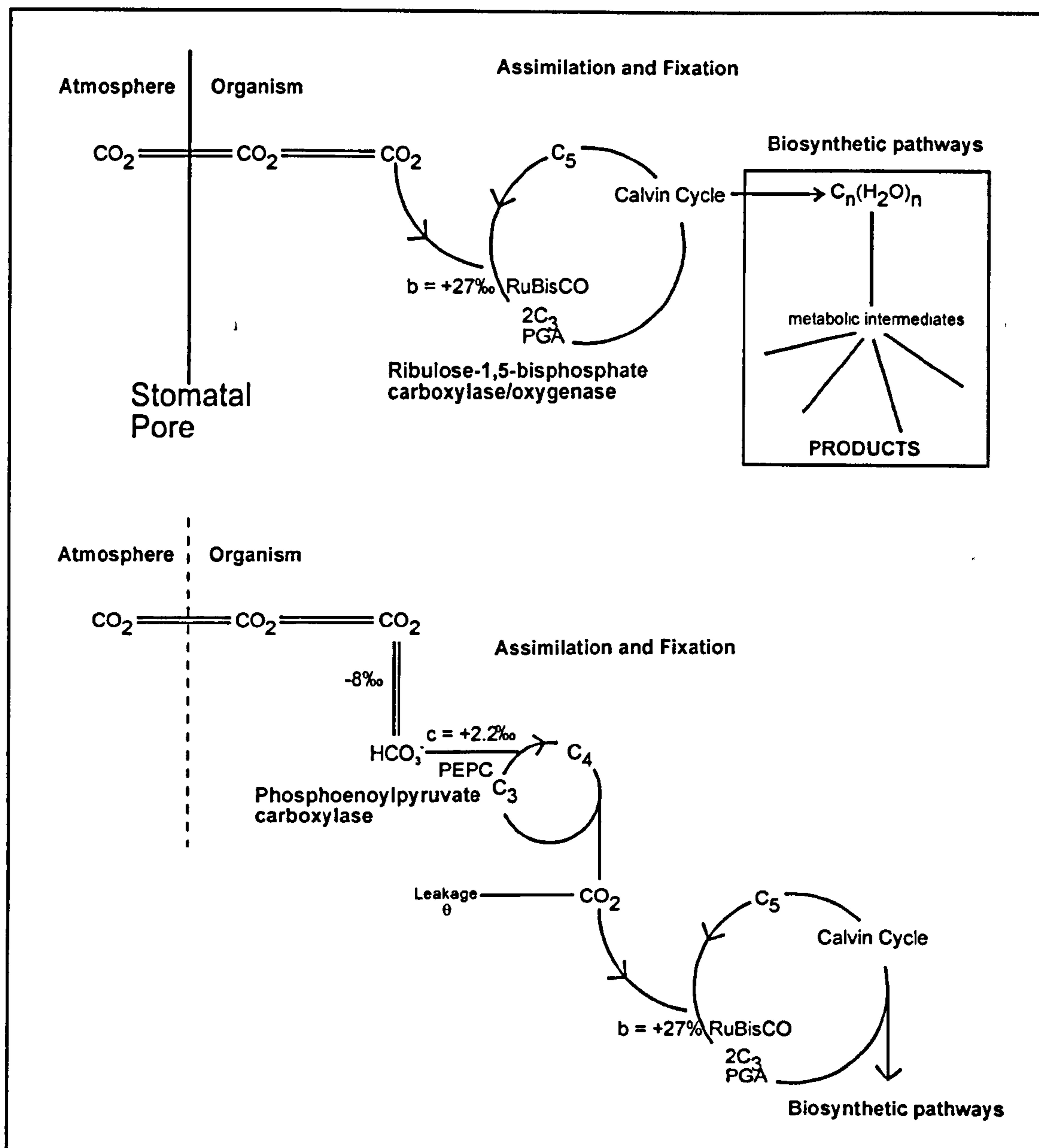


Figure 1.1. Isotopic fractionations which occur during the assimilation and fixation of CO₂ in C₃ (upper) and C₄ (lower) plants (from Hayes, 1983).

overall fractionation is *ca.* 5.8‰ (Gillon *et al.*, 1998). Some leakage of CO₂ occurs during decarboxylation and re-fixation in the bundle sheath and this results in the expression of a small portion of the expected isotope discrimination for RuBisCO (O'Leary, 1981).

The isotopic fractionation caused by different photosynthetic pathways is relevant to the field of palaeodietary reconstruction due to the differences in the $\delta^{13}\text{C}$ values of C_3 and C_4 plants. Based on hundreds of isotopic measurements it has been shown that C_3 and C_4 plants have average $\delta^{13}\text{C}$ values of -26.5‰ and -12.5‰ , respectively (Vogel *et al.*, 1978). C_3 plant $\delta^{13}\text{C}$ values can range from -20‰ to -35‰ whilst C_4 plant $\delta^{13}\text{C}$ values range from -9‰ to -16‰ . CAM plants can exhibit $\delta^{13}\text{C}$ values ranging from -28‰ to -10‰ , but they most commonly range between -20‰ and -10‰ (Boutton, 1991).

In the terrestrial carbon cycle, the primary source of carbon is atmospheric carbon dioxide. Therefore, if the isotopic composition of the source CO_2 changes, the isotopic composition of the plant will change by the same magnitude. This process is seen in the 'canopy effect' where leaves from the same tree in a dense forest may vary by up to 3‰ with leaves closer to the ground having the most depleted $\delta^{13}\text{C}$ values (Vogel, 1978b). This effect is due to the decomposition and respiration of plants, which produces CO_2 depleted in ^{13}C , which does not mix adequately with atmospheric CO_2 under the canopy and can lead to plants growing on the forest floor having $\delta^{13}\text{C}$ values as low as -36‰ (van der Merwe and Medina, 1991). Other environmental factors such as water availability, light intensity, temperature, partial pressure of CO_2 and nutrient availability can also lead to variations in the $\delta^{13}\text{C}$ values of similar species of plants growing in different environments (Farquhar *et al.*, 1989).

The isotopic compositions of aquatic plants vary between -11‰ and -39‰ (Farquhar *et al.*, 1989); however, with only a few exceptions aquatic plants fix carbon using the C_3 photosynthetic pathway (Chisholm *et al.*, 1982). The cause of these less depleted values observed for C_3 aquatic plants may be their source of carbon. Bicarbonate (HCO_3^-) constitutes ca. 95% of the dissolved inorganic carbon (DIC) in oceans, with CO_2 contributing approximately 1% and the remainder occurring as carbonate (CO_3^{2-}). Bicarbonate has a $\delta^{13}\text{C}$ value of ca. 0‰ in comparison with -7.8‰ for atmospheric CO_2 . Hence, if bicarbonate were the source carbon for aquatic plants they would be enriched in ^{13}C relative to terrestrial plants (Boutton, 1991).

1.3.2 Nitrogen isotopes in terrestrial and marine environments

Plants obtain virtually all of their nitrogen from inorganic ammonium and nitrate (NH_4^+ and NO_3^-) in the soil, or through symbiosis with atmospheric N_2 -fixing bacteria (Ambrose, 1991). Non-leguminous plants derive their nitrogen from the soil, whilst leguminous plants may derive their nitrogen both from the soil and from the atmosphere via symbiosis with N_2 -fixing bacteria. Plant $\delta^{15}\text{N}$ values mainly resemble source $\delta^{15}\text{N}$ values since there is only a slight fractionation of nitrogen when plants absorb nitrate (Garten, 1993), and little fractionation is associated with the fixation of atmospheric nitrogen by bacteria (Delwiche and Steyn, 1970).

Nitrogen isotope measurements are made relative to the AIR standard which has a designated $\delta^{15}\text{N}$ value of 0‰, but atmospheric nitrogen has an observed value of $+1.6 \pm 1.4\text{‰}$ (Owens, 1987). Different soils have distinct isotope signatures (Garten, 1993) and $\delta^{15}\text{N}$ values can vary from -7‰ to $+18\text{‰}$. Biological fixation of N_2 contributes ^{15}N -depleted nitrogen to the soil, but denitrification processes tend to increase soil $\delta^{15}\text{N}$ values. The wide range of observed soil $\delta^{15}\text{N}$ values is due to the balance of nitrification and denitrification processes. For example, soil dryness and high temperatures inhibit nitrification which leads to enriched soil $\delta^{15}\text{N}$ values in hot, arid environments in comparison with soils from cool, moist forests (Ambrose, 1991).

Therefore, leguminous plants are expected to exhibit lower $\delta^{15}\text{N}$ values than non-leguminous plants since they can obtain nitrogen from the atmosphere, which is generally more depleted in ^{15}N than soils. However, the mean $\delta^{15}\text{N}$ value for non-legumes is $+3 \pm 2.43\text{‰}$ and for legumes is $+3 \pm 2.5\text{‰}$ (Owens, 1987), although the maximum value for the legumes is lower than that for the non-legumes. Within the same environment it is possible to observe a clear distinction between leguminous and non-leguminous plants (Schoeninger and DeNiro, 1984), and this discrepancy is most likely due to the effect of environmental conditions on the availability of inorganic nitrate.

Marine plants obtain their nitrogen as dissolved ammonium and nitrate in the oceans. Marine nitrate can vary in different locations and has been found to range from +6‰ to +19‰ in the Pacific Ocean. These values are more enriched in ^{15}N than atmospheric nitrogen, hence marine plants have higher $\delta^{15}\text{N}$ values than terrestrial plants and can also vary widely.

1.3.3 Palaeodietary reconstruction based on stable isotopes

In 1964 it was first noted that marine animals display the same range of $\delta^{13}\text{C}$ values as the foods they eat, and it was suggested that stable carbon isotopes could be used as tracers (Parker, 1964). Since then, controlled animal feeding experiments have confirmed that the isotopic signature of different foodstuffs is passed on to a consumer's tissues (Ambrose and Norr, 1993; DeNiro and Epstein, 1978; DeNiro and Epstein, 1981; Tieszen *et al.*, 1983; Tieszen and Fagre, 1993). A small trophic enrichment of ca. 1‰ is observed for $\delta^{13}\text{C}$ values (DeNiro and Epstein, 1978), and a larger enrichment of ca. 3‰ is observed for $\delta^{15}\text{N}$ values (DeNiro and Epstein, 1981; Schoeninger and DeNiro, 1984). Due to the distinct isotopic signatures observed for C_3 and C_4 terrestrial and marine plants, it has been possible to use $\delta^{13}\text{C}$ and $\delta^{15}\text{N}$ values of consumer tissues to assess the consumption of C_3 vs. C_4 photosynthetically derived foods, the consumption of marine vs. terrestrial foods and protein vs. carbohydrate in the diets of ancient populations.

Hair, skin, flesh and bone have all been used in the stable isotope analysis of ancient diets. However, it is bone that is most commonly recovered in archaeological excavations and, therefore, this is where most of the research has been undertaken on the isotopic relationship between diet and consumer. More specifically, both the biomineral components and proteins preserved in ancient bones and teeth have been studied (Ambrose *et al.*, 1997; Ambrose and DeNiro, 1986; DeNiro and Schoeninger, 1983; Lee-Thorp *et al.*, 1989; Tieszen and Fagre, 1993; van der Merwe, 1978). The use of the stable isotopic compositions of bone components in palaeodietary reconstruction will be discussed in the following sections.

1.4 Bone collagen and apatite

Bone collagen has been the most widely used material for investigating the diets of ancient populations with stable isotopes and more recently the use of apatite has also been applied in this area. The turnover of bone is the slowest of all tissues in the body and the turnover of carbon in collagen has been estimated as being at least 30 years (Stenhouse and Baxter, 1979). Bone is a complex tissue, which is composed of collagen fibres permeated by hydroxyapatite crystals that lead to its strength and resiliency. Three major components comprise bone; these are the inorganic fraction, the organic matrix and water. By dry weight, the organic materials constitute about 30% and minerals about 70% of bone (Leblond and Weinstock, 1976). Collagen comprises ca. 90% of the organic component, lipids 0.4%, with the remainder consisting of non-collagenous proteins, glycosaminoglycans and glycoproteins (Herring, 1972).

Collagen is the most abundant protein of mammals and contains three helical polypeptide chains, each nearly 1000 residues long. It has a unique amino acid composition with two-thirds being comprised of just four amino acids. Collagen is ca. 33% glycine, 11% alanine and 22% proline and hydroxyproline. The remaining 34% consists glutamate (7%), arginine (5%), aspartate (5%), serine (4%), lysine, leucine, valine, threonine, phenylalanine, isoleucine, histidine, methionine, tyrosine and hydroxylysine (Herring, 1972). Collagen in bones is constantly deposited and recycled by growth and remodelling.

The composition of the inorganic matrix of bone is not precisely defined. It is considered to be a non-stoichiometric, carbonate-containing analogue of hydroxyapatite. Pure hydroxyapatite would have a formula of $\text{Ca}_5(\text{PO}_4)_3(\text{OH})$, however, carbonate ion substitutions can constitute as much as 5% of the inorganic matrix by structural substitution for phosphate groups, but also as a substitute in the hydroxyl position or attached in labile surface positions on the crystals in bone apatite (Krueger and Sullivan, 1984). It is thought that these carbonate ions are incorporated into the apatite structure from dissolved bicarbonate in body fluids during crystal growth.

1.4.1 Development of palaeodietary indicators

Bone collagen has been used since the 1970s and apatite since the 1980s to reconstruct the diets of ancient populations, and their use has been based on the fact that the isotopic composition of an animal's tissues is a direct and constant function of the diet. Accurate palaeodietary reconstruction demands firstly, that the bone component being analysed retains its isotopic integrity and has not been altered through diagenesis, and secondly, an understanding of the isotopic relationship between dietary macronutrients and different bone biochemical components.

The latter point has been the subject of some debate. Early field studies indicated that the enrichment in ^{13}C which occurs during collagen formation in the body was 6‰ (Vogel and van der Merwe, 1977). However, there were limitations to the conclusions that could be drawn from the results of these studies. Seasonal variation in the isotopic composition of the diet meant that unless recently synthesised tissue components were analysed the relationship between diet and consumer could not be accurately assessed. Also, selective feeding of wild animals would lead to inaccuracies in the interpretation of observed fractionation between diet and consumer. DeNiro and Epstein (1978) carried out controlled feeding experiments using mice to quantify the isotopic fractionation seen between diet and animal tissues. They found that collagen from mice raised on controlled diets was enriched in ^{13}C relative to whole diet by ca. 3‰, whilst an enrichment of 5.3‰ was observed for African ungulates (Vogel, 1978a). This wide range of $\Delta^{13}\text{C}_{\text{collagen-diet}}$ values ($\delta^{13}\text{C}_{\text{collagen}} - \delta^{13}\text{C}_{\text{diet}}$) was attributed to differences in metabolic rates of different animals and errors in the assumption of the isotopic composition of the diet (van der Merwe, 1982). Further controlled feeding experiments indicated that the fractionation was more complicated than initially suggested and these findings will be discussed in Section 1.4.2.

The palaeodietary interpretations based on the $\delta^{13}\text{C}$ values of bone collagen have raised some interesting questions. Palaeobotanical and faunal analyses suggest that Holocene hunter-gatherers in the Cape Province of South Africa stayed inland during the summer months and moved to the coast during the winter months to

exploit seasonally fluctuating resources (Parkington, 1972, 1976, 1977). If this were true, then $\delta^{13}\text{C}$ values of bone collagen from human skeletons from both inland and coastal sites should be similar, reflecting the same diet over a long period of time. However, bone collagen $\delta^{13}\text{C}$ values of individuals recovered from coastal and inland sites were found to differ ($\delta^{13}\text{C}_{\text{coll}}$ ranging from -14‰ to -16‰ for coastal individuals and ranging from -17‰ to -19‰ for inland individuals), which contradicted the seasonal mobility model for this population (Sealy and van der Merwe, 1985, 1986). From the isotopic analyses, it was postulated that the individuals from the inland and coastal sites were not part of a single population that moved in a regular pattern between inland and coastal sites; however Sealy and van der Merwe did not exclude the possibility that inland people visited the coast and stated that 'any seasonal round that inland people did engage in was different from that of people on the coast' (Sealy and van der Merwe, 1986).

This contradiction in results led to the palaeodietary information obtained from the $\delta^{13}\text{C}$ values of collagen to be questioned. Based on previous research it was observed that as long as protein is sufficient in the diet, it will preferentially be used to synthesise collagen and it was therefore assumed that 'not only all of the essential amino acids but also most of the inessential ones in human collagen come from protein in the food' (Parkington, 1991). It was also suggested that the high protein content of a marine diet would cause an increase in the turnover rate of bone collagen and this would exaggerate the marine signal and lead to an incorrect assumption of long-term dietary habits. It was further suggested that C_4 plants may have contributed to the enriched signals seen for the coastal individuals that would lead to a mistaken assumption of greater dependence on marine foodstuffs for the coastal individuals than was actually the case (Parkington, 1991).

This debate focussed attention on the fact that the relationship between diet and bone is dependent on many factors, including the turnover rates and biosynthetic pathways of bone biochemical components (Koch *et al.*, 1994). Thus it was evidenced that further investigation into the factors that affect the dietary signals

reflected in different bone biochemical components was required. These factors are discussed in the following sections.

1.4.2 Routing of dietary macronutrients

In order to interpret the $\delta^{13}\text{C}$ values obtained for collagen and apatite from ancient humans, it is necessary to understand how dietary macronutrients are incorporated into these bone components. The bulk of any diet will comprise carbohydrates, lipids and proteins, and each of these components will have a distinct isotopic signature that reflects its formation. Fundamental to the use of isotopes for palaeodietary reconstruction is the question of whether the carbon contained in these dietary macronutrients is pooled together for the synthesis of collagen and apatite or if certain dietary macronutrients are routed to specific body tissues. If the latter is the case, then different body tissues will reflect the isotopic composition of different macronutrients in the diet. Much work has focussed on attempting to answer this question (DeNiro and Epstein, 1978; Krueger and Sullivan, 1984; Lee-Thorp *et al.*, 1989; Schwarcz, 1991; van der Merwe, 1982).

It is through controlled feeding experiments that further understanding of the relationship between dietary macronutrients and bone component $\delta^{13}\text{C}$ values has been achieved (Ambrose and Norr, 1993; DeNiro and Epstein, 1978; Tieszen and Fagre, 1993). Initial work by DeNiro and Epstein (1978) showed an average enrichment of $0.8 \pm 1.1\text{‰}$ between the $\delta^{13}\text{C}$ values of the whole animal and the diet for a variety of animals (mice, nematodes, insects, shrimps and snails) raised on monotonous diets. They also found that the isotopic relationships of macronutrients in the diet e.g. $\delta^{13}\text{C}_{\text{lipid}} < \delta^{13}\text{C}_{\text{total organic matter}}$, $\delta^{13}\text{C}_{\text{lipid}} < \delta^{13}\text{C}_{\text{carbohydrate}}$ and $\delta^{13}\text{C}_{\text{lipid}} < \delta^{13}\text{C}_{\text{protein}}$ was also observed in the tissues of the animals raised on those diets. DeNiro and Epstein (1978) and Tieszen *et al.* (1983) also observed that the isotopic difference between diet and tissue ($\Delta^{13}\text{C}_{\text{diet-tissue}}$) for mice and gerbils, respectively, raised on monotonous diets varied widely depending on which tissue or organ was being analysed (e.g. fat, liver, muscle or hair). It was suggested that these differences reflected variation in the biochemical composition

of the tissues. For example, a tissue containing a high proportion of lipids would probably have a more depleted $\delta^{13}\text{C}$ values than a tissue with lower lipid content, since lipids are relatively depleted in ^{13}C (DeNiro and Epstein, 1977).

Following on from this work, results from the highly controlled feeding experiments undertaken by Ambrose and Norr (1993) and Tieszen and Fagre (1993) led to the conclusion that dietary macronutrients are routed to specific tissues. Figure 1.2 summarises the routing of dietary macronutrients to consumer tissues. Both studies found a high correlation between whole diet and apatite $\delta^{13}\text{C}$ values ($R^2 = 0.90$ for the Tieszen and Fagre study and $R^2 > 0.98$ for the Ambrose and Norr study), which suggested that the isotopic composition of apatite would provide more information on the isotopic composition of the whole diet than the $\delta^{13}\text{C}$ values of collagen. This was confirmed by the correlation of whole diet and bone collagen $\delta^{13}\text{C}$ values ($R^2 = 0.62$ and 0.28 for the Tieszen and Fagre study and Ambrose and Norr studies, respectively). Virtually all ingested carbon atoms leave the body as CO_2 respired by the lungs and, therefore, reflect the carbon from all dietary macronutrients according to their proportions in the diet (Lee-Thorp *et al.*, 1989; Schwarcz, 1991). Respired CO_2 is in equilibrium with blood bicarbonate and since apatite carbonate is derived from blood bicarbonate, the isotopic composition of apatite will reflect the isotopic composition of all dietary macronutrients. A further confirmation of this was obtained by Tieszen and Fagre (1993), who showed that the $\delta^{13}\text{C}$ values of respired CO_2 correlated highly with both whole diet ($R^2 = 0.92$) and apatite $\delta^{13}\text{C}$ values ($R^2 = 0.98$).

These isotopically controlled feeding experiments also revealed a correlation between bone collagen and dietary protein ($R^2 = 0.91$), although the collagen to dietary protein spacing did range from +2‰ to almost +6‰ for different diets (Tieszen and Fagre, 1993). The combination of this information suggested that the isotopic signal in collagen is largely determined by the isotopic signal of dietary protein, but is also affected by the percentage of protein in the diet and the $\delta^{13}\text{C}$ value of the other dietary macronutrients. Collagen is comprised of amino acids which can be classed as either essential or non-essential. Essential amino acids

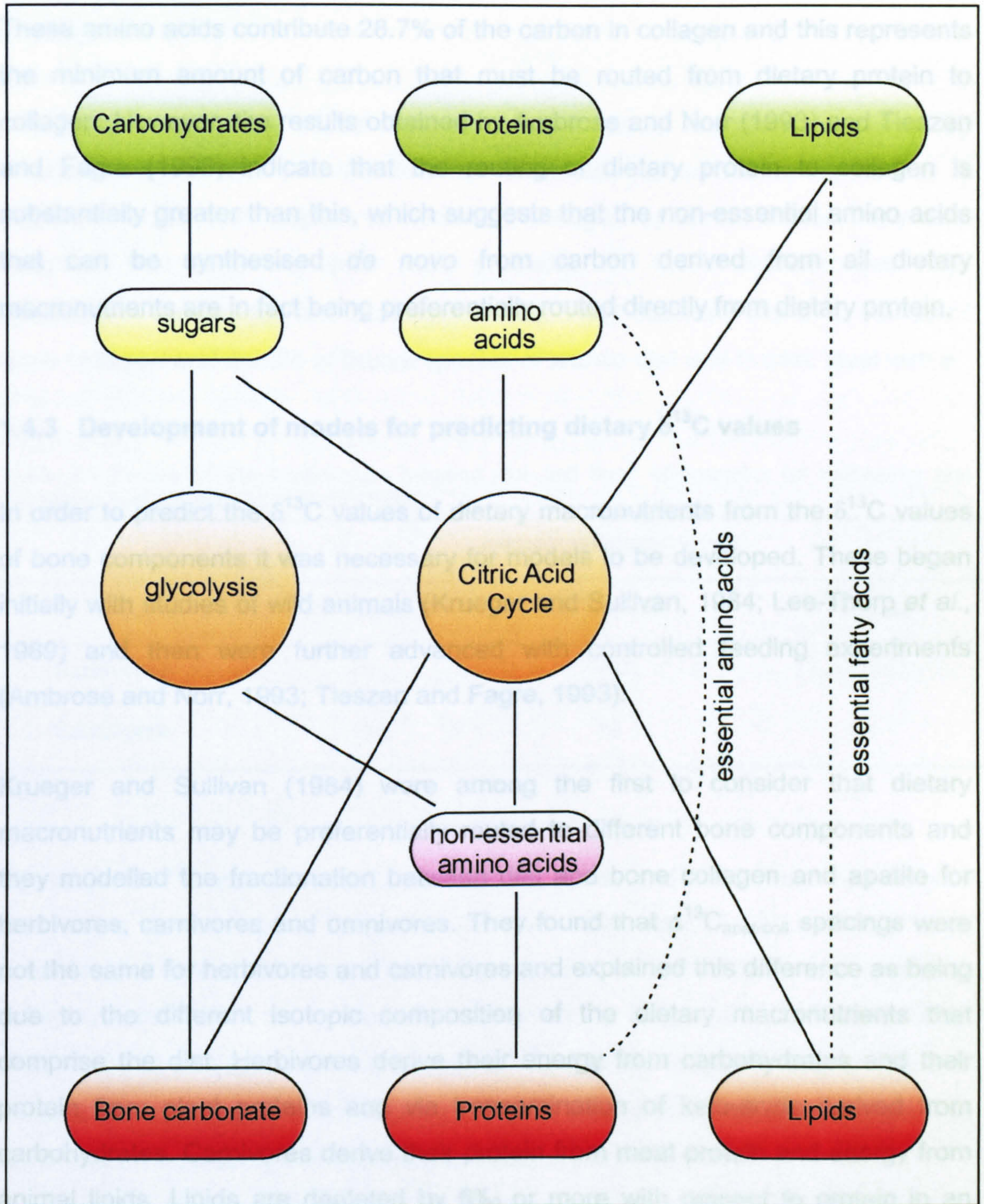


Figure 1.2. Summary of the fate of dietary macronutrients in relation to bone components. Adapted from Jim (2000).

cannot be synthesised by the body and must be obtained from dietary protein. These amino acids contribute 28.7% of the carbon in collagen and this represents the minimum amount of carbon that must be routed from dietary protein to collagen. However, the results obtained by Ambrose and Norr (1993) and Tieszen and Fagre (1993) indicate that the routing of dietary protein to collagen is substantially greater than this, which suggests that the non-essential amino acids that can be synthesised *de novo* from carbon derived from all dietary macronutrients are in fact being preferentially routed directly from dietary protein.

1.4.3 Development of models for predicting dietary $\delta^{13}\text{C}$ values

In order to predict the $\delta^{13}\text{C}$ values of dietary macronutrients from the $\delta^{13}\text{C}$ values of bone components it was necessary for models to be developed. These began initially with studies of wild animals (Krueger and Sullivan, 1984; Lee-Thorp *et al.*, 1989) and then were further advanced with controlled feeding experiments (Ambrose and Norr, 1993; Tieszen and Fagre, 1993).

Krueger and Sullivan (1984) were among the first to consider that dietary macronutrients may be preferentially routed to different bone components and they modelled the fractionation between diet and bone collagen and apatite for herbivores, carnivores and omnivores. They found that $\Delta^{13}\text{C}_{\text{apat-coll}}$ spacings were not the same for herbivores and carnivores and explained this difference as being due to the different isotopic composition of the dietary macronutrients that comprise the diet. Herbivores derive their energy from carbohydrates and their protein from plant proteins and via transamination of keto-acids derived from carbohydrates. Carnivores derive their protein from meat protein and energy from animal lipids. Lipids are depleted by 6‰ or more with respect to protein in an organism, and this depletion is due to a fractionation that occurs during the oxidation of pyruvate to acetyl CoA, which is the main source of carbon for lipid biosynthesis (DeNiro and Epstein, 1977). Therefore, carnivores derive their energy from lipids which have relatively depleted $\delta^{13}\text{C}$ values which leads to depleted $\delta^{13}\text{C}$ values of apatite, producing smaller $\Delta^{13}\text{C}_{\text{apat-coll}}$ spacings for carnivores than herbivores. A summary of their model is presented in Table 1.1. Omnivores

(including humans) have more complicated diets and have intermediate $\Delta^{13}\text{C}_{\text{apat-coll}}$ spacings.

Lee-Thorp *et al.* (1989) based their work on this model and further refined it by incorporating the fact that the flesh of herbivores consumed by carnivores is depleted in ^{13}C with respect to herbivore collagen by about 2-3‰. They also assumed that herbivore lipids were probably 1‰ more depleted than was assumed in the Kruger and Sullivan models. They obtained the $\delta^{13}\text{C}$ values of bone collagen and apatite of faunal species of known diet and trophic level with a

Table 1.1 Models of the fractionation between diet and bone components for herbivores and carnivores from Kruger and Sullivan (1984).

	Isotopic relationship (‰)		
	$\Delta^{13}\text{C}_{\text{coll-diet}}$	$\Delta^{13}\text{C}_{\text{apat-diet}}$	$\Delta^{13}\text{C}_{\text{apat-coll}}$
Herbivores	+5	+12	+7
Carnivores	+5	+8	+3

full range of $\delta^{13}\text{C}$ values from C_4 plants to C_3 plants and from these they derived the models summarised in Table 1.2. The main refinement of the Lee-Thorp *et al.* model is the fractionation of 2 to 2.5‰ between herbivore flesh and carnivore collagen rather than no fractionation assumed by Kruger and Sullivan (1984). Despite these differences, the proposed $\Delta^{13}\text{C}_{\text{apat-coll}}$ spacings are very similar and indicate the importance of measuring the $\delta^{13}\text{C}$ values of both bone collagen and apatite when assessing the isotopic compositions of diet.

The controlled feeding experiments carried out by Ambrose and Norr (1993) and Tieszen and Fagre (1993) provided important insights into the spacings between $\delta^{13}\text{C}$ values of diet and bone components. It was encouraging that they observed that $\Delta^{13}\text{C}_{\text{apat-diet}}$ spacings were fairly constant (from 8.4‰ to 11.1‰; Tieszen and Fagre (1993) and from 9.1‰ to 10.9‰; Ambrose and Norr (1993)) given the wide

Table 1.2 Models of the fractionation between diet and bone components for herbivores and carnivores from Lee-Thorp *et al.* (1989).

	Isotopic relationship (‰)		
	$\Delta^{13}\text{C}_{\text{coll-diet}}$	$\Delta^{13}\text{C}_{\text{apat-diet}}$	$\Delta^{13}\text{C}_{\text{apat-coll}}$
Herbivores	+5	+12	+7
Carnivores	+8	+12	+4

range of isotopic compositions of the diets. In comparison, the $\Delta^{13}\text{C}_{\text{coll-diet}}$ spacings ranged from 1.7‰ to 8.1‰ (Tieszen and Fagre, 1993). This wide range contrasted with the fixed 5‰ spacing that researchers had been applying based on results from field studies. A $\Delta^{13}\text{C}_{\text{coll-diet}}$ spacing of +5‰ was observed for animals raised on diets in which all dietary macronutrients had the same isotopic composition, but values varied amongst animals raised on diets which contained isotopically distinct macronutrients. Hence, it became apparent that the isotopic relationship between diet and bone components is more complicated than originally thought, leading to the conclusion that bone collagen largely reflects the dietary protein, with some influence from other dietary macronutrients.

1.4.4 Isotopic integrity of collagen and apatite

As mentioned previously, bone is the most common tissue uncovered at archaeological excavations and, therefore, it is the isotopic compositions of bone components that have been used to reconstruct ancient diets. However, buried bone is subject to diagenesis, which is the sum of the physical, chemical and biological processes that occur in the postmortem depositional environment (DeNiro, 1985). Fundamental to all palaeodietary reconstruction with stable isotopes is the assumption that the organic material being analysed is indigenous and that the indigenous material retains its original isotopic composition with high fidelity.

The preservation of collagen in bones is extremely variable as a function of time and is dependent on the burial environment. Bones buried in wet, warm soils can decompose very rapidly, whilst bones that have been preserved in permafrost or clay may contain more than 50% of their original collagen after 75,000 years (Tuross *et al.*, 1988).

Insoluble collagen is obtained for isotopic analysis by dissolving away biogenic and diagenetic minerals, non-collagenous proteins and contaminating organic material (Koch *et al.*, 1994). The simplest method to achieve this is to demineralise the bone with dilute hydrochloric acid, wash to neutralise with double distilled water and then to freeze-dry the organic residue (Tuross *et al.*, 1988). Collagen has a unique amino acid composition, and each amino acid has a unique $\delta^{13}\text{C}$ and $\delta^{15}\text{N}$ value. Therefore, the isotopic composition of bulk collagen is dependent on the isotopic composition of the amino acids that comprise it. The $\delta^{13}\text{C}$ and $\delta^{15}\text{N}$ values of individual amino acids from bone collagen have been found to vary by *ca.* 17‰ and 47‰, respectively (Tuross *et al.*, 1988); thus, any preferential loss of an amino acid will bias the isotopic measurement of the bulk collagen. To assess the isotopic integrity of collagen extracted from bones, researchers can measure the atomic C:N ratios. These ratios can rise or fall during diagenesis as a result of deamination of amino acids or invasion by soil humic acids or inorganic material (DeNiro, 1985). The C:N ratio of modern collagen ranges from 2.9 to 3.6 and archaeological samples that have ratios which fall within this range are thought to retain their original isotopic composition (DeNiro, 1985; Ambrose, 1990). Other protocols which can be applied to the isotopic integrity of archaeological collagen are the collagen yield and the percentage of carbon and nitrogen in the collagen sample (Ambrose, 1990). Additionally, the unique amino acid composition makes it possible to use the amino acid composition of isolated collagen samples to assess the effects of diagenesis (Tuross *et al.*, 1988).

Bone apatite is susceptible to leaching by groundwater as it contains many complex carbonates and phosphates. The carbonate in hydration layers is highly labile and may exchange with carbonate in burial fluids over time, and recrystallisation following burial can allow sediment-derived ions to infiltrate the

structural carbonate fractions (Kruger, 1991). To obtain reliable $\delta^{13}\text{C}$ values for apatite, it is thus necessary to remove all diagenetic carbonates. The accepted procedure for this is treatment of the sample with weak acetic acid to remove the diagenetic carbonate as this is more soluble than biogenic apatite due to its higher CO_3^{2-} content (Koch *et al.*, 1997). X-ray diffraction techniques and the monitoring of carbonate yield have also been applied to ensure isotopic integrity (Tuross *et al.*, 1989; Lee-Thorp and van der Merwe, 1991); unusually low carbonate yields may indicate recrystallisation to fluoroapatite, whereas high values suggest addition of exogenous sedimentary carbonates.

1.5 Bulk stable isotope analysis

The bulk stable isotope analysis of bone collagen ($\delta^{13}\text{C}$ and $\delta^{15}\text{N}$) and apatite ($\delta^{13}\text{C}$) has provided much information on palaeodiet including the detection of the introduction of maize into North America (Vogel and van der Merwe, 1977; van der Merwe and Vogel, 1978; Katzenberg *et al.*, 1995), and more subtle changes in diet such as the duration of nursing by prehistoric peoples (Tuross and Fogel, 1994). The dependence on marine sources has been assessed for populations from British Columbia (Chisholm *et al.*, 1982), Northern England (Mays, 1997) and Micronesia (Ambrose *et al.*, 1997), and the adaptation of Neanderthals from scavengers to effective predators has been observed (Richards *et al.*, 2000).

The stable isotope ratios of a variety of compounds can be measured using isotope ratio mass spectrometry (IRMS). The mass spectrometer used to make these measurements was designed by Nier (1947) and modified by McKinney *et al.* (1950) (See Figure 1.3). For IRMS analysis, all samples must first be converted into simple gases prior to introduction into the ion source. The isotope measurements of hydrogen ($^2\text{H}/^1\text{H}$), nitrogen ($^{15}\text{N}/^{14}\text{N}$), carbon ($^{13}\text{C}/^{12}\text{C}$), oxygen ($^{18}\text{O}/^{16}\text{O}$) and sulphur ($^{34}\text{S}/^{32}\text{S}$) are performed on gases of H_2 , N_2 , CO_2 , CO and SO_2 , respectively (Meier-Augenstein, 1999). Freeze-dried samples are combusted in sealed, evacuated quartz tubes with CuO as an oxidant, and the resultant gases are purified cryogenically before being subjected to IRMS analysis.

Almost 70% of all gas isotope analyses are made on CO₂, which is employed for both the ¹³C/¹²C and ¹⁸O/¹⁶O ratios. The CO₂ derived from the sample is introduced into the ion source under very high vacuum where it is ionised to a beam of positive ions. The ion beam passes through a magnetic field, which deflects the ions according to their mass to charge (*m/z*) ratios. The major ion currents of CO₂⁺ are resolved into three separate beams corresponding to *m/z* 44, 45 and 46. These ion beams are registered simultaneously by a multiple Faraday cup arrangement to measure the 6 isotopomers of CO₂ (¹²C¹⁶O₂, ¹²C¹⁶O¹⁷O, ¹³C¹⁶O₂, ¹²C¹⁶O¹⁸O, ¹²C¹⁷O₂ and ¹³C¹⁶O¹⁷O); the δ¹³C and δ¹⁸O values are then calculated via a system of equations (Santrock *et al.*, 1985).

The dual-inlet system devised by McKinney *et al.* (1950) requires sample sizes of approximately 20 mg and can measure the isotope ratios of gases with a precision of ±0.1‰. The isotope ratios are expressed relative to international standards, rather than the use of absolute isotope values. For carbon, the international standard is Pee Dee Belemnite (PDB). For oxygen and hydrogen measurements, the standard is Standard Mean Ocean Water (SMOW) and the standard is AIR for nitrogen measurements. All these standards have been assigned a value of 0.0‰. The recent coupling of an elemental analyser to an IRMS (termed continuous-flow IRMS) has allowed only micrograms of sample to be required for stable isotope analysis (Preston and Barrie, 1991). By this method samples are placed in tin or silver capsules and automatically dropped into a reactor filled with CuO. The combustion products are passed through a reduction furnace to reduce nitrous oxides to N₂ and to remove surplus oxygen. Water is then removed in a drying tube and the resultant gases separated chromatographically prior to introduction into the IRMS. It is necessary to remove water to prevent the formation of HCO₂⁺ ions in the ion source, which would contribute to the ion current at *m/z* 45.

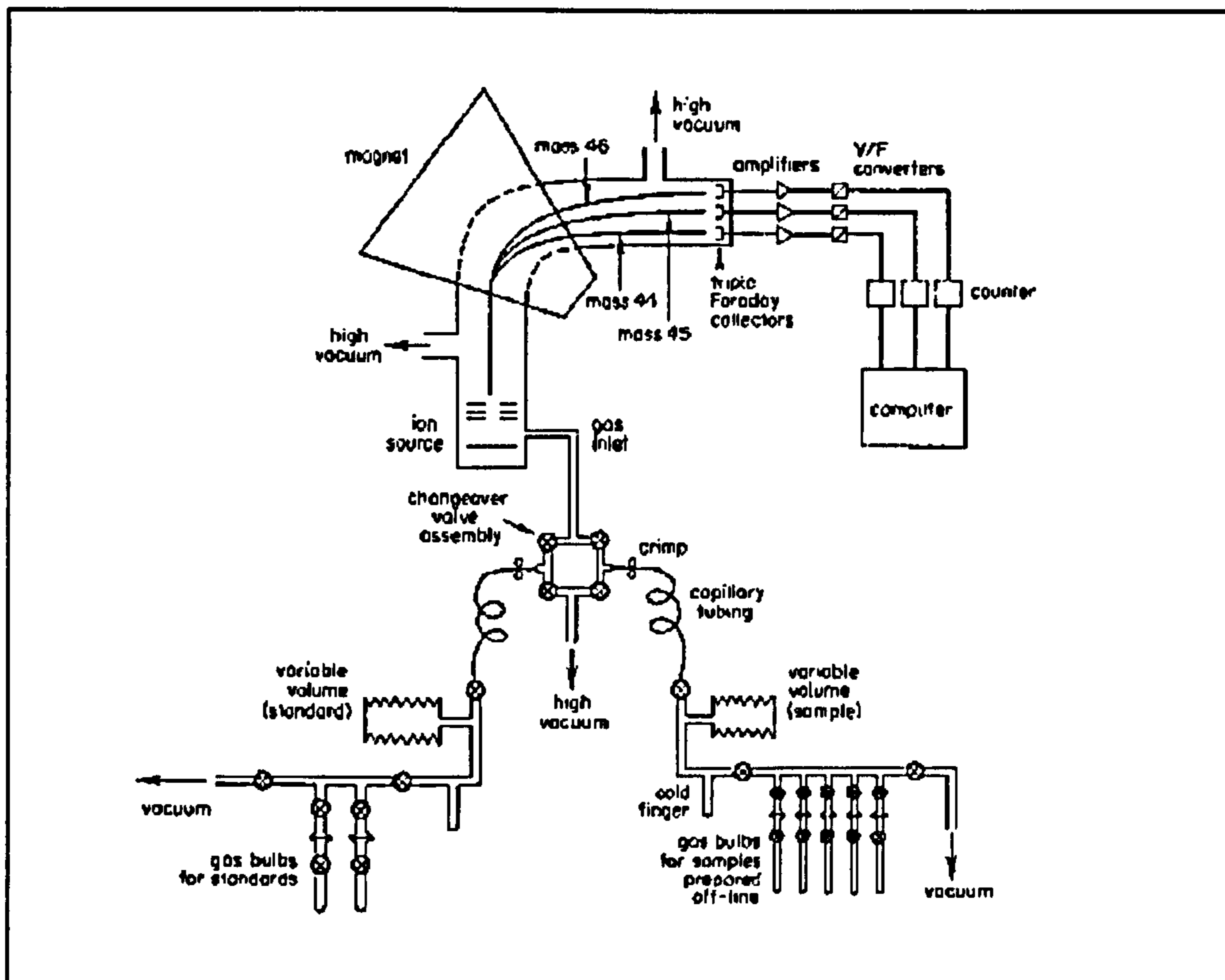


Figure 1.3. Schematic of the McKinney-Nier IRMS system (from Boutton, 1991).

1.6 Compound-specific stable isotope analysis

The previous sections have discussed the stable isotope analysis of bulk materials; however these materials are the weighted average of the compounds that comprise them, each of which has its own unique isotopic composition. Compound specific isotope analysis holds great potential in the field of palaeodietary reconstruction as well as for tracing the source, biochemistry, and diagenesis of a material (Macko, 1994). In materials such as collagen, analyses of the $\delta^{13}\text{C}$ and $\delta^{15}\text{N}$ values of the individual amino acids which comprise it may overcome the problems regarding the indigineity of the material obtained from fossil bones (see Section 1.4.4) (Hare *et al.*, 1991). Prior to the introduction of gas chromatography/combustion/isotope ratio mass spectrometry (GC/C/IRMS), which will be discussed in the following section, off-line isotopic analyses relied on obtaining ca. 10 μg to 1 mg of the pure compound to be measured, from which the

stable isotope ratios were obtained as described previously in Section 1.5. Abelson and Hoering (1961) were one of the first to measure compound-specific stable isotope ratios in this way. They analysed the $\delta^{13}\text{C}$ values of individual amino acids in algal and bacterial cultures and strengthened the understanding of biosynthetic pathways. In 1964, Parker measured the $\delta^{13}\text{C}$ values of individual fatty acids and showed that lipids were up to 15‰ depleted in ^{13}C relative to bulk organic carbon. The stable isotope ratios of hydrocarbons were also investigated in order to determine the biological origin of petroleum (Welte, 1968).

In 1991 Hare *et al.* measured the $\delta^{13}\text{C}$ and $\delta^{15}\text{N}$ values of individual amino acids from collagen from modern and archaeological bone using preparative HPLC followed by off-line combustion and IRMS. They observed a characteristic pattern among the $\delta^{13}\text{C}$ and $\delta^{15}\text{N}$ values and suggested that deviations from this pattern could indicate dietary stress or contamination from exogenous substances. Therefore, the compound-specific analysis of amino acids could provide information on the indigeneity and diagenesis of individual collagenous amino acids (Macko, 1994).

The introduction of GC/C/IRMS provided a much more sensitive and less laborious approach to compound-specific analyses and allowed the rapid analysis of stable isotope ratios of individual compounds occurring at trace levels in complex sample mixtures; this facilitated previously unobtainable stable isotope analyses in many new research fields. The first application of GC/C/IRMS measured the $\delta^{13}\text{C}$ values of essential oils (Barrie *et al.*, 1984) and since then, this technique has allowed the determination of alkane $\delta^{13}\text{C}$ values to deduce the sources of sedimentary lipids (Rieley *et al.*, 1991); carbohydrate $\delta^{13}\text{C}$ values to trace exogenous ^{13}C labelled glucose (Tissot *et al.*, 1990) and amino acid $\delta^{13}\text{C}$ values (Silfer *et al.*, 1991). The analysis of $\delta^{13}\text{C}$ values of individual fatty acid components of remnant fats preserved in archaeological pottery has shown that dairying was a component of archaeological economies (Dudd and Evershed, 1998), whilst $\delta^{13}\text{C}$ values of fatty acids of archaeological pottery and faunal remains have provided information on palaeodiet (Copley, 2001). The analysis of soils and plant remains has allowed manuring and other agricultural practices to be investigated (Bull *et al.*, 1999).

1.6.1 Measurement of stable isotope ratios of individual compounds by GC/C/IRMS

The technique of gas chromatography/combustion/isotope ratio mass spectrometry (GC/C/IRMS) was first reported by Barrie *et al.* (1984). This technique allows mixtures to be injected onto a GC column; the eluants are then combusted and the resultant gases purified on-line before being directly introduced into an IRMS. Such instruments first became commercially available in 1988 and Figure 1.4 depicts the machine schematically. The sample mixture is separated on a GC column and the eluants are fed via a post-column split to a vent outlet and the combustion furnace. The furnace consists of either a quartz glass or ceramic tube filled with CuO/Pt or CuO/NiO/Pt maintained at a temperature of 820 or 940°C, respectively (Freedman *et al.*, 1988; Merritt *et al.*, 1995). The combustion (or oxidation) furnace converts the sample to CO₂, H₂O and a variety of nitrogen compounds. If compounds being analysed contain nitrogen, then the effluent must next pass through a reduction furnace (see Section 3.3.2), which contains Cu, is maintained at a temperature of 600 °C, and reduces the nitrogen oxides to N₂ (Brand, 1996). It should be noted that the original instrumental design did not include a reduction reactor for obtaining $\delta^{13}\text{C}$ values of nitrogenous compounds (Freedman *et al.*, 1988). Water vapour is removed by a hygroscopic Nafion membrane. Nafion is a fluorinated polymer that acts as a semi-permeable membrane through which water passes freely while all the other combustion products are retained in the carrier gas stream (Meier-Augenstein, 1999). An open split connects the separator to the mass spectrometer in order to cope with the pressure fluctuations inherent with the combustion process (Brand, 1996).

As described previously, for stable carbon isotope analysis, ion currents at m/z 44, 45 and 46 are measured. These are presented in two types of traces, which are illustrated in Figure 1.5. The lower trace depicts the m/z 44 ion current at a period of time during analysis when the CO₂ resulting from the combustion of a hydrocarbon was detected by the Faraday cups. The upper trace depicts the instantaneous ratio of the m/z 45/44 ion current over the same time period. An S-

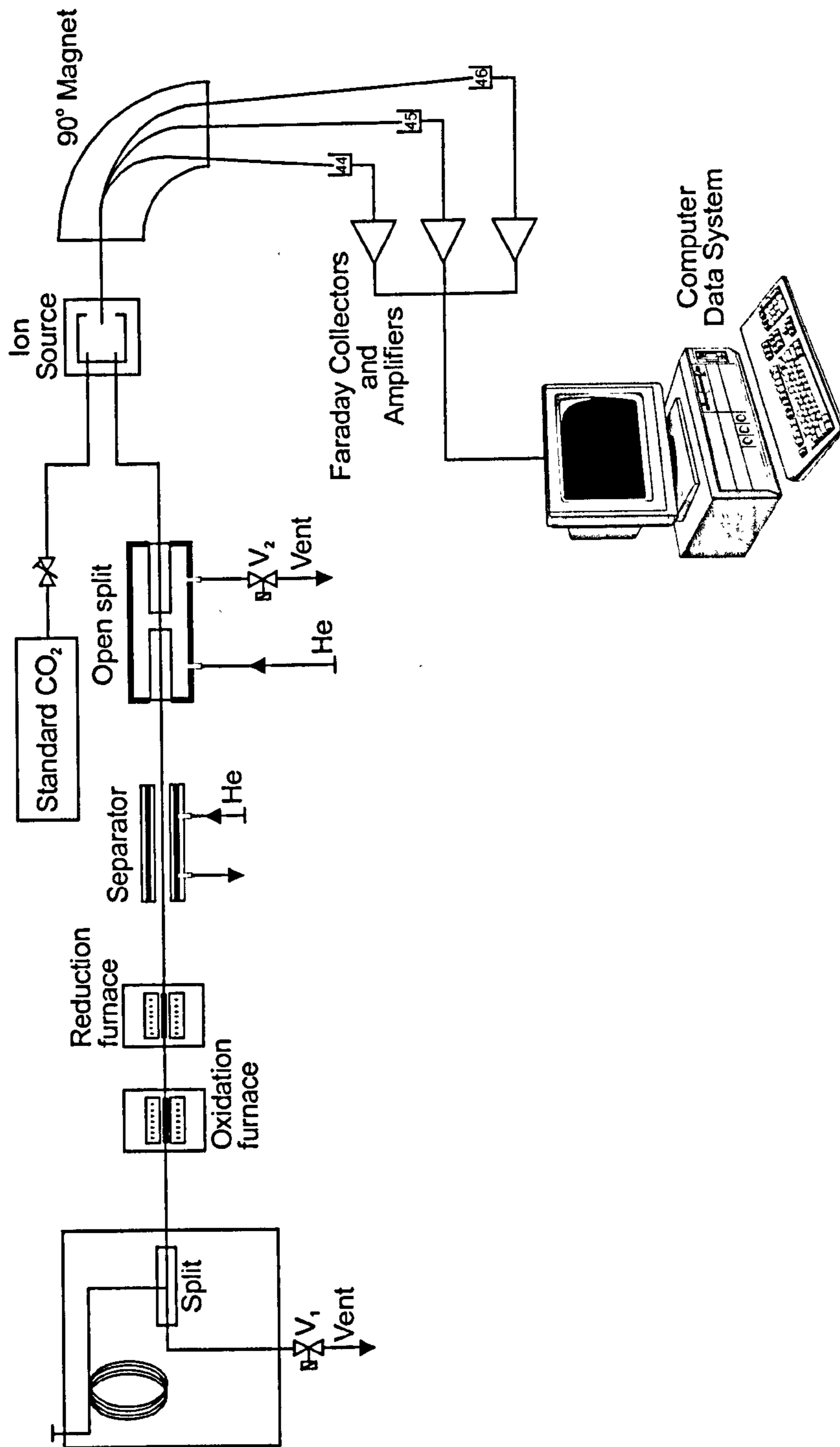


Figure 1.4. Schematic of the GC/C/IRMS system adapted from Brand (1996).

shaped curve is observed due to the m/z 45 signal preceding the m/z 44 signal by ca. 150 ms (Habfast, 1991). This chromatographic isotope effect is a result of different solute/stationary phase interactions caused by lower molar volumes of the heavier compounds due to increased bond strength and thus shortened bond lengths involving the heavier isotope (Meier-Augenstein, 1999). This chromatographic separation thus demands that the entire peak must be integrated to obtain an accurate $\delta^{13}\text{C}$ value (Brand, 1996).

1.7 Further Development of palaeodietary reconstruction models

The advent of GC/C/IRMS led to the possibility of measuring the $\delta^{13}\text{C}$ values of cholesterol in ancient bones. Lipids are preserved in association with archaeological artefact and ecofact (Evershed *et al.*, 1999), and in 1995, Evershed *et al.* first reported the preservation of cholesterol in ancient human and animals bones. A relatively high concentration of cholesterol (1.5 to 46.5 $\mu\text{g g}^{-1}$) was detected in bone samples of varying age (75,000 B.P. to 19th century) recovered from different burial environments. The possibility of diffusion of soil lipids into bone samples during burial was investigated, but soil lipid compositions associated with the samples were in total contrast to the bone lipid compositions; thus, the indigeneity of cholesterol in bone was assured. Due to its preservation and retention of biogenic integrity, cholesterol's potential as a palaeodietary indicator was suggested. Preliminary investigations of the isotopic composition of bone cholesterol from animals from controlled feeding experiments and from archaeological samples of 'known diet' revealed that the $\delta^{13}\text{C}$ values of cholesterol did reflect the $\delta^{13}\text{C}$ value of the diet (Stott *et al.*, 1997; Stott *et al.*, 1999). Further insight into the exact dietary information supplied by cholesterol was obtained by comparing bone collagen, apatite and cholesterol $\delta^{13}\text{C}$ values from the same samples. From this small sample set it was suggested that the dietary signal of cholesterol reflected whole diet $\delta^{13}\text{C}$ values, consistent with its *de novo* synthesis predominantly from non-protein sources (Jim, 2000).

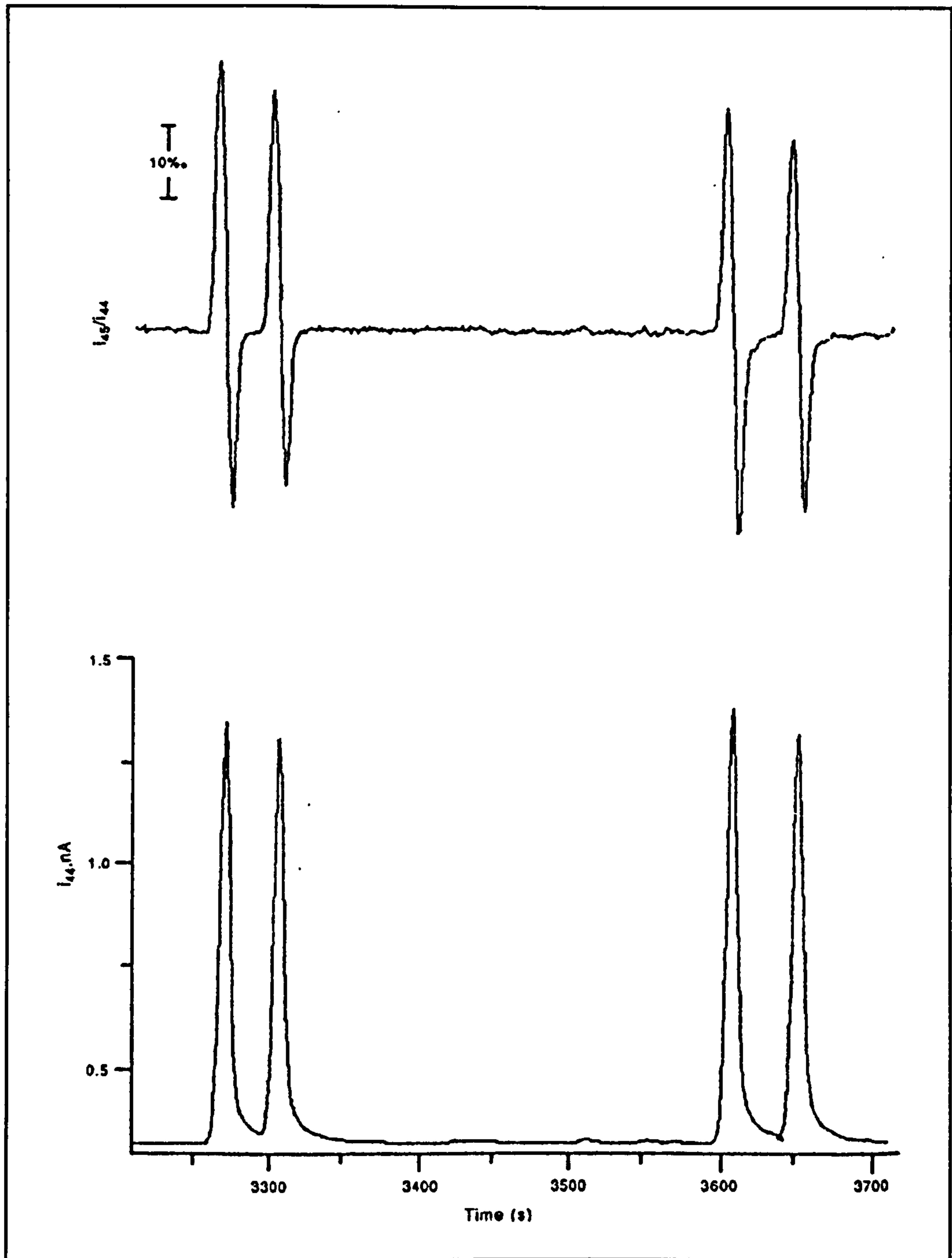


Figure 1.5. An example of partial traces obtained from the $\delta^{13}\text{C}$ analysis of hydrocarbons. The lower chromatogram represents the m/z 44 ion current as a function of time, whilst the upper chromatogram represents the instantaneous ratio of the m/z 45/44 ions. From Ricci *et al.* (1994).

Based on $\delta^{13}\text{C}$ analysis of collagen, apatite and cholesterol from the controlled feeding experiment carried out by Ambrose and Norr (1993), recent work in this laboratory by Jim (2000) assessed the use of cholesterol as a palaeodietary indicator. This work revealed that the majority of cholesterol in bone is synthesised *de novo* in the body and has a mean 99% turnover time of 289 days ($\delta^{13}\text{C}$ values obtained from the bone cholesterol of rats of ages 131-251 days). Bone cholesterol $\delta^{13}\text{C}$ values correlated well with whole diet $\delta^{13}\text{C}$ values, and models were constructed to exploit the differences observed in dietary signals and turnover rates of the bone biochemical components. Bone component spacings were used to gain an insight into the long-term isotopic relationship between whole diet and dietary protein $\delta^{13}\text{C}$ values and also into the changes in whole diet $\delta^{13}\text{C}$ values over time. The linear relationship between diet and bone $\delta^{13}\text{C}$ values and their $\Delta^{13}\text{C}$ spacings were used to construct models that enabled the prediction of long- and short-term whole diet, dietary energy and dietary protein $\delta^{13}\text{C}$ values from bone component $\delta^{13}\text{C}$ values. These models were then applied to archaeological populations in the reconstruction of palaeodiet.

1.8 Amino acids as palaeodietary indicators

Collagen is the most abundant protein in mammalian tissue and is comprised of 19 amino acids that can be supplied by dietary protein or synthesised *de novo*. Thus, the $\delta^{13}\text{C}$ value of collagen is a weighted average of the $\delta^{13}\text{C}$ values of the individual amino acids that comprise it. The amino acids found in collagen are presented in Table 1.3. Nine of the amino acids found in collagen are essential and thus cannot be synthesised by the body; they must be provided by dietary protein. Non-essential amino acids may be provided by dietary protein, but can also be synthesised *de novo*.

Considerable potential exists for the use of individual collagenous amino acids in the field of palaeodietary reconstruction, however, only a handful of studies have so far measured the $\delta^{13}\text{C}$ values of individual amino acids in bone collagen (Hare and Estep, 1983; Hare *et al.*, 1991; Tuross *et al.*, 1988). In 1983, Hare and Estep

Table 1.3 Amino acids found in collagen (residues per 1000 are in parentheses) from Vaughan (1970).

Essential amino acids	Non-essential amino acids
isoleucine (11)	alanine (119)
leucine (24)	serine (28)
lysine (29)	glycine (328)
methionine (8)	glutamate (75)
phenylalanine (15)	proline (114)
threonine (20)	aspartate (45)
valine (20)	tyrosine (4)
arginine ¹ (52)	3-hydroxyproline (2)
histidine (5)	4-hydroxyproline (97)
	hydroxylysine (6)

¹conditionally essential as synthesised at rates inadequate to support rapid growth

were the first to measure the $\delta^{13}\text{C}$ and $\delta^{15}\text{N}$ values of amino acids in modern and fossil collagens. The purpose of the work was to determine a labelling pattern of the isotopic compositions of amino acids in modern collagen and the relationship of these compounds to total protein. They then compared the observed pattern with that seen for 10,000-year-old bison collagen. They observed a wide range of amino acid $\delta^{13}\text{C}$ values within a sample (ca. -24‰ to -8‰), but this pattern was preserved in modern and fossil collagen. They noted that the analysis of $\delta^{13}\text{C}$ values of individual amino acids in collagen overcame the problem of contamination of bulk collagen with exogenous compounds. Tuross *et al.* (1988) measured the $\delta^{13}\text{C}$ values of individual amino acids in modern and fossil whale bones. Once again, they observed a wide range of $\delta^{13}\text{C}$ values within one sample (ca. 20‰), but found that the pattern of values observed was very similar for both the modern and fossil collagens.

Only one study has used controlled feeding experiments to investigate the $\delta^{13}\text{C}$ values of individual amino acids in bone collagen. Hare *et al.* (1991) measured the $\delta^{13}\text{C}$ and $\delta^{15}\text{N}$ values of amino acids from the bone collagen of modern (including pigs raised on isotopically defined diets) and archaeological bone. They observed a wide range of $\delta^{13}\text{C}$ values for individual amino acids separated from the bone collagen of pigs raised on controlled diets (Figure 1.6). This pattern of isotope fractionation was very similar for the pigs whether they were raised on diets comprised of either C_3 or C_4 foodstuffs. Incorporation of dietary isotopic signals and biosynthesis related isotope effects were observed. Glycine in the diet was 8‰ more positive than the bulk diet and the isotope value was incorporated almost directly into the tissue. Since glycine comprises one third of the carbon in collagen, this enriched signal contributed to the bulk collagen being several per mil more positive than the bulk diet. This study also allowed an insight into the metabolic pathways that govern these amino acid $\delta^{13}\text{C}$ values; aspartate and glutamate were 3‰ and 6‰ more enriched, respectively, in collagen than diet, and this shows how fractionation during metabolism can cause an enrichment in bulk values. The $\delta^{13}\text{C}$ values of proline and glutamate in collagen were found to be different, despite proline being formed directly from glutamate. Therefore, it was suggested that proline was being incorporated directly from the diet as well as being synthesised *de novo*.

Hare *et al.* also measured the $\delta^{13}\text{C}$ and $\delta^{15}\text{N}$ values of individual amino acids from the bone collagen of herbivores and terrestrial and marine carnivores and observed that the isotopic distributions shown in Figure 1.6 were consistent across trophic levels, environments and diets. The $\delta^{13}\text{C}$ and $\delta^{15}\text{N}$ values for individual amino acids from bone collagen of two terrestrial carnivores, the lion and the lynx, are presented in Figure 1.7. Hare *et al.* observed that both animals had identical patterns of carbon isotope fractionation even though the absolute values differed. These differences reflected the differences in diets; lions feed on animals subsisting on C_4 plants, whilst the lynx relies on small mammals, which primarily consume C_3 plants. The $\delta^{13}\text{C}$ and $\delta^{15}\text{N}$ values of individual amino acids from the bone collagen of modern and fossil whale were also compared (Figure 1.8); the pattern of isotopic fractionation was similar for both samples.

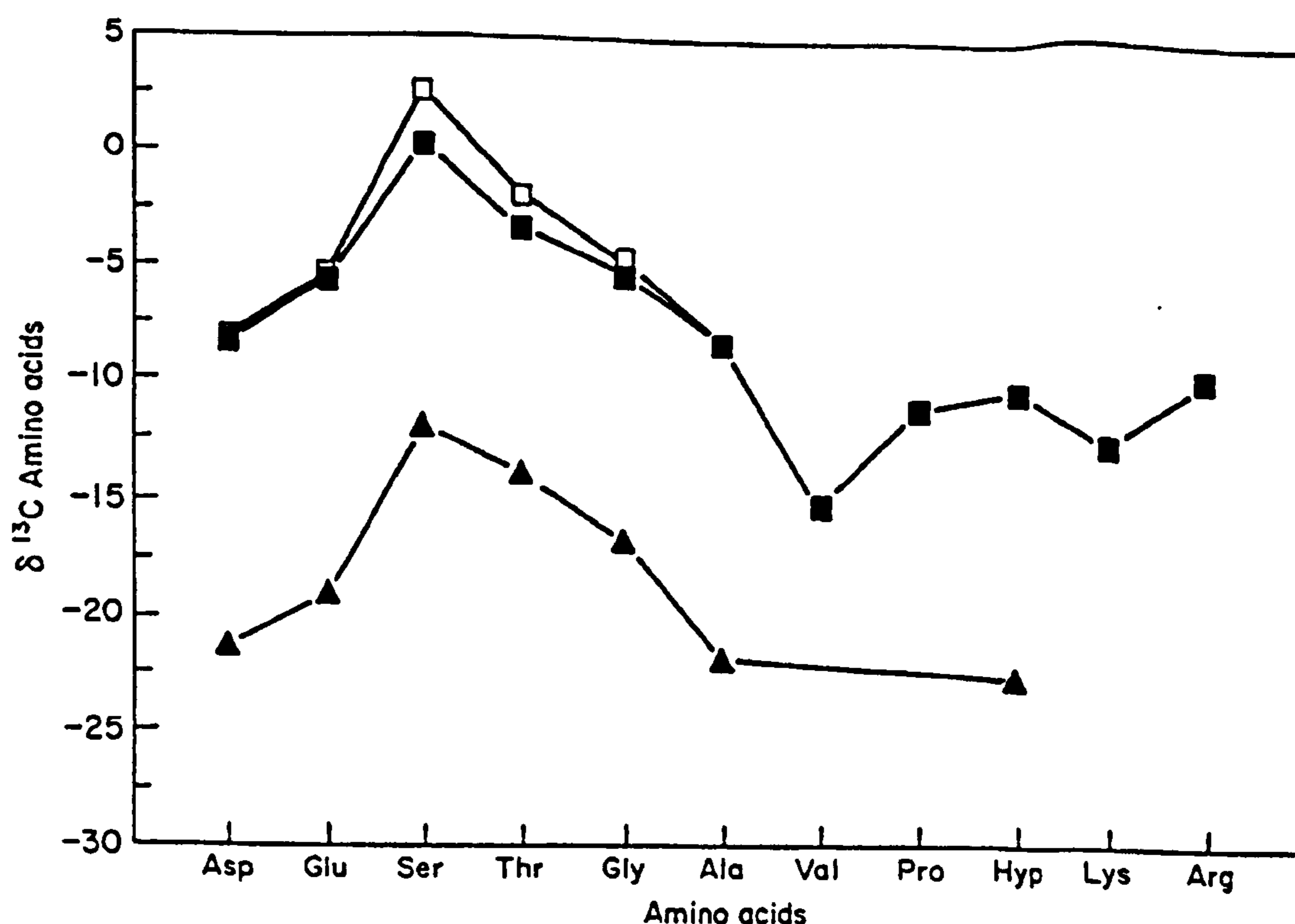


Figure 1.6 $\delta^{13}\text{C}$ values of individual amino acids separated from bone collagen of pigs raised on controlled diets. Pigs were raised on diets containing either C₃ (triangles) or C₄ (open squares – pig 1, filled squares - pig 2) foodstuffs. From Hare *et al.* (1991).

Therefore, it was suggested that any deviation from this pattern could indicate diagenesis or contamination from exogenous substances,

This study illustrated for the first time the processes that contribute to the isotopic fractionation between an animal and its diet and how the $\delta^{13}\text{C}$ values of individual amino acids can be used to investigate this. It also provided an insight into the use of $\delta^{13}\text{C}$ values of individual amino acids to study the metabolic pathways that involve these amino acids and how individual amino acids could be used to overcome some of the problems associated with diagenesis and contamination in the stable isotope analysis of bone components for palaeodietary reconstruction.

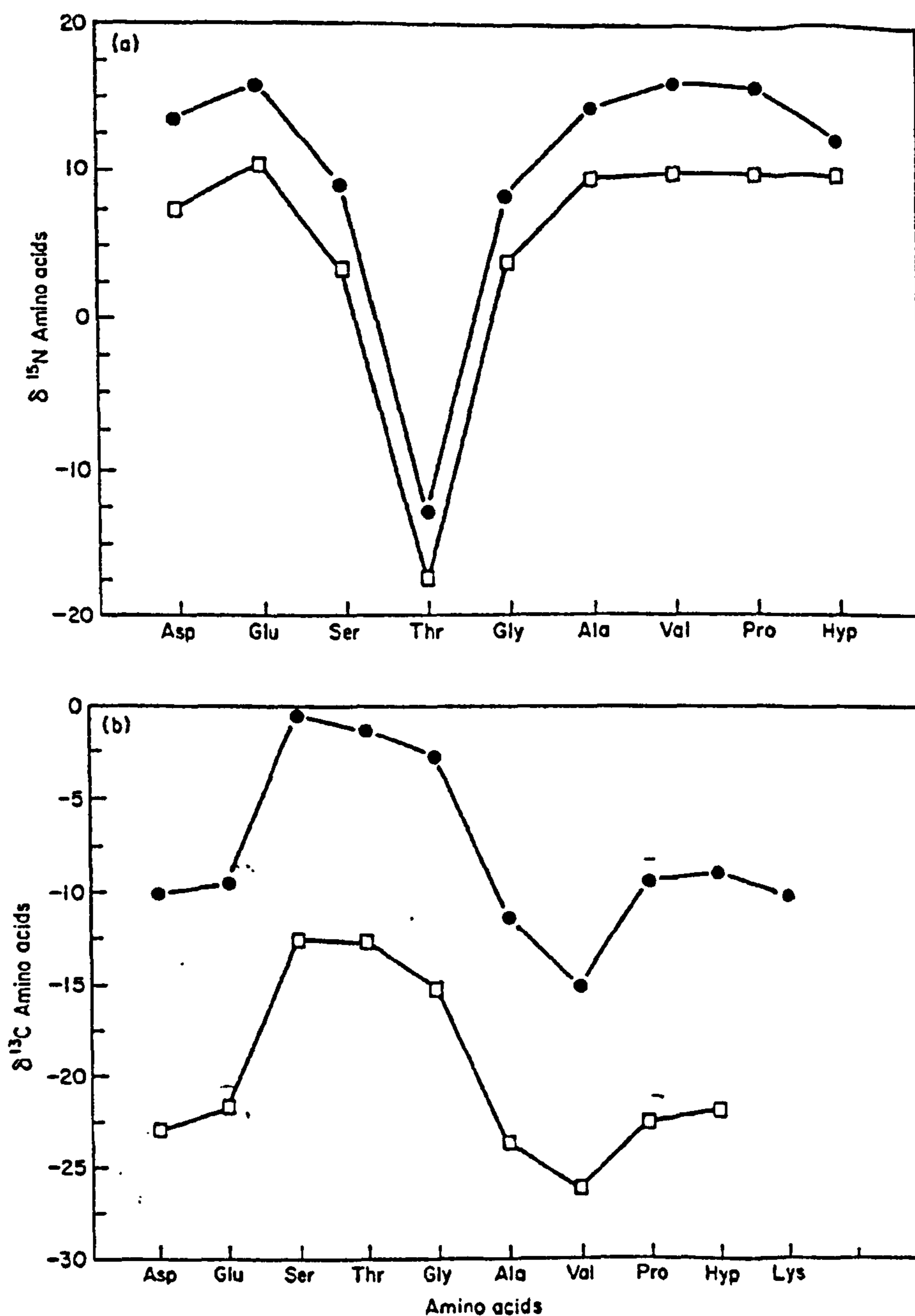


Figure 1.7 (a) $\delta^{15}\text{N}$ and (b) $\delta^{13}\text{C}$ values for individual amino acids from the bone collagen of a lion (circles) and a lynx (squares). From Hare *et al.* (1991).

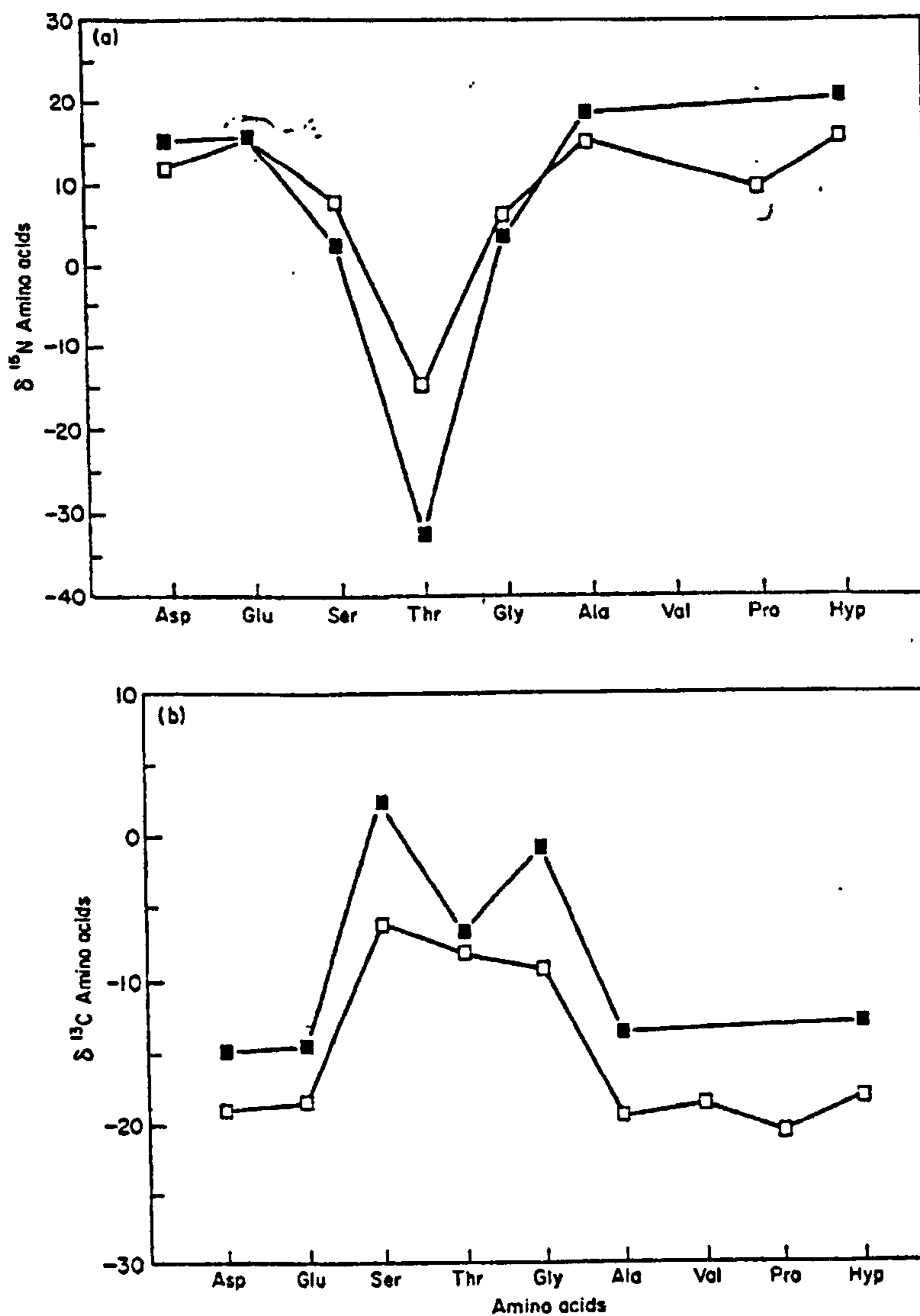


Figure 1.8 (a) $\delta^{15}\text{N}$ and (b) $\delta^{13}\text{C}$ values for individual amino acids from the bone collagen of fossil whale (clear squares) and modern whale (black squares). From Hare *et al.* (1991).

1.9 Biosynthesis of amino acids

The body lacks the enzymatic capability to synthesise essential amino acids; hence, they must be provided by the diet. However, non-essential amino acids can be synthesised *de novo*, and an overview of their biosynthesis is shown in Figure 1.9.

Alanine has the simplest biosynthetic pathway. It is formed by a one-step transamination of pyruvate (Figure 1.10b). Transamination reactions convert one amino acid into another and they are catalysed by aminotransferases, which

transfer the α -amino group (NH_3^+) to an α -keto acid (either pyruvate, oxaloacetate or α -ketoglutarate). In alanine biosynthesis, the α -amino group is transferred from glutamate or aspartate to pyruvate to form alanine. Pyruvate itself is formed from carbohydrates by glycolysis; therefore, the carbon skeleton of alanine formed *de novo* will comprise carbohydrate carbons.

There are a number of different pathways available in the synthesis of serine. The main pathway (shown in Figure 1.10a) is the phosphorylated pathway where serine is formed from 3-phosphoglycerate (a pyruvate precursor and glycolytic intermediate). It involves three steps: firstly, the α -hydroxyl group of 3-phosphoglycerate is oxidised to form phosphohydroxypyruvate; secondly, an α -amino group is transferred from glutamate to form phosphoserine; and finally, this compound is hydrolysed to serine. As with alanine, because 3-phosphoglycerate is a glycolytic intermediate, the carbon skeleton of serine will be formed *de novo* from carbohydrate carbons. Serine can also be synthesised from glycine by serine hydroxymethyl transferase. This is a reversible reaction and is therefore also a pathway for glycine synthesis. Glycine can also be formed from CO_2 , NH_4^+ and N^5N^{10} -methylene tetrahydrofolate in a reaction catalysed by glycine synthase.

Aspartate is formed by the transamination of oxaloacetate (Figure 1.10d). An α -amino group of glutamate is transferred to oxaloacetate by aspartate aminotransferase to form aspartate. Oxaloacetate is an intermediate of the citric acid cycle and as shown in Figure 1.2, dietary lipids, carbohydrates and proteins all contribute carbon to this cycle. Glutamate is formed from another intermediate of the citric acid cycle, α -ketoglutarate, via reductive deamination (Figure 1.10c) by glutamate dehydrogenase. Proline is synthesised from glutamate in three steps (see Figure 1.11). Glutamate is first reduced to glutamate- γ -semialdehyde, a spontaneous cyclisation forms pyrroline-5-carboxylate and finally it is reduced to proline. Arginine is biosynthesised from an intermediate in the formation of proline (Figure 1.11). Glutamate- γ -semialdehyde is transaminated to ornithine, which is metabolised by the urea cycle to form arginine

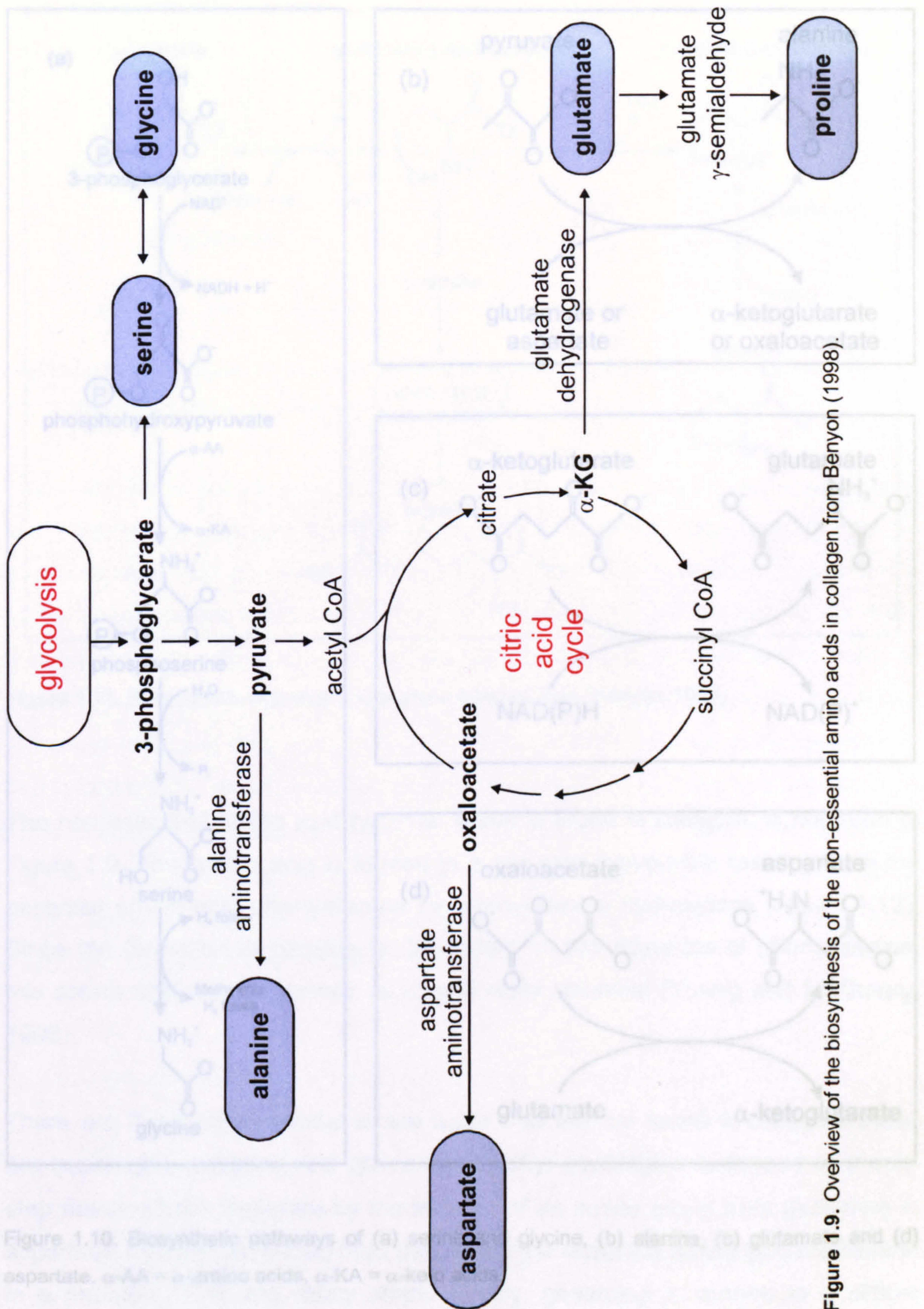


Figure 1.9. Overview of the biosynthesis of the non-essential amino acids in collagen from Benyon (1998).

Figure 1.10. Biosynthetic pathways of (a) serine, (b) glycine, (c) glutamate, and (d) aspartate. α-AA = α-amino acids, α-KA = α-ketoglutarate.

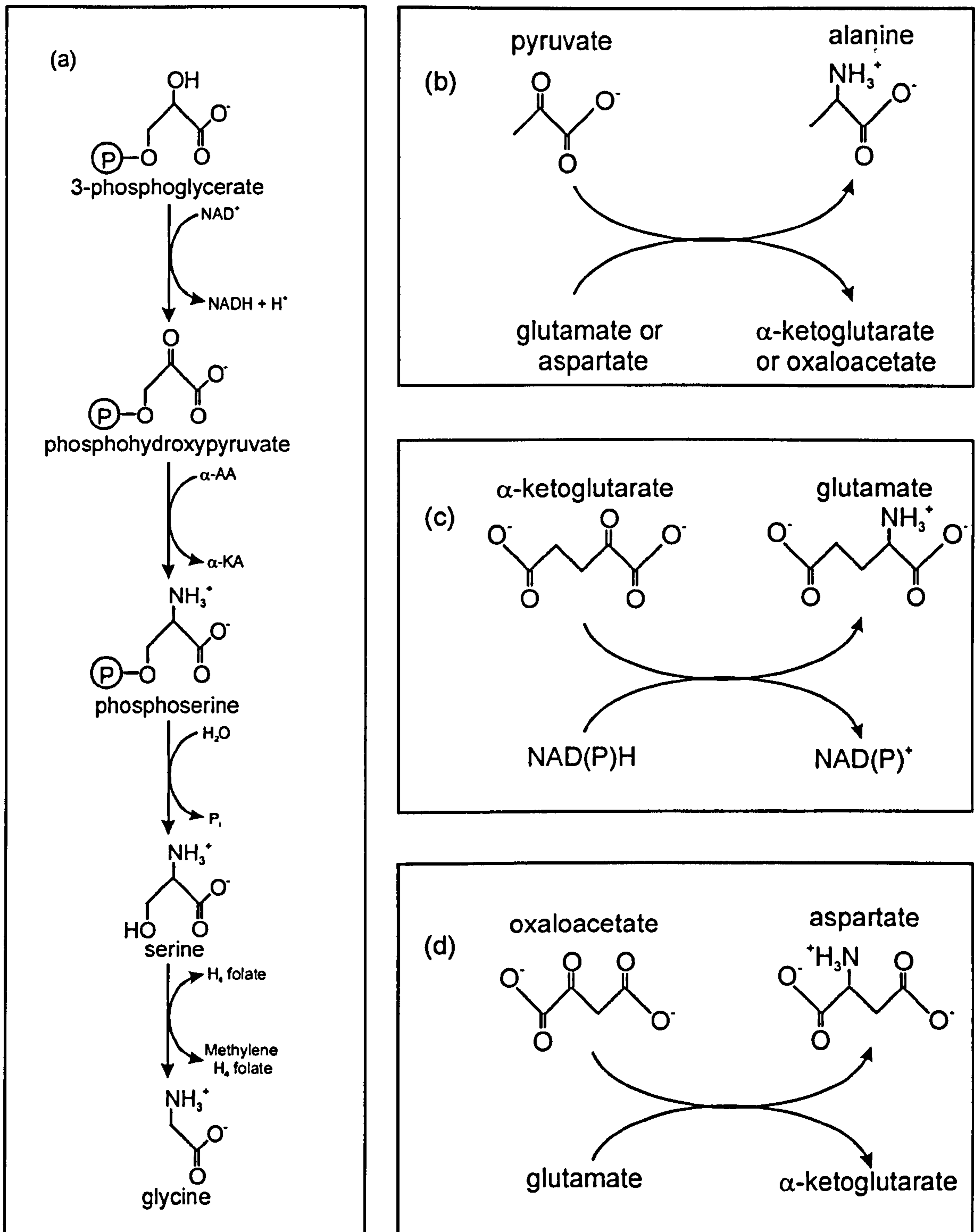


Figure 1.10. Biosynthetic pathways of (a) serine and glycine, (b) alanine, (c) glutamate and (d) aspartate. α -AA = α -amino acids, α -KA = α -keto acids.

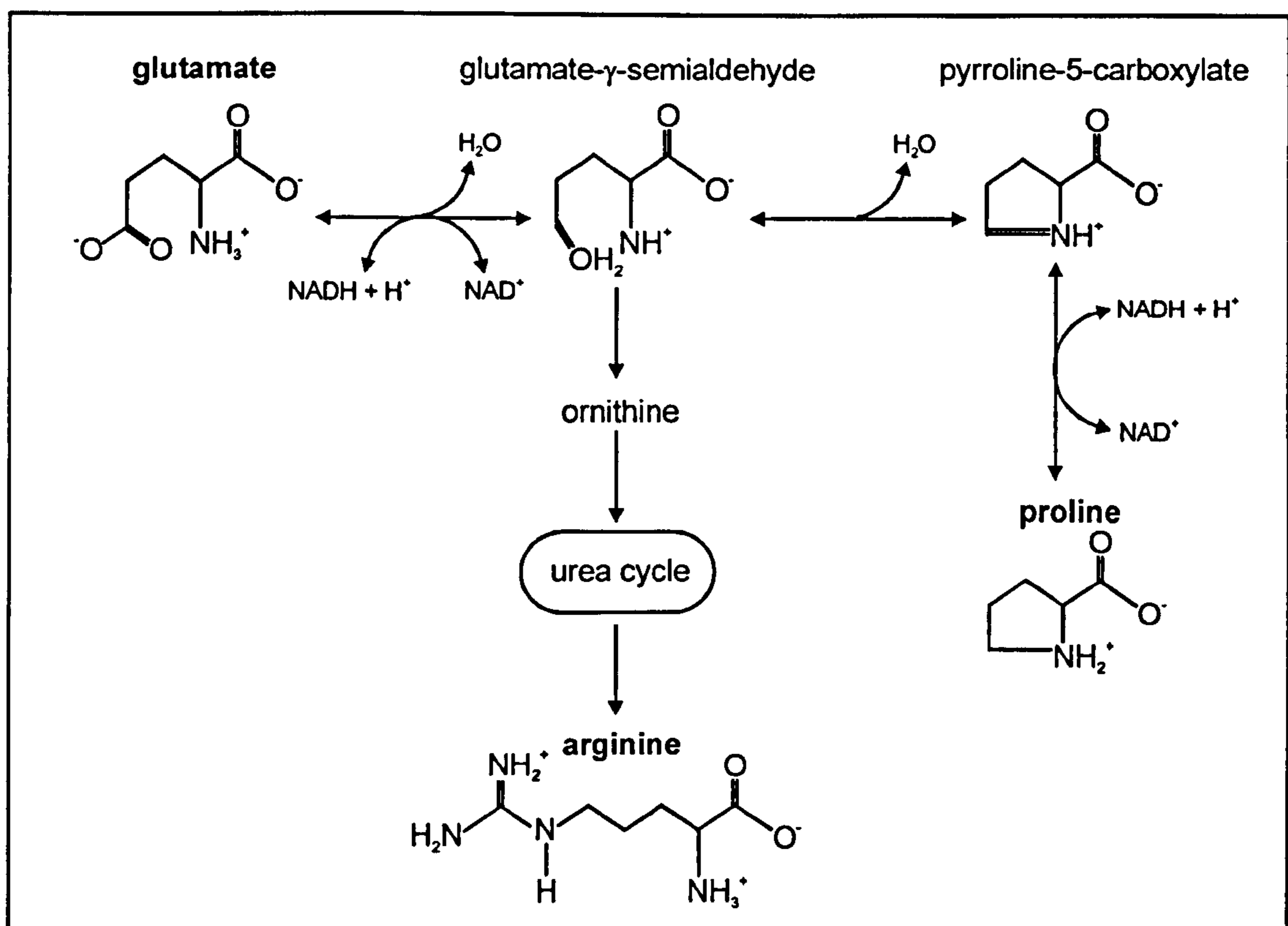


Figure 1.11. Biosynthesis of proline and arginine adapted from (Benyon, 1998).

The non-essential amino acid tyrosine, which is found in collagen, is not seen in Figure 1.9. This amino acid is formed in a one-step irreversible reaction from the essential amino acid phenylalanine by phenylalanine hydroxylase (Figure 1.12). Since the formation of tyrosine is dependent on the presence of phenylalanine, this amino acid can be termed as conditionally essential (Young and El-Khoury, 1995).

There are three non-essential amino acids that are not found in collagen, these are asparagine, cysteine and glutamine. Briefly, asparagine is formed in a one-step reaction from aspartate by the transfer of an amide group from glutamine to aspartate. Cysteine is formed from serine and the essential amino acid methionine in a process containing many steps. Finally, glutamine is formed in a simple amidation reaction of glutamate.

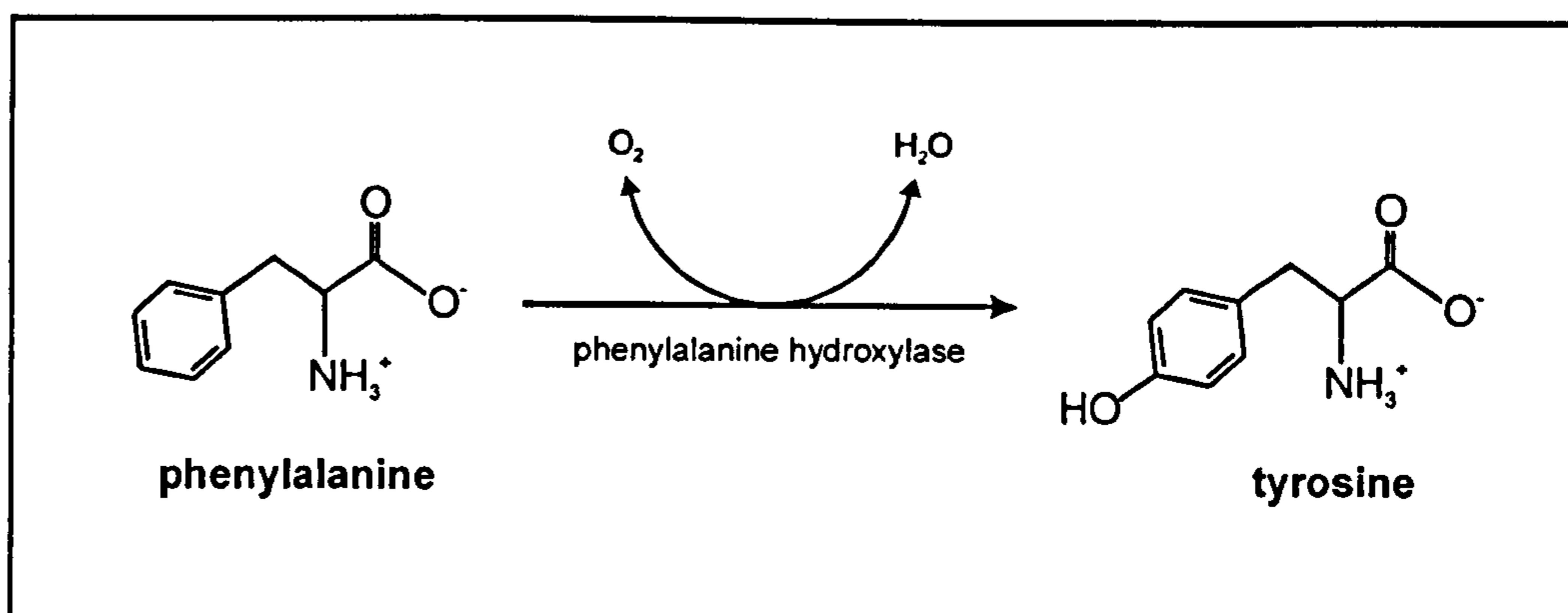


Figure 1.12. Biosynthesis of tyrosine. Tyrosine is formed by the hydroxylation of the essential amino acid phenylalanine by phenylalanine hydroxylase.

There are three remaining non-essential amino acids found in collagen whose biosynthesis has not yet been described in this thesis; these are 3- and 4-hydroxyproline and hydroxylysine (see Figure 1.13 for structures). These three amino acids are not necessary for protein synthesis but are formed during post-translational processing of collagen. An unusual feature of these amino acids is that they cannot be incorporated into proteins from the diet; however, proline is the precursor to 3- and 4-hydroxyproline and lysine is the precursor to hydroxylysine. The hydroxylation is catalysed by prolyl hydroxylase or by lysyl hydroxylase and these enzymes also require molecular O_2 , ascorbate, Fe^{2+} and α -ketoglutarate (Figure 1.14). For every mole of proline or lysine hydroxylated, 1 mole of α -ketoglutarate is decarboxylated to succinate and during this process, one atom of molecular O_2 is incorporated into proline and one into succinate.

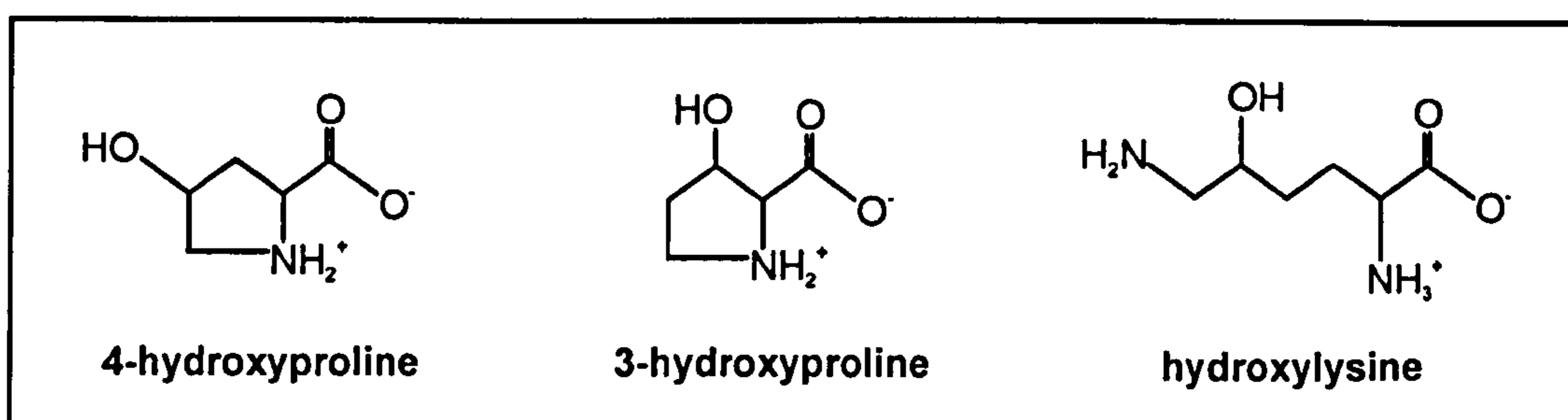


Figure 1.13. Chemical structures of the non-essential amino acids, 3- and 4-hydroxyproline and hydroxylysine.

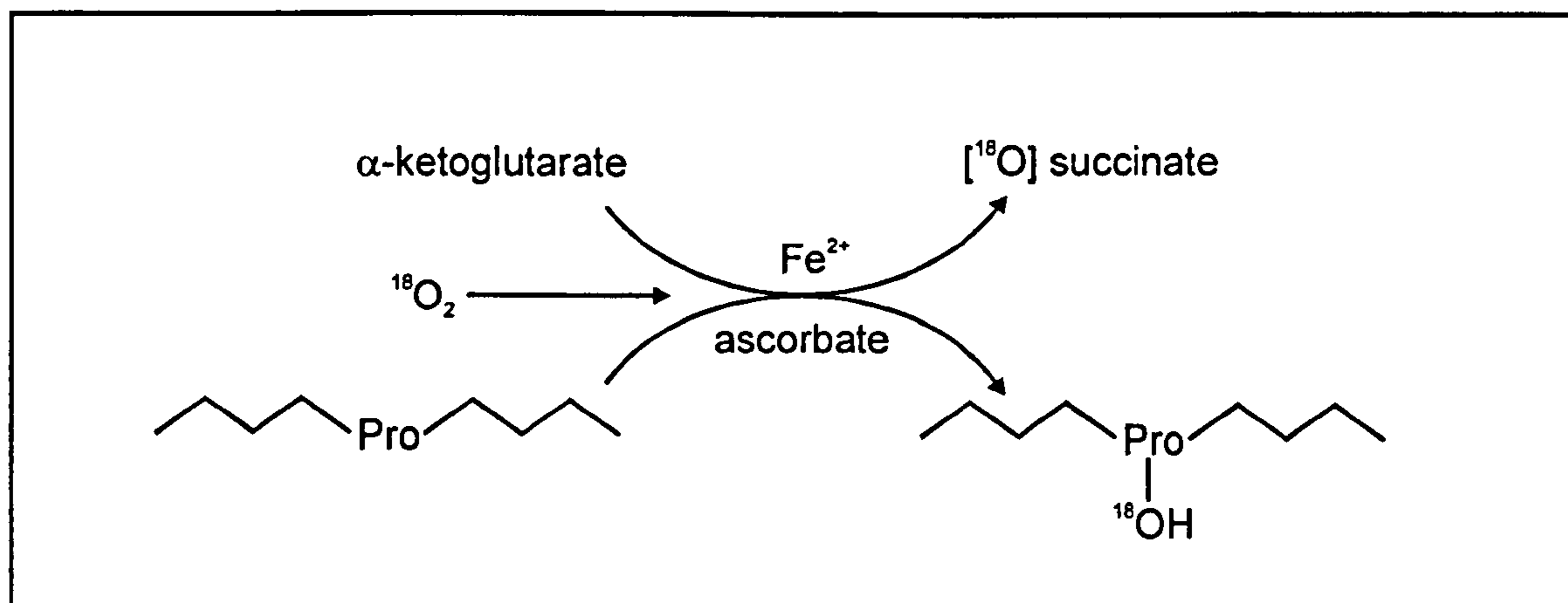


Figure 1.14. Prolyl hydroxylase reaction that converts proline to 3- and 4-hydroxyproline and lysine to hydroxylysine.

1.10 Aims and Objectives

1.10.1 Aims

The main aim of this thesis is to investigate the routing and synthesis of amino acids from the diet into bone collagen using $\delta^{13}\text{C}$ analysis; and from these results, discover how the carbon isotopic analysis of individual amino acids could be used in addition to the $\delta^{13}\text{C}$ values of other bone components (cholesterol, collagen, apatite, fatty acids) in the field of palaeodietary reconstruction.

Authentic amino acids will be used in the method development of compound-specific stable isotope analysis of amino acids to assess and correct for any isotope effects that may be incurred during the hydrolysis and derivatisation procedures involved in obtaining $\delta^{13}\text{C}$ values. Authentic amino acids will also be used to investigate the errors associated with $\delta^{13}\text{C}$ values.

The amino acids from bone collagen of rats from a controlled feeding experiment (Ambrose and Norr, 1993) will be used to study the synthesis and routing of dietary amino acids. The results will be used to identify the dietary macronutrients used in the synthesis of bone collagen, with the aim of providing new insights into the factors that influence the $\delta^{13}\text{C}$ values of bone and interpreting bulk $\delta^{13}\text{C}$ values in palaeodietary reconstruction. In conjunction with previously obtained $\delta^{13}\text{C}$ values (bone collagen, apatite and cholesterol) for the animals from the controlled feeding experiment, individual amino acids in bone collagen will be used to construct a quantitative model that will compliment previous methods of predicting whole diet, protein and energy $\delta^{13}\text{C}$ values (Jim, 2000).

This model will then be applied archaeologically to assess the applicability of compound-specific amino acid $\delta^{13}\text{C}$ analyses to palaeodietary reconstruction and identify additional information that may be gained from the $\delta^{13}\text{C}$ values of collagenous amino acids.

1.10.2 Objectives

The specific objectives of the research described in this thesis are to:

- i) measure the $\delta^{13}\text{C}$ values of authentic amino acids to assess the effects of the hydrolysis and derivatisation procedures and to undertake a rigorous investigation of the precision of the carbon isotopic analysis of individual amino acids.
- ii) measure the $\delta^{13}\text{C}$ values of amino acids in bone collagen of rats from a controlled feeding experiment ($n = 24$) and in the diets themselves, thereby tracing the routing and synthesis of individual amino acids from dietary macronutrients into bone collagen. Also, to assess the rate of incorporation of dietary signals into bone collagen amino acids.
- iii) construct a quantitative model to predict dietary $\delta^{13}\text{C}$ values from $\delta^{13}\text{C}$ values of individual amino acids in addition to the $\delta^{13}\text{C}$ values of bone cholesterol, collagen and apatite, and then to test the model on $\delta^{13}\text{C}$ values

of diets and bone components from a controlled feeding experiment (unpublished data).

- iv) measure the $\delta^{13}\text{C}$ values of bulk collagen and apatite and individual amino acids from archaeological bone ($n = 27$), apply information gained on the routing and synthesis of amino acids in bone collagen and the quantitative model to these samples, and assess the palaeodietary information that can be obtained from the $\delta^{13}\text{C}$ values of individual amino acids and the applicability of the model to archaeological samples. Also to compare palaeodietary information gained from $\delta^{13}\text{C}$ values of individual amino acids to that obtained from other bone components (collagen, apatite and fatty acids), thereby developing a multi-proxy approach to palaeodietary reconstruction.

CHAPTER 2

MATERIALS AND METHODS

Chapter 2 Materials and Methods

2.1 Chemicals and standards

All solvents used were of HPLC grade and purchased from Rathburn chemicals. All authentic amino acids and derivatising reagents were purchased from Sigma-Aldrich Co. Ltd (Poole, Dorset, UK). Bleach and acetic acid for apatite preparation were purchased from BDH Laboratory Supplies (Merck Ltd, Poole, Dorset, UK).

2.2 Sample Information

Tables 4.1 and 4.2 list all the modern samples from the rat feeding experiment (diets and bones). These samples were received after they had been powdered and lipid extracted and were stored at room temperature until required for analysis. Table 6.1 lists the archaeological samples from Qasr Ibrim, these were received in powdered form after lipid extraction, as described below, and stored at room temperature.

2.3 Preparation of modern samples

Sample preparation was undertaken by Dr S. Jim in our laboratory for an earlier study of bone cholesterol. The rat forelimbs were manually cleaned of adhering flesh, cartilage and tendons with a scalpel. Rat bone and diet pellets were then ground to a powder in a pestle and mortar with liquid nitrogen to aid the crushing process. The powdered samples were then lipid extracted as described in Section 2.5.

2.4 Preparation of archaeological samples

Some of the archaeological bones were prepared in our laboratory by Dr M. Copley as part of an earlier study of fatty acids in the bones. The surfaces of the archaeological bones were cleaned using a modelling drill to remove any adhering

soil or exogenous lipids introduced during handling. After cleaning, the bones were crushed to a powder in a pestle and mortar with the aid of liquid nitrogen. The powdered samples were then lipid extracted as described in Section 2.5.

2.5 Solvent extraction of samples

Lipids were extracted from the powdered samples in large screw-capped vials with chloroform/methanol (2:1 v/v, 10 mL) by ultrasonication (3 x 30 min, Decon F5200b). The powdered sample was then left open to the air to dry and then stored at room temperature until required for analysis.

2.6 Collagen extraction

To obtain collagen from the archaeological samples, ca. 200 mg of powdered bone samples were demineralised in Pyrex tubes with Teflon-lined caps with 0.5 M HCl (10 mL) for 24 h at room temperature. The samples were agitated ca. 3 times during this period. They were then rinsed twice with 10 mL of double distilled water, centrifuging between washes to minimise sample loss. The residues were gelatinised in 10 mL of 0.001 M HCl at 75 °C for 48 h. The samples were then filtered through 8 µm polyethylene 'Ezee' filters, into centrifuge tubes and freeze dried (ca. 24 h). The dried collagens were then stored at room temperature until required for analysis.

2.7 Hydrolysis of rat bone and diets and archaeological collagen

To obtain individual amino acids, ca. 200 mg of lipid extracted rat bone and diet and archaeological collagen were placed in a Young's tube with 6 M HCl (500:1 v:w). The samples were evacuated and heated for 24 h at 100 °C. After heating, the tubes were allowed to cool and the samples were transferred to screw-capped vials with 2 x 0.5 mL double distilled H₂O and 2 x 0.5 mL MeOH to ensure quantitative recovery from the Young's tube. The solution was blown to dryness

under nitrogen and redissolved in 2 mL MeOH and stored at $-20\text{ }^{\circ}\text{C}$ until required for analysis.

2.8 Apatite extraction

Approximately 2 g of lipid extracted powdered bone was placed in conical flasks and 4% bleach was added (0.04 mL mg^{-1} of bone). The flasks were placed on a shaker bed at 140 rpm at room temperature for 3 days. The samples were then washed five times with double distilled water. After washing, 1 M acetic acid (0.04 mL mg^{-1} sample) was added to the samples and the flasks were returned to the shaker bed (140 rpm, room temperature, 24 h). The samples were then transferred to centrifuge tubes and washed five times with double distilled water, centrifuging between washes to minimise sample loss. After washing, the samples were frozen, freeze dried and stored at room temperature until required for analysis.

2.9 Derivatisation of amino acids

For the modern and archaeological samples, 0.5 ml aliquots of the hydrolysates obtained from the hydrolysis of lipid extracted modern bones and diet and archaeological collagen (Section 2.7) were placed in Pyrex tubes and blown to dryness. For the authentic amino acids used to obtain correction factors, a $40\text{ }\mu\text{l}$ aliquot of the mixture (0.2 mg mL^{-1} in 0.1 M HCl) was removed, placed in a Pyrex tube and blown to dryness. Forty microlitres of γ -amino-*n*-butyric acid (0.2 mg mL^{-1} in 0.1 M HCl) was added to all samples as an internal standard. Acidified iso-propanol (0.5 ml, 2.8 M with acetyl chloride) was added to the Pyrex tubes, sealed with Teflon-lined caps and heated to $100\text{ }^{\circ}\text{C}$ for 1 h. The reaction was quenched by placing the tubes in a freezer. The residual iso-propanol was removed under a gentle stream of nitrogen at $40\text{ }^{\circ}\text{C}$. Dichloromethane (DCM, $2 \times 0.25\text{ ml}$) was then added and evaporated at room temperature to remove excess iso-propanol and water. Trifluoroacetic acid (TFAA, 0.5 ml) and DCM were added to the Pyrex tubes, sealed with Teflon-lined caps and heated for 10 min at $100\text{ }^{\circ}\text{C}$. The tubes were then placed in an ice bath where the excess TFAA and DCM were removed

under a gentle stream of nitrogen. The derivatised amino acids were then dissolved in an appropriate volume of DCM before analysis by gas chromatography (GC), gas chromatography/mass spectrometry (GC/MS) and gas chromatography/combustion/isotope ratio mass spectrometry (GC/C/IRMS).

2.10 Gas chromatography analyses (GC)

GC analyses were performed using a Hewlett-Packard 5890 series II gas chromatograph using He carrier gas. Derivatised amino acids were analysed on a fused silica capillary column (60 m x 0.32 mm x 0.25 μ m) coated with a 5% phenyl 95% methyl polysiloxane stationary phase. The temperature was programmed from 40 °C (1 min) to 70 °C at 10 °C min⁻¹ then to 170 °C at 3 °C min⁻¹ and then to 250 °C at 15 °C min⁻¹ with an isothermal of 10 min. Flame ionisation detection (FID) was used to monitor the column effluent and data were acquired and analysed using HP Chemstation software.

2.11 Gas chromatography/mass spectrometry analyses (GC/MS)

Compound identification was by GC/MS using a Carlo Erba 5160 gas chromatograph coupled, via a heated transfer line, to a Finnigan MAT 4500 quadrupole mass spectrometer (electron voltage 70 eV, electron current 0.35 mA, electron multiplier 2 kV, source temperature 280 °C). The GC was fitted with the same column as was used for GC analyses and the same temperature programme and carrier gas was employed. Compounds were identified by the use of authentic amino acids and literature mass spectra (Leimer *et al.*, 1977). Mass spectra of trifluoroacetyl isopropyl ester derivatives of all amino acids studied in this thesis are presented in Appendix 1.

2.12 Stable carbon isotope analyses (IRMS and GC/C/IRMS)

GC/C/IRMS analyses were performed using a Hewlett-Packard 6890 GC coupled to a Finnigan MAT DELTA^{plus} XL isotope ratio mass spectrometer (electron

ionisation 100 eV, three Faraday cup collectors m/z 44, 45 and 46) via a Finnigan MAT GC III combustion interface (CuO/ NiO/ Pt combustion reactor set to 940 °C, Cu reduction reactor set to 600 °C). The GC was fitted with the same column as was used for GC analyses and the same temperature programme was employed.

Samples were calibrated against reference CO₂ of known carbon isotopic composition which was introduced directly into the source three times at the beginning and end of every run. All $\delta^{13}\text{C}$ values are reported relative to the PeeDee Belemnite international isotope standard. Each sample was run in triplicate to obtain reliable mean $\delta^{13}\text{C}$ values. Data were collected and processed using Finnigan MAT Isobase software.

Three pre-derivatised trifluoroacetyl methyl ester amino acids (alanine, phenylalanine and lysine) of known $\delta^{13}\text{C}$ values were employed as secondary standards. They were co-injected with every sample in order to monitor instrument performance.

A mixture of authentic amino acids of known $\delta^{13}\text{C}$ values were derivatised using the same derivatising reagents as was used for all samples. The $\delta^{13}\text{C}$ values of these derivatised amino acid standards were obtained via GC/C/IRMS to allow the calculation of correction factors required to establish the contribution of derivative carbon and a kinetic isotope effect. The standard mixture was run at regular intervals, typically every 15 runs.

On-line bulk carbon isotope analyses were performed using a Carlo Erba NC2500 elemental analyser coupled to the same Finnigan MAT DELTA^{plus} XL.

2.13 Quantification of amino acids

All quantifications of amino acids were performed on GC traces. Due to the structural difference between the amino acids their FID response factors vary i.e. equivalent amounts of internal standard and amino acids will not provide the same GC peak area. To overcome this, a mixture of the authentic amino acids of known

concentration, including the internal standard, γ -amino-*n*-butyric acid, was analysed by GC. From this FID correction factors were determined for each amino acid relative to the internal standard and were calculated as follows:

$$(\text{area of aa} / \text{area of IS}) * \text{concentration of IS} = \text{apparent concentration of aa}$$

Equation 2.1

where aa = amino acid; IS = internal standard and area = GC peak area

$$\text{actual concentration of aa} / \text{apparent concentration of aa} = \text{FID correction factor}$$

Equation 2.2

These correction factors were tested for their accuracy over a range of different concentrations ($0.04 \mu\text{g } \mu\text{l}^{-1}$ to $0.2 \mu\text{g } \mu\text{l}^{-1}$), and it was found that the derivatisation process did not produce evaporative effects. The FID correction factors are presented in Table 2.1.

Table 2.1. FID correction factors for quantifying amino acids by GC. Standards deviations from correction factors measured at nine different concentrations.

Amino acid	FID correction factor
Ala	1.86 \pm 0.1
Gly	1.95 \pm 0.1
Thr	2.06 \pm 0.2
Ser	1.81 \pm 0.1
Val	2.21 \pm 0.2
Leu	1.35 \pm 0.1
Ile	2.73 \pm 0.2
Pro	1.41 \pm 0.1
Hyp	1.52 \pm 0.1
Asp	1.45 \pm 0.1
Glu	1.45 \pm 0.1
Phe	1.19 \pm 0.1

CHAPTER 3

METHOD DEVELOPMENT OF COMPOUND-SPECIFIC ISOTOPE ANALYSIS OF AMINO ACIDS

Chapter 3 Method development of compound-specific isotope analysis of amino acids

3.1 Objectives

The compound-specific stable isotope analysis of individual amino acids requires the hydrolysis of proteins to their constituent amino acids and then the derivatisation of these individual amino acids to a form suitable for gas chromatographic analysis. This chapter presents results describing the effects of these procedures on the isotopic composition of authentic amino acids. The hydrolysis of proteins to their individual amino acids introduces the possibility of isotopic fractionation due to incomplete hydrolysis of the protein, whilst the derivatisation requires that consideration be given to the correction of the $\delta^{13}\text{C}$ values due to carbon added during derivatisation, and the identification and correction for any kinetic isotope effects associated with the derivatisation reactions. Due to the aforementioned points it is also necessary to undertake a rigorous treatment of the precision of the analysis in order to obtain meaningful $\delta^{13}\text{C}$ values for individual amino acids.

Authentic amino acids were used to obtain the correction factors required to account for a kinetic isotope effect associated with the derivatisation procedure. The authentic amino acids are also used to assess the magnitude of the errors associated with the carbon isotope analysis of individual amino acids. The requirement for specific configurations for the GC/C/IRMS instrument for these analyses is discussed and the need for pre-derivatised authentic amino acids is shown in order to monitor instrument performance.

Authentic poly amino acids are used to investigate any isotope effects that may be associated with the hydrolysis of proteins to amino acids. Single and mixed poly amino acids are both utilised in order to investigate the effects of varying lengths of hydrolysis times and the effect on the isotopic composition of individual amino acids.

Some of the results presented here have been reported in Docherty *et al.* (2001).

3.2 Introduction

Abelson and Hoering (1961) published one of the first investigations of the $\delta^{13}\text{C}$ values of individual amino acids. Liquid chromatographic separation was used to isolate micro-molar quantities of each pure amino acid; these were combusted and the resulting CO_2 was purified and analysed to determine the $\delta^{13}\text{C}$ values. This off-line method for determining $\delta^{13}\text{C}$ values of amino acids has been used in many studies (Hare and Estep, 1983; Hare *et al.*, 1991; Macko *et al.*, 1983; Macko *et al.*, 1987; Tuross *et al.*, 1988); however, this technique involves numerous preparative steps and has the potential for isotopic fractionation.

In 1984, Barrie *et al.* reported a new technique called gas chromatography combustion isotope ratio mass spectrometry (GC/C/IRMS). This allowed the separation and measurement of the stable carbon isotope ratios of individual compounds in a sample mixture. After compounds are separated in a GC column, the eluants are combusted and generated water is removed before CO_2 is directly introduced into an IRMS. Further discussion of the development and applications of this instrument can be found in Section 1.6.1. GC/C/IRMS eliminated the preparative steps associated with off-line analyses and allowed rapid determination of the $\delta^{13}\text{C}$ values of individual compounds in complex mixtures. It also allowed analyses of samples with low concentrations, as only nanograms of material were required for determinations that produced precisions of $\pm 0.3\%$. The instruments became commercially available in 1988, and in 1990 Engel *et al.* first reported the use of GC/C/IRMS to determine the $\delta^{13}\text{C}$ values of individual amino acids from the Murchison meteorite. This study would not have been possible using conventional methods due to the low abundances of amino acids in the sample material.

However, amino acids are non-volatile polyfunctional compounds that require derivatisation prior to GC separation and several different approaches have been utilised which are discussed in the following section.

3.3 Measuring the $\delta^{13}\text{C}$ values of amino acids using GC/C/IRMS

3.3.1 Derivatisation of amino acids

Amino acids are non-volatile polyfunctional molecules that require derivatisation to allow separation by gas chromatography. All amino acids have at least two functional groups, i.e. carboxylic acid and amine groups, that require derivatising. Ethyl and methyl chloroformates have been used as derivatives (Husek, 1995; Montigon *et al.*, 2001) but this has the risk of non-quantitative reactions which would lead to a loss of information (Meier-Augenstein, 1999); a formation of sub-products has also been noted in some cases (Pelaez *et al.*, 2000).

Silyl derivatives have found widespread use in the analysis of amino acids by GC/MS using either the trimethylsilyl (TMS) or tertiary butyl dimethylsilyl (*t*-BDMS) derivatives (Fortier *et al.*, 1986; Schwenk *et al.*, 1984), as they are prepared by a simple one-step reaction. These silyl derivatives have also been used for GC/C/IRMS analyses, but there are problems associated with these derivatives. Derivatisation with TMS leads to the formation of several derivatives for one compound, whilst *t*-BDMS derivatives are unstable, lasting only a matter of days when kept in the dark at sub-zero temperatures (Hofmann *et al.*, 1995). Some chemically different amino acids become difficult to separate by GC as derivatisation to *t*-BDMS derivatives makes them chromatographically similar (Meier-Augenstein, 1997). Additionally, derivatisation with TMS or *t*-BDMS adds a large number of additional carbons to the compound of interest; for example, an alanine *t*-BDMS derivative would contain only 3 indigenous carbons out of a total of 15 carbons. This amount of additional carbon leads to imprecision in the $\delta^{13}\text{C}$ determinations. The larger the relative contribution of derivative carbon to the derivatised compound, the greater the imprecision (Rieley, 1994); therefore, in carbon isotope analyses it is necessary to minimise the amount of carbon added during derivatisation. Furthermore, silyl derivatives can quickly contaminate the analytical system: SiO_2 can form in the oxidation reactor and coat the active components, preventing complete combustion of the sample (Montigon *et al.*, 2001).

The combined esterification and acetylation of amino acids has emerged as the derivatisation method of choice in $\delta^{13}\text{C}$ analyses. This procedure has been used since the 1970s in gas chromatographic analyses of individual amino acids (Adams, 1974; Moss and Lambert, 1971) and has now been used extensively in GC/C/IRMS analyses (Demmelmair and Schmidt, 1993; Fantle *et al.*, 1999; Johnson *et al.*, 1993; Metges and Daenzer, 2000; Metges *et al.*, 1996; Silfer *et al.*, 1991; Silfer *et al.*, 1994; Simpson *et al.*, 1997). The derivatisation comprises the esterification of the carboxyl group with an acidified alcohol and the acetylation of the amine group with an anhydride and leads to stable derivatives from a simple two-step procedure that can be carried out in a screw-capped vial. Table 3.1 presents the three different combinations of derivative groups that have been used in the esterification and acetylation of amino acids, and Figure 3.1 presents the structure of the amino acid alanine as these three different derivatives.

Table 3.1. Different combinations of esterification and acetylation groups used in the derivatisation of amino acids.

Esterification derivative	Acetylation derivative	Reference
isopropyl	acetyl	Demmelmair and Schmidt 1993 Metges <i>et al.</i> 1996 Metges and Daenzer 2000
isopropyl	pivaloyl	Simpson <i>et al.</i> 1997 Metges and Daenzer 2000
isopropyl	trifluoroacetyl	Silfer <i>et al.</i> 1991 Johnson <i>et al.</i> 1993 Fantle <i>et al.</i> 1999

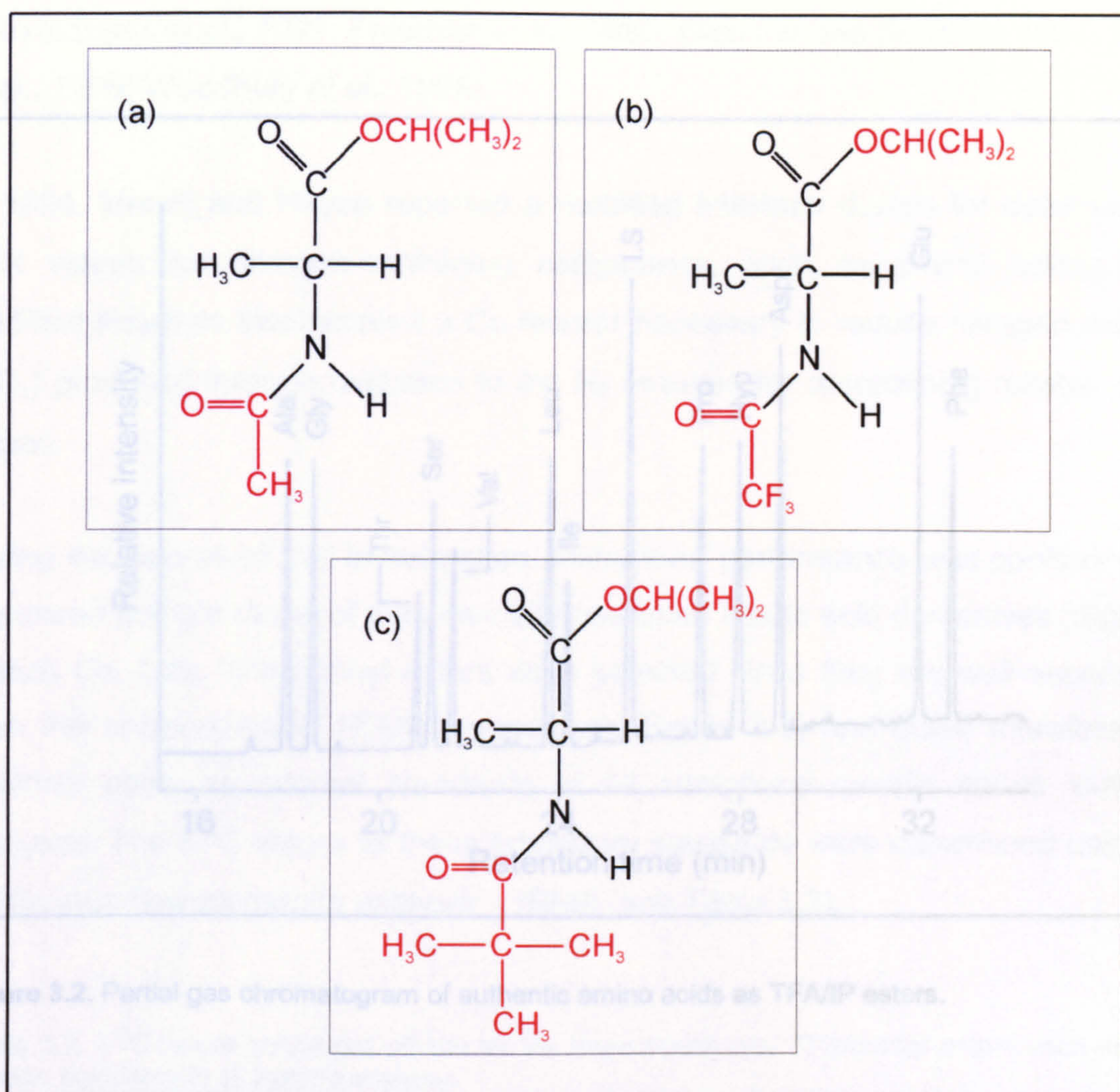


Figure 3.1. Alanine derivatised to (a) an acetyl isopropyl ester, (b) a trifluoroacetyl isopropyl ester and (c) a pivaloyl isopropyl ester. Derivative groups are indicated in red.

From Figure 3.1 it can be seen that the pivaloyl isopropyl ester (c) has the most additional derivative carbon and is, therefore, the least suitable for compound-specific carbon isotope analyses as discussed above. The acetyl isopropyl ester (Figure 3.1(a)) has the least amount of additional derivative carbon; however, Metges *et al.* (1996) found that gas chromatographic baseline separation was not achieved for threonine and serine, aspartic acid and methionine, and lysine and histidine. Therefore, since baseline separation is essential when obtaining compound-specific carbon isotope values, it was decided that the amino acids investigated in this work would be derivatised to trifluoroacetyl isopropyl (TFA/IP) esters. Figure 3.2 presents a partial gas chromatogram of twelve authentic amino

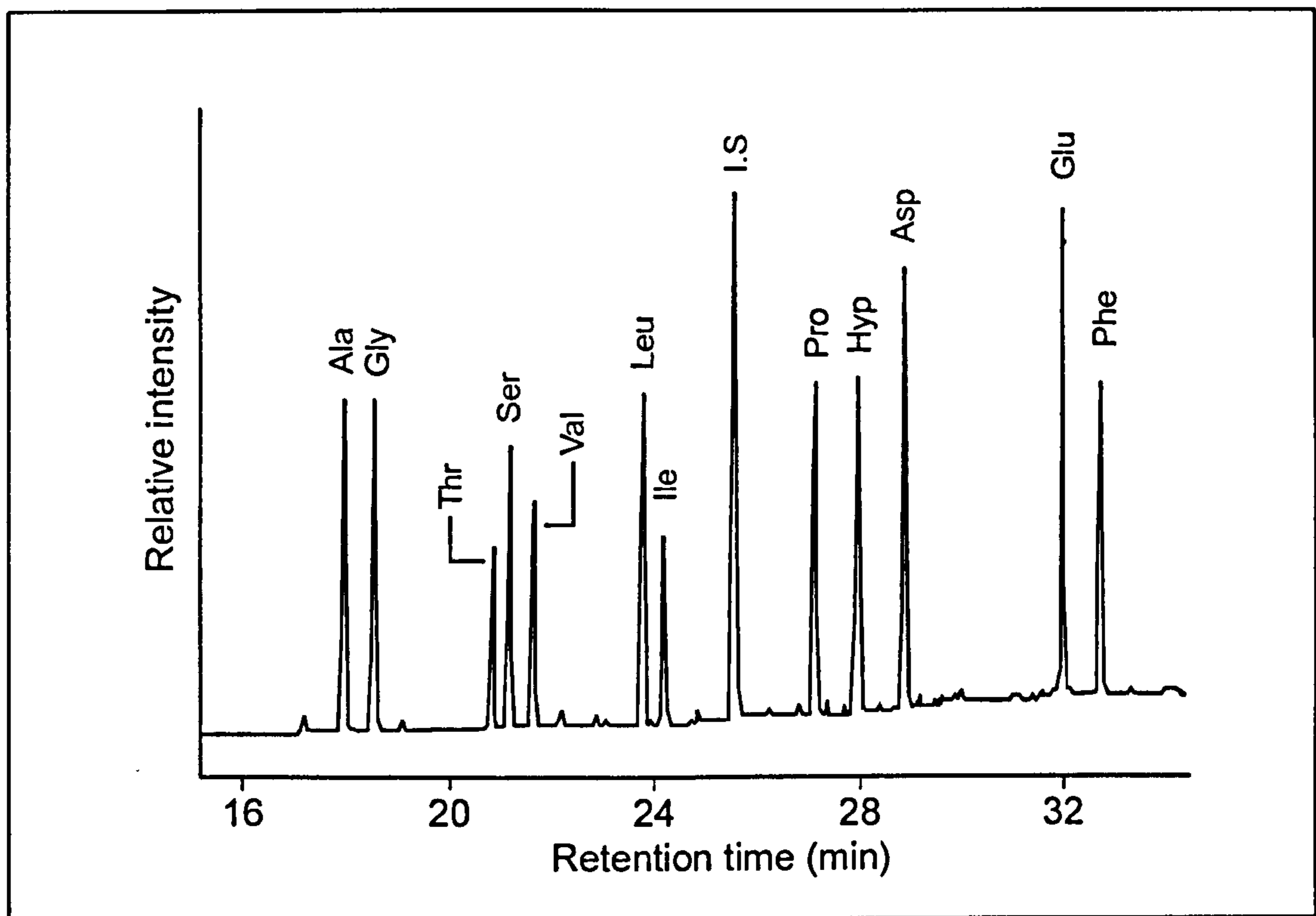


Figure 3.2. Partial gas chromatogram of authentic amino acids as TFA/IP esters.

acids derivatised to TFA/IP esters. It can be seen that the chromatography achieved was excellent.

3.3.2 Obtaining carbon isotope data

The $\delta^{13}\text{C}$ values of derivatised amino acids are readily determined using gas chromatography combined with isotope ratio mass spectrometry (IRMS), via the interface configuration described in Section 1.6.1. GC/C/IRMS analyses of alkanes and oxygenated organic compounds require only a single stage combustion reactor and water removal system (Nafion tubing) to provide a pure CO_2 pulse into the ion source of the IRMS (Merritt *et al.*, 1995). Reliable $\delta^{13}\text{C}$ values have been obtained for a wide range of compound classes, including alkanes, fatty acids, alcohols, sugars, etc. using this configuration (Copley *et al.*, 2001a; Copley *et al.*,

2001b; Dudd *et al.*, 1999; Freeman *et al.*, 1990; Gleixner and Schmidt, 1997; Stott *et al.*, 1999; Woodbury *et al.*, 1995).

In 1994, Merritt and Hayes reported a modified interface design for determining $\delta^{15}\text{N}$ values for nitrogen-containing compounds, such as amino acids. The modified interface incorporated a Cu reactor necessary to reduce nitrogen oxides (NO_x) produced through oxidation to the N_2 required for determining reliable $\delta^{15}\text{N}$ values.

During the course of this investigation, instrument performance was continuously monitored using a range of commercially produced amino acid derivatives (Sigma-Aldrich Co. Ltd). TFA/methyl esters were selected since they are well separated from the corresponding TFA/IP esters (see Figure 3.3) and could therefore be routinely used as internal standards in all compound-specific stable isotope analyses. The $\delta^{13}\text{C}$ values of these laboratory standards were determined using a continuous-flow elemental analyser – IRMS (see Table 3.2).

Table 3.2. $\delta^{13}\text{C}$ values measured off-line for the three amino acid TFA/methyl esters used as co-injected standards in all isotope analyses.

standard	$\delta^{13}\text{C}$ value (‰)				mean
	run 1	run 2	run 3		
Ala	-30.1	-30.2	-30.2		-30.2
Phe	-30.0	-30.0	-29.9		-30.0
Lys	-26.2	-26.1	-26.1		-26.1

Figure 3.4 shows the variation in the $\delta^{13}\text{C}$ values of the 3 standards during a continuous sequence of over 700 GC/C/IRMS analyses. It can be clearly seen that during the initial runs, where no reduction reactor was used, the measured $\delta^{13}\text{C}$ values vary from the values recorded off-line by up to 5‰. Once the Cu reactor was introduced into the system, the $\delta^{13}\text{C}$ values of the standards became comparable

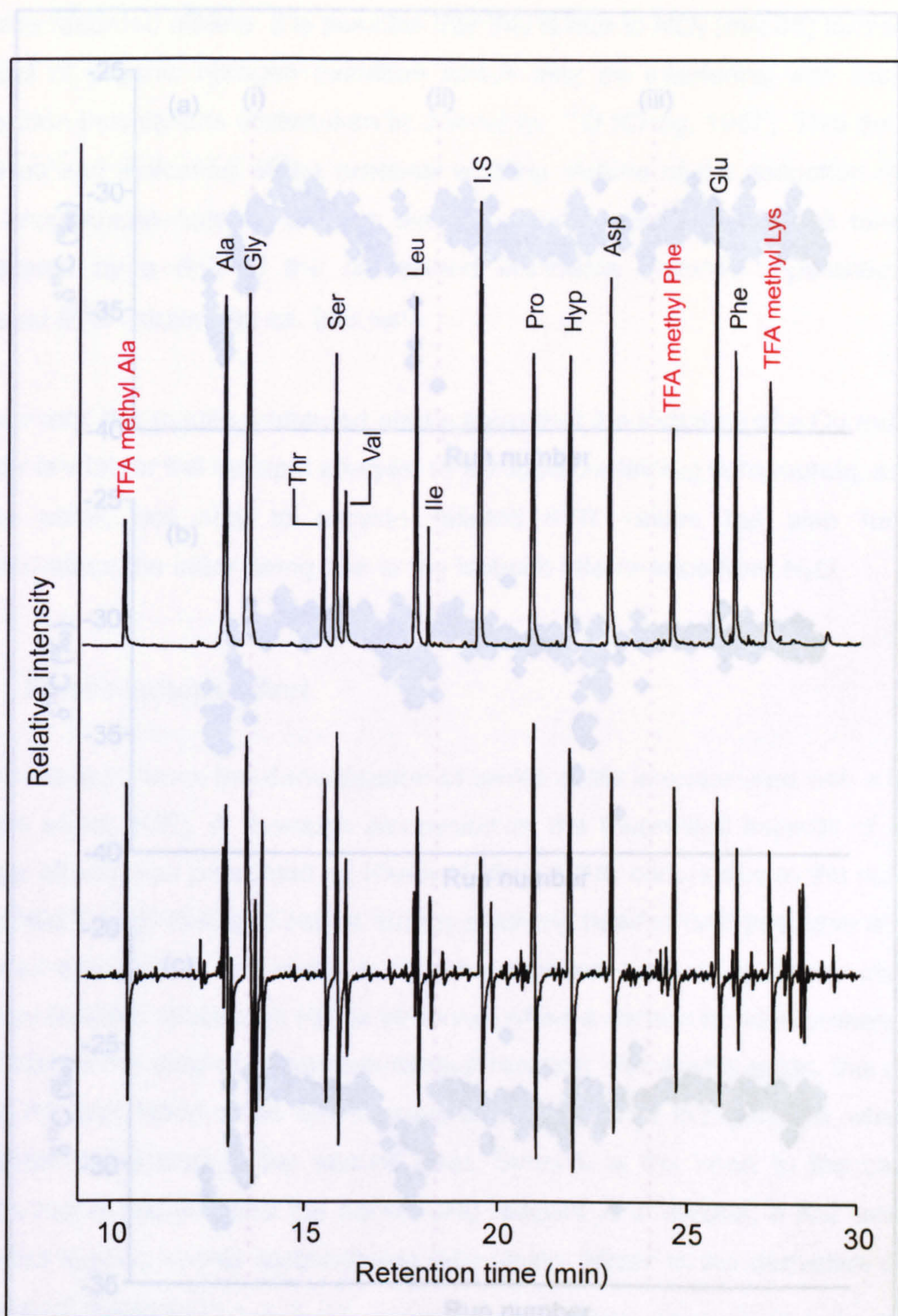


Figure 3.3. Partial GC/C/IRMS profiles of authentic amino acids derivatised to TFA/IP esters. The upper chromatogram represents the m/z 44 ion current, whilst the lower chromatogram represents the instantaneous ratio of the m/z 45/44 ions. The compounds indicated in red are commercially produced amino acid TFA/methyl esters, which were used to monitor the performance of the reduction reactor. The internal standard is γ -amino-*n*-butyric acid.

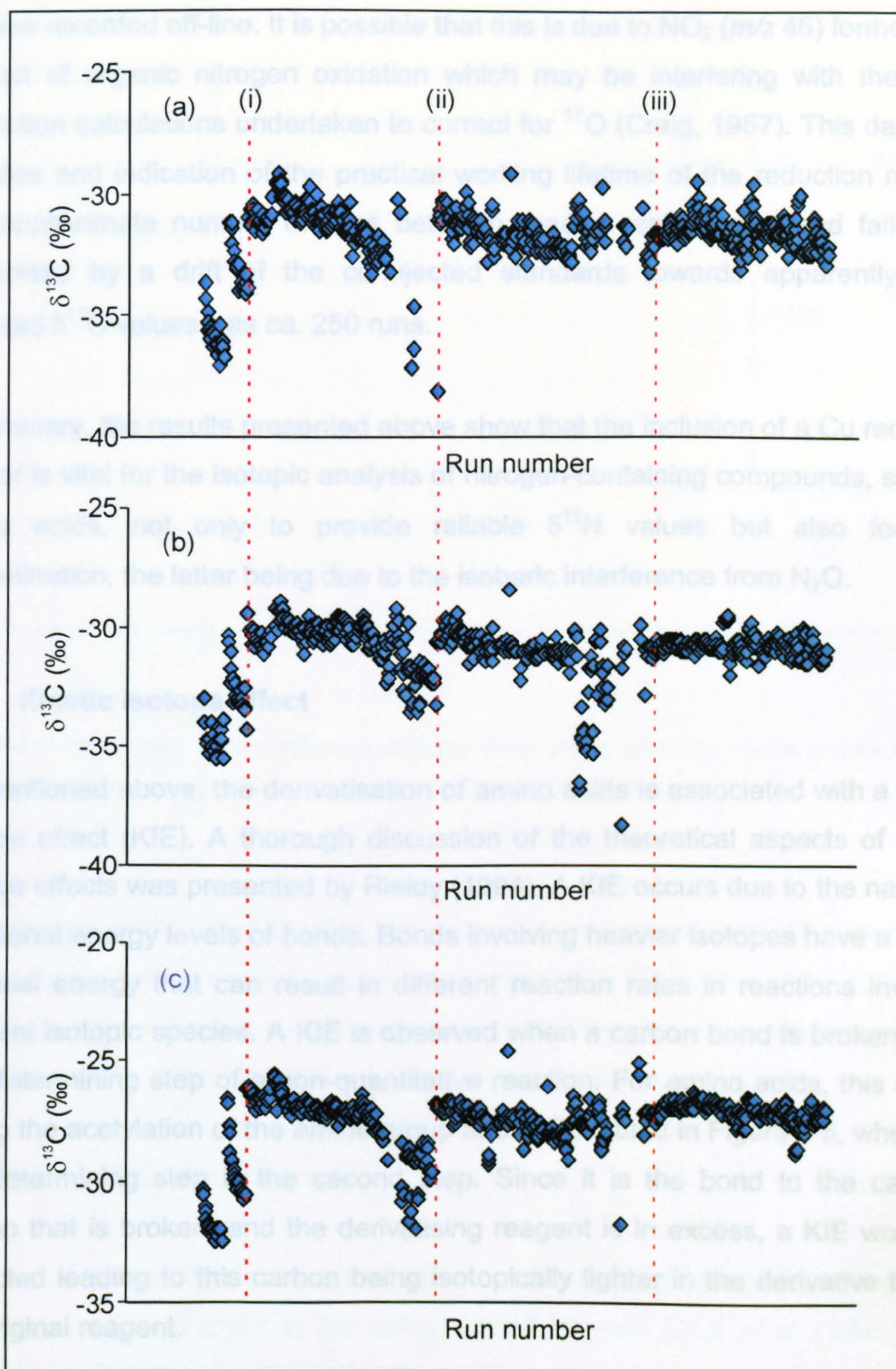


Figure 3.4. Graph showing the effect of reduction reactor performance when determining the $\delta^{13}\text{C}$ values of TFA methyl esters of (a) alanine, (b) phenylalanine and (c) lysine. Dashed red lines indicate where (i) reduction reactor was introduced and (ii) and (iii) where it was replaced.

to those recorded off-line. It is possible that this is due to NO_2 (m/z 46) formed as a product of organic nitrogen oxidation which may be interfering with the Craig Correction calculations undertaken to correct for ^{17}O (Craig, 1957). This data also provides an indication of the practical working lifetime of the reduction reactor. The approximate number of runs between reactor replacement and failure as interpreted by a drift of the co-injected standards towards apparently more depleted $\delta^{13}\text{C}$ values was ca. 250 runs.

In summary, the results presented above show that the inclusion of a Cu reduction reactor is vital for the isotopic analysis of nitrogen-containing compounds, such as amino acids, not only to provide reliable $\delta^{15}\text{N}$ values but also for $\delta^{13}\text{C}$ determination, the latter being due to the isobaric interference from N_2O .

3.4 Kinetic isotope effect

As mentioned above, the derivatisation of amino acids is associated with a kinetic isotope effect (KIE). A thorough discussion of the theoretical aspects of kinetic isotope effects was presented by Rieley (1994). A KIE occurs due to the nature of vibrational energy levels of bonds. Bonds involving heavier isotopes have a higher potential energy that can result in different reaction rates in reactions involving different isotopic species. A KIE is observed when a carbon bond is broken in the rate-determining step of a non-quantitative reaction. For amino acids, this occurs during the acetylation of the amine group and is illustrated in Figure 3.5, where the rate-determining step is the second step. Since it is the bond to the carbonyl carbon that is broken, and the derivatising reagent is in excess, a KIE would be expected leading to this carbon being isotopically lighter in the derivative than in the original reagent.

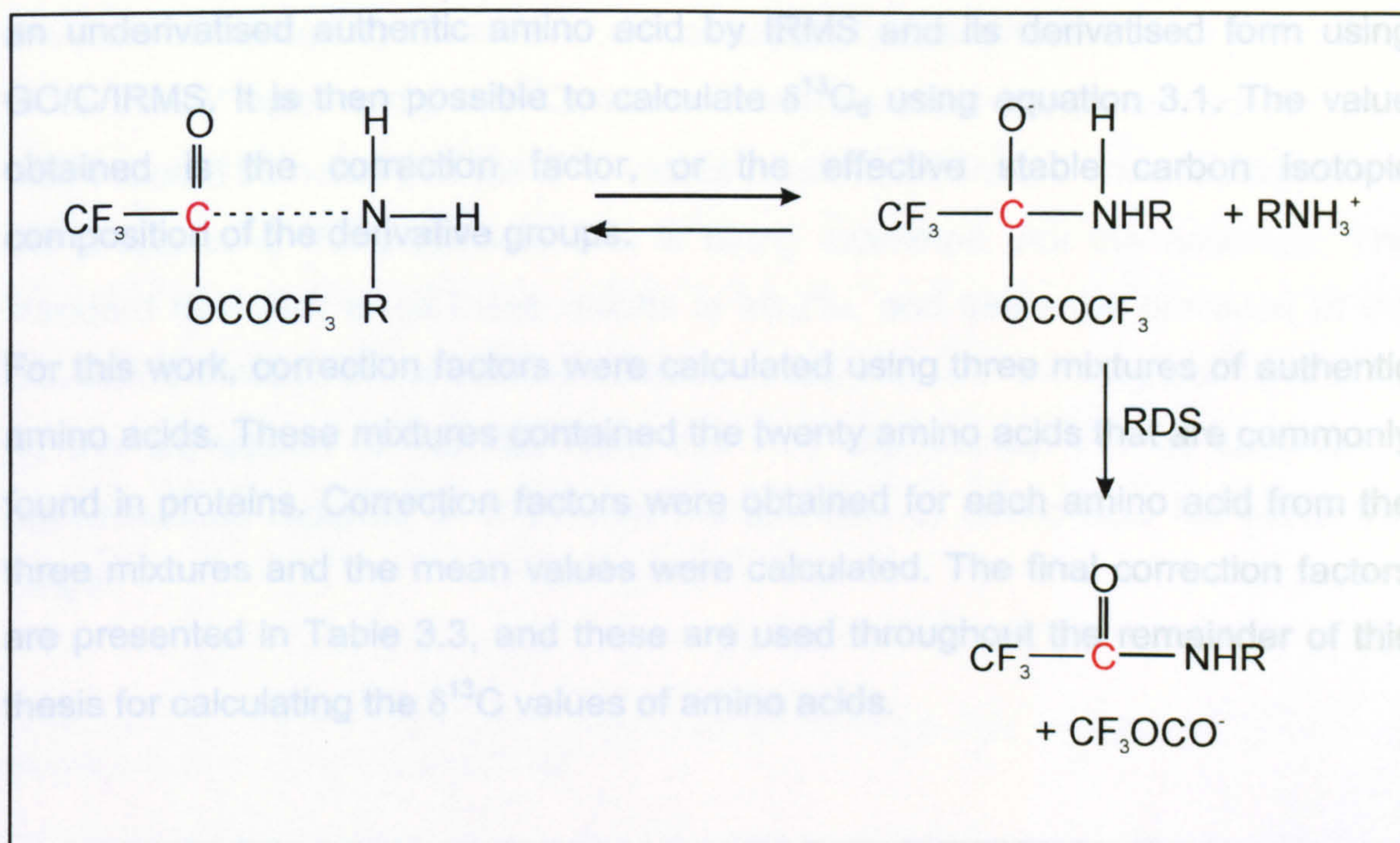


Table 3.3. Correction factors determined in order to calculate the original $\delta^{13}\text{C}$ value of amino acids.

Figure 3.5. Mechanism for the trifluoroacetylation of an amino acid. The kinetic isotope effect is associated with the carbon atom, indicated in red. From Rieley (1994).

This isotopic fractionation precludes the use of simple mass balance equations to correct for the added derivative carbon and obtain the $\delta^{13}\text{C}$ value of the compound of interest. When there is no KIE associated with a derivatisation reaction then the following equation can be used to correct for exogenous carbon:

$$n_{cd}\delta^{13}\text{C}_{cd} = n_c\delta^{13}\text{C}_c + n_d\delta^{13}\text{C}_d \quad \text{Equation 3.1}$$

Where n is the number of moles of carbon, cd is the derivatised compound, d is the derivative group and c is the compound of interest. Silfer *et al.* (1991) found that when correcting for the exogenous carbon from the derivatisation of amino acids, equation 3.1 gave results that did not agree with the values they obtained from IRMS analyses. However, they found that the isotopic fractionation caused by the KIE was reproducible for each amino acid if the same reagents and reaction conditions were used and, therefore, could be accounted for by using correction factors. These correction factors are determined by measuring the $\delta^{13}\text{C}$ value of

an underivatized authentic amino acid by IRMS and its derivatized form using GC/C/IRMS. It is then possible to calculate $\delta^{13}\text{C}_d$ using equation 3.1. The value obtained is the correction factor, or the effective stable carbon isotopic composition of the derivative groups.

For this work, correction factors were calculated using three mixtures of authentic amino acids. These mixtures contained the twenty amino acids that are commonly found in proteins. Correction factors were obtained for each amino acid from the three mixtures and the mean values were calculated. The final correction factors are presented in Table 3.3, and these are used throughout the remainder of this thesis for calculating the $\delta^{13}\text{C}$ values of amino acids.

Table 3.3. Correction factors determined in order to calculate the original $\delta^{13}\text{C}$ value of amino acids.

Amino acid	Correction factor (‰)
Ala	-34.8 ±0.8
Gly	-31.9 ±1.1
Thr	-36.9 ±0.8
Ser	-36.9 ±1.0
Val	-40.7 ±0.6
Leu	-35.1 ±0.6
Ile	-37.1 ±0.6
Pro	-38.7 ±0.6
Hyp	-37.2 ±0.7
Asp	-33.0 ±0.9
Glu	-32.4 ±0.8
Phe	-35.5 ±0.5
Orn	-38.5 ±0.7

The KIE occurs due to the non-quantitative reaction of the trifluoroacetic anhydride with the amino acid; therefore, it is possible that if the amount of analyte being derivatized is varied the expression of the KIE may be affected. In order to assess

this possibility, varying amounts of an authentic alanine standard were derivatised to its TFA/IP ester and the $\delta^{13}\text{C}$ values determined and are presented in Figure 3.6. It should be noted that the $\delta^{13}\text{C}$ values presented here are uncorrected, as it is the precision of the procedure that is being examined, not the accuracy. The standard deviation of all these results is $\pm 0.2\text{‰}$, and since the precision of the GC/C/IRMS instrument is $\pm 0.3\text{‰}$, it can be stated that over the range of 10 to 2000 μg the expression of the KIE does not vary significantly. For all subsequent derivatisations reported in this thesis the amounts of amino acid fall within this range.

Table 3.4. Influence of the correction for added carbon on the standard deviation of $\delta^{13}\text{C}$ values for leucine and serine TFA/IP esters. (n=3).

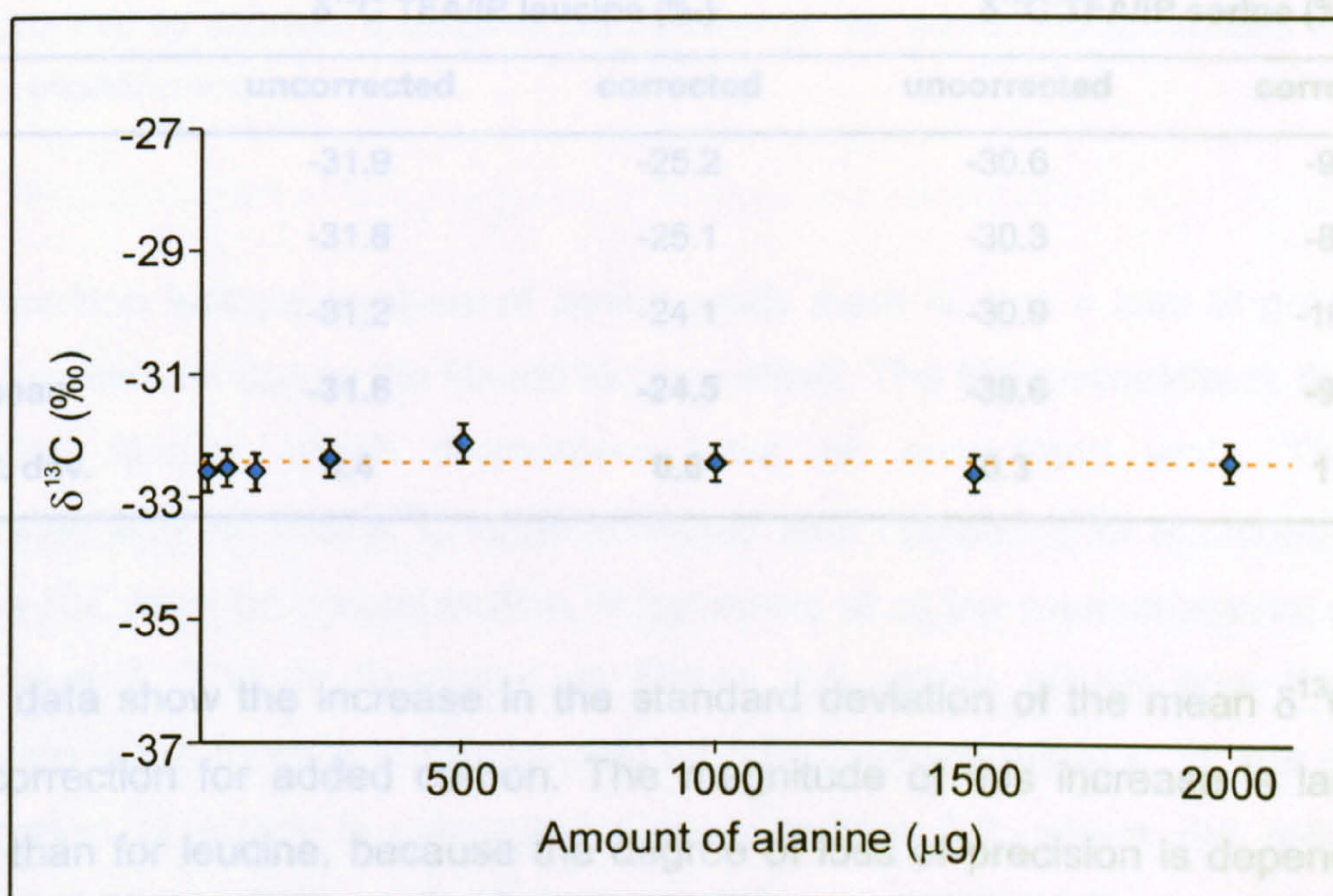


Figure 3.6. Variation in the expression of the KIE during the derivatisation of varying amounts of alanine. $\delta^{13}\text{C}$ values determined by GC/C/IRMS.

3.5 Errors

The assessment of the errors associated with the carbon isotope analysis of amino acids is imperative in order to justify the interpretations of the results within the precision of the analyses. There is a loss in precision associated with the addition of extra carbon to the compound of interest during derivatisation. Since amino acids vary in their carbon number and the number of functional groups that require derivatisation, the precision will be different for each amino acid, as illustrated by the $\delta^{13}\text{C}$ values presented in Table 3.4.

Table 3.4. Influence of the correction for added carbon on the standard deviation of $\delta^{13}\text{C}$ values for leucine and serine TFA/IP esters, (n=3).

	$\delta^{13}\text{C}$ TFA/IP leucine (‰)		$\delta^{13}\text{C}$ TFA/IP serine (‰)	
	uncorrected	corrected	uncorrected	corrected
	-31.9	-25.2	-30.6	-9.1
	-31.8	-25.1	-30.3	-8.2
	-31.2	-24.1	-30.9	-10.2
mean	-31.6	-24.5	-30.6	-9.2
std. dev.	0.4	0.6	0.3	1.0

These data show the increase in the standard deviation of the mean $\delta^{13}\text{C}$ value after correction for added carbon. The magnitude of this increase is larger for serine than for leucine, because the degree of loss of precision is dependent on the molar ratio of derivative carbon to sample carbon. This is illustrated in Figure 3.7, where it can be seen that the different structures of serine and leucine lead to different molar ratios of derivative carbon to sample carbon. Leucine contains six carbon atoms and has only two functional groups that require derivatisation, whilst serine contains three carbon atoms and due to an additional hydroxyl group, has three functional groups that require derivatisation.

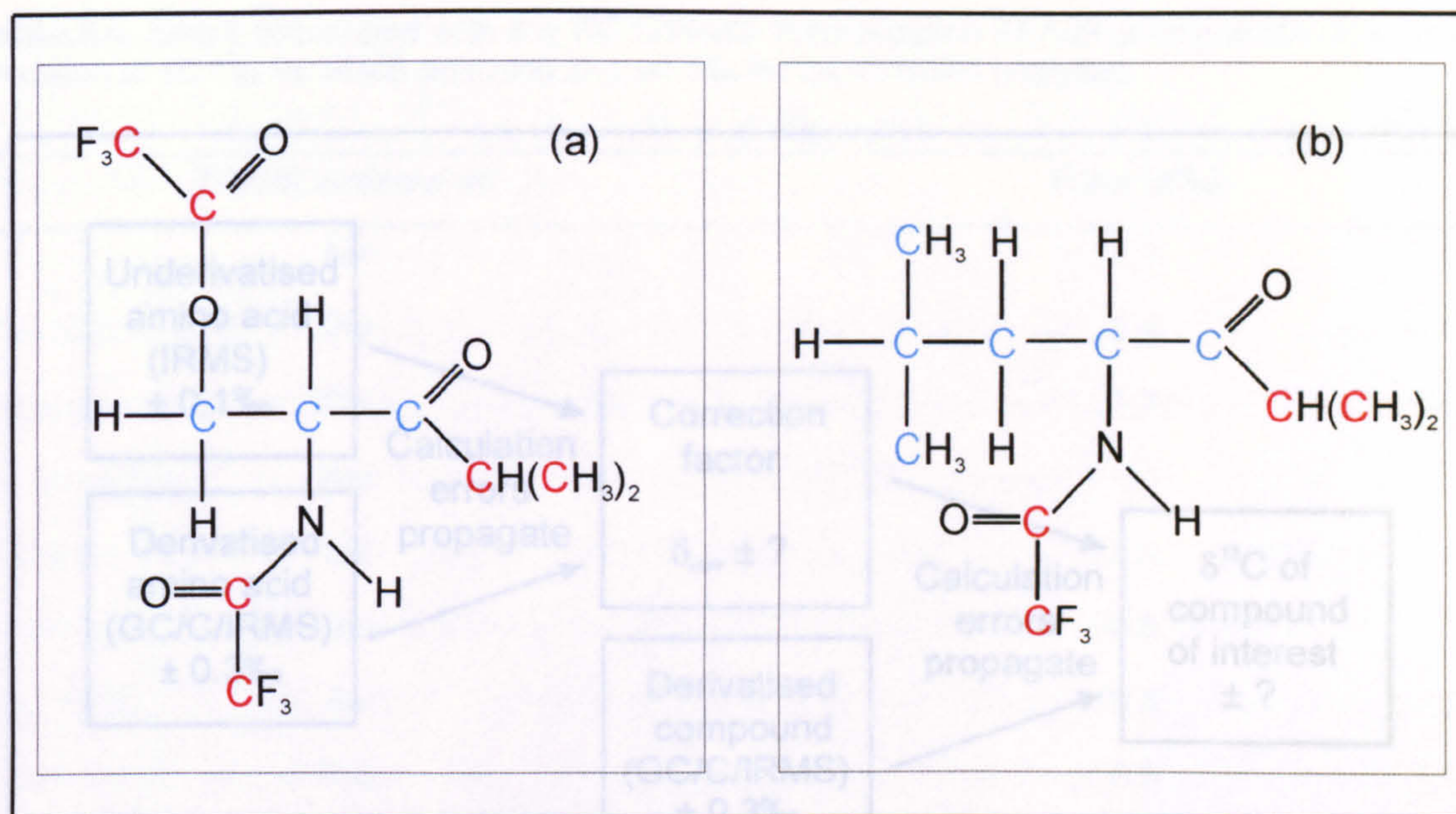


Figure 3.7. Comparison of the structures of TFA/IP esters of (a) serine and (b) leucine. The carbon atoms provided by derivatising reagents are indicated in red, carbon atoms indicated in blue are from the original amino acid.

Figure 3.8. GC/C/IRMS error propagation associated with derivatisation, from Docherty et al. (2001).

In the carbon isotope analysis of amino acids there is also a loss of precision in the measurement due to the kinetic isotope effect. The KIE necessitates the use of correction factors, which themselves have an associated error. The error associated with the final $\delta^{13}\text{C}$ value achieved after correcting for additional carbon and the KIE must be a combination of the errors of all the measurements required to achieve it. This is illustrated in Figure 3.8, which shows how the errors propagate when there is a KIE associated with the derivatisation. In this case the propagation of errors is calculated using equation 3.2, where the subscript s denotes the standard used in correction factor determination and sd is the derivatised standard.

$$\sigma_c^2 = \sigma_s^2 (n_s/n_c)^2 + \sigma_{sd}^2 ((n_s + n_d)/n_c)^2 + \sigma_{cd}^2 ((n_c + n_d)/n_c)^2 \quad \text{Equation 3.2}$$

This equation accounts for the loss of precision, which is dependent on the molar ratio of derivative carbon to sample carbon, as well as the error associated with correction factor determination. Due to the nature of amino acids, as mentioned above, errors must be calculated for each amino acid individually. The errors

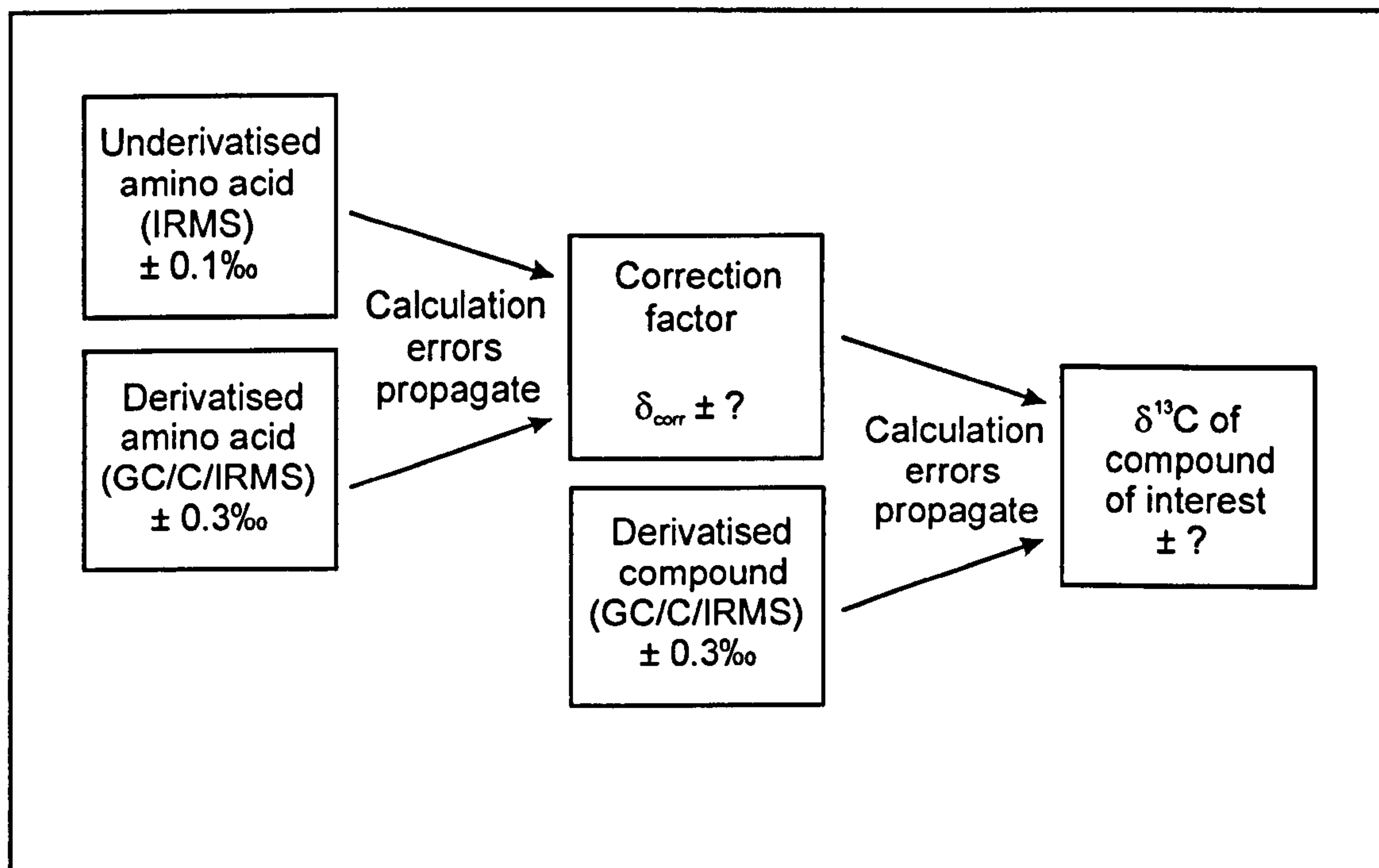


Figure 3.8. GC/C/IRMS error propagation associated with derivatisation, from Docherty *et al.* (2001).

associated with each amino acid, assuming a precision of $\pm 0.1\text{‰}$ for bulk IRMS analyses and $\pm 0.3\text{‰}$ for GC/C/IRMS analyses, are presented in Table 3.5 and it is clear that the errors involved are more than simply the precision of the GC/C/IRMS instrument. These errors are used throughout this thesis when quoting amino acid $\delta^{13}\text{C}$ values, although sometimes standard deviations of $>0.3\text{‰}$ were observed for GC/C/IRMS analyses. In these cases, a new error was calculated using equation 3.2 and the observed standard deviation. If the standard deviation of GC/C/IRMS analyses is $\leq 0.3\text{‰}$ the errors quoted in Table 3.5 are applicable to all GC/C/IRMS analyses of TFA/IP amino acids.

Table 3.5. Errors associated with the GC/C/IRMS determination TFA/IP amino acids, assuming a precision of $\pm 0.1\%$ for IRMS analyses and $\pm 0.3\%$ for GC/C/IRMS analyses.

TFA/IP amino acid	Error ($\pm\%$)
Ala	1.1
Gly	1.5
Thr	1.2
Ser	1.4
Val	0.9
Leu	0.8
Ile	0.8
Pro	0.9
Hyp	1.1
Asp	1.3
Glu	1.1
Phe	0.7
Orn	1.0

3.6 Poly amino acids

As part of the developmental work undertaken to verify the analytical protocol used in this thesis, two different types of poly amino acids were used to investigate any isotope effects that might be associated with the hydrolysis of proteins to amino acids. Poly amino acids are polypeptide chains that have been synthesised to contain known amounts of specific amino acids. The poly amino acids used here were obtained from Sigma-Aldrich Co. Ltd (Poole, Dorset, UK). The first type of poly amino acids studied are termed 'single poly amino acids' (SPAAs), and consist of a polypeptide chain comprising only one repeating amino acid residue. Five different SPAAs were used; these were poly alanine, poly serine, poly glutamic acid, poly phenylalanine and poly ornithine. They were chosen to encompass the molecular weight range and differing structures seen in the twenty amino acids commonly found in proteins. The second type of poly amino acids studied are termed 'mixed poly amino acids' (MPAAs), and their polypeptide

chains comprise two different amino acids. Five MPAAAs were investigated; these were poly glutamic acid/leucine, poly glutamic acid/proline, poly ornithine/serine, poly glutamic acid/serine and poly proline/glycine.

The SPAAs were hydrolysed for varying lengths of time and the $\delta^{13}\text{C}$ values of the released amino acids were determined by GC/C/IRMS as their TFA/IP derivatives, as described in Sections 2.7, 2.9 and 2.12, to assess the effect of different reaction times on the isotopic composition of the products. The MPAAAs were hydrolysed for 24 h as is widely used in the hydrolysis of protein (Hare *et al.*, 1991; Ho, 1967; Simpson *et al.*, 1997) and the $\delta^{13}\text{C}$ values of the component amino acids were determined. The results were used to investigate possible effects of hydrolysis on the isotopic composition of individual amino acids in a polypeptide. The bulk isotopic compositions of all the poly amino acids were measured off-line as described in Section 2.12.

3.6.1 Single poly amino acids (SPAAs)

Approximately 2 mg of each SPAA was hydrolysed for 4, 10, 24 and 48 h. One quarter of the resulting hydrolysate was derivatised and analysed in order to quantify the amount of poly amino acid released after different reaction times. Quantification of the amino acids (Table 3.6) was achieved by gas chromatography, as described in Section 2.13, using calculated FID correction factors, a known amount of internal standard and by then comparing peak areas. As expected, the amount of amino acid recovered increases with increasing hydrolysis time.

There was no detectable hydrolysis of poly phenylalanine after 4 or 10 h and the recovery after 24 and 48 hours was very low. This low recovery must be related to the nature of this synthetic poly amino acid that causes it to be resistant to hydrolysis, as recovery of phenylalanine from both ancient and modern collagen is comparable to the other amino acids (see Chapters 4 and 5). Unlike poly phenylalanine, the amino acid sequence in collagen does not contain sequential

Table 3.6. Expected and measured yields of amino acids recovered after hydrolysis of SPAA. No detectable product was present after 4 h hydrolysis of poly glutamic acid and poly phenylalanine and 10 h hydrolysis of poly phenylalanine, as no detectable hydrolysis of the SPAA had occurred.

hydrolysis time	Amount of hydrolysed amino acid (μg)		
	measured	expected	% recovery
Ala			
4 h	52	500	10.0
10 h	272	470	57.9
24 h	297	490	60.1
48 h	615	650	94.6
Ser			
4 h	72	520	13.8
10 h	190	440	43.2
24 h	201	440	45.7
48 h	356	450	79.1
Glu			
4 h	n.d.	n.d.	n.d.
10 h	137	315	43.5
24 h	152	400	38.0
48 h	214	442	48.4
Phe			
4 h	n.d.	n.d.	n.d.
10 h	n.d.	n.d.	n.d.
24 h	3	250	1.4
48 h	85	1970	4.3
Orn			
4 h	127	268	47.4
10 h	128	268	47.8
24 h	137	283	48.4
48 h	136	217	62.7

Table 3.7. $\delta^{13}\text{C}$ values and associated errors for the single poly amino acids.

	$\delta^{13}\text{C}$ values (‰)				
	bulk	4 hr	10 hr	24 hr	48 hr
Ala	-22.4 ±0.1	-23.8 ±1.1	-22.7 ±1.3	-22.5 ±1.6	-22.2 ±1.1
Ser	-12.6 ±0.1	-15.1 ±1.4	-14.8 ±1.4	-11.3 ±1.4	-12.7 ±1.4
Glu	-14.2 ±0.1	n.d.	-14.3 ±1.3	-14.1 ±1.1	-15.1 ±1.3
Phe	-30.6 ±0.1	n.d.	n.d.	-31.1 ±0.7	-31.5 ±0.8
Orn	-10.8 ±0.1	-13.8 ±1.0	-12.8 ±1.0	-11.5 ±1.0	-11.3 ±1.0

phenylalanine molecules, and hydrolysis of the peptide bond may be inhibited by sequential phenylalanine molecules due to their bulky structure.

The data presented in Table 3.7 and Figure 3.9 show that most of the $\delta^{13}\text{C}$ values obtained for the amino acids from the hydrolysed SPAAs are in agreement with the bulk $\delta^{13}\text{C}$ values of the unhydrolysed SPAAs. Only after either 4 or 10 h hydrolysis times are the isotopic compositions of some of the released amino acids significantly different from the bulk values. Therefore, if a polypeptide is hydrolysed for 24 h the isotopic composition of the individual amino acids has probably been unaffected by the procedure.

3.6.2 Mixed poly amino acids (MPAAs)

Approximately 0.5 mg of each of the five MPAAs were hydrolysed as described in Section 2.7. The resulting hydrolysate was then derivatised and quantified using gas chromatography and the $\delta^{13}\text{C}$ values of the individual amino acids comprising the MPAAs measured by GC/C/IRMS as described in Section 2.12. In order to assess whether the $\delta^{13}\text{C}$ values obtained for the individual amino acids from the MPAA hydrolysates had been fractionated during hydrolysis it was necessary to estimate the bulk $\delta^{13}\text{C}$ values using mass balance. To use mass balance equations it is necessary to know the molar ratios of the individual amino acids

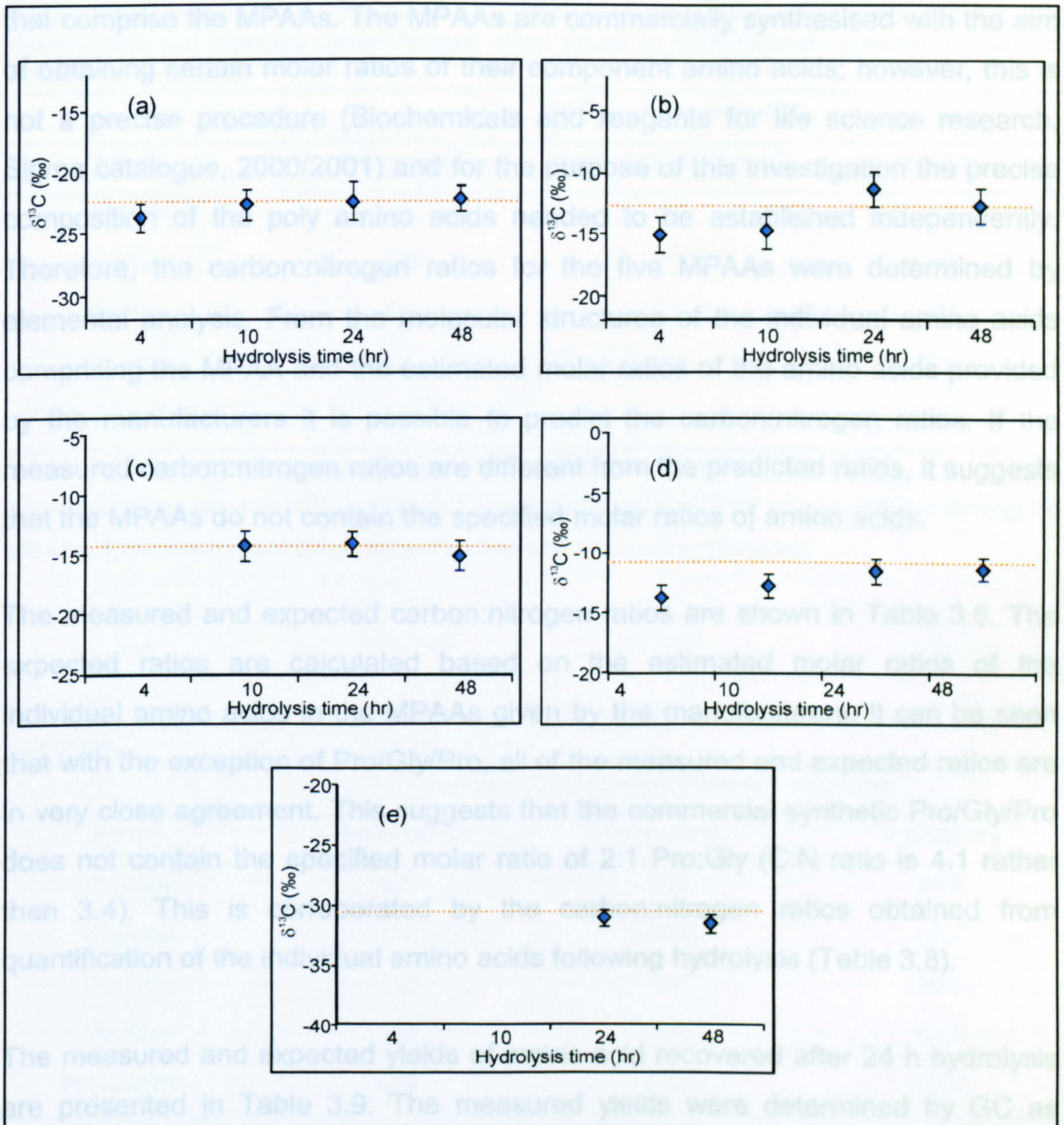


Figure 3.9. Compound-specific $\delta^{13}\text{C}$ values of (a) poly alanine, (b) poly serine, (c) poly glutamic acid, (d) poly ornithine and (e) poly phenylalanine measured after different hydrolysis times. Dotted orange line represents bulk $\delta^{13}\text{C}$ values obtained off-line from unhydrolysed samples.

that comprise the MPAAAs. The MPAAAs are commercially synthesised with the aim of obtaining certain molar ratios of their component amino acids; however, this is not a precise procedure (Biochemicals and reagents for life science research, Sigma catalogue, 2000/2001) and for the purpose of this investigation the precise composition of the poly amino acids needed to be established independently. Therefore, the carbon:nitrogen ratios for the five MPAAAs were determined by elemental analysis. From the molecular structures of the individual amino acids comprising the MPAA and the estimated molar ratios of the amino acids provided by the manufacturers it is possible to predict the carbon:nitrogen ratios. If the measured carbon:nitrogen ratios are different from the predicted ratios, it suggests that the MPAAAs do not contain the specified molar ratios of amino acids.

The measured and expected carbon:nitrogen ratios are shown in Table 3.8. The expected ratios are calculated based on the estimated molar ratios of the individual amino acids in the MPAAAs given by the manufacturers. It can be seen that with the exception of Pro/Gly/Pro, all of the measured and expected ratios are in very close agreement. This suggests that the commercial synthetic Pro/Gly/Pro does not contain the specified molar ratio of 2:1 Pro:Gly (C:N ratio is 4.1 rather than 3.4). This is corroborated by the carbon:nitrogen ratios obtained from quantification of the individual amino acids following hydrolysis (Table 3.8).

The measured and expected yields of amino acid recovered after 24 h hydrolysis are presented in Table 3.9. The measured yields were determined by GC as described in Section 2.13. It can be seen that there is substantial variation in the yields of amino acids.

The $\delta^{13}\text{C}$ values of the individual amino acids obtained from the MPAAAs after hydrolysis are shown in Table 3.10. The estimated bulk values for the poly amino acids were obtained using mass balance equations and the amino acid ratios consistent with the C:N values shown in Table 3.8. The errors associated with the estimated bulk value were obtained by combining the errors for each of the individual amino acids as described previously in Section 3.5. A comparison of the

Table 3.8. Carbon:nitrogen ratios of the MPAAAs determined by elemental analysis and quantification and expected carbon:nitrogen ratios based on manufacturers specified amino acid compositions.

MPAA	carbon: nitrogen ratio		
	measured ^a	from quantification ^b	expected
Glu/Ala	4.1	4.2	4.2
Glu/Leu	5.3	5.1	5.2
Glu/Phe	6.0	5.5	5.8
Orn/Ser	2.3	2.6	2.6
Pro/Gly/Pro	4.1	3.9	3.4

^a actual carbon:nitrogen ratios were determined by elemental analysis of MPAAAs

^b Relative molar ratios estimated from GC quantification of individual amino acids comprising the MPAAAs. From these molar ratios, the carbon:nitrogen ratios were estimated.

Table 3.9. Expected and measured amounts of mixed poly amino acids recovered after 24 h hydrolysis.

MPAA	Amount of hydrolysed amino acid (μg)		
	measured	expected	% recovery
Glu/Ala	493	520	94.8
Glu/Leu	152	348	43.7
Glu/Phe	153	430	35.6
Orn/Ser	190	301	63.1
Pro/Gly/Pro	873	1003	87.0

estimated bulk $\delta^{13}\text{C}$ values and the measured $\delta^{13}\text{C}$ values is presented in Figure 3.10.

For three of the five MPAAAs, estimated and experimentally determined $\delta^{13}\text{C}$ values agree within experimental error. It is unclear why the remaining two are not in such close agreement, although their estimated and measured values are still very similar. Especially significant is the agreement of the two measurements for Pro/Gly/Pro. The $\delta^{13}\text{C}$ values for proline and glycine differ by over 40‰. If there had been any isotopic fractionation or differential recoveries for the two amino

acids during hydrolysis of this MPAA, or the estimated composition had been erroneous then the estimated and measured $\delta^{13}\text{C}$ values would have shown considerable divergence. Thus, these results show that the $\delta^{13}\text{C}$ values of individual amino acids obtained from the hydrolysis of peptides are reliable.

Table 3.10. $\delta^{13}\text{C}$ values of individual amino acids comprising the mixed poly amino acids measured by GC/C/IRMS and the estimated bulk values calculated from these values by mass balance. Actual bulk values were measured by off-line IRMS.

MPAA	individual amino acid	$\delta^{13}\text{C}$ values (‰)	
		estimated bulk	measured bulk
Glu/Ala			
Glu	-33.2 ±1.1		
Ala	-21.9 ±1.8	-29.4 ±2.1	-25.8 ±0.1
Glu/Leu			
Glu	-26.4 ±1.3		
Leu	-26.3 ±0.9	-26.4 ±1.6	-25.0 ±0.1
Glu/Phe			
Glu	-27.2 ±1.1		
Phe	-27.5 ±0.8	-27.3 ±1.4	-25.6 ±0.1
Orn/Ser			
Orn	-13.3 ±1.0		
Ser	-12.8 ±1.4	-13.2 ±1.7	-10.1 ±0.1
Pro/Gly/Pro			
Pro	-8.1 ±0.9		
Gly	-50.6 ±1.5	-17.1 ±1.7	-17.3 ±0.1

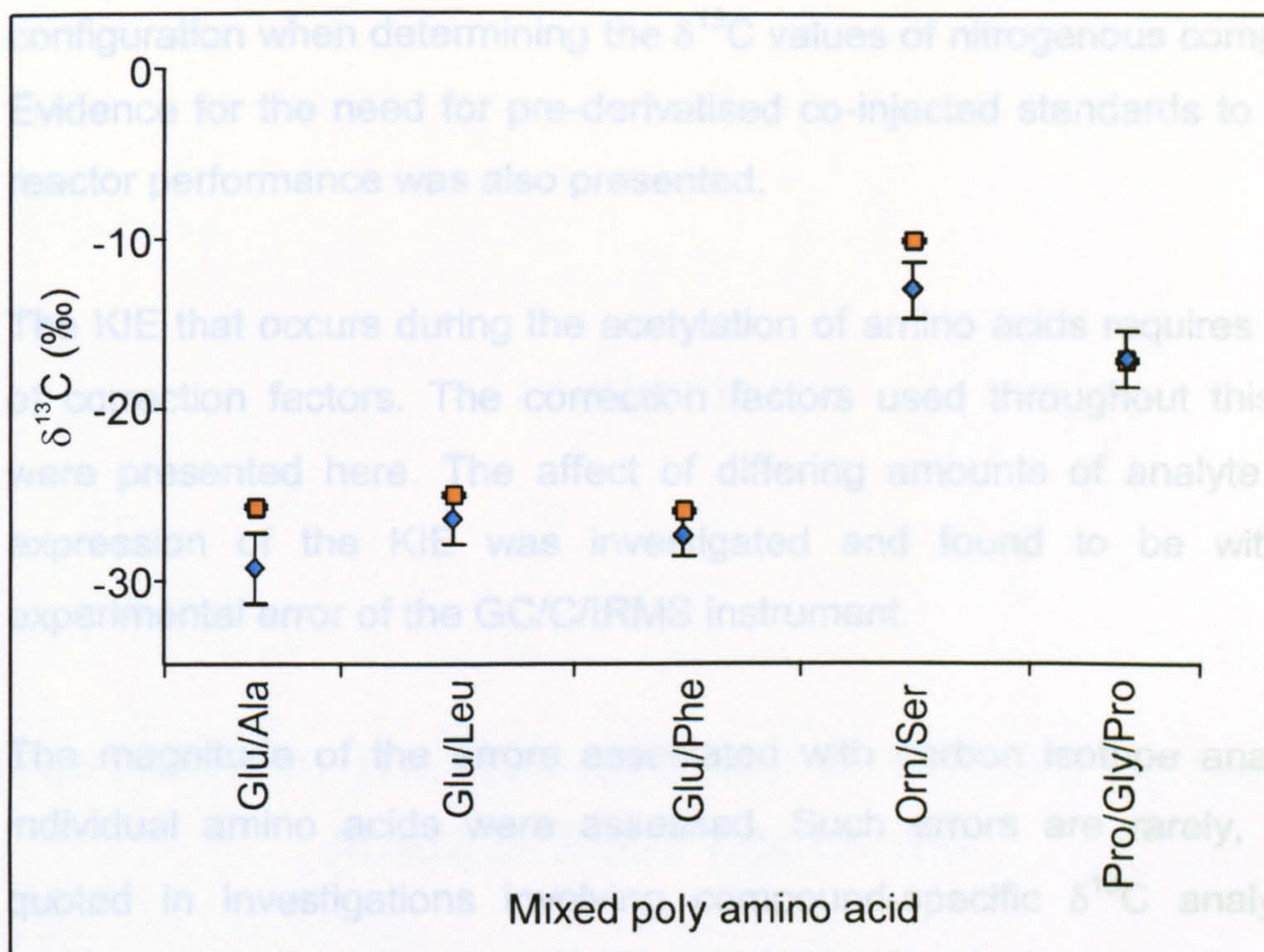


Figure 3.10. Comparison of $\delta^{13}\text{C}$ values of MPAAAs obtained from bulk analysis (orange squares) and those obtained by mass balance of $\delta^{13}\text{C}$ values of individual amino acids comprising them (blue diamonds).

3.7 Summary

This chapter has presented the results of analyses undertaken to investigate likely sources of errors in the analytical protocol employed in the stable carbon isotope analysis of individual amino acids in proteins. The following points were investigated:

- (i) The choice of derivatives for isotope analysis was discussed. Trifluoroacetyl isopropyl ester derivatives were chosen for the investigations in this thesis and the chromatographic resolution for these derivatives was shown to be excellent.

- (ii) It was shown that a reduction reactor is required in the GC/C/IRMS configuration when determining the $\delta^{13}\text{C}$ values of nitrogenous compounds. Evidence for the need for pre-derivatised co-injected standards to monitor reactor performance was also presented.
- (iii) The KIE that occurs during the acetylation of amino acids requires the use of correction factors. The correction factors used throughout this thesis were presented here. The affect of differing amounts of analyte on the expression of the KIE was investigated and found to be within the experimental error of the GC/C/IRMS instrument.
- (iv) The magnitude of the errors associated with carbon isotope analysis of individual amino acids were assessed. Such errors are rarely, if ever, quoted in investigations involving compound-specific $\delta^{13}\text{C}$ analyses of amino acids (Demmelair and Schmidt, 1993; Fantle *et al.*, 1999; Johnson *et al.*, 1998; Silfer *et al.*, 1994) and may affect the interpretations of the results. The errors were evaluated for each amino acid and found to vary from $\pm 0.7\text{‰}$ to $\pm 1.5\text{‰}$.
- (v) The effect of hydrolysis of proteins on the isotopic composition of the individual amino acids that comprise them was investigated using authentic poly amino acids. It was found that after 24 and 48 h the isotopic composition of individual amino acids was unaffected by the hydrolysis procedure. Shorter hydrolysis times did not show such close agreement between estimated and measured $\delta^{13}\text{C}$ values and so are not recommended for use in such work.

CHAPTER 4

INVESTIGATING THE ROUTING AND SYNTHESIS OF AMINO ACIDS IN BONE COLLAGEN

Chapter 4 Investigating the routing and synthesis of amino acids in bone collagen

4.1 Objectives

This chapter presents the results of the isotopic analysis of individual amino acids from an isotopically controlled animal feeding experiment. The $\delta^{13}\text{C}$ values of individual amino acids in dietary protein and rat bone collagen were measured. The aim of this work was to gain a better understanding of the routing and synthesis of individual amino acids by identifying the dietary macronutrients used in the synthesis of bone collagen. It was anticipated that elucidating the factors that influence the carbon isotopic composition of bone, would explain the fractionation observed from diet to bone collagen and offer new insights into interpreting bulk isotopic data in palaeodietary reconstruction.

Professor Stanley Ambrose at the University of Illinois undertook the controlled feeding experiment that provided the samples for this work. All carbon isotopic data relating to the bulk collagen, apatite and dietary macronutrients were measured by Ambrose and co-workers, some of which were reported previously (Ambrose and Norr, 1993), but the majority of which are unpublished.

4.2 Influences on the $\delta^{13}\text{C}$ value of bone collagen

The average adult has a requirement for dietary protein of about 80 g day⁻¹. Proteins are digested in the stomach and small intestine to release amino acids, which are then taken up by cells and used for the synthesis of the 50,000 different proteins and polypeptides in the body as well as a variety of other molecules, such as purines and pyrimidines. Any amino acid that is present in excess of the body's requirements, can be used directly as fuel or converted to glycogen or fat and stored for later use, however amino acids are never stored as proteins. An overview of protein metabolism can be seen in Figure 4.1.

Collagen is the most abundant protein in humans, comprising 20-25 % of total body protein. Proteins are continually being broken down and replaced, but for collagen this happens so slowly it is almost impossible to measure the rate. It has been estimated that the half-life of collagen in adults is about 300 days. This slow process means that collagen is significantly less sensitive to nutritional deficiency than other proteins in the body. Collagen consists of 19 amino acids, which must either be supplied directly from the diet or synthesised *de novo*. The $\delta^{13}\text{C}$ value of bone collagen reflects the individual $\delta^{13}\text{C}$ values of these amino acids. Therefore it is the $\delta^{13}\text{C}$ values of the individual amino acids that influence the isotopic composition of bone collagen.

4.2.1 Essential amino acids

Ten of the amino acids that comprise collagen are essential amino acids and they contribute *ca.* 29% of the carbon in collagen. The pathways for their formation do not occur in mammals and, therefore, they must be provided in the diet. It has been postulated that the carbon isotopic composition of essential amino acids will be identical to the carbon isotopic composition of those amino acids in the diet, bar any fractionation during transport and assimilation (Hare *et al.*, 1991). For an omnivorous diet, the amino acids will be provided mainly from animal protein and the essential amino acids in the animal protein will derive from plants. Therefore, the $\delta^{13}\text{C}$ values of essential amino acids in the omnivore's bone

4.2.2 Non-essential amino acids

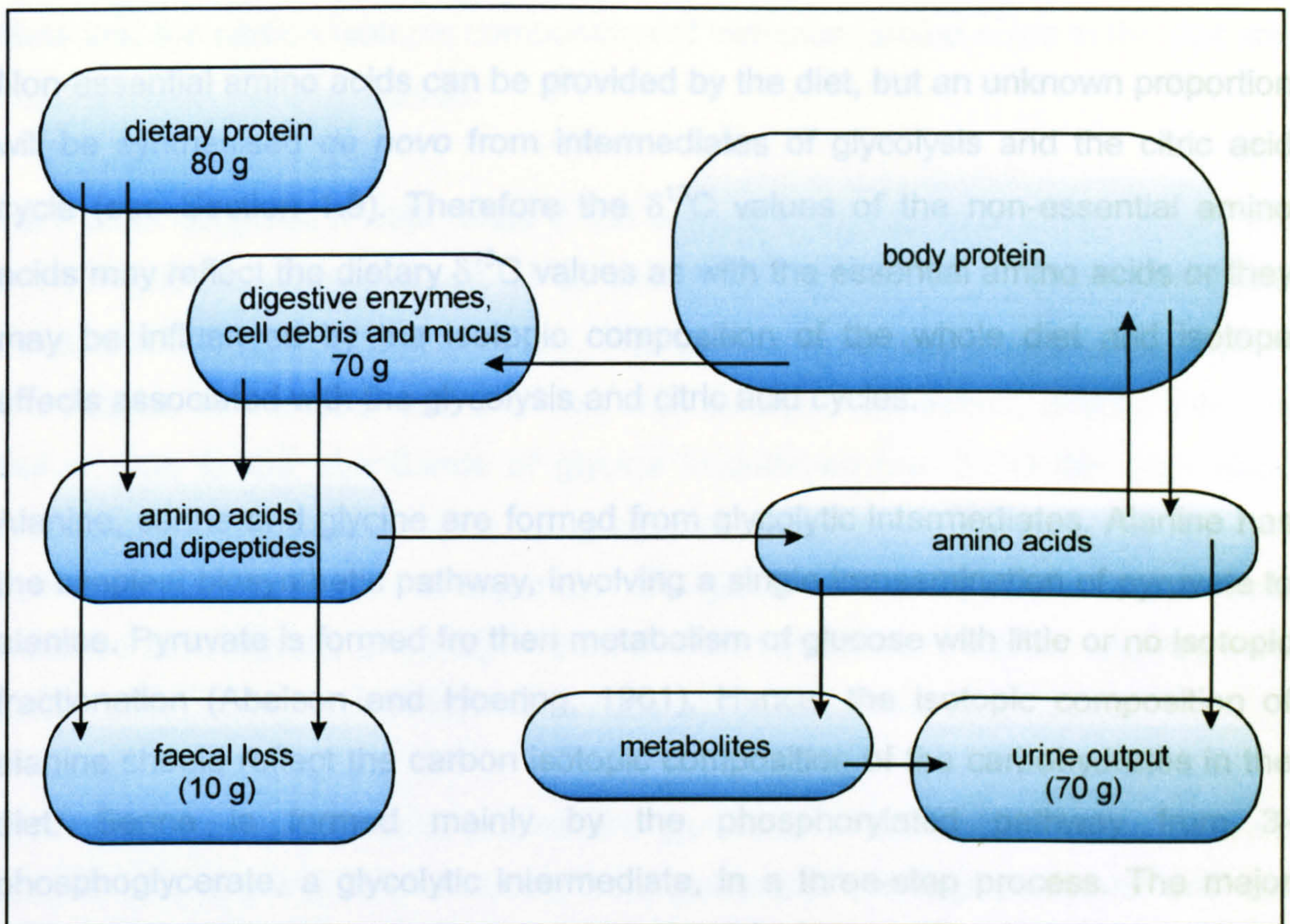


Figure 4.1. An overview of protein metabolism. (From Bender, 1997)

Aspartate and glutamate are both formed by transamination of intermediates of the citric acid cycle, oxalobacelate and α -ketoglutarate, respectively. Proline is formed from glutamate via a three-step process involving a spontaneous cyclisation. Carbohydrates, lipids and proteins all contribute to the citric acid cycle. Therefore, collagen will ultimately reflect the $\delta^{13}\text{C}$ values of those amino acids in plant material.

Although they cannot be synthesised, essential amino acids can be degraded if the diet provides excess, so unless the concentrations of amino acids in the diet are identical to those in the consumer's tissues, alteration of the $\delta^{13}\text{C}$ value could occur (Fogel *et al.*, 1997).

4.2.2 Non-essential amino acids

Non-essential amino acids can be provided by the diet, but an unknown proportion will be synthesised *de novo* from intermediates of glycolysis and the citric acid cycle (see Section 1.9). Therefore the $\delta^{13}\text{C}$ values of the non-essential amino acids may reflect the dietary $\delta^{13}\text{C}$ values as with the essential amino acids or they may be influenced by the isotopic composition of the whole diet and isotope effects associated with the glycolysis and citric acid cycles.

Alanine, serine and glycine are formed from glycolytic intermediates. Alanine has the simplest biosynthetic pathway, involving a single transamination of pyruvate to alanine. Pyruvate is formed from the metabolism of glucose with little or no isotopic fractionation (Abelson and Hoering, 1961). Hence, the isotopic composition of alanine should reflect the carbon isotopic composition of the carbohydrates in the diet. Serine is formed mainly by the phosphorylated pathway from 3-phosphoglycerate, a glycolytic intermediate, in a three-step process. The major metabolic source of glycine is serine via serine hydroxymethyl transferase. These two amino acids should also reflect the carbohydrate isotopic composition.

Aspartate and glutamate are both formed by transamination of intermediates of the citric acid cycle, oxaloacetate and α -ketoglutarate, respectively. Proline is formed from glutamate via a three-step process involving a spontaneous cyclisation. Carbohydrates, lipids and proteins all contribute to the citric acid cycle. Therefore, the isotopic composition of these amino acids should reflect a mixture of all dietary components.

4.3 Other controlled feeding experiments and amino acid analyses

Controlled feeding experiments were performed to gain a better understanding of the factors that influence the carbon isotope fractionations observed between diet and tissue, and thus the metabolic controls on the isotopic composition of bone (Ambrose and Norr, 1993; DeNiro and Epstein, 1978; Tieszen and Fagre, 1993). However, only one study (Hare *et al.*, 1991) involved measuring the $\delta^{13}\text{C}$ values of

individual amino acids. Domestic pigs were reared on 100% C₃ or 100% C₄ plant diets and the carbon isotopic composition of individual amino acids in the diet and bone collagen were measured.

Hare *et al.* observed a wide range in the isotopic composition of amino acids from the diet and bone collagen (ca. 18‰) and found that this range, in part, lead to a fractionation from bulk diet to tissue. The glycine in the diet was 8‰ enriched in ¹³C relative to the bulk diet and that was incorporated almost directly into the tissue. Due to the abundance of glycine in collagen (ca. 33%) this high value contributed to the bulk collagen being several per mil more ¹³C-enriched than the bulk diet. They also found aspartate and glutamate to be 3‰ and 6‰ more enriched respectively, in collagen than diet and interpreted this as showing how fractionation during metabolism can cause an enrichment in bulk values.

The isotopic compositions of proline and glutamate in the collagen were different despite proline being formed directly from glutamate. The explanation for this was that proline was being incorporated directly from the diet, as well as being synthesised *de novo*.

This study revealed some important processes that contribute to the isotopic fractionation between an animal and its diet and showed for the first time how the δ¹³C values of individual amino acids can be utilised for such work. The work presented in this chapter builds on these foundations with the use of isotopically distinct dietary macronutrients to further investigate routing and synthesis of amino acids in bone collagen.

4.4 Sample description

The rat tissues and diets provided for analysis were part of a larger isotopically controlled feeding experiment undertaken by Ambrose and co-workers at the University of Illinois (Ambrose and Norr, 1993). Holtzman albino rats were raised on a variety of isotopically distinct purified and pellatised diets in which the proportions of protein, starch, sucrose and oil were varied.

4.4.1 Experimental approach

Female Holtzman albino rats were placed on the diet that their offspring would consume, 1 day after insemination. Birth occurred 21 days later and weaning began 21-23 days subsequently. Male and Female pairs were sacrificed at 91, 131 and 171 days after birth. To investigate the turnover rates of different bone components, two groups of animals were subjected to a diet switch experiment whereby animals were raised on either a pure C₃ or pure C₄ diet and then switched to the other diet at 131 days after weaning. The rats were sacrificed at 40, 80 and 120 days after this.

Twenty rats raised on ten isotopically distinct diets were sampled for stable carbon isotope analysis of individual amino acids, two rats from each of the diet switch experiments were also analysed. The diet compositions and carbon isotope values of individual components can be seen in Table 4.1. The experimental animals studied fell into three main groups, those that were raised on 20% protein diets, those that were raised on 70% protein diets and those that came from the diet switch experiments. Details of all studied animals can be seen in Table 4.2. The animals raised on 20% and 70% diets can be used to compare the routing and synthesis of amino acids from dietary macronutrients to bone collagen, whilst the diet switch animals provide information on the rate of incorporation of different amino acids into bone collagen.

4.5 Results and Discussion

4.5.1 Amino acid composition of diet and bone collagen

Individual amino acids were obtained from the diets and bone collagen as described in Sections 2.7 and 2.9. Figure 4.2(a) shows a partial gas chromatogram of diet D7K2, where it can be seen that eleven amino acids were successfully separated. The variation in the relative abundances of the amino acids in the diets can be seen in Figure 4.3. All of the terrestrial protein diets (diets

Table 4.1. Diet composition and $\delta^{13}\text{C}$ values . Carbon isotope values for individual components are given in parentheses (from Ambrose and Norr, 1993; Ambrose, unpublished data).

Diet	Composition		Components ($\delta^{13}\text{C}$ ‰)						
	protein	energy	protein (20%)	sucrose (50.2%)	starch (15.5%)	oil (5.0%)	cellulose (5.0%)	whole diet	
D2A4	C ₃	C ₃	milk casein (-24.5)	beet (-24.2)	rice (-26.4‰)	cottonseed (-27.9)	wood (-17.0)	-24.9	
D3G	C ₃	C ₄	milk casein (-26.3)	cane (-11.0)	corn (-10.3)	corn (-14.9)	corn (-17.0)	-14.7	
D4H	C ₄	C ₄	milk casein (-14.6)	cane (-11.4)	corn (-10.6)	corn (-14.9)	corn (-16.9)	-12.2	
D5I	C ₄	C ₃	milk casein (-14.6)	beet (-24.2)	rice (-26.4)	cottonseed (-27.9)	wood (-16.9)	-22.3	
D6J2	marine	C ₃	tuna fish (-17.8)	beet (-24.2)	rice (-26.4)	cottonseed (-28.3)	wood (-20.7)	-23.3	
D7K2	marine	C ₄	tuna fish (-17.8)	cane (-11.3)	corn (-10.6)	corn (-15.0)	corn (-20.7)	-12.9	
D8L2	marine	C ₃ +C ₄	tuna fish (-17.8)	beet + cane (-17.6)	rice + corn (-18.3)	cottonseed + corn (-21.6)	wood + corn (-20.7)	-18.3	
			protein (70%)	sucrose (12.5%)	starch (3.6%)	oil (5.0%)	cellulose (5.0%)		
D9J3	marine	C ₃	tuna fish (-17.8)	beet (-24.2)	rice (-26.4)	cottonseed (-28.3)	wood (-20.7)	-19.4	
D10K3	marine	C ₄	tuna fish (-17.8)	cane (-11.3)	corn (-10.6)	corn (-15.0)	corn (-20.7)	-16.0	
D11L3	marine	C ₃ + C ₄	tuna fish (-17.8)	beet + cane (-17.6)	rice + corn (-18.3)	cottonseed + corn (-21.6)	wood + corn (-20.7)	-17.7	

Table 4.2. Diet, tissue code, sex and pair of individual animals that were analysed. Pair indicates age of animal at sacrifice. First, second and third pair are 91, 131 and 171 days old, respectively for 20% and 70% protein diets, whilst first, second and third pair are 171, 211, and 251 days old for the diet switch animals.

Diet	Tissue Code	No. of Animals	Sex	Pair
D2A4	Pure C ₃	2	m, f	2, 2
D3G	C ₃ /C ₄	2	m, f	3, 2
D4H	Pure C ₄	2	m, m	1, 2
D5I	C ₄ /C ₃	2	f, m	2, 3
D6J2	MP/C ₃	2	f, f	1, 2
D7K2	MP/C ₄	2	m, m	1, 2
D8L2	MP/C ₃ +C ₄	2	f, m	1, 2
D9J3	70%MP/C ₃	2	m, f	1, 1
D10K3	70%MP/C ₄	2	m, f	1, 1
D11L3	70%MP/C ₃ +C ₄	2	m, f	1, 1
D2A4 to D4H	pure C ₃ to pure C ₄	2	m, f	3, 3
D4H to D2A4	pure C ₄ to pure C ₃	2	m, f	3, 3

D2A4, D3G, D4H and D5I) have comparable distributions, as do the marine protein diets (D6J2, D7K2 and D8L2), although there is a significant variation between the terrestrial protein diets and the marine protein diets. This variation reflects the different sources of protein comprising these diets, *i.e.* milk casein for the terrestrial protein diets and tuna fish for the marine protein diets. A typical amino acid distribution for the rat bone collagen can be seen in Figure 4.2(b). The same eleven amino acids were separated as well as one additional amino acid, hydroxyproline. This compound was not present in the diet, as it is synthesised solely in the animal after incorporation of proline into proteins (Udenfriend, 1966). As would be expected for bone collagen, the relative abundances of the amino acids were very similar for all samples, regardless of their sources of protein (Table 4.3.). The relative abundances observed for the amino acids isolated from

the bone can be compared with theoretical relative abundances based on the known amino acid composition of mammalian collagen (Vaughan, 1970). Figure 4.4 compares the relative abundances in a typical rat bone with the theoretical relative abundances. They are quite similar, with the exception of proline, hydroxyproline and glutamic acid. This may indicate preferential loss of these compounds during the hydrolysis and derivatisation procedures, although this is not thought to affect the stable carbon isotope values observed.

Table 4.3. Relative abundances of amino acids in bone collagen of rats raised on controlled diets. Values for each diet are an average of two animals.

	% abundance relative to glycine						
	Tissue code						
	pure C ₃	pure C ₄	C ₃ /C ₄	C ₄ /C ₃	MP/C ₃	MP/C ₄	MP/C ₃ +C ₄
Ala	35	35	43	32	37	35	39
Gly	100	100	100	100	100	100	100
Thr	7	8	8	6	9	8	9
Ser	6	12	12	8	16	9	15
Val	9	9	9	5	8	7	9
Leu	11	10	13	8	10	10	11
Ile	4	4	5	3	4	4	4
Pro	28	28	37	23	26	25	26
Hyp	27	29	37	24	28	28	30
Asp	16	15	18	11	13	13	15
Glu	21	18	25	14	18	14	16
Phe	7	8	9	7	8	7	8

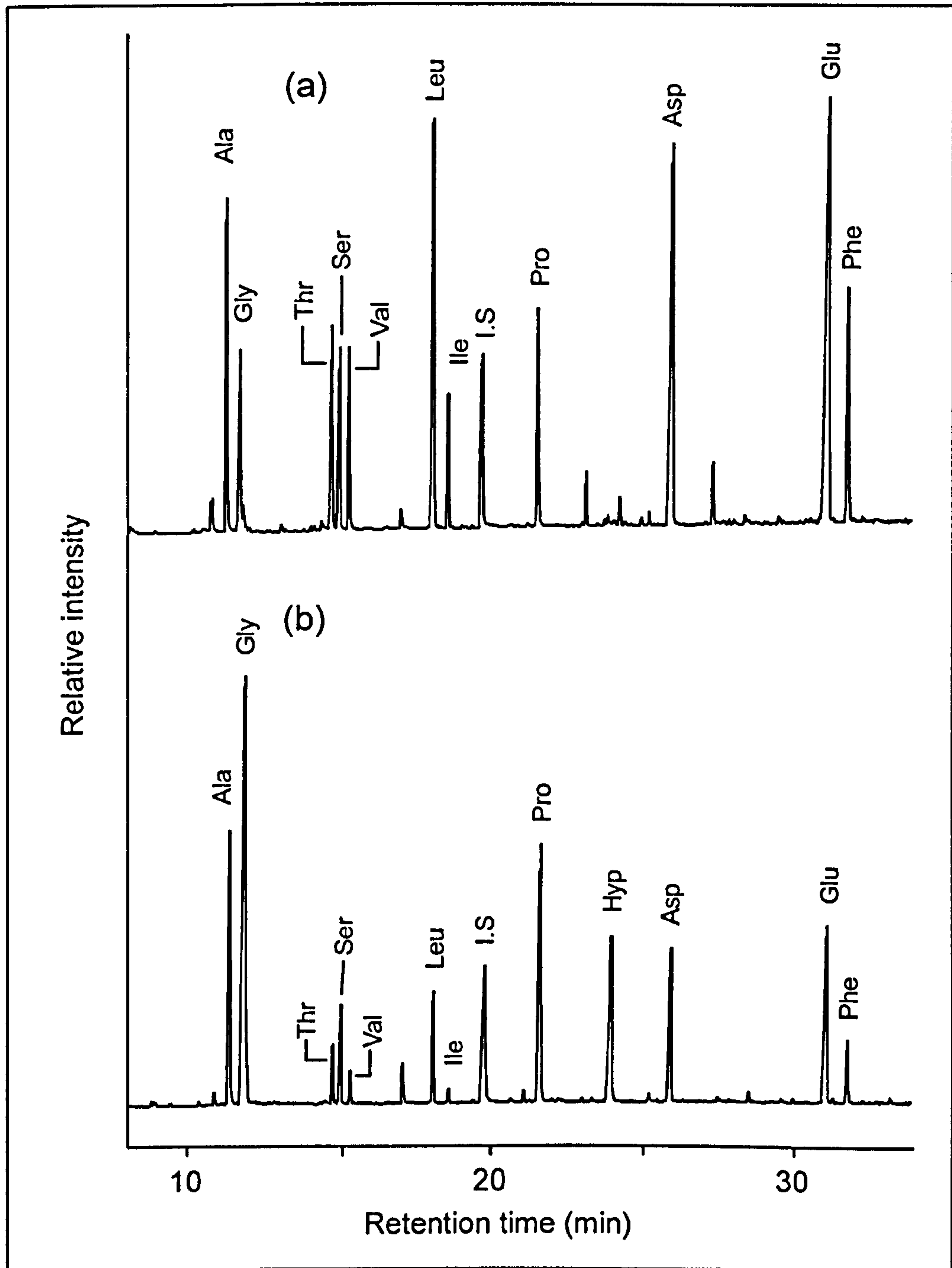


Figure 4.2. Typical partial gas chromatograms of individual amino acids in (a) dietary protein and (b) rat collagen.

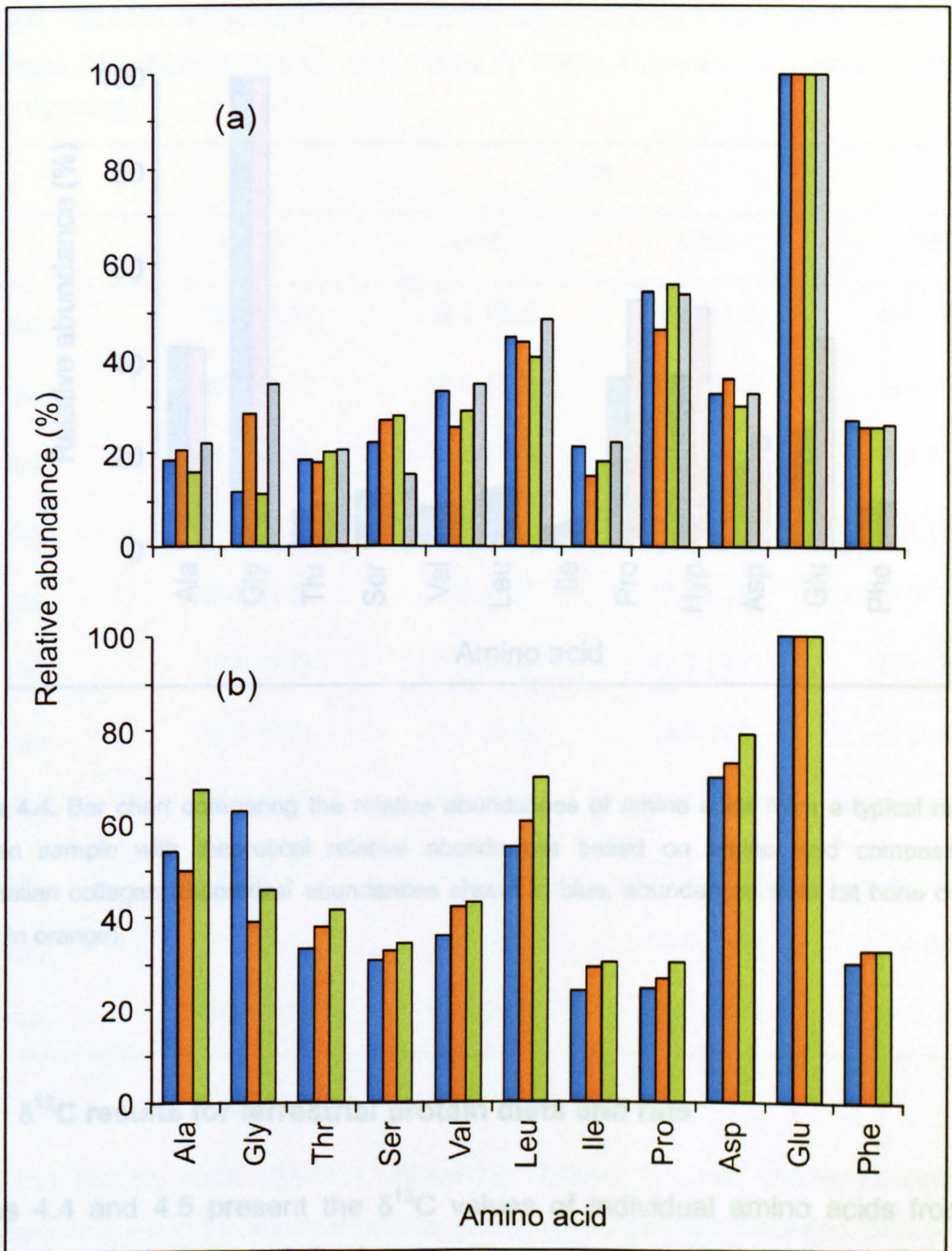


Figure 4.3. Bar charts showing relative abundances of amino acids in (a) terrestrial protein diets, diets D2A4, D3G, D4H and D5I indicated by the blue, orange, green and grey bars, respectively and (b) marine protein diets, diets D6J2, D7K2 and D8L2 indicated by blue, orange and green bars respectively.

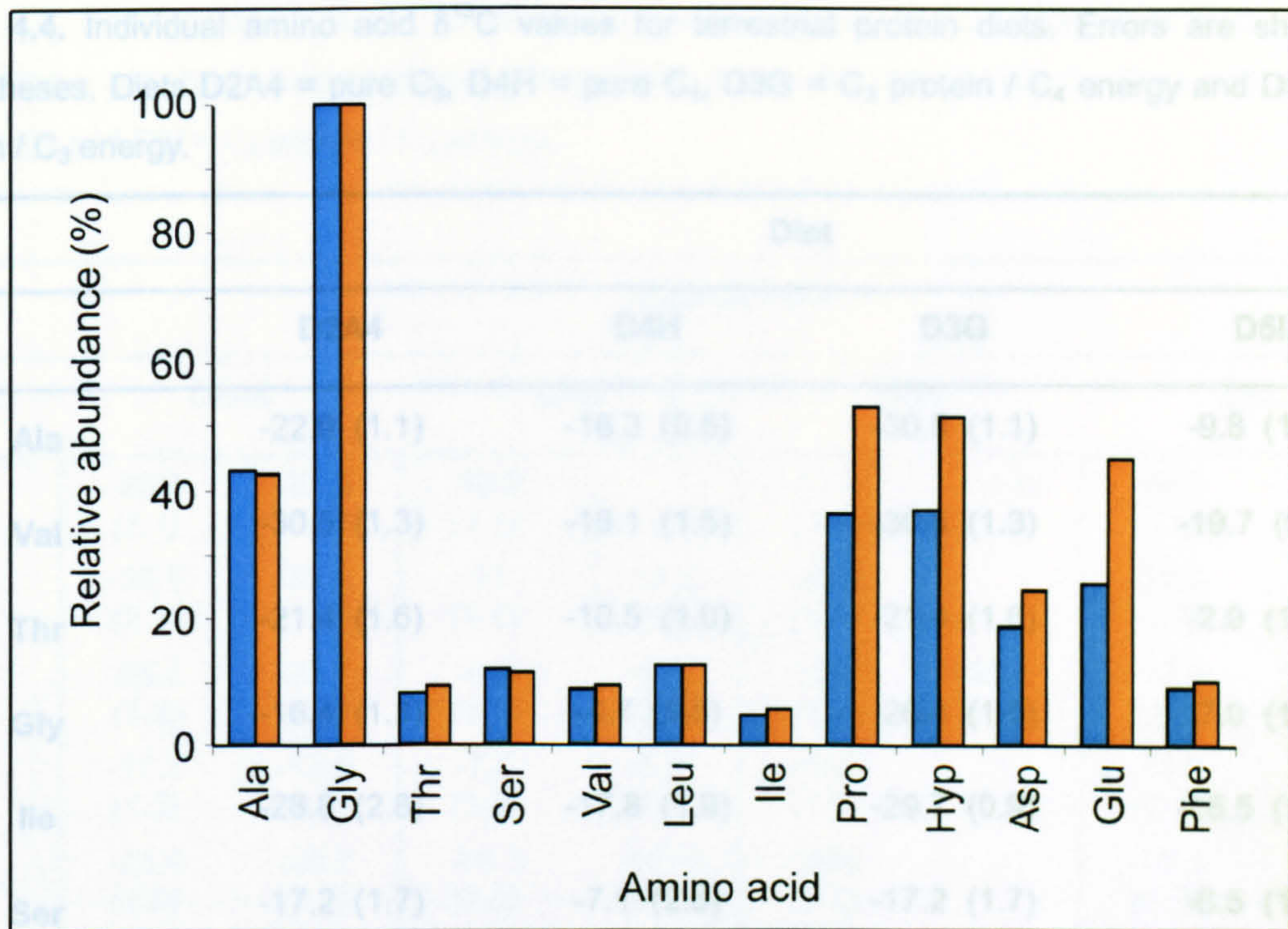


Figure 4.4. Bar chart comparing the relative abundances of amino acids from a typical rat bone collagen sample with theoretical relative abundances based on amino acid composition of mammalian collagen (theoretical abundances shown in blue, abundances from rat bone collagen shown in orange).

4.5.2 $\delta^{13}\text{C}$ results for terrestrial protein diets and rats

Tables 4.4 and 4.5 present the $\delta^{13}\text{C}$ values of individual amino acids from the terrestrial protein diets and the bone collagen of rats raised on these diets. Two animals from each diet were studied. The isotope values for individual amino acids from diet and bone collagen for the pure C_3 and pure C_4 diets are shown in Figure 4.5. A range of 16.5‰ and 19.6‰ was observed for the pure C_3 and pure C_4 dietary values, respectively. A slightly larger range of 21.5‰ and 23.6‰ was observed for individual amino acids in the bone collagen of rats fed on the pure C_3 and pure C_4 diets, respectively. This large range is comparable to that observed in other studies (Hare *et al.*, 1991; Johnson *et al.*, 1998). In general, the acidic amino acids (aspartate and glutamate) were relatively enriched with respect to the

Table 4.4. Individual amino acid $\delta^{13}\text{C}$ values for terrestrial protein diets. Errors are shown in parentheses. Diets D2A4 = pure C_3 , D4H = pure C_4 , D3G = C_3 protein / C_4 energy and D5I = C_4 protein / C_3 energy.

	Diet			
	D2A4	D4H	D3G	D5I
Ala	-22.9 (1.1)	-16.3 (0.8)	-30.5 (1.1)	-9.8 (1.8)
Val	-30.5 (1.3)	-16.1 (1.5)	-30.5 (1.3)	-19.7 (0.9)
Thr	-21.4 (1.6)	-10.5 (1.0)	-21.4 (1.6)	-2.9 (1.4)
Gly	-16.4 (1.3)	-4.7 (1.5)	-26.4 (1.5)	-7.0 (1.5)
Ile	-28.8 (2.8)	-17.8 (1.9)	-29.7 (0.9)	-16.5 (1.2)
Ser	-17.2 (1.7)	-7.1 (2.5)	-17.2 (1.7)	-6.5 (1.7)
Leu	-32.9 (0.8)	-21.7 (0.8)	-33.3 (0.8)	-21.3 (0.8)
Pro	-18.4 (0.7)	-7.6 (0.6)	-19.7 (0.9)	-9.8 (1.0)
Asp	-21.7 (1.1)	-11.0 (0.9)	-23.9 (1.3)	-12.9 (1.5)
Glu	-16.8 (0.8)	-2.1 (0.9)	-18.5 (1.1)	-5.2 (0.9)
Phe	-30.9 (0.5)	-15.6 (0.5)	-29.0 (0.7)	-16.9 (0.7)

remaining amino acids (glycine, threonine, serine, proline, hydroxyproline and phenylalanine), and the neutral amino acids were relatively depleted with respect to the remaining amino acids. The enrichment seen in the former is caused by the extra carboxyl group, which is enriched in ^{13}C (ca. 20‰) relative to the remainder of the molecule (Abelson and Hoering, 1961). The depletion seen in the neutral amino acids is due to a fractionation in the enzymatic conversion of pyruvate to acetyl CoA, an ubiquitous precursor in their biosynthesis (DeNiro and Epstein, 1977).

Table 4.5. Individual amino acid $\delta^{13}\text{C}$ values from bone collagen of rats raised on terrestrial protein diets. Errors are shown in parentheses. Diets D2A4 = pure C_3 , D4H = pure C_4 , D3G = C_3 protein / C_4 energy and D5I = C_4 protein / C_3 energy.

	Tissue code							
	D2A4		D4H		D3G		D5I	
Ala	-26.8 (1.1)	-21.9 (1.1)	-10.8 (1.1)		-12.4 (1.1)	-14.6 (2.0)	-28.7 (1.0)	-30.2 (0.8)
Val	-30.7 (2.3)	-32.8 (1.2)	-17 (1.5)	-15.9 (0.9)	-26.2 (1.3)		-19.6 (1.2)	-18.5 (0.9)
Thr	-25.2 (1.2)	-23.1 (1.6)	-8.5 (1.8)	-5.3 (0.9)	-19.7 (1.2)	-22.7 (1.8)	-12.4 (1.0)	-8.9 (0.8)
Gly	-17.3 (1.3)	-12.9 (1.5)	-7.2 (1.3)	-5.9 (1.8)	-15.9 (1.8)		-13.3 (1.1)	-11.7 (1.3)
Ile	-25.4 (1.9)	-26.7 (1.1)	-16.3 (3.0)	-17.4 (0.9)	-29.0 (1.2)		-15.5 (1.7)	-16.5 (1.6)
Ser	-14.0 (2.2)	-13.2 (1.4)	-2.7 (1.1)	-1.7 (2.2)	-9.6 (1.7)		-13.5 (1.2)	-11.4 (1.0)
Leu	-34.1 (0.6)	-34.4 (0.8)	-23.6 (0.6)	-24 (0.7)	-34.5 (0.9)	-32.2 (0.8)	-26.4 (1.4)	-26.0 (0.6)
Pro	-15.6 (0.7)	-15.4 (0.9)	-4.5 (0.9)	-3.8 (1.5)	-14.9 (0.9)	-14.8 (1.7)	-4.7 (1.0)	-5.6 (0.6)
Hyp	-21.9 (1.0)	-23.1 (1.4)	-10.1 (0.9)	-11.1 (0.7)	-22.4 (0.7)		-13.4 (0.6)	-13.1 (0.7)
Asp	-20.7 (0.9)	-21.8 (1.1)	-8.8 (1.5)	-9.7 (1.8)	-12.6 (1.5)		-15.3 (1.3)	-15.2 (1.0)
Glu	-15.8 (0.8)	-15.2 (0.9)	0.0 (0.8)	-2.3 (0.9)	-6.0 (0.9)	-6.0 (1.7)	-12.5 (1.1)	-11.5 (0.8)
Phe		-30.4 (0.6)	-13.2 (0.6)	-13.5 (0.5)	-28.7 (0.8)	-32.1 (1.0)	-15.0 (0.9)	-14.5 (0.8)

The incorporation of the isotopic signal from dietary amino acids to tissue amino acids can clearly be seen, although as expected this is not uniform. Interestingly the varying $\Delta^{13}\text{C}_{\text{collAA-dietAA}}$ values observed for the essential and non-essential amino acids are statistically identical (students t-test), despite the fact that the non-essential amino acids can be synthesised by the body from a variety of different carbon sources. Significantly, fractionation of the essential amino acids was observed even though they must derive directly from the diet. Only if all essential amino acids provided in the diet are incorporated into tissue protein will there be

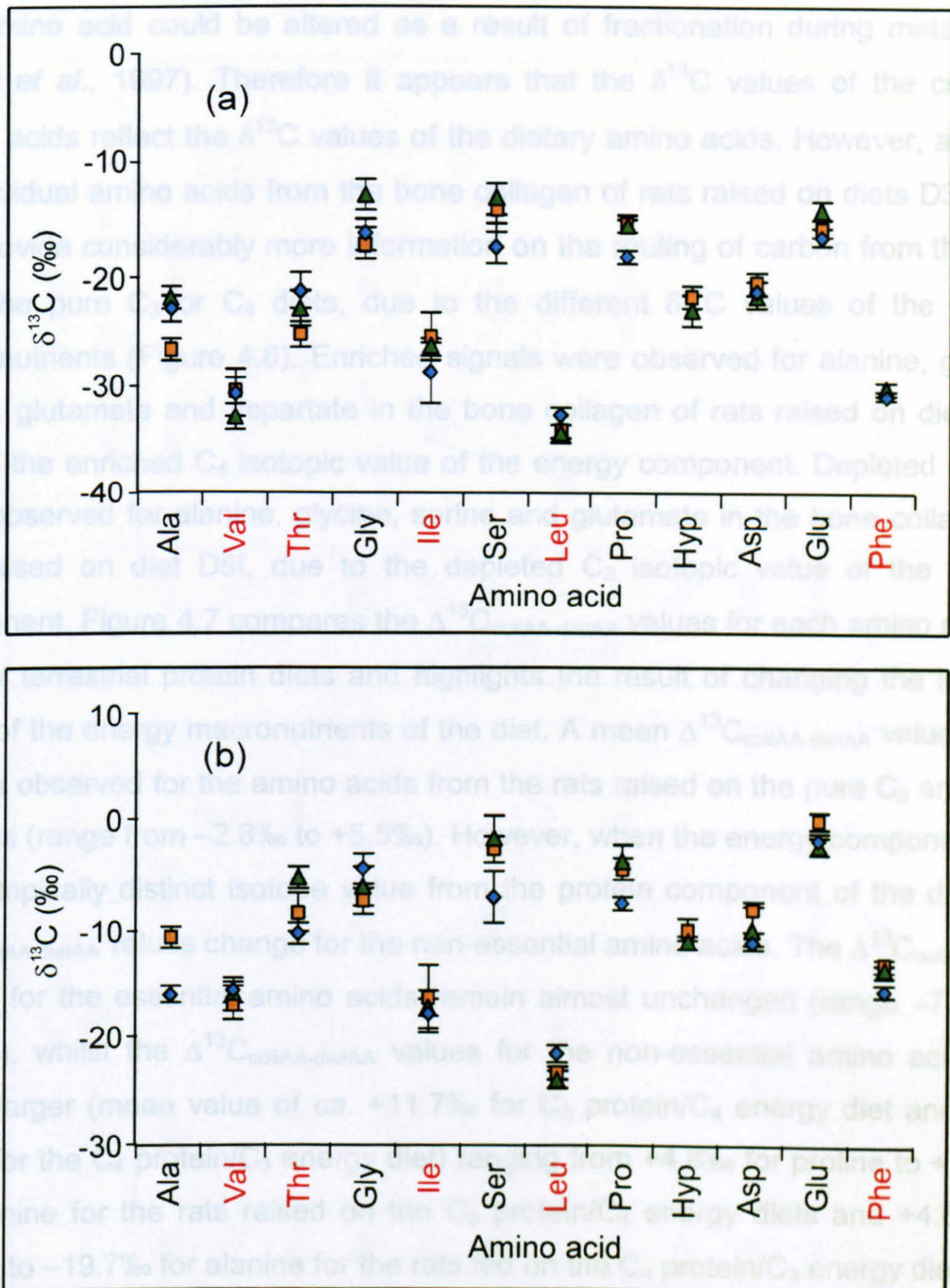


Figure 4.5. Graph showing the $\delta^{13}\text{C}$ values of individual amino acids from the diet (diamonds) and bone collagen from two rats raised on the diet (squares and triangles), for (a) the pure C₃ diet and (b) the pure C₄ diet. Essential amino acids are indicated in red.

no fractionation. Hence, if an amino acid is consumed in excess, the $\delta^{13}\text{C}$ value of that amino acid could be altered as a result of fractionation during metabolism (Fogel *et al.*, 1997). Therefore it appears that the $\delta^{13}\text{C}$ values of the collagen amino acids reflect the $\delta^{13}\text{C}$ values of the dietary amino acids. However, analysis of individual amino acids from the bone collagen of rats raised on diets D3G and D5I provide considerably more information on the routing of carbon from the diet, than the pure C_3 or C_4 diets, due to the different $\delta^{13}\text{C}$ values of the dietary macronutrients (Figure 4.6). Enriched signals were observed for alanine, glycine, serine, glutamate and aspartate in the bone collagen of rats raised on diet D3G due to the enriched C_4 isotopic value of the energy component. Depleted signals were observed for alanine, glycine, serine and glutamate in the bone collagen of rats raised on diet D5I, due to the depleted C_3 isotopic value of the energy component. Figure 4.7 compares the $\Delta^{13}\text{C}_{\text{collAA-dietAA}}$ values for each amino acid for all four terrestrial protein diets and highlights the result of changing the isotopic value of the energy macronutrients of the diet. A mean $\Delta^{13}\text{C}_{\text{collAA-dietAA}}$ value of ca. +2‰ is observed for the amino acids from the rats raised on the pure C_3 and pure C_4 diets (range from -2.8‰ to +5.5‰). However, when the energy component has an isotopically distinct isotope value from the protein component of the diet, the $\Delta^{13}\text{C}_{\text{collAA-dietAA}}$ values change for the non-essential amino acids. The $\Delta^{13}\text{C}_{\text{collAA-dietAA}}$ values for the essential amino acids remain almost unchanged (range -7.8‰ to +4.3‰), whilst the $\Delta^{13}\text{C}_{\text{collAA-dietAA}}$ values for the non-essential amino acids are much larger (mean value of ca. +11.7‰ for C_3 protein/ C_4 energy diet and ca. -6.0‰ for the C_4 protein/ C_3 energy diet) ranging from +4.8‰ for proline to +17.0‰ for alanine for the rats raised on the C_3 protein/ C_4 energy diets and +4.6‰ for proline to -19.7‰ for alanine for the rats fed on the C_4 protein/ C_3 energy diet.

The fractionations from diet amino acid to collagen amino acid can be compared with the fractionation from bulk dietary protein to bulk collagen (see Table 4.6). The fractionation observed for the pure C_3 and pure C_4 diets correlate well with the fractionations seen for the individual amino acids, however the bulk fractionations for the mixed protein/energy diets obscure some of the large $\Delta^{13}\text{C}_{\text{collAA-dietAA}}$ values seen in the individual amino acids. For example, a difference of +9.4‰ is observed for the C_3 protein/ C_4 energy diet, which is larger than the differences seen for the

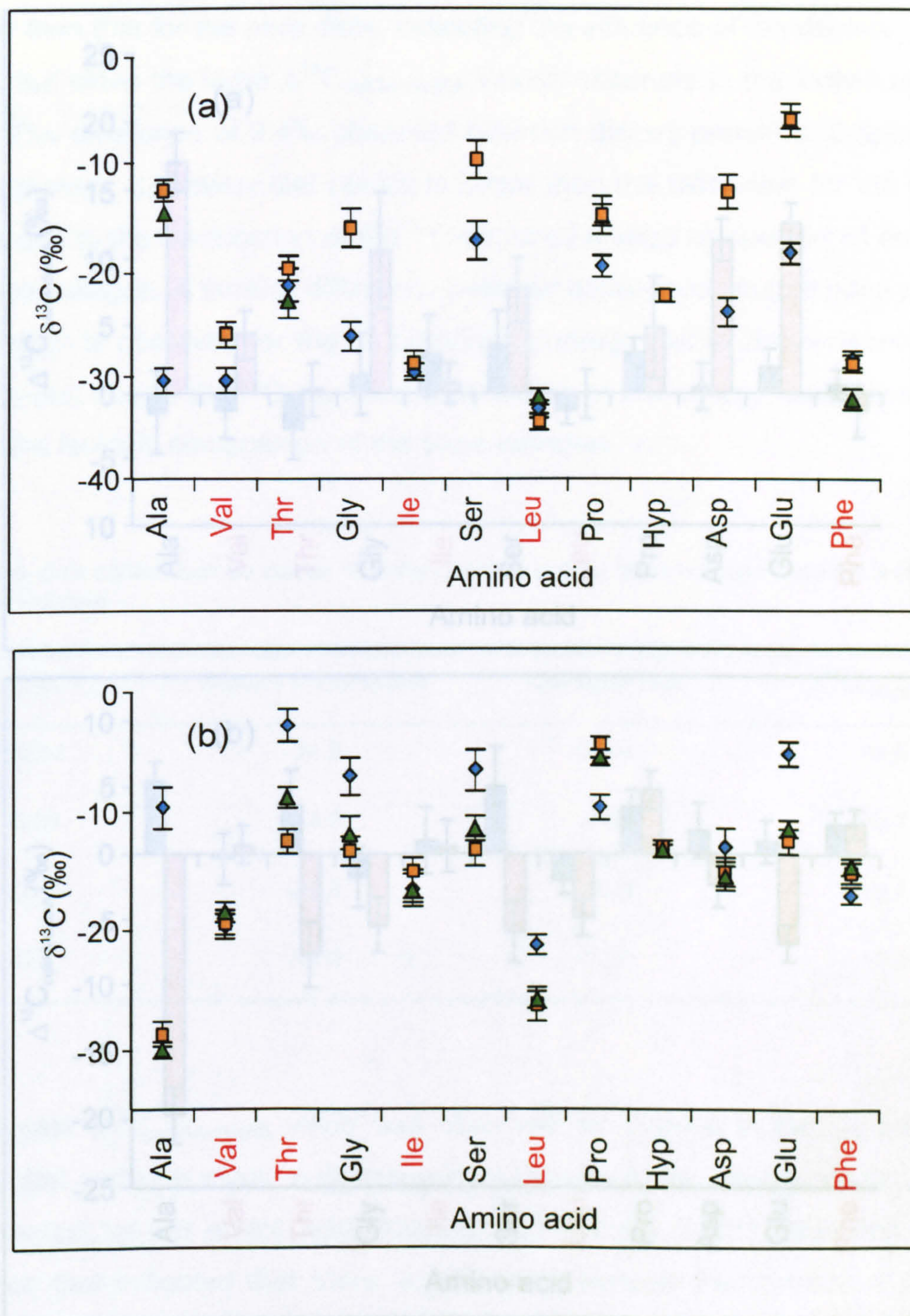


Figure 4.6. Graph showing the $\delta^{13}\text{C}$ values of individual amino acids from the diet (diamonds) and bone collagen from two rats raised on the diet (squares and triangles), for (a) the C_3/C_4 diet and (b) the C_4/C_3 diet. Essential amino acids are indicated in red.

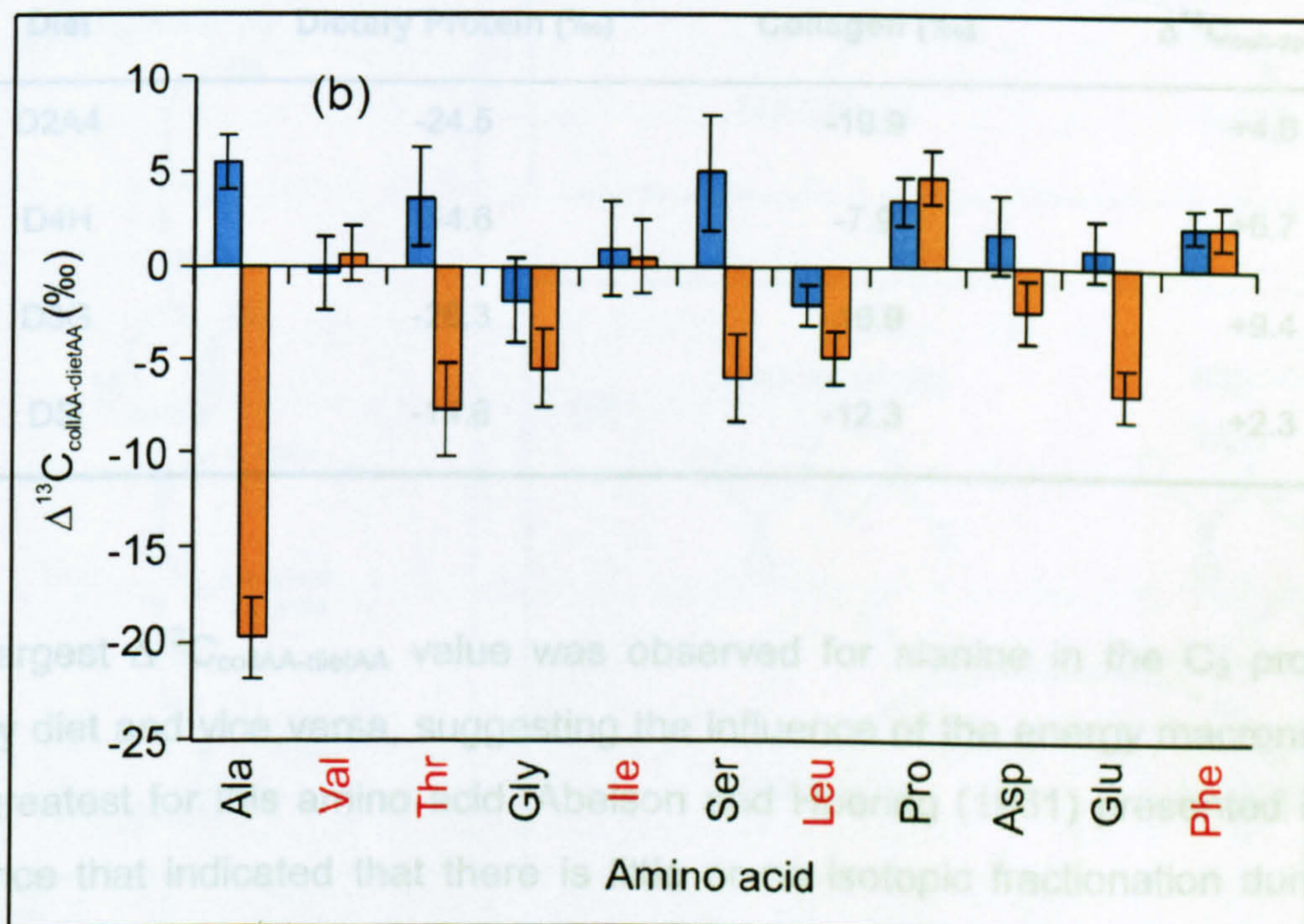
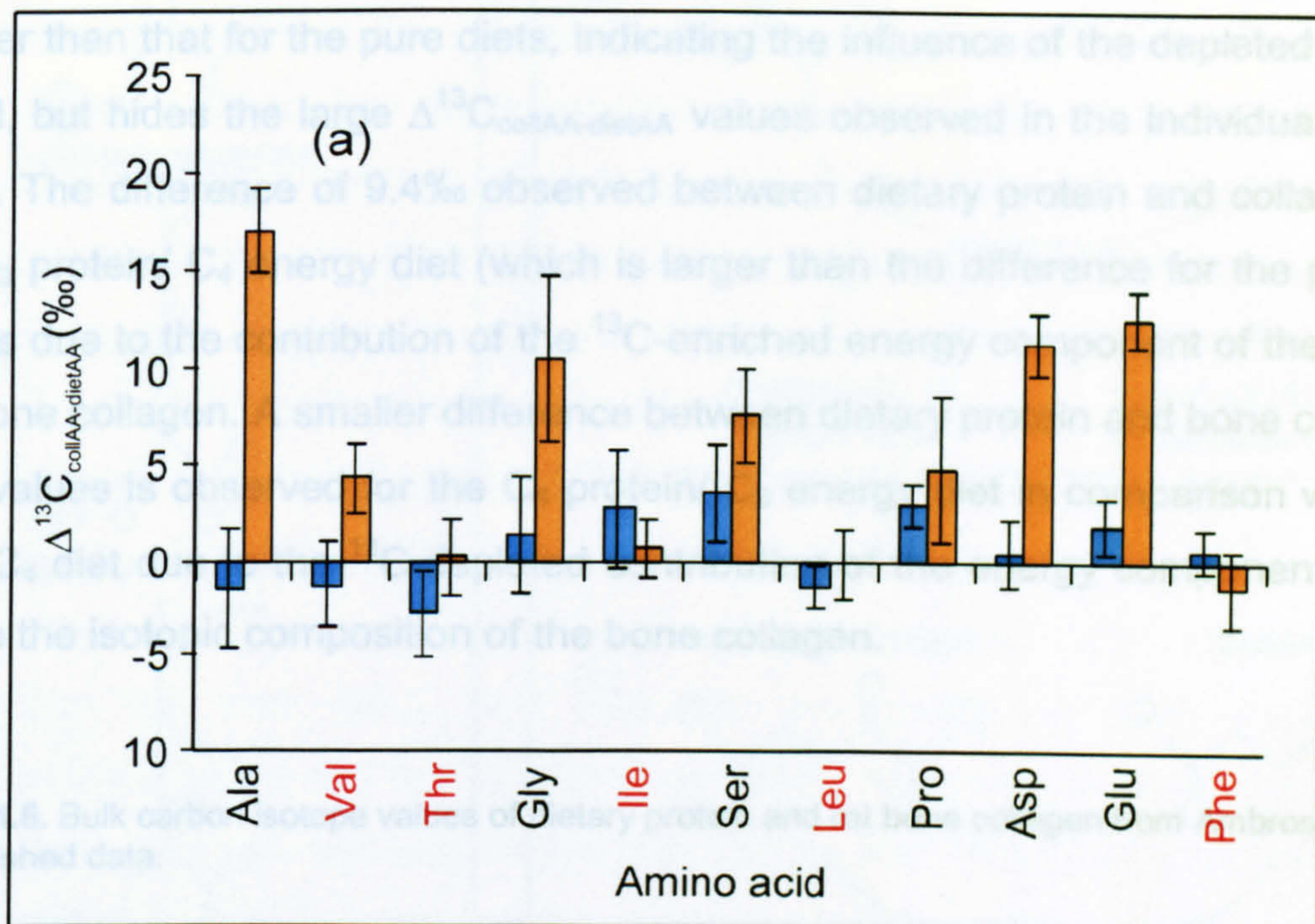


Figure 4.7. Histograms showing the $\Delta^{13}\text{C}_{\text{collIAA-dietAA}}$ values for each amino acid for (a) the pure C_3 and C_3/C_4 diet and (b) the pure C_4 and C_4/C_3 diet; where $\Delta^{13}\text{C}_{\text{collIAA-dietAA}} = \delta^{13}\text{C}_{\text{collIAA}} - \delta^{13}\text{C}_{\text{dietAA}}$. Pure diets are shown in blue and mixed diets in orange. Essential amino acids are indicated in red.

pure diets, but it conceals the very large $\Delta^{13}\text{C}_{\text{collAA-dietAA}}$ value of +17‰ for alanine. The same applies to the C₄ protein/C₃ energy diet which shows a bulk fractionation smaller than that for the pure diets, indicating the influence of the depleted energy signal, but hides the large $\Delta^{13}\text{C}_{\text{collAA-dietAA}}$ values observed in the individual amino acids. The difference of 9.4‰ observed between dietary protein and collagen for the C₃ protein/ C₄ energy diet (which is larger than the difference for the pure C₃ diet) is due to the contribution of the ¹³C-enriched energy component of the diet to the bone collagen. A smaller difference between dietary protein and bone collagen $\delta^{13}\text{C}$ values is observed for the C₄ protein/ C₃ energy diet in comparison with the pure C₄ diet due to the ¹³C-depleted contribution of the energy component of the diet to the isotopic composition of the bone collagen.

Table 4.6. Bulk carbon isotope values of dietary protein and rat bone collagen from Ambrose, unpublished data.

Diet	Dietary Protein (‰)	Collagen (‰)	$\Delta^{13}\text{C}_{\text{coll-dp}}$ (‰)
D2A4	-24.5	-19.9	+4.6
D4H	-14.6	-7.9	+6.7
D3G	-26.3	-16.9	+9.4
D5I	-14.6	-12.3	+2.3

The largest $\Delta^{13}\text{C}_{\text{collAA-dietAA}}$ value was observed for alanine in the C₃ protein/C₄ energy diet and vice versa, suggesting the influence of the energy macronutrients was greatest for this amino acid. Abelson and Hoering (1961) presented indirect evidence that indicated that there is little or no isotopic fractionation during the metabolism of glucose to pyruvate. Since alanine is formed directly from pyruvate in a one step transamination reaction, (Figure 4.8b) it follows that alanine will have a carbohydrate isotopic signature. Glycine and serine also show the incorporation of the energy signal, although not as dramatically as for alanine, despite their formation from 3-phosphoglycerate, an intermediate in the formation of pyruvate from glucose. This may be because serine is formed via a three-step pathway (see

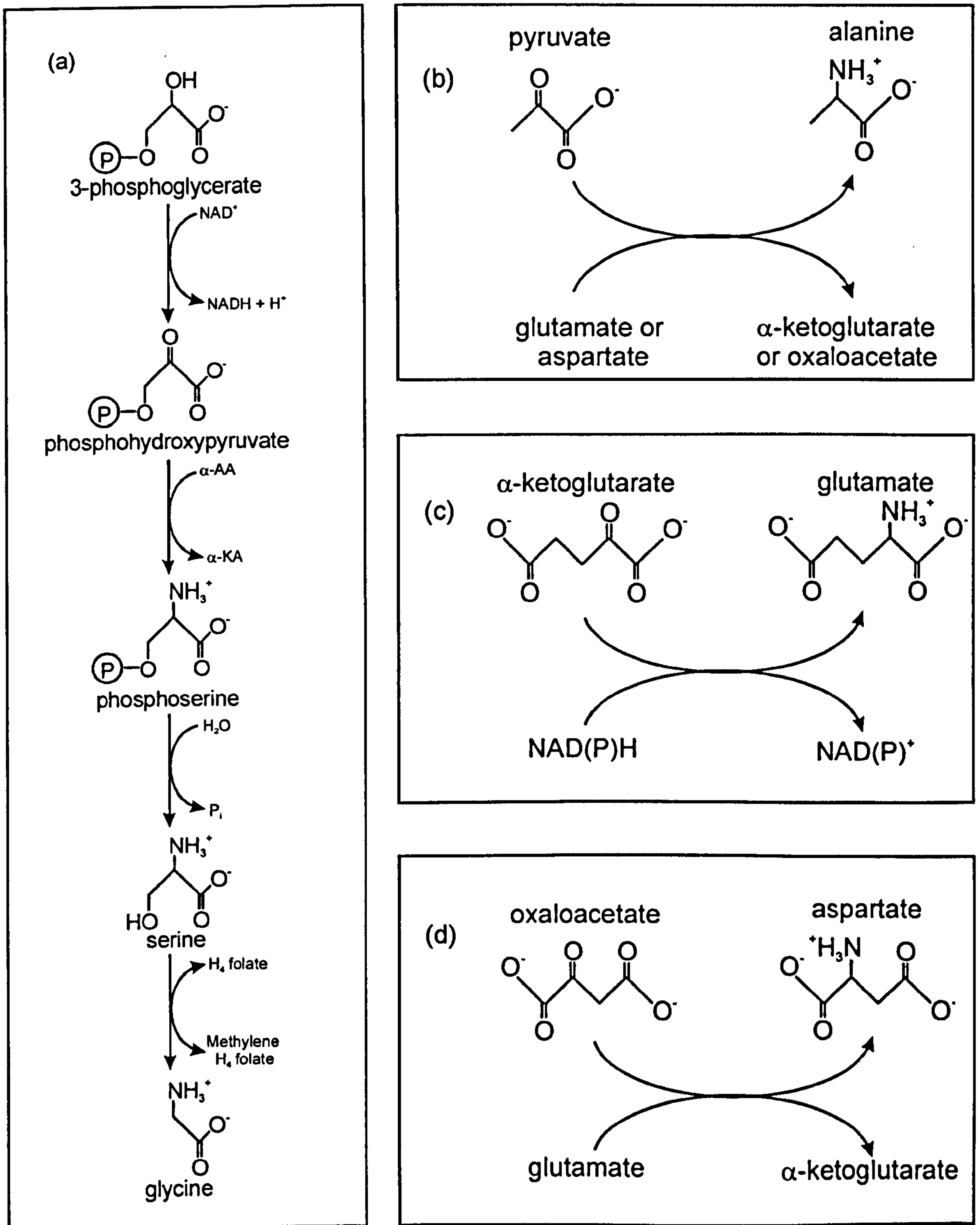


Figure 4.8. Biosynthetic pathways of (a) serine, (b) alanine, (c) glutamate and (d) aspartate. Serine is formed from the glycolytic intermediate 3-phosphoglycerate via a 3-step process. $\alpha\text{-AA}$ = α -amino acids, $\alpha\text{-KA}$ = α -keto acids. Alanine is formed via the transamination of pyruvate. Glutamate and aspartate are formed by the reductive amination of α -ketoglutarate and oxaloacetate, respectively.

Figure 4.8a) and, therefore, it is more energetically efficient to use serine provided in the diet. Since the majority of glycine is formed from serine, its isotopic signature will reflect the isotopic signature of serine (either dietary or biosynthesised), as well as dietary glycine. The C₃ protein/C₄ energy diet indicates that aspartate and glutamate are not directly incorporated from dietary protein. These amino acids are biosynthesised from oxaloacetate and α -ketoglutarate, respectively (see Figure 4.8c and d), which are intermediates of the citric acid cycle, so their isotopic signal is a mixture of the isotopic signal of protein, carbohydrates and lipids in the diet. It is unclear why the aspartate and glutamate from the C₄ protein/C₃ energy diet do not show the same large $\Delta^{13}\text{C}_{\text{collAA-dietAA}}$ values. The $\Delta^{13}\text{C}_{\text{collAA-dietAA}}$ values observed for proline are no larger in the mixed diets than the pure diets. This suggests that proline in bone collagen is incorporated from the diet rather than being biosynthesised from glutamate. These findings are in agreement with work carried out by Bier (1989), who compared the whole body flux of specific amino acids in healthy adults with the relative concentrations of these amino acids in proteins. He found evidence for substantial *de novo* synthesis of some of the non-essential amino acids, including glutamate, glutamine, glycine and alanine, whilst the close agreements of fluxes with concentration in proteins for proline and arginine indicated much lower rates of *de novo* synthesis. Although no data is available here for arginine or glutamine, the remaining amino acids agree with these observations.

4.5.3 $\delta^{13}\text{C}$ values for the amino acids of marine protein diet and rat collagen

Tables 4.7 to 4.9 present the $\delta^{13}\text{C}$ values of individual amino acids from the three marine protein diets and the bone collagen of rats raised on these diets. Twelve such rat collagens have been analysed with six being raised, two each, on the three 20% marine protein diets. Another six rats were raised, two each, on diets which were essentially isotopically identical to the former diets, but which contained 70% marine protein. Therefore isotope data for diets D9J3, D10K3 and D11L3 are isotopically identical to diets D6J2, D7K2 and D8L2, respectively. A range in dietary amino acid $\delta^{13}\text{C}$ values of *ca.* 20‰ was observed, which is

comparable to that observed in the terrestrial protein diets. There were differences in the relative isotopic pattern and amino acid distribution between the terrestrial and marine protein diets due to the different sources of protein.

Figure 4.9 compares the $\Delta^{13}\text{C}_{\text{collAA-dietAA}}$ values for all three 20% marine protein diets. Differences in spacings between amino acids are less obvious in these diets

Table 4.7. Individual amino acid $\delta^{13}\text{C}$ values for marine protein diets. Errors are shown in parentheses.

	Diet (‰)		
	D6J2	D7K2	D8L2
Ala	-17.7 (1.1)	-15.2 (1.1)	-14.4 (2.5)
Val	-20.1 (1.2)	-17.5 (0.9)	-18.1 (0.9)
Thr	-14.7 (1.0)	-10.5 (1.4)	-13.4 (1.2)
Gly	-6.1 (2.4)	-3.4 (1.5)	-1.5 (1.8)
Ile	-19.0 (0.8)	-18.7 (1.1)	-17.8 (1.1)
Ser	-6.8 (1.4)	-1.7 (1.4)	-4.2 (1.7)
Leu	-25.9 (1.4)	-24.6 (0.8)	-24.9 (0.8)
Pro	-9.5 (1.0)	-9.7 (1.2)	-9.6 (1.1)
Asp	-19.1 (1.3)	-18.6 (1.3)	-17.2 (1.3)
Glu	-10.6 (1.1)	-11.4 (1.1)	-11.1 (1.1)
Phe	-25.6 (0.7)	-25.1 (0.7)	-24.9 (0.7)

Table 4.8. Individual amino acid $\delta^{13}\text{C}$ values from bone collagen of rats raised on 20% marine protein diets. Errors are shown in parentheses.

	Tissue Code					
	MP/C ₃		MP/C ₄		MP/C ₃ + C ₄	
Ala	-24.4 (1.6)	-17.4 (1.1)	-12.2 (1.1)	-7.1 (1.0)	-16.1 (1.1)	-14.3 (1.0)
Val	-22.2 (1.5)	-21.9 (1.0)	-26.3 (1.5)	-19.8 (0.9)	-22.3 (1.9)	-21.5 (0.6)
Thr	-14.4 (1.8)	-11.6 (1.2)	-17.9 (0.9)	-9.5 (1.6)	-9.6 (1.4)	-10.0 (1.6)
Gly	-11.3 (1.8)	-12.9 (1.3)	-4.1 (1.1)	-2.5 (1.3)	-10.2 (2.4)	-7.5 (1.3)
Ile	-15.6 (0.6)	-17.6 (0.8)		-15.5 (1.6)		-17.4 (1.1)
Ser	-13.2 (1.4)	-8.9 (1.9)	-8.5 (1.4)	0.5 (1.2)	-6.9 (1.9)	-3.4 (1.1)
Leu	-28.5 (0.9)	-30.3 (0.8)	-30.3 (0.9)	-26.7 (0.6)	-29.4 (0.6)	-31.6 (1.9)
Pro	-10.2 (1.0)	-9.6 (0.7)	-6.4 (1.0)	-6.6 (1.2)	-7.6 (0.7)	-7.4 (0.6)
Hyp	-17.6 (0.9)	-16.1 (0.9)	-13.3 (0.9)	-11.9 (0.6)	-14.3 (0.7)	-12.8 (1.0)
Asp	-19.0 (1.3)	-21.4 (1.3)	-12.4 (1.3)	-12.2 (1.3)	-14.1 (1.3)	-14.7 (1.1)
Glu	-15.8 (0.9)	-13.6 (1.1)	-3.1 (1.1)	-1.4 (1.3)	-6.4 (0.8)	-6.8 (0.8)
Phe	-23.3 (0.7)	-24.0 (0.6)	-24.7 (0.6)	-23.7 (0.5)	-23.3 (0.5)	-22.9 (0.5)

Table 4.9. Individual amino acid $\delta^{13}\text{C}$ values from bone collagen of rats raised on 70% marine protein diets. Errors are shown in parentheses.

	Tissue Code					
	MP/C ₃		MP/C ₄		MP/C ₃ + C ₄	
Ala	-17.4 (1.6)	-15.4 (1.3)	-13.3 (1.1)	-8.5 (1.3)	-17.7 (0.8)	-13.9 (1.0)
Val	-24.4 (4.6)	-17.6 (2.1)	-19.4 (0.9)	-16.9 (1.5)		-16.0 (1.5)
Thr	-15.7 (1.6)	-9.5 (1.2)	-12.5 (2.9)	-12.5 (1.4)	-14.8 (1.2)	-14.3 (1.4)
Gly	-5.1 (1.8)	-9.3 (1.1)	-11.3 (1.5)	-7.0 (1.1)	-7.1 (1.3)	-8.1 (1.1)
Ile		-16.2 (1.6)	-15.9 (1.2)	-14.8 (0.8)		-15.0 (2.8)
Ser	-9.1 (1.7)	-6.5 (1.1)	-8.1 (1.2)	-3.9 (1.4)	-8.9 (1.7)	-5.0 (1.7)
Leu	-26.8 (0.7)	-24.9 (0.6)	-29.8 (0.9)	-25.7 (0.6)	-26.6 (0.9)	-26.7 (1.1)
Pro	-7.9 (0.6)	-7.8 (0.6)	-9.8 (0.9)	-6.1 (0.7)	-7.9 (0.6)	-5.0 (0.7)
Hyp	-15.6 (0.6)	-18.2 (0.6)	-16.1 (0.9)	-15.5 (0.9)	-15.5 (1.0)	-15.3 (1.0)
Asp	-15.4 (1.5)	-15.4 (1.1)	-16.9 (2.0)	-12.2 (1.3)	-15.5 (1.3)	-13.5 (1.5)
Glu	-9.0 (0.9)	-9.3 (1.3)	-9.4 (0.9)	-5.1 (1.1)	-7.7 (1.1)	-5.3 (0.5)
Phe	-24.2 (0.9)	-23.7 (0.8)	-26.0 (0.5)	-23.7 (0.8)	-23.7 (0.5)	-22.9 (0.7)

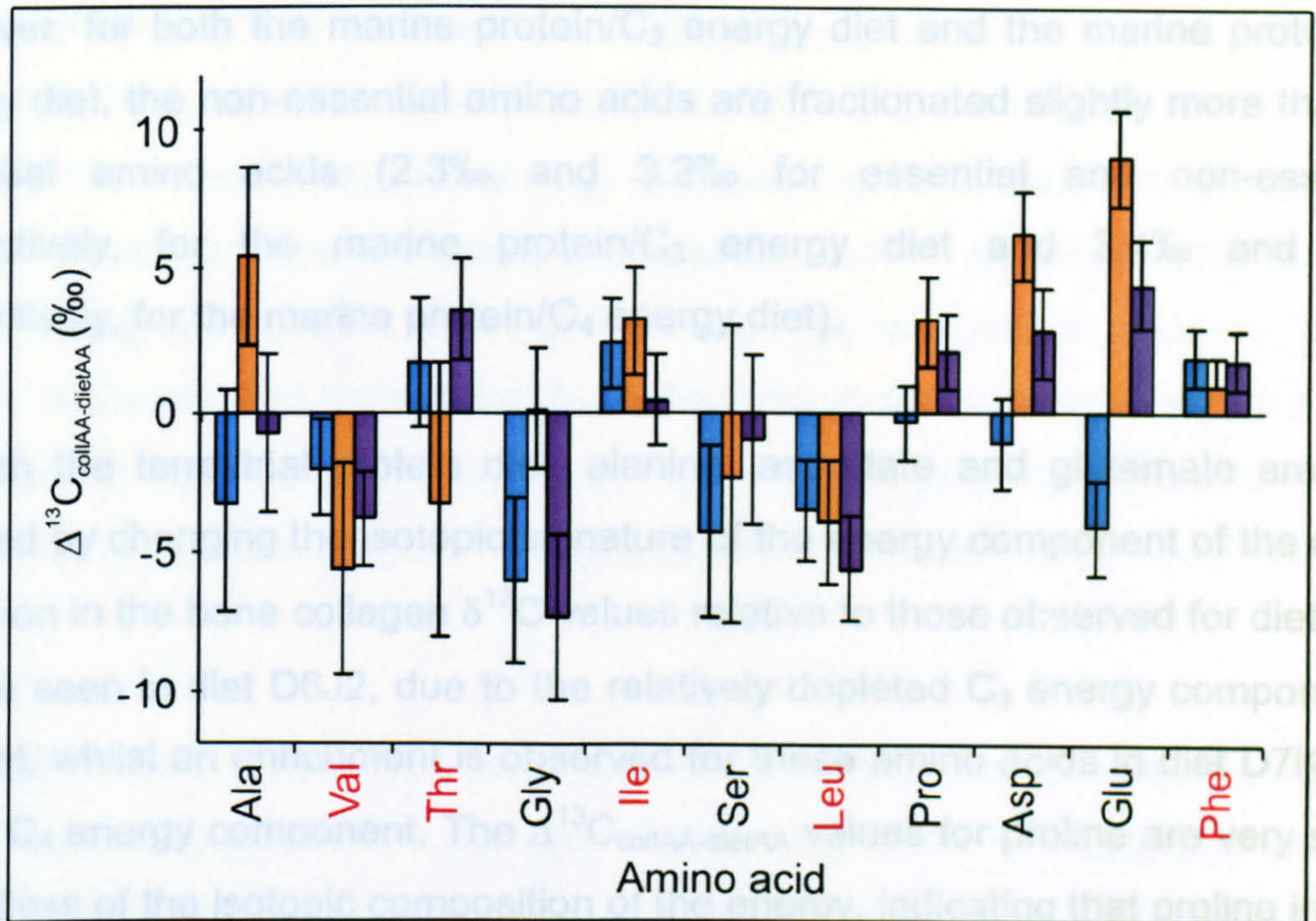


Figure 4.9. Bar chart showing the $\Delta^{13}\text{C}_{\text{collAA-dietAA}}$ values for each amino acid for the 20% marine protein diets. MP/C₃ in blue, MP/C₄ in orange and MP/C₃+C₄ in purple. Essential amino acids are indicated in red.

than for those seen previously in Section 4.5.2. The reason for this is two-fold. Firstly, the differences in the isotopic compositions of the dietary protein and energy are much smaller than for the mixed terrestrial protein diets; in fact the largest isotopic difference is only 7.3‰ for the marine protein/C₃ energy diet. The second obstacle to interpretation of these results is the increased size of the errors for this data. However, some conclusions can be drawn from this data. For the marine protein diets, diet D8L2 can be assumed to be comparable with a pure diet as the isotopic composition of the protein and energy components is very similar. Therefore changes in $\Delta^{13}\text{C}_{\text{collAA-dietAA}}$ values for diets D6J2 and D7K2 can be assessed relative to D8L2. An average $\Delta^{13}\text{C}_{\text{collAA-dietAA}}$ value of 3‰ was observed for both essential and non-essential amino acids in the marine protein /C₃ + C₄ energy diet. As with the pure C₃ and C₄ diets it is impossible to draw conclusions as to the contribution of the energy component of the diet to the non-essential amino acids in the bone collagen.

However, for both the marine protein/C₃ energy diet and the marine protein/ C₄ energy diet, the non-essential amino acids are fractionated slightly more than the essential amino acids (2.3‰ and 3.2‰ for essential and non-essential, respectively, for the marine protein/C₃ energy diet and 3.4‰ and 4.4‰ respectively, for the marine protein/C₄ energy diet).

As with the terrestrial protein diet, alanine, aspartate and glutamate are most affected by changing the isotopic signature of the energy component of the diet. A depletion in the bone collagen $\delta^{13}\text{C}$ values relative to those observed for diet D8L2 can be seen in diet D6J2, due to the relatively depleted C₃ energy component of the diet, whilst an enrichment is observed for these amino acids in diet D7K2 due to the C₄ energy component. The $\Delta^{13}\text{C}_{\text{collAA-dietAA}}$ values for proline are very similar regardless of the isotopic composition of the energy, indicating that proline in bone collagen is routed directly from dietary proline as suggested by the terrestrial protein results.

The remaining two non-essential amino acids, glycine and serine, give more ambiguous $\Delta^{13}\text{C}_{\text{collAA-dietAA}}$ values. Serine from the marine protein/C₃ energy diet shows the expected depletion, but the error bar on the marine protein/C₄ energy diet is so large as to make the unexpected observed depletion meaningless. Once again, glycine from the marine protein/C₃ energy diet shows the expected depletion, but there is no evidence for the incorporation of the C₄ energy component into glycine and the marine protein/C₃ + C₄ energy diet shows an uncharacteristically large depletion for an essentially pure diet.

It is interesting to note that there is a pattern in the isotopic fractionation seen for some of the essential amino acids resulting from assimilation and transport processes. Leucine in bone collagen is consistently depleted with respect to dietary leucine, whilst phenylalanine and isoleucine are enriched relative to their dietary sources. This may suggest that the fractionations are not random but can be attributed to specific processes that occur for these amino acids.

Figures 4.10 and 4.11 compare the $\Delta^{13}\text{C}_{\text{collAA-dietAA}}$ values for the 20% and 70% marine protein diets. Increased incorporation of dietary protein can clearly be seen for the 70% marine protein/ C_3 energy diet (see Figure 4.10a). The $\Delta^{13}\text{C}_{\text{collAA-dietAA}}$ values for the non-essential amino acids, which showed evidence of incorporation of the energy component when 20% of the diet was protein (alanine, glycine, serine, aspartate and glutamate), have become more consistent with the values expected for a pure diet. This incorporation of dietary protein is also evidenced by the decrease in the average $\Delta^{13}\text{C}_{\text{collAA-dietAA}}$ value for these amino acids from 3.7‰ to 1.7‰.

The 70% marine protein/ C_4 energy diet also indicates increased incorporation of the protein component of the diet (see Figure 4.10b). The $\Delta^{13}\text{C}_{\text{collAA-dietAA}}$ values for alanine, aspartate and glutamate have moved away from the 20% values towards those observed for the 'pure' marine protein/ $\text{C}_3 + \text{C}_4$ energy diet, indicating less incorporation of the enriched C_4 energy component into these amino acids. The ambiguous results seen previously for glycine and serine lead to difficulties in interpreting changes caused by increasing the protein content of the diet. The change in the $\Delta^{13}\text{C}_{\text{collAA-dietAA}}$ value for serine is inconclusive due to the large error bar for serine in the 20% protein diet. It is not possible to say whether there is a significant change, and the 70% protein value does show more incorporation of dietary serine. The isotope value for glycine from the 70% marine protein/ C_4 energy diet is depleted relative to the value for the 20% protein diet as expected when decreasing the amount of C_4 signal in the diet. However the depletion of 7.4‰ from the dietary glycine value is surprisingly large when an increase in the incorporation of dietary glycine is expected. Although this depletion is larger than others observed for the pure terrestrial protein diets, it is in agreement with the large $\Delta^{13}\text{C}_{\text{collAA-dietAA}}$ value observed for glycine in the marine protein/ $\text{C}_3 + \text{C}_4$ energy diets.

The spacings observed for the essential amino acids in all the marine protein diets remain unchanged when the percentage of protein in the diet is changed. This is as expected as the essential amino acids will be routed from dietary protein regardless of the protein content of the diet.

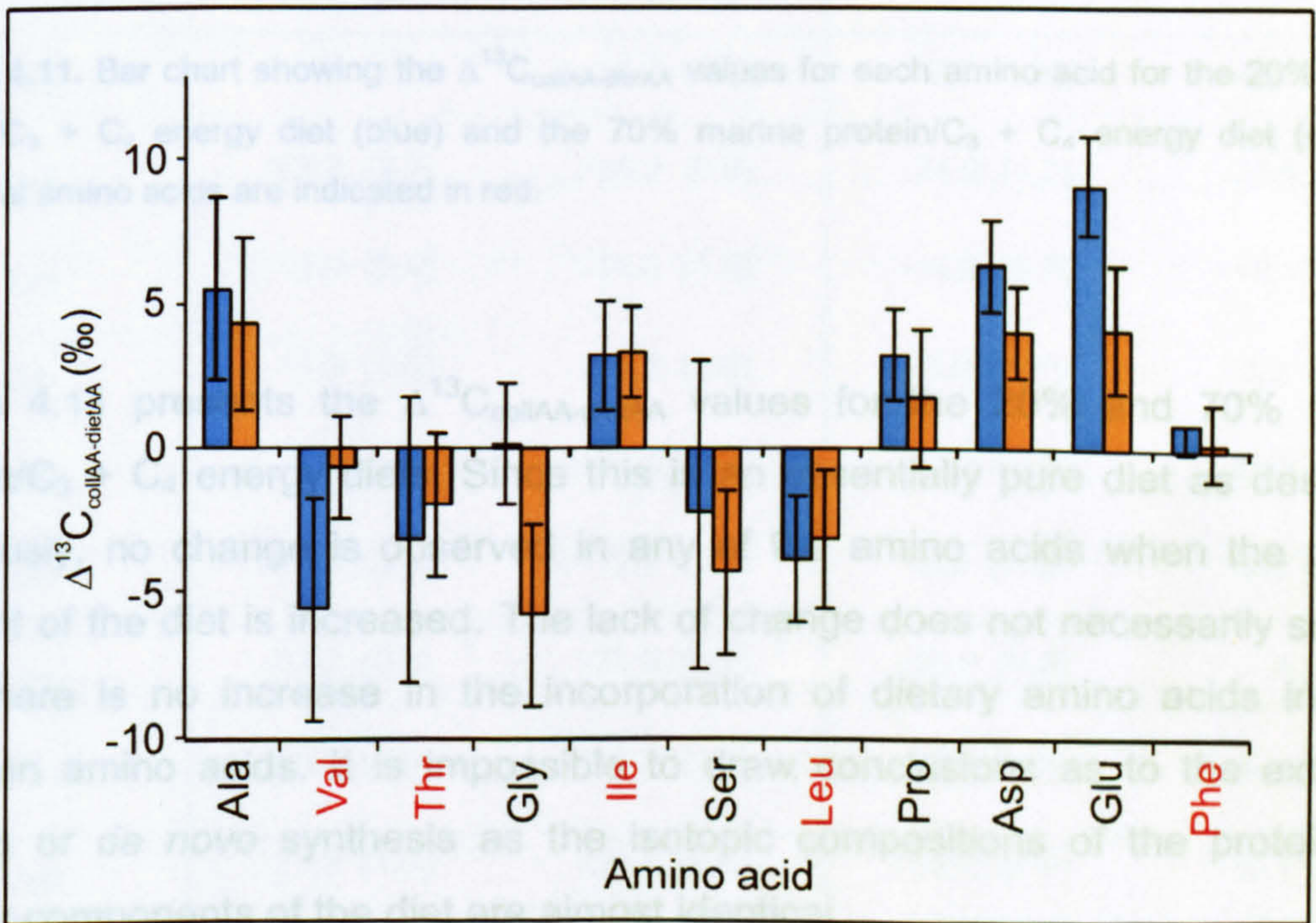
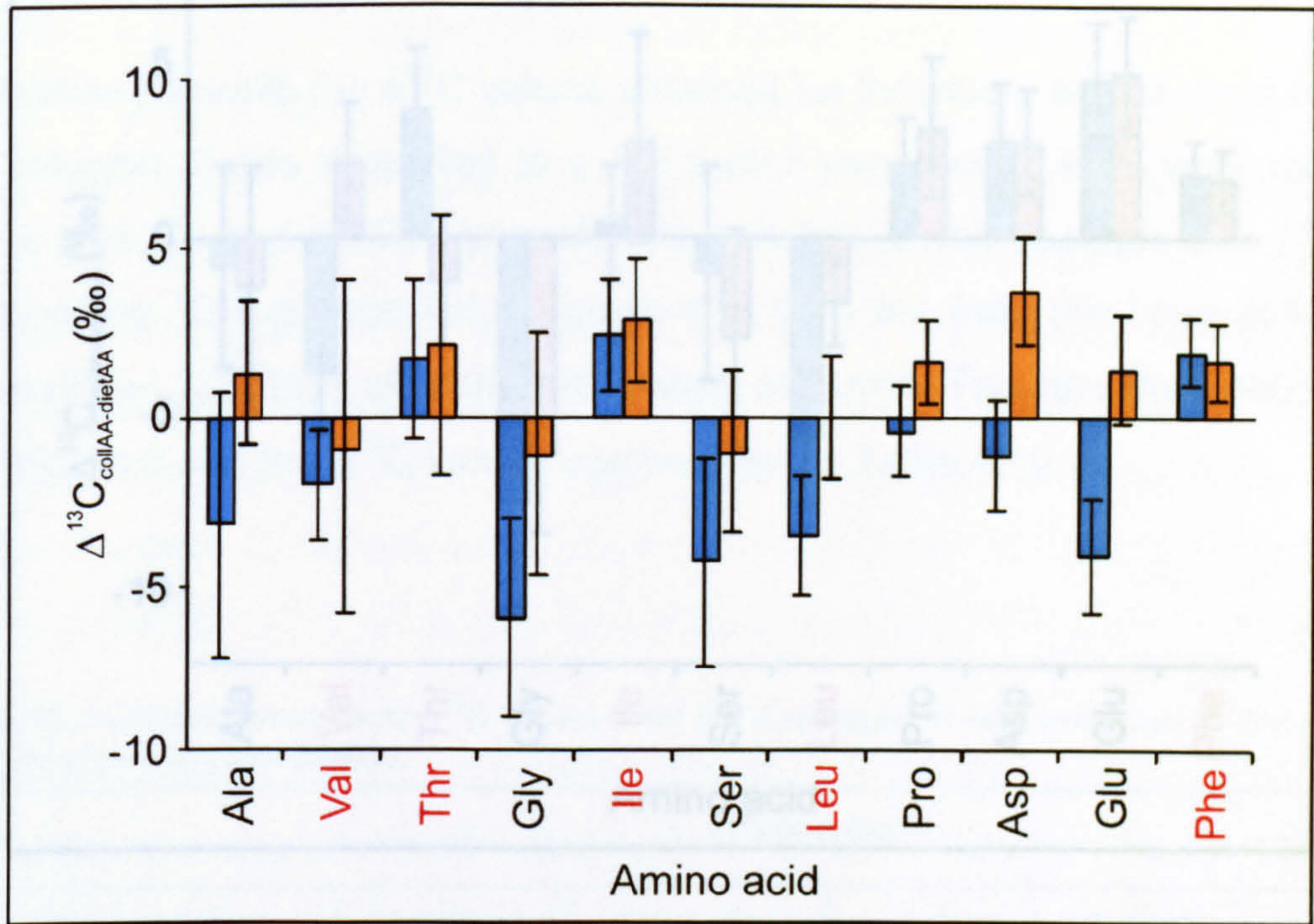


Figure 4.10. Bar chart showing the $\Delta^{13}C_{collIAA-dietAA}$ values for each amino acid for (a) the marine protein/ C_3 energy diets and (b) the marine protein/ C_4 energy diets. The 20% protein diets are in blue and 70% protein diets are in orange. Essential amino acids are indicated in red.

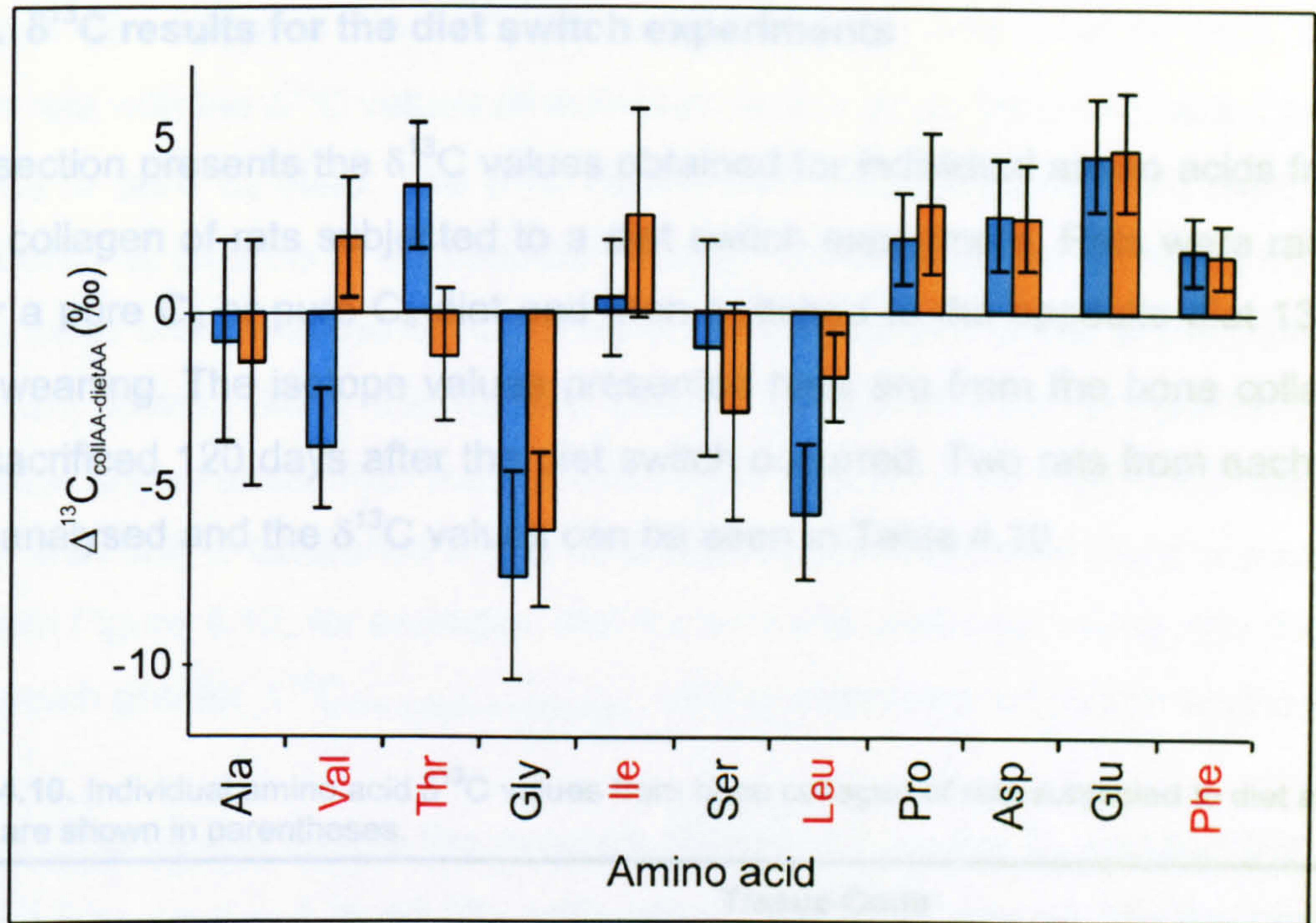


Figure 4.11. Bar chart showing the $\Delta^{13}\text{C}_{\text{collIAA-dietAA}}$ values for each amino acid for the 20% marine protein/ $\text{C}_3 + \text{C}_4$ energy diet (blue) and the 70% marine protein/ $\text{C}_3 + \text{C}_4$ energy diet (orange). Essential amino acids are indicated in red.

Figure 4.11 presents the $\Delta^{13}\text{C}_{\text{collIAA-dietAA}}$ values for the 20% and 70% marine protein/ $\text{C}_3 + \text{C}_4$ energy diets. Since this is an essentially pure diet as described previously, no change is observed in any of the amino acids when the protein content of the diet is increased. The lack of change does not necessarily suggest that there is no increase in the incorporation of dietary amino acids in bone collagen amino acids. It is impossible to draw conclusions as to the extent of routing or *de novo* synthesis as the isotopic compositions of the protein and energy components of the diet are almost identical.

In general the results of these experiments have shown that increasing the protein content of the diet does increase the incorporation of the dietary protein signal into the non-essential amino acids.

4.5.4. $\delta^{13}\text{C}$ results for the diet switch experiments

This section presents the $\delta^{13}\text{C}$ values obtained for individual amino acids from the bone collagen of rats subjected to a diet switch experiment. Rats were raised on either a pure C_3 or pure C_4 diet and then switched to the opposite diet 131 days after weaning. The isotope values presented here are from the bone collagen of rats sacrificed 120 days after the diet switch occurred. Two rats from each switch were analysed and the $\delta^{13}\text{C}$ values can be seen in Table 4.10.

Table 4.10. Individual amino acid $\delta^{13}\text{C}$ values from bone collagen of rats subjected to diet switches. Errors are shown in parentheses.

	Tissue Code			
	C_3 to C_4		C_4 to C_3	
Ala	-17.0 (1.0)	-14.7 (1.6)	-9.4 (1.1)	-6.4 (1.0)
Val	-23.7 (3.3)	-24.2 (0.9)	-24.9 (1.2)	-27.6 (2.3)
Thr	-13.9 (2.4)	-14.8 (1.0)	-14.9 (3.7)	-15.1 (3.7)
Gly	-16.5 (1.5)	-17.2 (1.8)	-6.5 (1.8)	-4.8 (1.1)
Ile	n.d.	-23.2 (1.1)	-17.3 (1.6)	-18.8 (0.9)
Ser	-10.5 (3.5)	-12.2 (1.2)	-8.2 (1.9)	-8.3 (1.7)
Leu	-33.2 (0.8)	-31.9 (0.7)	-25.5 (0.8)	n.d.
Pro	-16.1 (0.9)	-13.8 (1.2)	-5.6 (0.9)	-4.1 (0.7)
Hyp	-21.3 (1.0)	-24.1 (0.6)	-12.0 (0.7)	-10.1 (0.9)
Asp	-20.4 (1.5)	-16.5 (2.0)	-13.5 (1.1)	-13.9 (1.1)
Glu	-14.9 (1.1)	-10.4 (1.7)	-7.1 (1.3)	-5.0 (1.3)
Phe	-25.9 (0.6)	-25.1 (0.5)	-17.6 (0.7)	-14.8 (0.6)

Figure 4.12 compares the $\delta^{13}\text{C}$ values of individual amino acids from the diet switch rats with the $\delta^{13}\text{C}$ values of individual amino acids from rats raised on either pure C_3 or pure C_4 diets. The $\delta^{13}\text{C}$ values from rats raised on pure diets can be considered as controls or endmember values. It is immediately apparent that some amino acids show enhanced incorporation of the isotopic signal of the post-switch diet than others. Since the relative pattern of the isotopic composition of the individual amino acids from the bone collagen of pure C_3 and pure C_4 rats is very similar with only a difference in the absolute values of *ca.* 10-15‰ it is possible to say from Figure 4.12, for example, that for both diet switches, valine and threonine have much greater $\Delta^{13}\text{C}_{\text{diet switch-endmember}}$ values compared with other amino acids.

For the C_3 to C_4 diet switch, the average difference from the C_3 endmember values ($\Delta^{13}\text{C}_{\text{diet switch-endmember}}$) is +3.5‰ with values ranging from -1.8‰ for glycine to +9.8‰ for threonine. For the C_4 to C_3 diet switch, the average $\Delta^{13}\text{C}_{\text{diet switch-endmember}}$ value is -3.0‰ with values ranging from +2.9‰ for alanine to -9.8‰ for valine. These differences can be compared to the differences observed in the bulk collagen values for these rats (Table 4.11). The mean difference for the individual amino acid $\delta^{13}\text{C}$ values is larger than the differences between endmember and diet switch bulk collagen values.

In fact, the bulk collagen values mask some of the large incorporations seen for the individual amino acids. This is possible due to the fact that those amino acids which comprise a large proportion of collagen, namely glycine, proline and hydroxyproline show no incorporation at all of the isotopic signal of the post-switch diet. Glycine, proline and hydroxyproline show differences of -1.8, +0.5 and -0.2, respectively, for the C_3 to C_4 diet switch and +0.9, -0.7 and -0.5 for the C_4 to C_3 diet switch. These differences are well within the margin of error. These three amino acids comprise 44.2% of the carbon in collagen; therefore it is unsurprising that if these individual amino acids show little effect of the diet switch, the bulk collagen values will also appear to show little incorporation. This is coupled with the fact that the amino acids that show the largest incorporation of the diet contribute a relatively small amount of carbon to collagen.

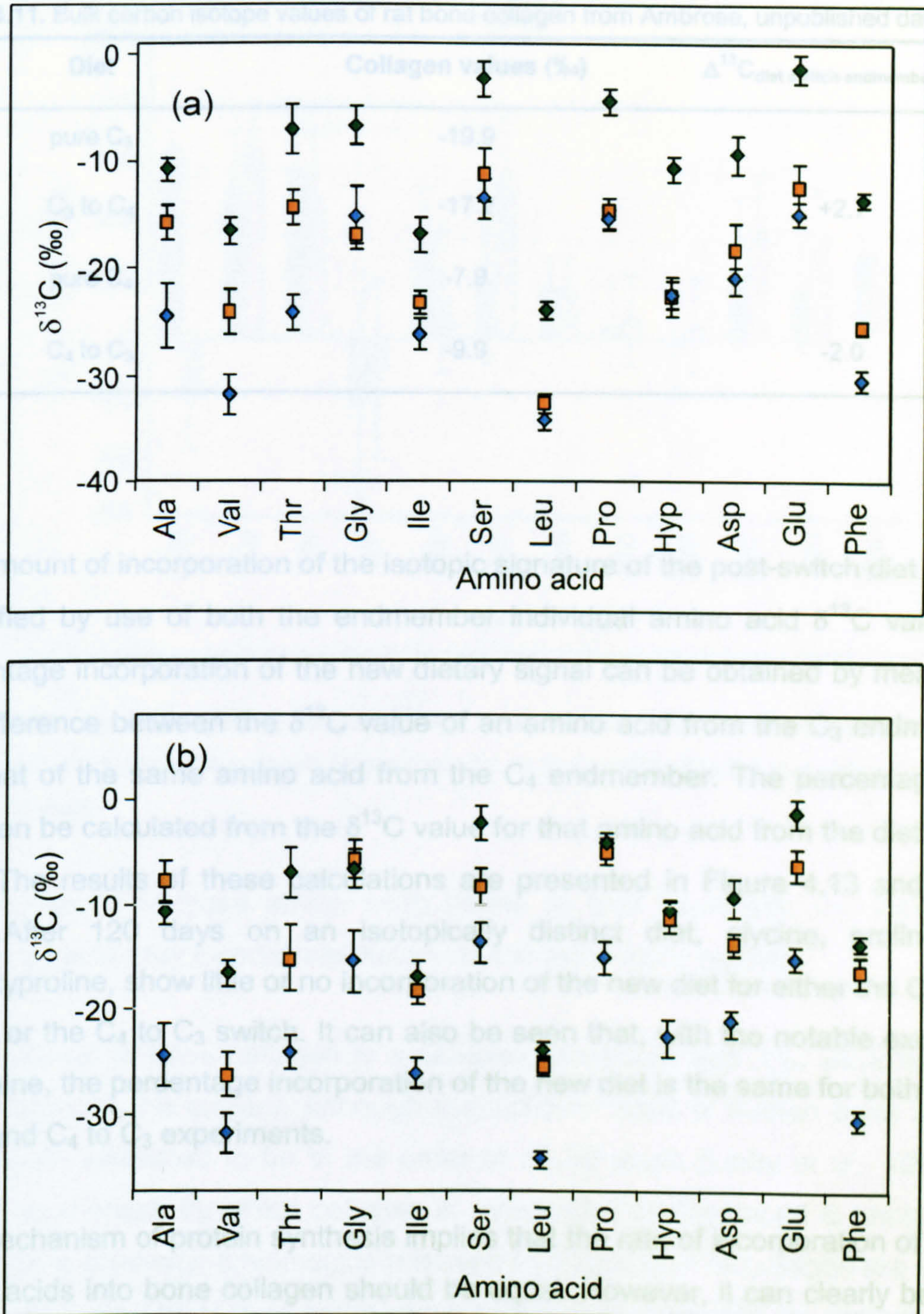


Figure 4.12. Scattergrams comparing the individual amino acid $\delta^{13}\text{C}$ values from bone collagen of rats from (a) pure C_3 diet (blue diamonds), C_3 to C_4 diet switch (squares) and pure C_4 diet (green diamonds) and (b) pure C_4 diet (green diamonds), C_4 to C_3 diet switch (squares) and pure C_3 diet (blue diamonds). All values are an average from two rats.

Table 4.11. Bulk carbon isotope values of rat bone collagen from Ambrose, unpublished data.

Diet	Collagen values (‰)	$\Delta^{13}\text{C}_{\text{diet switch-endmember}}$ (‰)
pure C ₃	-19.9	
C ₃ to C ₄	-17.2	+2.7
pure C ₄	-7.9	
C ₄ to C ₃	-9.9	-2.0

The amount of incorporation of the isotopic signature of the post-switch diet can be quantified by use of both the endmember individual amino acid $\delta^{13}\text{C}$ values. A percentage incorporation of the new dietary signal can be obtained by measuring the difference between the $\delta^{13}\text{C}$ value of an amino acid from the C₃ endmember and that of the same amino acid from the C₄ endmember. The percentage shift can then be calculated from the $\delta^{13}\text{C}$ value for that amino acid from the diet switch data. The results of these calculations are presented in Figure 4.13 and Table 4.12. After 120 days on an isotopically distinct diet, glycine, proline and hydroxyproline, show little or no incorporation of the new diet for either the C₃ to C₄ switch or the C₄ to C₃ switch. It can also be seen that, with the notable exception of alanine, the percentage incorporation of the new diet is the same for both the C₃ to C₄ and C₄ to C₃ experiments.

The mechanism of protein synthesis implies that the rate of incorporation of all the amino acids into bone collagen should be equal. However, it can clearly be seen from Figure 4.13 and Table 4.12 that the relative amount of post-switch diet amino acids incorporated into bone collagen after 120 days is very different for each of the amino acids. Since the turnover times of all the amino acids in bone collagen must be the same, these differences must be due to the availability of other sources of amino acids for protein synthesis. This diet switch experiment only allows the rate of incorporation of dietary amino acids into bone collagen to be studied, whilst in practice amino acids for protein synthesis can be provided by *de novo* synthesis and protein breakdown. It is also likely that the intracellular

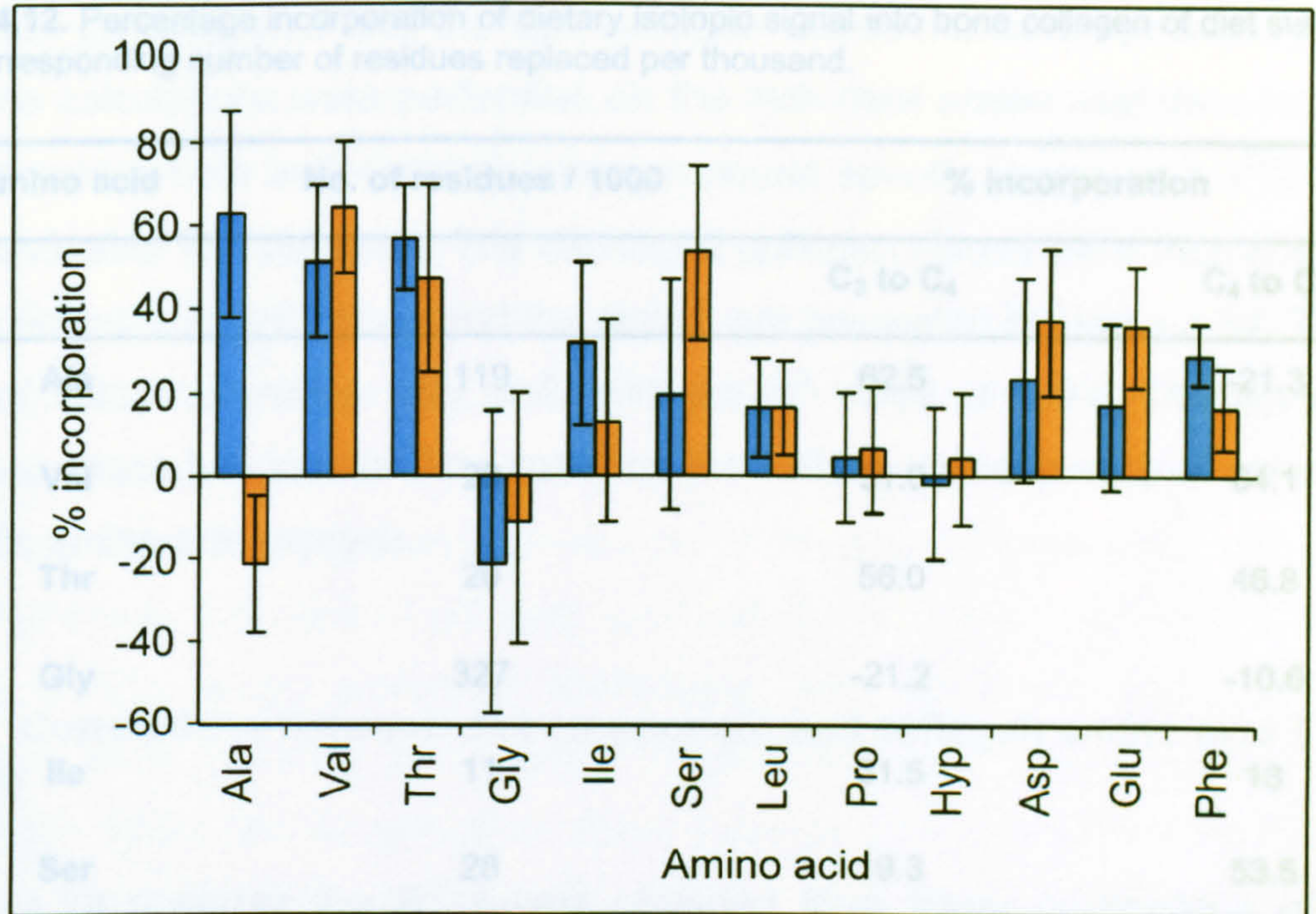


Figure 4.13. Bar chart showing the percentage incorporation of the isotopic signal into individual amino acids from the bone collagen of rats from the C₃ to C₄ diet switch (blue) and the C₄ to C₃ diet switch (orange).

concentrations of these amino acids varies so that those with low intracellular concentrations may incorporate dietary amino acids more readily.

The turnover of bone collagen is a complex procedure and little work has been undertaken on the subject. Although the turnover rates of human bone collagen have been estimated to be in the order of 10-30 years (Libby *et al.*, 1964), the actual mechanism by which collagen is remodelled and replaced is unclear. It is known that generally, amino acids released by breakdown of collagen are used as metabolic fuels rather than being reused in protein synthesis, so dietary protein should provide most of the new amino acids used for collagen synthesis. However, it has not yet been realised why some dietary amino acids should be incorporated into bone collagen faster than others.

The amino acids for which $\delta^{13}\text{C}$ values have been obtained comprise 83.5% of the carbon in collagen. Since the number of residues of each amino acid in collagen is known, it is possible using mass balance equations to obtain an estimated bulk $\delta^{13}\text{C}$ value for the bone collagen from the individual amino acid data. This value

Table 4.12. Percentage incorporation of dietary isotopic signal into bone collagen of diet switch rats and corresponding number of residues replaced per thousand.

Amino acid	No. of residues / 1000	% incorporation	
		C ₃ to C ₄	C ₄ to C ₃
Ala	119	62.5	-21.3
Val	20	51.0	64.1
Thr	20	56.0	46.8
Gly	327	-21.2	-10.6
Ile	11	31.5	13
Ser	28	19.3	53.5
Leu	24	16.2	16.2
Pro	113	4.4	6.2
Hyp	96	-1.7	4.2
Asp	45	23.3	36.7
Glu	75	16.7	35.5
Phe	15	28.8	16.5

4.6. Correlations of the isotope data

4.6.1. Mass balance of individual amino acid bone collagen data

The amino acids for which $\delta^{13}\text{C}$ values have been obtained comprise 83.5% of the carbon in collagen. Since the number of residues of each amino acid in collagen is known, it is possible using mass balance equations to obtain an estimated bulk $\delta^{13}\text{C}$ value for the bone collagen from the individual amino acid data. This value

can then be compared with the bulk collagen values measured previously. Mass balance calculations were performed on the individual amino acid data for all the rats for which both bulk collagen and compound specific amino acid $\delta^{13}\text{C}$ values were available (23 samples). The estimated collagen values were then compared to the actual collagen values and the results are presented in Figure 4.14. The two sets of values correlate very well, with an R^2 value of 0.91. The agreement between these two sets of data confirms the validity and accuracy of compound-specific amino acid analysis.

4.6.2 Correlations between diet component and collagen amino acid $\delta^{13}\text{C}$ values

Table 4.13 presents the R^2 values obtained from linear correlations of bone collagen amino acids versus dietary and tissue components. As expected, the essential amino acids correlated highly with the protein component of the diet and the dietary amino acids. This is expected due to the routing that must occur for these amino acids (see Figure 4.15a).

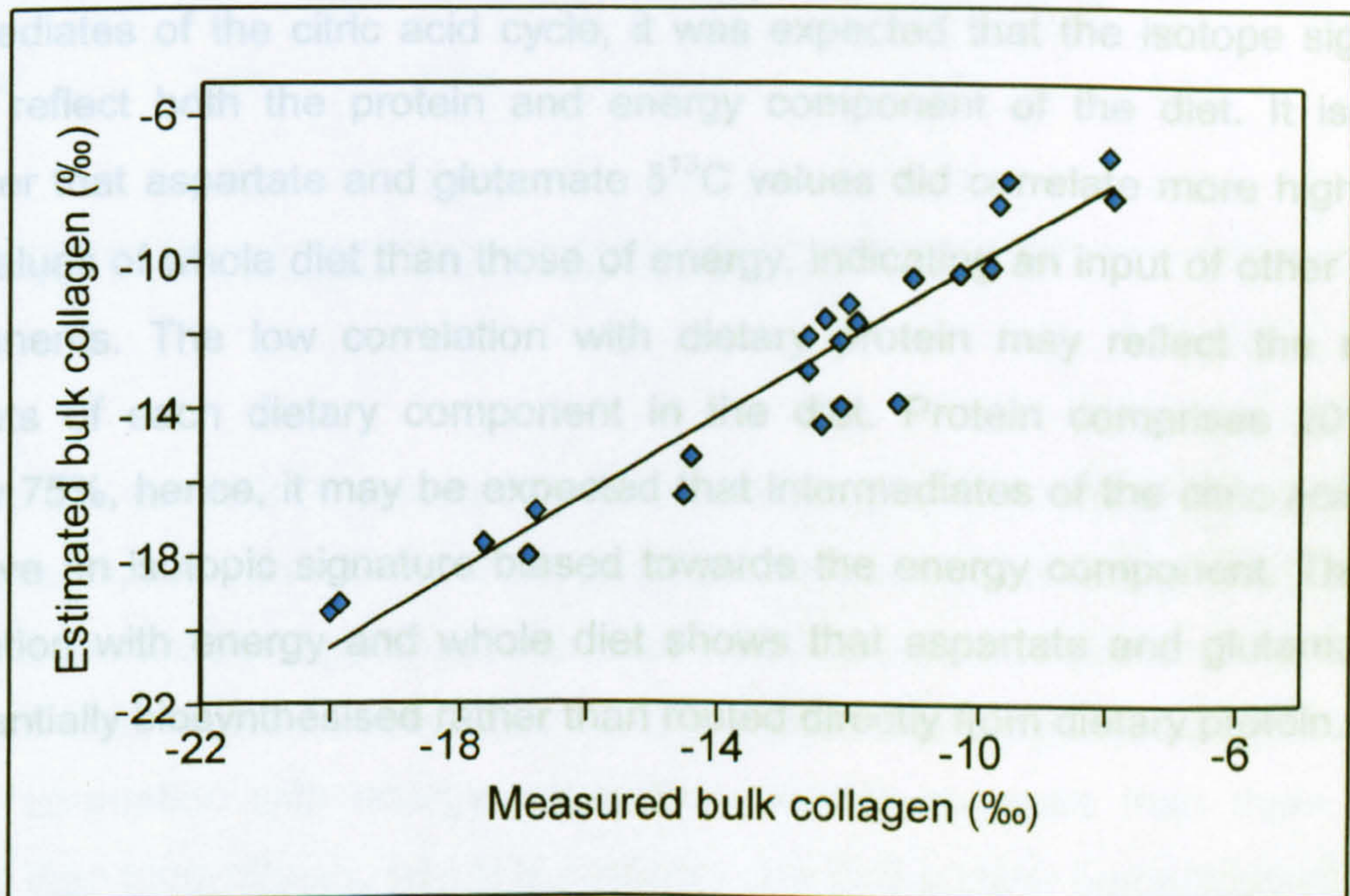


Figure 4.14. Correlation of measured bulk collagen values with estimated bulk collagen values from mass balance of individual amino acid $\delta^{13}\text{C}$ values.

Proline and hydroxyproline correlate extremely well with dietary protein and dietary amino acids, which confirms that despite its status as a non-essential amino acid, proline is primarily routed directly from dietary protein. Since hydroxyproline is formed from proline after incorporation into collagen ($R^2 = 0.95$), it follows that it will also correlate well with dietary protein. As a non-essential amino acid, it might be expected that proline $\delta^{13}\text{C}$ values in bone collagen would correlate with collagen glutamate $\delta^{13}\text{C}$ values since proline is synthesised *de novo* from glutamate. However, this correlation has an R^2 value of 0.22 indicating a lack of *de novo* synthesis. The lack of *de novo* synthesis for proline can further be seen in Figure 4.15(b). Since proline is synthesised from glutamate and if *de novo* synthesis were occurring then it would be expected that proline would correlate highly with whole diet, as glutamate does. It can be seen that in fact proline has a very low correlation with whole diet ($R^2 = 0.14$).

Dietary energy $\delta^{13}\text{C}$ values correlate best with alanine, aspartate and glutamate, confirming that despite the availability of dietary alanine, it is preferentially biosynthesised from pyruvate. To see such high correlation for aspartate and glutamate with energy may be slightly surprising. Due to their formation from intermediates of the citric acid cycle, it was expected that the isotope signature would reflect both the protein and energy component of the diet. It is noted however that aspartate and glutamate $\delta^{13}\text{C}$ values did correlate more highly with $\delta^{13}\text{C}$ values of whole diet than those of energy, indicating an input of other dietary components. The low correlation with dietary protein may reflect the relative amounts of each dietary component in the diet. Protein comprises 20% and energy 75%, hence, it may be expected that intermediates of the citric acid cycle will have an isotopic signature biased towards the energy component. This high correlation with energy and whole diet shows that aspartate and glutamate are preferentially biosynthesised rather than routed directly from dietary protein.

Table 4.13. R² values from linear correlations of diet components and bone collagen amino acid $\delta^{13}\text{C}$ values. Essential amino acids are indicated in red.

Diet and bone components R ² values						
Collagen amino acid	Protein	Energy	Whole diet	Diet amino acid	Collagen	Apatite
Ala	0.01	0.76	0.72	0.07	0.17	0.72
Gly	0.32	0.42	0.53	0.51	0.68	0.54
Thr	0.78	0.02	0.11	0.56	0.72	0.09
Ser	0.16	0.59	0.66	0.29	0.55	0.64
Val	0.76	0.09	0.21	0.69	0.71	0.18
Leu	0.78	0.03	0.13	0.80	0.73	0.12
Ile	0.88	2 ⁻⁰⁶	0.04	0.94	0.61	0.03
Pro	0.92	0.03	0.14	0.86	0.88	0.14
Hyp	0.85	0.16	0.32	n.d ^a	0.91	0.30
Asp	0.21	0.74	0.85	0.31	0.67	0.82
Glu	0.05	0.86	0.94	0.08	0.51	0.94
Phe	0.82	0.01	0.01	0.97	0.58	0.01

^a No R² value since hydroxyproline is not present in the diet.

Glycine and serine $\delta^{13}\text{C}$ values did not correlate highly with any of the diet or bone components, but they did show a high degree of correlation with whole diet. Since they are formed from glycolytic intermediates this indicates that in bone collagen they are both routed directly from dietary protein and synthesised *de novo*. The higher correlation with energy rather than protein suggests that there is less routing than biosynthesis, which is probably due to the lower percentage of protein in the diet.

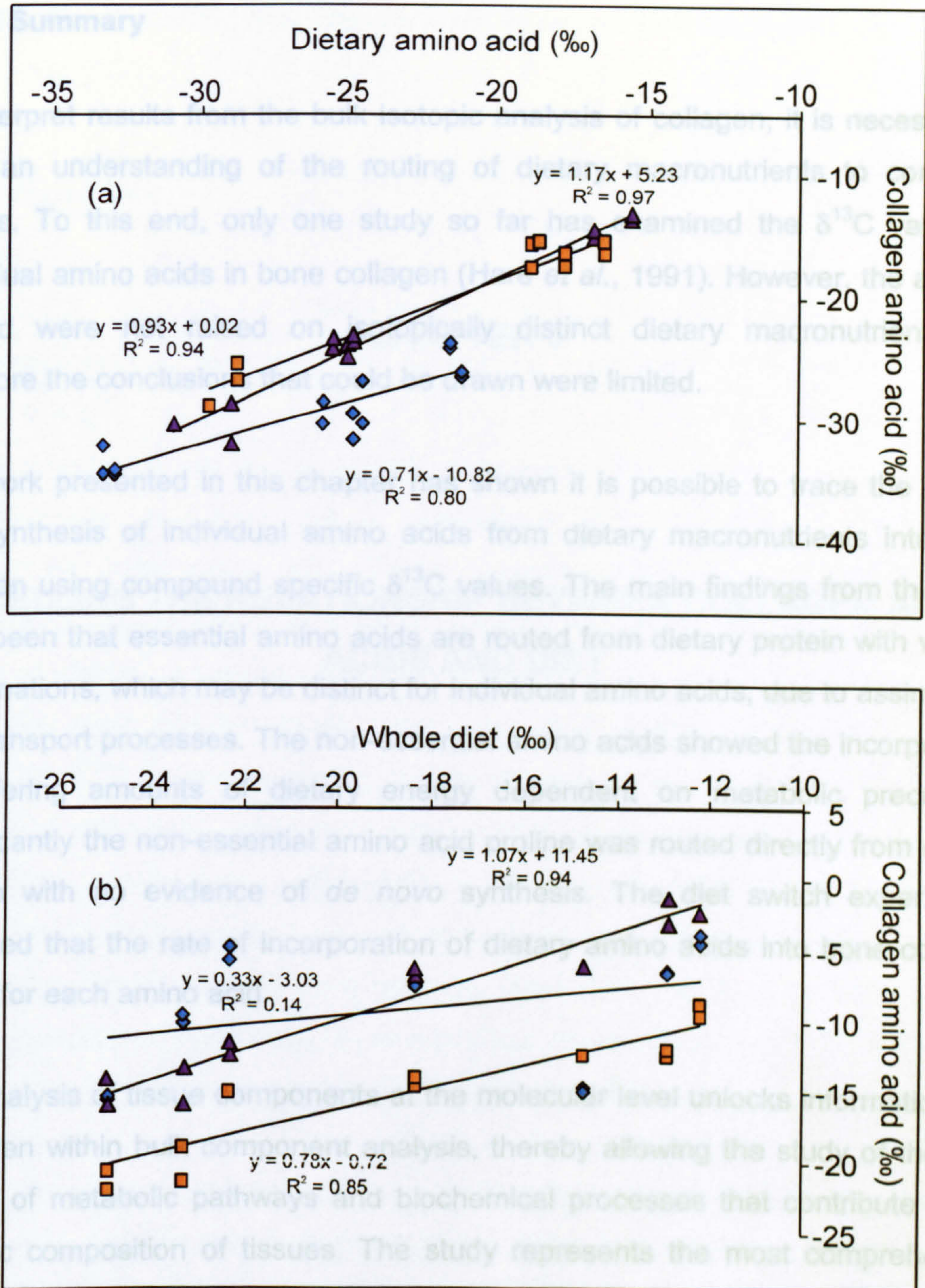


Figure 4.15. Correlations for bone collagen amino acids with (a) dietary amino acids (diamonds = leucine, squares = isoleucine, triangles = phenylalanine) and (b) whole diet (diamonds = proline, squares = aspartate, triangles = glutamate).

4.7 Summary

To interpret results from the bulk isotopic analysis of collagen, it is necessary to have an understanding of the routing of dietary macronutrients to consumer tissues. To this end, only one study so far has examined the $\delta^{13}\text{C}$ values of individual amino acids in bone collagen (Hare *et al.*, 1991). However, the animals studied were not raised on isotopically distinct dietary macronutrients and therefore the conclusions that could be drawn were limited.

The work presented in this chapter has shown it is possible to trace the routing and synthesis of individual amino acids from dietary macronutrients into bone collagen using compound specific $\delta^{13}\text{C}$ values. The main findings from this work have been that essential amino acids are routed from dietary protein with varying fractionations, which may be distinct for individual amino acids, due to assimilation and transport processes. The non-essential amino acids showed the incorporation of differing amounts of dietary energy dependent on metabolic precursors. Significantly the non-essential amino acid proline was routed directly from dietary protein with no evidence of *de novo* synthesis. The diet switch experiments indicated that the rate of incorporation of dietary amino acids into bone collagen varies for each amino acid.

The analysis of tissue components at the molecular level unlocks information that is hidden within bulk component analysis, thereby allowing the study of the finer details of metabolic pathways and biochemical processes that contribute to the isotopic composition of tissues. The study represents the most comprehensive analysis of individual amino acids from a controlled feeding experiment to date and provides new evidence for the metabolic and energetic controls on bone collagen biosynthesis.

CHAPTER 5

MODELLING THE RELATIONSHIP BETWEEN COLLAGEN AMINO ACIDS AND DIET

Chapter 5 Modelling the relationship between collagen amino acids and diet

5.1 Objectives

This chapter presents the results of linear regression analysis of diet and bone component isotope data from the rat feeding experiment. The previous chapter utilised the $\delta^{13}\text{C}$ values of individual amino acids to investigate the influences of dietary macronutrients on the isotopic composition of collagen, and in so doing it was discovered that there existed correlations between individual amino acids, other bone components and dietary macronutrients. In this chapter these correlations are exploited to produce models that allow the prediction of $\delta^{13}\text{C}$ values of dietary macronutrients. Two approaches to constructing these models have been used. The first model used only individual amino acid isotopic data to predict the $\delta^{13}\text{C}$ values of dietary macronutrients, whilst the second investigates the use of other bone component isotope data (bone collagen, apatite and bone cholesterol) in conjunction with individual amino acids. All $\delta^{13}\text{C}$ values relating to bulk collagen, apatite and dietary macronutrients were measured by Ambrose and co-workers, some of which were reported previously (Ambrose and Norr, 1993), but the majority of which remains unpublished. Bone cholesterol $\delta^{13}\text{C}$ values were measured by Dr Susan Jim in our laboratory (Jim, 2000).

The two models constructed are tested using the isotopic data from a controlled pig feeding experiment. Individual amino acid and bone cholesterol isotope analyses were undertaken in our laboratory, whilst all other isotopic analyses were carried out at Harvard University. All data is unpublished.

5.2 Previous models for diet reconstruction

For it to be possible to use the isotope values of bone components to reconstruct the $\delta^{13}\text{C}$ values of the diet, it is necessary for the relationship between diet and bone components to be fully understood. To achieve this end, models must be

constructed where the spacing between (i) diet and bone components and (ii) bone components and bone components are explained. Krueger and Sullivan (1984) were one of the first groups to consider that dietary macronutrients may be preferentially routed to different bone components. They suggested that protein may be routed into collagen, whilst the energy component of the diet may be routed into apatite. Apatite is always more enriched in ^{13}C than bone collagen; however, the $\Delta^{13}\text{C}_{\text{apat-coll}}$ spacings are not consistent and differences have been observed between herbivores and carnivores. Krueger and Sullivan explain this difference as being due to the different isotopic composition of the dietary macronutrients that comprise the diets. Herbivores derive their energy from carbohydrates and their protein from plant proteins and transamination of keto-acids derived from carbohydrates. Carnivores derive their protein from meat protein and energy from animal lipids. Since lipids are known to be depleted in ^{13}C with respect to proteins and carbohydrates this produces a smaller gap between collagen and apatite for carnivores than herbivores. Data collected from wild animals fits this model very well.

Lee-Thorp *et al.* (1989) based their work on this model and further refined it by incorporating the fact that the flesh of herbivores consumed by carnivores is depleted in ^{13}C with respect to herbivore collagen. Despite refinements, the basic principle remained that the study of both apatite and bone collagen from archaeological remains yielded different information about the diet.

However, uncertainty in diet is a problem inherent with studies based on wild animals and there was a need for controlled feeding experiments was required. Two studies investigating the routing of dietary carbon into bone components via the use of controlled feeding experiments were undertaken by Ambrose and Norr (1993) and Tieszen and Fagre (1993). Both of these studies included many different diets with different isotopic compositions and this lead to the possibility of using linear regression analysis to create more sophisticated models for predicting protein and whole diet $\delta^{13}\text{C}$ values from collagen and apatite $\delta^{13}\text{C}$ values. These studies proved conclusively that dietary carbon is routed from dietary

macronutrients into specific consumer bone components and that the isotopic composition of collagen and apatite reflect different dietary signals.

More recently a third component, bone cholesterol, has been used to gain further insight into reconstructing diet composition (Jim, 2000). Bone cholesterol was shown to be an accurate proxy for short-term whole diet and in combination with collagen and apatite isotopic data, it was possible to predict dietary protein, energy and short-term and long-term whole diet isotopic compositions.

The individual amino acids that comprise collagen each have a unique isotopic composition that reflects the isotopic composition of its precursors. The previous chapter has shown that some amino acids reflect the isotopic composition of protein in the diet, whilst others incorporate the isotopic signal of the whole diet. This observation suggests that a mathematical relationship may exist between the isotopic composition of the suite of twelve amino acids that have been measured and the isotopic composition of the dietary macronutrients. It is hoped that the construction of models using individual amino acid $\delta^{13}\text{C}$ values from bone collagen will offer a reliable method of predicting the isotopic composition of dietary macronutrients from just one set of isotopic data. As well as new models based solely on individual amino acids, the models presented by Jim (2000) that were constructed from the same data set, are also utilised in order to predict the isotopic composition of dietary macronutrients.

5.3 Models for dietary reconstruction using amino acid $\delta^{13}\text{C}$ values

5.3.1 A quantitative model for predicting $\delta^{13}\text{C}$ values of dietary macronutrients and bone components from single amino acids

To discover which amino acids may be used to calculate the $\delta^{13}\text{C}$ values of dietary macronutrients and bone components, linear regression analysis was undertaken on each of the individual amino acids in bone collagen versus diet and tissue

Table 5.1. R² values from linear correlations of diet and bone components with bone collagen amino acid $\delta^{13}\text{C}$ values. * Indicates that no value is available as no hydroxyproline was observed in the diet.

Collagen amino acid	Diet and bone components R ² values						
	Protein	Energy	Whole diet	Diet amino acid	Collagen	Apatite	b chol
Ala	0.01	0.76	0.72	0.07	0.17	0.72	0.48
Gly	0.32	0.42	0.53	0.51	0.68	0.54	0.49
Thr	0.78	0.02	0.11	0.56	0.72	0.09	0.23
Ser	0.16	0.59	0.66	0.29	0.55	0.64	0.54
Val	0.76	0.09	0.21	0.69	0.71	0.18	0.37
Leu	0.78	0.03	0.13	0.80	0.73	0.12	0.30
Ile	0.88	2 ⁻⁰⁶	0.04	0.94	0.61	0.03	0.10
Pro	0.92	0.03	0.14	0.86	0.88	0.15	0.31
Hyp	0.85	0.16	0.32	*	0.91	0.30	0.44
Asp	0.21	0.75	0.85	0.31	0.67	0.82	0.95
Glu	0.05	0.86	0.94	0.08	0.51	0.94	0.89
Phe	0.82	0.01	0.01	0.97	0.58	0.01	0.12

components. The R^2 values obtained for these correlations are presented in Table 5.1. From these values it can be seen that seven correlations had an R^2 value greater than 0.9 and these correlations were therefore deemed suitable for deriving $\delta^{13}\text{C}$ values of dietary and tissue components. These correlations are presented in Table 5.2.

Table 5.2. Linear correlations where $R^2 > 0.9$. Equation of the line follows the form $y = mx + c$, where x and y are variables, m is the gradient of the line and c is the y intercept. $n = 14$

Components of linear equation $y = mx + c$				
x	y	m	c	R^2
diet phe	collagen phe	1.17	5.23	0.97
bone cholesterol	collagen asp	0.98	6.21	0.95
diet ile	collagen ile	0.93	0.02	0.94
whole diet	collagen glu	1.07	11.49	0.94
apatite	collagen glu	1.15	1.90	0.94
dietary protein	collagen pro	0.95	9.06	0.92
collagen	collagen hyp	1.07	-1.57	0.91

It can be seen from Table 5.1 that only the energy component of the diet does not have a linear correlation with an individual amino acid in bone collagen with an $R^2 > 0.9$. Each of the observed correlations with the diet components reflects the incorporation of the dietary signal into bone collagen amino acids. Whole diet correlates with glutamate since this amino acid incorporates carbon from all the dietary macronutrients (see Section 1.9). Proline constitutes 14.7% of the carbon in collagen and correlates with dietary protein since it is routed into collagen from dietary protein (see Section 4.5.2). The correlation of collagen amino acids with tissue components supports previous observations of the incorporation of dietary signals into tissue components (Ambrose and Norr, 1993; Krueger and Sullivan, 1984; Lee-Thorp *et al.*, 1989; Schwarcz, 1991; Tieszen and Fagre, 1993b). It is

known that the $\delta^{13}\text{C}$ value of apatite reflects the $\delta^{13}\text{C}$ value of whole diet; in fact, the correlation of apatite and whole diet values obtained from these experiments

gave an R^2 value of 0.99, therefore it is unsurprising that glutamate correlates strongly with apatite as well as whole diet. Bone cholesterol has been found to be a short-term indicator of whole diet $\delta^{13}\text{C}$ values (Jim, 2000). Cholesterol is synthesised *de novo* from acetyl CoA which is produced through the catabolism of dietary proteins, lipids and carbohydrates. Since aspartate is formed from an intermediate of the citric acid cycle, it will also incorporate the isotopic signal of proteins, lipids and carbohydrates. From Table 5.2 it appears that bone collagen aspartate and bone cholesterol $\delta^{13}\text{C}$ values correlate highly, reflecting the similar sources of carbon for both of these bone components. However, the turnover time of bone aspartate will be analogous to bone collagen (6.9 years), whilst the turnover time of bone cholesterol is 289 days (Jim, 2000). Therefore $\delta^{13}\text{C}_{\text{coll asp}}$ values cannot be used to predict $\delta^{13}\text{C}_{\text{bchol}}$ values. These two bone components do correlate well in this instance since the rats from which this data was obtained were raised on monotonous diets whose isotopic composition did not vary over time. It is expected that had the diet varied over time, these bone components would not have been found to have a high correlation.

These correlations can be applied to the prediction of dietary macronutrient $\delta^{13}\text{C}$ values via the following equations derived from the data in Table 5.1:

$\delta^{13}\text{C}_{\text{whole diet}}$ can be obtained from $\delta^{13}\text{C}_{\text{coll glu}}$ values using:

$$\delta^{13}\text{C}_{\text{whole diet}} = (\delta^{13}\text{C}_{\text{coll glu}}/1.07) - 11.45 \quad \text{equation 5.1}$$

$\delta^{13}\text{C}_{\text{diet prot}}$ can be obtained from $\delta^{13}\text{C}_{\text{coll pro}}$ values using:

$$\delta^{13}\text{C}_{\text{diet prot}} = (\delta^{13}\text{C}_{\text{coll pro}}/0.95) - 9.06 \quad \text{equation 5.2}$$

Since the whole diet $\delta^{13}\text{C}$ value is comprised of the protein and energy $\delta^{13}\text{C}$ values, they can be related with the following mass balance equation where x is the fraction of protein in the diet.

$$\delta^{13}\text{C}_{\text{whole diet}} = x * \delta^{13}\text{C}_{\text{diet prot}} + (1-x) * \delta^{13}\text{C}_{\text{energy}} \quad \text{equation 5.3}$$

Therefore $\delta^{13}\text{C}$ energy values can be calculated as follows:

$$\delta^{13}\text{C}_{\text{diet energy}} = (\delta^{13}\text{C}_{\text{whole diet}} - 0.20 * \delta^{13}\text{C}_{\text{diet prot}}) / 0.80 \quad \text{equation 5.4}$$

The $\delta^{13}\text{C}$ values of bone components can be estimated using the following equations:

$\delta^{13}\text{C}_{\text{coll}}$ can be obtained from $\delta^{13}\text{C}_{\text{coll hyp}}$ values using:

$$\delta^{13}\text{C}_{\text{coll}} = (\delta^{13}\text{C}_{\text{coll hyp}} / 1.07) + 1.57 \quad \text{equation 5.5}$$

$\delta^{13}\text{C}_{\text{apat}}$ can be obtained from $\delta^{13}\text{C}_{\text{coll glu}}$ values using:

$$\delta^{13}\text{C}_{\text{apat}} = (\delta^{13}\text{C}_{\text{coll glu}} / 1.15) - 1.90 \quad \text{equation 5.6}$$

Alternatively, it is also possible to obtain $\delta^{13}\text{C}$ values of dietary macronutrients using the $\delta^{13}\text{C}$ values of bone components from collagen amino acids and then use these estimated values in models that have been previously constructed (Jim, 2000). The following equations were constructed using the $\delta^{13}\text{C}$ values of dietary macronutrients and bone collagen and apatite from the same rat feeding experiment as used here and are presented in Jim (2000).

From the collagen and apatite $\delta^{13}\text{C}$ values it is possible to calculate:

$$\delta^{13}\text{C}_{\text{whole diet}} \text{ from: } (\delta^{13}\text{C}_{\text{apat}} - 8.34) / 0.94 \quad \text{equation 5.7}$$

$$\delta^{13}\text{C}_{\text{prot}} \text{ from: } (\delta^{13}\text{C}_{\text{coll}} - (0.40 \cdot \delta^{13}\text{C}_{\text{apat}}) - 1.68)/0.60$$

equation 5.8

$$\delta^{13}\text{C}_{\text{energy}} \text{ from: } (\delta^{13}\text{C}_{\text{apat}} - (0.37 \cdot \delta^{13}\text{C}_{\text{coll}}) - 7.60)/0.63$$

equation 5.9

$$\delta^{13}\text{C}_{\text{whole diet (short term)}} \text{ from: } (\delta^{13}\text{C}_{\text{bchol}} + 6.77)/0.82$$

equation 5.10

$\delta^{13}\text{C}$ values for the dietary macronutrients obtained using the above equations can be compared to the actual $\delta^{13}\text{C}$ values for the dietary macronutrients to obtain an R^2 value (approach 2). This value can then be compared with the R^2 value obtained when the $\delta^{13}\text{C}$ values of the dietary macronutrients are calculated directly from collagen amino acids using equations 5.1, 5.2 and 5.4 (approach 1). The results are presented in Table 5.3.

Table 5.3 Comparison of R^2 values obtained when comparing calculated $\delta^{13}\text{C}$ values of dietary macronutrients with actual value using two different approaches.

dietary component	R^2 value	
	directly from amino acid $\delta^{13}\text{C}$ value	from estimated bone component $\delta^{13}\text{C}$ value
whole diet	0.94	0.94
protein	0.92	0.95
energy	0.93	0.96

It can be seen that when calculating protein and energy $\delta^{13}\text{C}$ values it is more accurate to use the $\delta^{13}\text{C}$ values of bone components obtained from collagen amino acids and then use the models that have been previously constructed for calculating dietary macronutrient $\delta^{13}\text{C}$ values from bone component $\delta^{13}\text{C}$ values (Jim, 2000). The two different approaches for calculating whole diet lead to almost identical R^2 values, due to the very high correlation between apatite and whole diet ($R^2 = 0.99$). Since whole diet and apatite $\delta^{13}\text{C}$ values are both calculated from

glutamate using approach 1 and there is a high degree of correlation between apatite and whole diet, it follows that the difference between approach 1 and approach 2 is too small to be detected via R^2 values.

To summarise, the most accurate way to calculate the $\delta^{13}\text{C}$ values of dietary macronutrients and bone components using only the $\delta^{13}\text{C}$ values of collagen amino acids is as follows:

- (1) Use $\delta^{13}\text{C}$ values of glutamate to calculate both whole diet and apatite $\delta^{13}\text{C}$ values, using equations 5.1 and 5.6, respectively.
- (2) Use hydroxyproline to calculate bone collagen $\delta^{13}\text{C}$ values with equation 5.5.
- (3) Use equation 5.8 and the apatite and collagen $\delta^{13}\text{C}$ values from (1) and (2) above to calculate the $\delta^{13}\text{C}$ value of dietary protein.
- (4) Use apatite and collagen $\delta^{13}\text{C}$ values from (1) and (2) above to calculate dietary energy $\delta^{13}\text{C}$ value using equation 5.9.

5.3.2. Combined use of bone component $\delta^{13}\text{C}$ values

A combined approach to calculating the $\delta^{13}\text{C}$ values of dietary macronutrients, whereby the measured $\delta^{13}\text{C}$ values of bone collagen, apatite and cholesterol are used in conjunction with the measured $\delta^{13}\text{C}$ values of collagen amino acids, was investigated. To ascertain any relationships that existed between all the bone components further correlations were employed. In addition to direct 'one-to-one' correlations where one diet or bone component was compared with another, the spacings between bone components and bone components (BC-BC), dietary components and dietary components (DC-DC) and bone components and dietary components (BC-DC) were also correlated. Investigating these spacings makes it possible to gain greater insights into the relationship between dietary macronutrients and bone components since these spacings are altered by differences in the isotopic composition of the dietary macronutrients.

The eight different $\delta^{13}\text{C}$ values that were measured for the diet and bone components leads to 28 $\Delta^{13}\text{C}$ spacings for each amino acid. All 36 variables are listed in Table 5.4. Linear regression analysis produced 651 correlations for each of the twelve amino acids studied, with the exception of hydroxyproline. Due to the lack of hydroxyproline in the diet, only 393 correlations were produced. Out of all the linear regressions possible, 16.2% had an $R^2 > 0.9$. Appendix 2 lists all of these correlations.

To find correlations that may be suitable for combining bone component $\delta^{13}\text{C}$ values to calculate the $\delta^{13}\text{C}$ values of dietary macronutrients, all correlations with an $R^2 > 0.9$ were studied to find those that contained a collagen amino acid, one other bone component and a dietary macronutrient. The relevant correlations are presented in Tables 5.5, 5.6 and 5.7. An R^2 value for the correlation between the predicted dietary macronutrient $\delta^{13}\text{C}$ values and the actual values can be used, as in the previous section, to assess the degree of correlation. The idea of the combined approach is to improve on the R^2 values obtained when using only individual amino acids. Therefore, the R^2 values were calculated for the correlation between actual dietary macronutrient $\delta^{13}\text{C}$ values and $\delta^{13}\text{C}$ values calculated using equations 1-48 in Tables 5.5, 5.6 and 5.7. Those R^2 values that were less than those already obtained from the use of individual amino acids alone (whole diet $R^2 = 0.94$; protein $R^2 = 0.94$; energy $R^2 = 0.96$) were disregarded. The remainder are presented in Table 5.8.

When calculating dietary protein, it can be seen that the combined use of collagen and glutamate $\delta^{13}\text{C}$ values improves the R^2 value obtained. Although this approach yields a slightly poorer correlation than when using collagen and apatite values to calculate dietary protein (Jim, 2000), it does have the advantage of being independent of apatite $\delta^{13}\text{C}$ values, since palaeodietary interpretations based on apatite have been the subject of some debate (Schoeninger and DeNiro, 1982; Schoeninger and DeNiro, 1983; Sullivan and Krueger, 1983). Most significantly, bone apatite is susceptible to contamination by diagenetic carbonates due to leaching by groundwater in the burial environment. A variety of experimental

Table 5.4. Diet and bone components and $\Delta^{13}\text{C}$ spacings subjected to linear regression analysis. wdiet = whole diet, prot = protein, AA_{diet} = dietary amino acid, coll = collagen, apat = apatite, bchol = bone cholesterol, AA_{coll} = collagen amino acid.

Variables				
wdiet	wdiet-prot	prot- AA_{diet}	energy-bchol	coll- AA_{coll}
prot	wdiet-energy	prot-coll	energy- AA_{coll}	apat-bchol
energy	wdiet- AA_{diet}	prot-apat	AA_{diet} -coll	apat- AA_{coll}
AA_{diet}	wdiet-coll	prot-bchol	AA_{diet} -apat	bchol- AA_{coll}
coll	wdiet-apat	prot- AA_{coll}	AA_{diet} -bchol	
apat	wdiet-bchol	energy- AA_{diet}	AA_{diet} - AA_{coll}	
bchol	wdiet- AA_{coll}	energy-coll	coll-apat	
AA_{coll}	prot-energy	energy-apat	coll-bchol	

Table 5.5. Linear correlations for calculating dietary protein $\delta^{13}\text{C}$ values from bone component $\delta^{13}\text{C}$ values where $R^2 > 0.9$. Equation of the line follows the form $y = mx + c$, where x and y are variables, m is the gradient of the line and c is the y intercept. n = 14

Components of linear equation $y = mx + c$					
Equation No.	x	y	m	c	R^2
1	prot-glu _{coll}	coll-glu _{coll}	0.617	1.59	0.98
2	prot-ala _{coll}	coll-ala _{coll}	0.74	5.36	0.98
3	prot-apat	apat-pro _{coll}	-0.84	-8.33	0.97
4	prot-bchol	pro _{coll} -bchol	0.80	10.54	0.96
5	prot-coll	prot-glu _{coll}	2.50	3.51	0.96
6	prot-asp _{coll}	prot-bchol	0.99	6.67	0.95
7	prot-apat	prot-glu _{coll}	1.01	-0.50	0.94
8	prot-apat	apat-ile _{coll}	1.07	0.08	0.92
9	prot-apat	apat-hyp _{coll}	-0.77	-0.89	0.92
10	ile _{coll} -bchol	prot-bchol	0.80	1.35	0.91

Table 5.6. Linear correlation for calculating dietary energy $\delta^{13}\text{C}$ values from bone component $\delta^{13}\text{C}$ values where $R^2 > 0.9$. Equation of the line follows the form $y = mx + c$, where x and y are variables, m is the gradient of the line and c is the y intercept.

Components of linear equation $y = mx + c$					
Equation No.	x	y	m	c	R^2
11	energy-coll	energy-pro _{coll}	1.24	3.07	0.99
12	energy-ile _{coll}	apat-ile _{coll}	0.76	9.85	0.99
13	energy-phe _{coll}	apat-phe _{coll}	0.78	10.32	0.99
14	energy-pro _{coll}	apat-pro _{coll}	0.70	6.72	0.99
15	energy-leu _{coll}	apat-leu _{coll}	0.69	12.90	0.98
16	energy-coll	energy-hyp _{coll}	1.20	3.56	0.98
17	energy-hyp _{coll}	apat-hyp _{coll}	0.70	8.77	0.98
18	energy-phe _{coll}	phe _{coll} -bchol	0.64	1.94	0.97
19	energy-thr _{coll}	apat-thr _{coll}	0.77	8.55	0.97
20	energy-coll	energy-ile _{coll}	1.51	9.02	0.97
21	energy-val _{coll}	apat-val _{coll}	0.75	10.73	0.96
22	energy-pro _{coll}	pro _{coll} -bchol	0.54	7.74	0.95
23	energy-leu _{coll}	leu _{coll} -bchol	0.52	-1.78	0.94
24	energy-leu _{coll}	energy-bchol	0.48	-1.78	0.93
25	energy-ile _{coll}	ile _{coll} -bchol	0.64	2.94	0.93
26	energy-pro _{coll}	energy-bchol	0.46	7.74	0.93
27	energy-coll	energy-leu _{coll}	1.15	16.86	0.93
28	energy-asp _{coll}	energy-bchol	0.86	6.21	0.93
29	energy-apat	energy-pro _{coll}	3.09	20.04	0.92
30	energy-thr _{coll}	thr _{coll} -bchol	0.64	4.97	0.92
31	energy-apat	energy-ile _{coll}	3.74	36.87	0.91
32	energy-apat	energy-leu _{coll}	2.96	39.17	0.91
33	energy-phe _{coll}	energy-bchol	0.36	1.94	0.91
34	energy-gly _{coll}	apat-gly _{coll}	0.65	6.80	0.91
35	energy-val _{coll}	val _{coll} -bchol	0.58	1.49	0.91

Table 5.7. Linear correlations for calculating whole diet $\delta^{13}\text{C}$ values from bone component $\delta^{13}\text{C}$ values, where $R^2 > 0.9$. Equation of the line follows the form $y = mx + c$, where x and y are variables, m is the gradient of the line and c is the y intercept.

Components of liner equation $y = mx + c$					
Equation No.	x	y	m	c	R^2
36	wdiet-phe _{coll}	phe _{coll} -bchol	-0.81	2.61	0.98
37	wdiet-coll	wdiet-pro _{coll}	1.35	2.48	0.98
38	wdiet-coll	wdiet-hyp _{coll}	1.31	4.13	0.96
39	wdiet-thr _{coll}	thr _{coll} -bchol	-0.83	4.15	0.96
40	wdiet-coll	pro _{coll} -bchol	-1.01	7.62	0.96
41	wdiet-ile _{coll}	ile _{coll} -bchol	-0.83	3.19	0.96
42	wdiet-pro _{coll}	pro _{coll} -bchol	-0.74	5.83	0.96
43	wdiet-ala _{coll}	ala _{coll} -bchol	-1.29	3.26	0.96
44	wdiet-leu _{coll}	leu _{coll} -bchol	-0.73	0.41	0.95
45	wdiet-coll	wdiet-ile _{coll}	1.77	10.39	0.95
46	wdiet-val _{coll}	val _{coll} -bchol	-0.78	2.39	0.95
47	wdiet-ile _{coll}	coll-ile _{coll}	0.47	5.85	0.93
48	wdiet-hyp _{coll}	hyp _{coll} -bchol	-0.76	4.04	0.91

Table 5.8. Linear correlations for calculating the $\delta^{13}\text{C}$ values of dietary macronutrients using the combined approach where R^2 values are greater than those already obtained from the use of individual amino acids alone. Equation of the line follows the form $y = mx + c$, where x and y are variables, m is the gradient of the line and c is the y intercept.

Components of linear equation $y = mx + c$					
Equation No.	x	y	m	c	R^2
Calculating dietary protein					
1	prot-glu _{coll}	coll-glu _{coll}	0.62	1.59	0.97
5	prot-coll	prot-glu _{coll}	2.50	3.51	0.97
Calculating dietary energy					
12	energy-ile _{coll}	apat-ile _{coll}	0.76	9.85	0.99
14	energy-pro _{coll}	apat-pro _{coll}	0.70	6.72	0.98
17	energy-hyp _{coll}	apat-hyp _{coll}	0.70	8.77	0.98
15	energy-leu _{coll}	apat-leu _{coll}	0.69	12.90	0.98
13	energy-phe _{coll}	apat-phe _{coll}	0.78	10.32	0.97
21	energy-val _{coll}	apat-val _{coll}	0.75	10.73	0.96
Calculating whole diet					
43	wdiet-ala _{coll}	ala _{coll} -bchol	-1.29	3.26	0.98
36	wdiet-phe _{coll}	phe _{coll} -bchol	-0.81	2.61	0.96
44	wdiet-leu _{coll}	leu _{coll} -bchol	-0.73	0.41	0.95
42	wdiet-pro _{coll}	pro _{coll} -bchol	-0.74	5.83	0.95

methods have been proposed to remove this diagenetic contamination (Krueger, 1991; Lee-Thorp and van der Merwe, 1991), but controversy still remains over which approach is most effective and whether the apatite obtained retains its isotopic integrity (Koch *et al.*, 1997).

The combined approach for calculating the $\delta^{13}\text{C}$ value of dietary energy shows that although there are six approaches that give a better correlation than any using individual amino acids alone, only one approach (equation 12) yields an R^2 value greater than the 0.98 obtained when calculating dietary energy $\delta^{13}\text{C}$ values from apatite and collagen $\delta^{13}\text{C}$ values using the model developed by Jim (2000). So, from equation 12 it can be seen that the combined use of bone collagen isoleucine and apatite $\delta^{13}\text{C}$ values for predicting dietary energy $\delta^{13}\text{C}$ values does improve on the previous models.

It is known that apatite reflects the long-term isotopic signal of whole diet (Ambrose and Norr, 1993; Lee-Thorp *et al.*, 1989; Schwarcz, 1991; Tieszen and Fagre, 1993b), whilst bone cholesterol reflects the short-term isotopic signal of whole diet (Jim, 2000). The correlations that give an R^2 value greater than the 0.94 obtained from the use of individual amino acids to calculate whole diet $\delta^{13}\text{C}$ values all include the $\delta^{13}\text{C}$ values of bone cholesterol, indicating that they will reflect the short-term whole diet $\delta^{13}\text{C}$ value. Therefore, the combined approach cannot improve on the long-term whole diet $\delta^{13}\text{C}$ values obtained either from individual amino acids or from bulk apatite $\delta^{13}\text{C}$ values. However, previous models for calculating $\delta^{13}\text{C}$ values of short-term whole diet have relied solely on the use of bone cholesterol with an R^2 value of 0.92. Equation 43 shows that the combined use of alanine from bone collagen and bone cholesterol significantly improves the approach to calculating short-term whole diet $\delta^{13}\text{C}$ values.

To summarise the findings of the combined approach: when all bone component $\delta^{13}\text{C}$ values are available (individual amino acids, collagen, apatite and bone cholesterol), the use of individual amino acids and apatite leads to a slight improvement when calculating dietary energy $\delta^{13}\text{C}$ values. The most accurate methods for predicting long-term whole diet and protein $\delta^{13}\text{C}$ values remains the use of collagen and apatite as described by equations 5.7 and 5.8. However, it should be noted that the collagen and apatite $\delta^{13}\text{C}$ values required for predicting protein and long-term whole diet $\delta^{13}\text{C}$ values, can themselves be predicted from individual amino acid $\delta^{13}\text{C}$ values (see Section 5.3.1) which overcomes the

diagenetic contamination problems mentioned above. The accuracy of calculating short-term whole diet $\delta^{13}\text{C}$ values is greatly improved by the combined use of individual amino acids and bone cholesterol.

When apatite $\delta^{13}\text{C}$ values are not available, the use of individual amino acids and collagen $\delta^{13}\text{C}$ values significantly improves on previous models for calculating the $\delta^{13}\text{C}$ values of dietary macronutrients. The lack of $\delta^{13}\text{C}_{\text{apat}}$ values previously led to a correlation with an R^2 of 0.70 when predicting dietary protein and it was not possible to predict whole diet or energy $\delta^{13}\text{C}$ values at all (Jim, 2000). Using the models developed in this chapter, dietary protein can now be calculated from $\delta^{13}\text{C}_{\text{coll glu}}$ and $\delta^{13}\text{C}_{\text{coll}}$ values with an R^2 value of 0.97. The accuracy of this method can also be compared to the previous model presented by Jim (2000). The average difference between actual and predicted $\delta^{13}\text{C}$ values has a magnitude of $1.0\text{‰} \pm 0.7\text{‰}$ when using $\delta^{13}\text{C}_{\text{coll glu}}$ and $\delta^{13}\text{C}_{\text{coll}}$ values whilst the difference has a magnitude of $2.0\text{‰} \pm 1.3\text{‰}$ for the previous model. This method of predicting protein $\delta^{13}\text{C}$ values is also more accurate than predicting apatite $\delta^{13}\text{C}$ values from $\delta^{13}\text{C}_{\text{glu}}$ values and then using equation 5.8. The most accurate prediction of dietary energy $\delta^{13}\text{C}$ values when $\delta^{13}\text{C}_{\text{apat}}$ values are not available remains the use of estimated bone component $\delta^{13}\text{C}$ values being utilised in the models presented by Jim (2000), since the combined approach requires $\delta^{13}\text{C}_{\text{apat}}$ values. It should be noted that even if predicted $\delta^{13}\text{C}_{\text{apat}}$ values are used in the combined approach this results in a smaller R^2 value than that obtained using amino acid $\delta^{13}\text{C}$ values alone. When $\delta^{13}\text{C}_{\text{apat}}$ values are not available, the most accurate whole diet $\delta^{13}\text{C}$ values can be obtained directly from amino acid $\delta^{13}\text{C}$ values since from Table 5.8 it can be seen that the combined approach requires $\delta^{13}\text{C}_{\text{bchol}}$ values. Therefore $\delta^{13}\text{C}_{\text{whole diet}}$ values obtained using the combined approach will be predicting short-term rather than long-term whole diet $\delta^{13}\text{C}$ values, as it is known that bone cholesterol is a proxy for short-term whole diet (Jim, 2000).

5.3.3 Testing the models

To assess the accuracy of the models constructed in the previous sections, it is necessary to apply them to isotopic data obtained from independent feeding studies. Apart from the rat feeding experiment that forms the basis of this research, only Hare *et al.* (1991) have published $\delta^{13}\text{C}$ values for individual porcine amino acids from a feeding experiment and this study was rather limited in scope with respect to our requirements since data was only obtained from pigs fed on either pure C_3 or pure C_4 diets. Therefore, the isotope data used to test these models comes from unpublished results obtained from analyses performed in our laboratory from a pig feeding experiment carried out at Harvard University under the supervision of Professor van der Merwe. Dietary macronutrient and collagen $\delta^{13}\text{C}$ values were measured at Harvard University. Individual amino acid and bone cholesterol $\delta^{13}\text{C}$ values were obtained in our laboratory by Mark Howland and Lorna Corr, respectively. The thirteen different diets used in this study comprised of varying percentages of energy and protein components. The energy was provided by whole wheat (-27.4‰) and whole maize (-13.2‰), whilst protein was provided by casein (-16.9‰), soy beans (-33.5‰) and fish meal (-18.7‰). Further details of the diets used in this study are given in Table 5.9, whilst the $\delta^{13}\text{C}$ values for the bone components for the 28 pig bones are listed in Appendix 3.

Following the procedure for estimating dietary macronutrient and bone component $\delta^{13}\text{C}$ values from individual amino acids presented in Section 5.3.1, bone and dietary component $\delta^{13}\text{C}$ values were obtained. Tables listing the predicted and measured $\delta^{13}\text{C}$ values can be found in Appendix 4. Measures of correlation and differences between predicted and measured values are summarised in Table 5.10.

The accuracy of the model for predicting bone component $\delta^{13}\text{C}$ values was first examined. $\delta^{13}\text{C}_{\text{apat}}$ values were estimated from $\delta^{13}\text{C}_{\text{coll glu}}$ values using equation 5.6. Unfortunately, no measured $\delta^{13}\text{C}_{\text{apat}}$ values were available to test the accuracy of the model. Collagen $\delta^{13}\text{C}$ values were estimated from hydroxyproline $\delta^{13}\text{C}$ values using equation 5.5; Figure 5.1 shows the correlation between estimated

Table 5.9. Diet composition and bulk diet $\delta^{13}\text{C}$ values for the diets used in the Harvard pig feeding experiment (personal communication).

Diet No.	Bulk diet (‰)	Diet constituents (%)				
		Whole wheat	Whole maize	casein	Soy beans	Fish meal
1	-13.0	-	85	15	-	-
2	-15.4	-	70	30	-	-
3	-23.3	10	70	20	-	-
4	-20.2	30	50	20	-	-
5	-17.8	50	30	20	-	-
6	-15.9	70	10	20	-	-
7	-13.4	-	80	20	-	-
9	-16.0	-	80	-	20	-
10	-14.9	-	80	-	-	20
11	-22.1	20	60	20	-	-
12	-16.3	60	20	20	-	-
13	-20.9	50	30	-	-	20
14	-18.5	30	50	-	-	20

Table 5.10. Correlations and differences between measured bone and dietary component $\delta^{13}\text{C}$ values and those predicted from the individual amino acid model. R^2_1 is a measure of the correlation between predicted values and actual values. R^2_2 is a measure of the accuracy of the predicted values and is calculated with reference to the $x = y$ line.

	Bone dietary components					
	Bone cholesterol	Collagen	Long-term whole diet	Short-term whole diet	Protein	Energy
R^2_1	0.78	0.80	0.81	0.83	0.21	0.89
R^2_2	0.88	0.78	0.81	0.88	0.36	0.72
$\Delta^{13}\text{C}_{\text{pred-meas}}$	1.1‰	1.6‰	2.3‰	1.6‰	1.6‰	4.4‰

values and measured values. Although there is a reasonable correlation between predicted and measured $\delta^{13}\text{C}_{\text{coll}}$ values ($R^2_1 = 0.80$) the line of best fit through these points does not coincide with the dashed $x = y$ line leading to an R^2_2 value of 0.78 indicating that there is a systematic inaccuracy occurring in the calculation causing the predicted values to be more enriched in ^{13}C than the measured values. A possible source of this discrepancy could be differences in the way the diets were formulated in the rat and pig feeding experiments. The data that was used to construct the models came from rats that were fed on purified diets; the only protein present in the diet was supplied by the milk casein and its $\delta^{13}\text{C}$ value was well characterised. The dietary formulation for the pig feeding experiment is complicated by the fact that carbohydrates in the diet are supplied by whole wheat and maize which themselves also contain protein, thus leading to two different sources of protein in the diets. Therefore uncertainty exists as to which of the two protein components provide the amino acids in collagen. Investigation of the processes that are occurring here are beyond the scope of this thesis. Another possible reason for the observed discrepancy could be differences in the physiologies of rats and pigs.

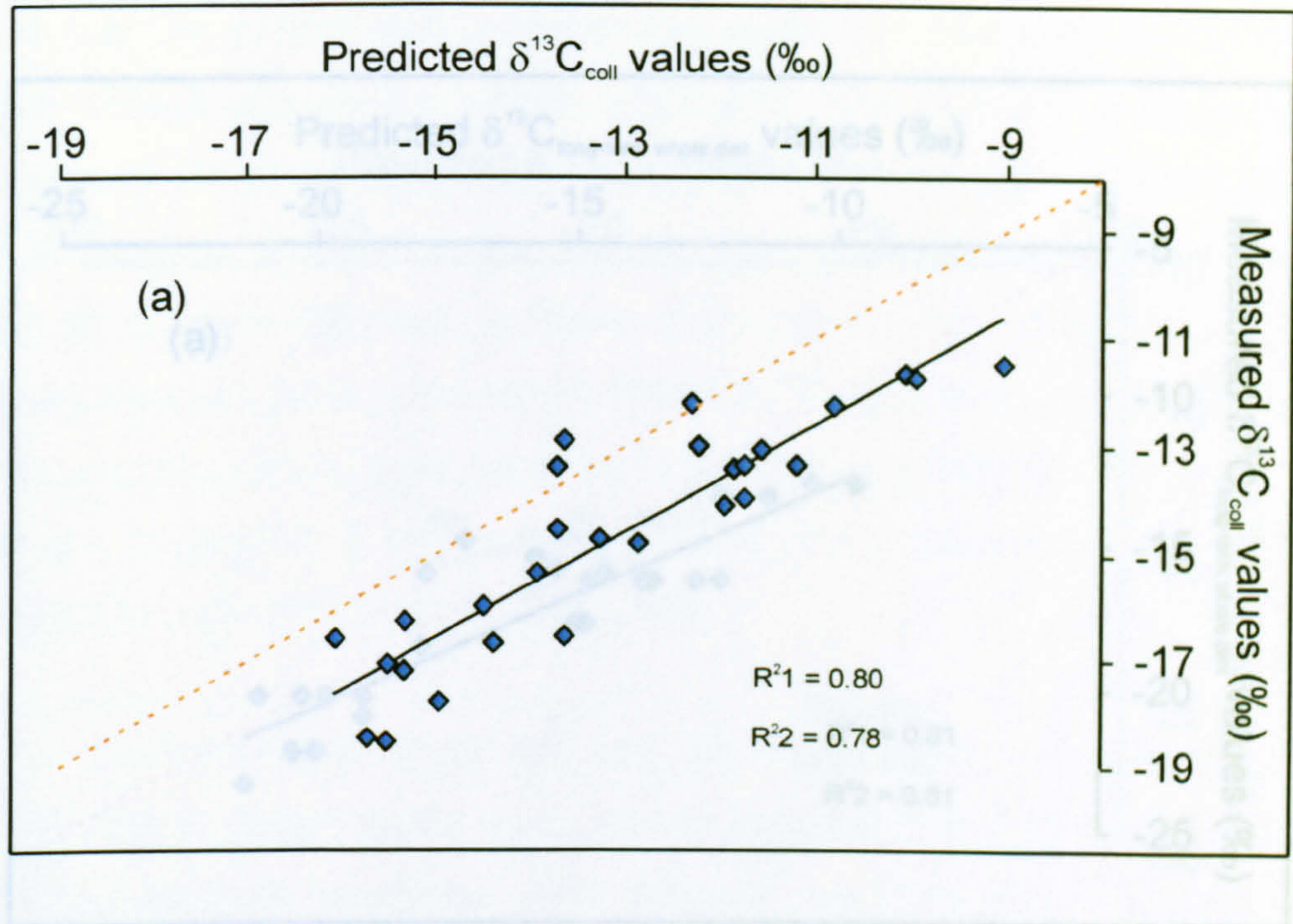


Figure 5.1. Comparison of measured bone component $\delta^{13}\text{C}$ values from the pig feeding experiment with those predicted by the individual amino acid rat model for collagen. Dashed line is the theoretical $x = y$ line.

The results from testing the accuracy of the model for predicting dietary macronutrient $\delta^{13}\text{C}$ values from individual amino acids are summarised in Figure 5.2 and 5.3. Figure 5.2 presents the comparison of long-term predicted and measured $\delta^{13}\text{C}_{\text{whole diet}}$ values. The whole diet $\delta^{13}\text{C}$ values were predicted using glutamate $\delta^{13}\text{C}$ values. There is a strong correlation between predicted and measured values, although it appears that the predicted values slightly overestimate the amount of C_4 components in the diet. Despite this discrepancy the model is still accurate, yielding an R^2 value of 0.81 for the correlation between measured and predicted long-term whole diet. Unlike the protein values discussed above, there is not a constant difference between predicted and measured values, which suggests that this inaccuracy is not due to physiological differences between rats and pigs. It may be that differences exist in amino acid composition and digestibility of the dietary macronutrients that leads to a preferential incorporation of the C_3 signal into collagen glutamate.

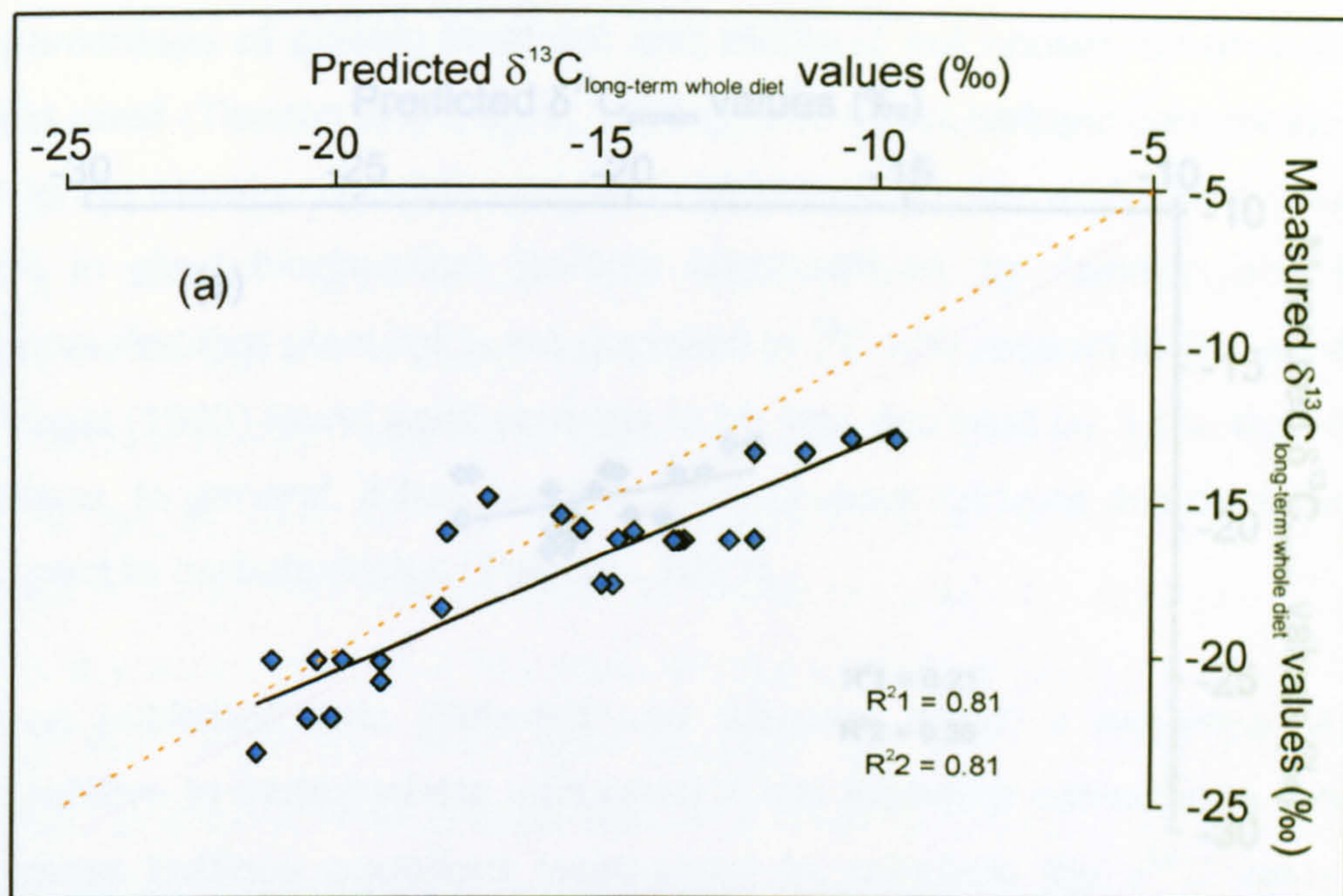


Figure 5.2. Comparison of measured long-term whole diet $\delta^{13}\text{C}$ values from the pig feeding experiment with those predicted by the individual amino acid rat model. Dashed line is the theoretical $x = y$ line.

Using equation 5.8, long-term whole diet values were calculated from apatite $\delta^{13}\text{C}$ values estimated using glutamate $\delta^{13}\text{C}$ values. The resulting correlation between predicted and measured values gave an R^2 value of 0.81. Although no apatite $\delta^{13}\text{C}$ values were available to test the accuracy of calculating apatite values from glutamate, this degree of correlation indirectly indicates that the method is accurate.

The dietary protein and energy $\delta^{13}\text{C}$ values were predicted using the estimated collagen and apatite isotope values and compared with measured values; the results are presented in Figure 5.3. Some difficulties were encountered in assessing the actual dietary protein $\delta^{13}\text{C}$ values. Clearly the dietary protein $\delta^{13}\text{C}$ value did not simply reflect that of the casein in the diet, since as mentioned before, additional protein was provided by the wheat and maize components of the diet. To establish the correct $\delta^{13}\text{C}$ value of the dietary protein, the percentage and

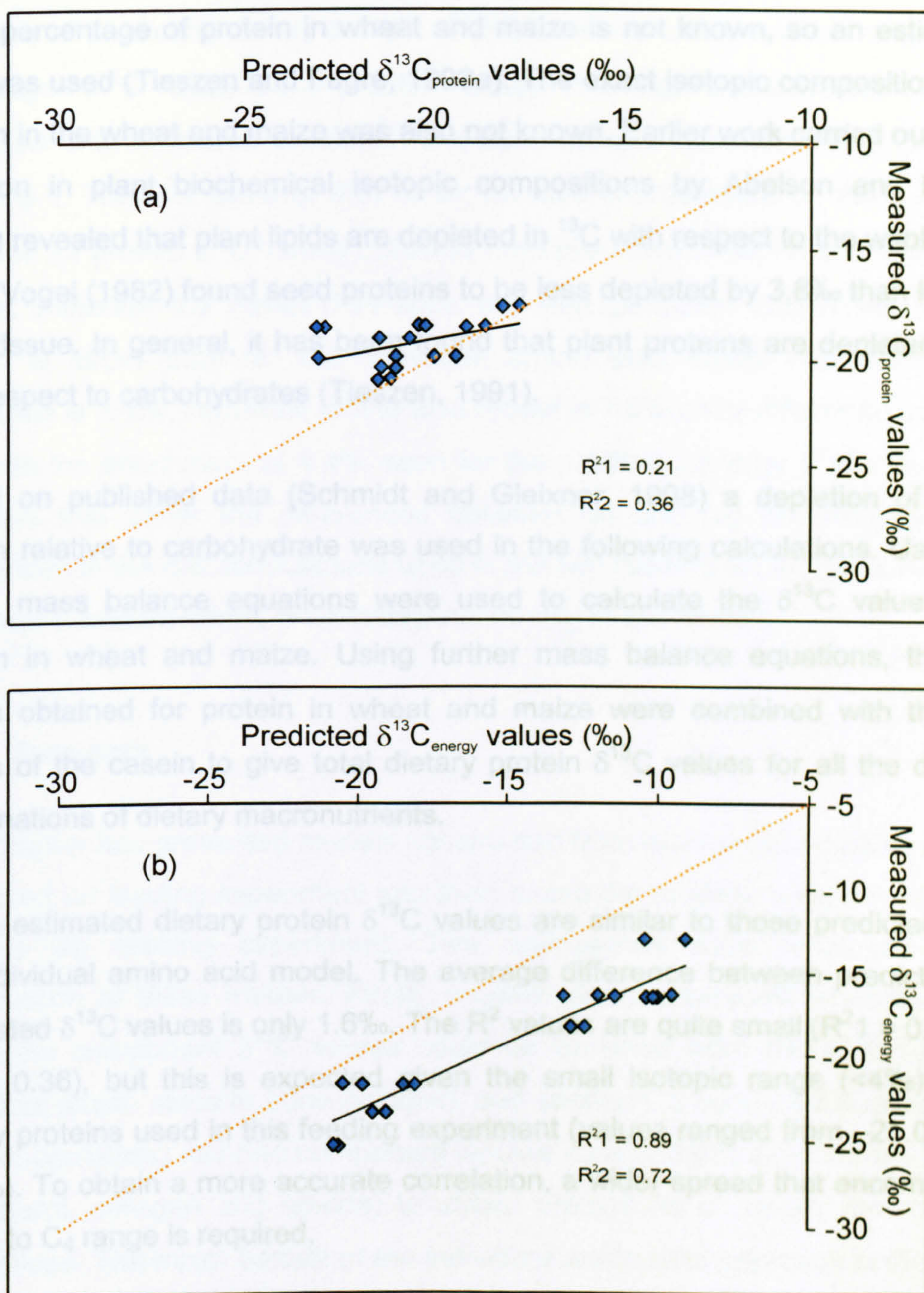


Figure 5.3. Comparison of measured dietary component $\delta^{13}\text{C}$ values from the pig feeding experiment with those predicted by the individual amino acid rat model for (a) dietary protein and (b) dietary energy. Dashed line is the theoretical $x = y$ line.

$\delta^{13}\text{C}$ value of the protein in the wheat and maize needed to be calculated. The exact percentage of protein in wheat and maize is not known, so an estimate of 10% was used (Tieszen and Fagre, 1993a). The exact isotopic composition of the protein in the wheat and maize was also not known. Earlier work carried out on the variation in plant biochemical isotopic compositions by Abelson and Hoering (1961) revealed that plant lipids are depleted in ^{13}C with respect to the whole plant, whilst Vogel (1982) found seed proteins to be less depleted by 3.8‰ than leaf and stem tissue. In general, it has been found that plant proteins are depleted in ^{13}C with respect to carbohydrates (Tieszen, 1991).

Based on published data (Schmidt and Gleixner, 1998) a depletion of 6‰ of protein relative to carbohydrate was used in the following calculations. Using this figure, mass balance equations were used to calculate the $\delta^{13}\text{C}$ value of the protein in wheat and maize. Using further mass balance equations, the $\delta^{13}\text{C}$ values obtained for protein in wheat and maize were combined with the $\delta^{13}\text{C}$ values of the casein to give total dietary protein $\delta^{13}\text{C}$ values for all the different combinations of dietary macronutrients.

These estimated dietary protein $\delta^{13}\text{C}$ values are similar to those predicted using the individual amino acid model. The average difference between predicted and calculated $\delta^{13}\text{C}$ values is only 1.6‰. The R^2 values are quite small ($R^2_1 = 0.21$ and $R^2_2 = 0.36$), but this is expected given the small isotopic range (<4‰) of the dietary proteins used in this feeding experiment (values ranged from -21.0‰ to -17.5‰). To obtain a more accurate correlation, a wider spread that encompasses the C_3 to C_4 range is required.

A comparison of the predicted and actual dietary energy $\delta^{13}\text{C}$ values is presented in Figure 5.3(b). Dietary energy $\delta^{13}\text{C}$ values cover a much larger range than that seen for the protein and this leads to a much greater R^2_1 value of 0.89. On average the predicted $\delta^{13}\text{C}_{\text{energy}}$ values are enriched in ^{13}C by 4.4‰ relative to the measured values. This difference may arise from the predicted collagen values which were enriched relative to the measured collagen values and were used in the prediction of $\delta^{13}\text{C}_{\text{energy}}$ values.

It was found that the use of glutamate and collagen $\delta^{13}\text{C}$ values improved the accuracy of predicting dietary protein $\delta^{13}\text{C}$ values over the use of either glutamate or collagen $\delta^{13}\text{C}$ values alone (Section 5.3.2). The degree of correlation between predicted and measured protein $\delta^{13}\text{C}$ values using this method is presented in Figure 5.4. The R^2 value of 0.67 is an obvious improvement on the 0.21 value obtained for protein $\delta^{13}\text{C}$ values obtained from predicted collagen and apatite $\delta^{13}\text{C}$ values. Although the mean difference between predicted and measured $\delta^{13}\text{C}$ values is larger than for the individual amino acid model (combined model difference is 3.4‰, individual amino acid model is 1.6‰), this difference compares well with the enrichment of 4.4‰ seen for the predicted energy $\delta^{13}\text{C}$ values. This indicates that either the differences between rat and pig physiologies or the differences in the diet formulations used in the two feeding experiments result in a systematic, and therefore, predictable inaccuracy in the models.

5.4 Summary

This chapter has presented models constructed from isotope data obtained from a controlled rat feeding experiment and then tested the models using data obtained from a pig feeding experiment. Two approaches were employed in the construction of these models. Firstly, models were constructed whereby dietary and bone component $\delta^{13}\text{C}$ values could be obtained from the $\delta^{13}\text{C}$ values of individual amino acids in bone collagen, and secondly a combined approach was utilised, containing all bone component isotope data (individual amino acids, bone cholesterol, collagen and apatite) to obtain predictions of dietary macronutrient $\delta^{13}\text{C}$ values. The major benefit of the individual amino acid approach in the field of palaeodietary reconstruction is the requirement of only one set of isotope data to provide all the dietary isotope information. The motivation behind the combined approach was to improve on models already available that utilised only collagen and apatite $\delta^{13}\text{C}$ values.

It was found that even from individual amino acids alone it was possible to reconstruct the isotopic composition of all dietary macronutrients. Whole diet $\delta^{13}\text{C}$

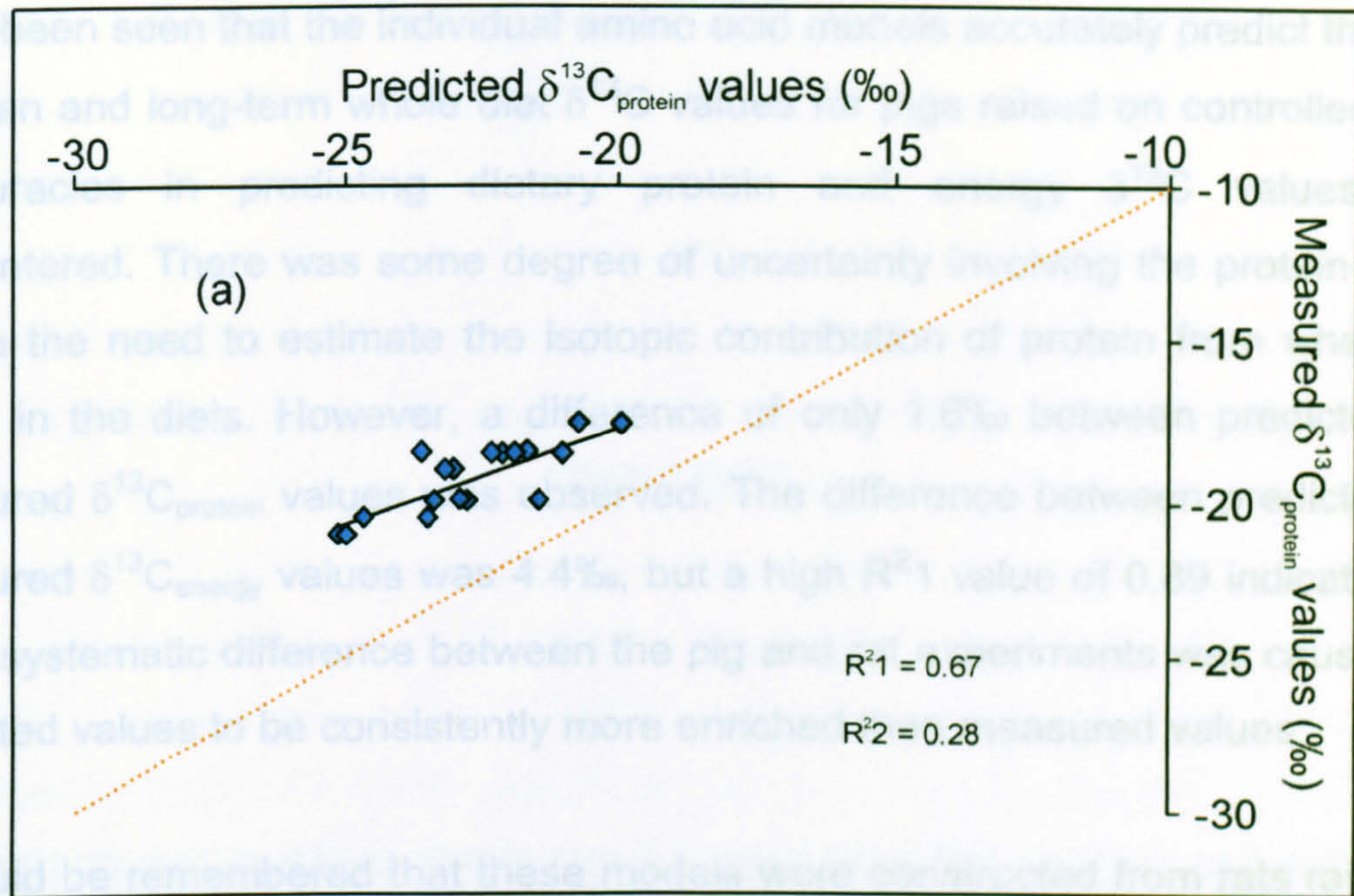


Figure 5.4. Comparison of measured dietary protein $\delta^{13}\text{C}$ values from the pig feeding experiment with those predicted by the combined approach rat model. Dashed line is the theoretical $x = y$ line.

values were predicted from glutamate $\delta^{13}\text{C}$ values and protein and energy $\delta^{13}\text{C}$ values were predicted from hydroxyproline and glutamate values, respectively. When the dietary macronutrient $\delta^{13}\text{C}$ values obtained from individual amino acids were correlated with the actual $\delta^{13}\text{C}$ values, a very high degree of accuracy for these models was observed.

The models constructed for the combined approach showed that using glutamate and collagen values together could improve the prediction of dietary protein $\delta^{13}\text{C}$ values. Previous models using only collagen to predict dietary protein $\delta^{13}\text{C}$ values led to a correlation with an R^2 of only 0.67, so the R^2 of 0.97 obtained here is a clear improvement. It also provides a strong prediction of dietary protein without the need for apatite $\delta^{13}\text{C}$ values.

It has been seen that the individual amino acid models accurately predict the bone collagen and long-term whole diet $\delta^{13}\text{C}$ values for pigs raised on controlled diets. Inaccuracies in predicting dietary protein and energy $\delta^{13}\text{C}$ values were encountered. There was some degree of uncertainty involving the protein values due to the need to estimate the isotopic contribution of protein from wheat and maize in the diets. However, a difference of only 1.6‰ between predicted and measured $\delta^{13}\text{C}_{\text{protein}}$ values was observed. The difference between predicted and measured $\delta^{13}\text{C}_{\text{energy}}$ values was 4.4‰, but a high R^2 value of 0.89 indicated that some systematic difference between the pig and rat experiments was causing the predicted values to be consistently more enriched than measured values.

It should be remembered that these models were constructed from rats raised on 20% protein diets with purified natural ingredients and will accurately predict dietary $\delta^{13}\text{C}$ values from data obtained under similar conditions. Higher or lower protein contents of the diets, or other differences in nutritional status may impose limits on the accuracy of these models. When applying them to $\delta^{13}\text{C}$ values obtained from different species care should be taken to consider any differences from the data from which these models were constructed such as diet formulation and animal physiologies and the possible effects any differences may have on predicted values.

CHAPTER 6

**AMINO ACID ANALYSIS OF ARCHAEOLOGICAL COLLAGEN
FROM QASR IBRIM**

Chapter 6 Carbon isotope analysis of archaeological data

6.1 Objectives

This chapter presents results from the compound specific $\delta^{13}\text{C}$ analyses of individual amino acids from the collagen of twenty-seven animal bones recovered from the archaeological site of Qasr Ibrim, Egypt. The bones were a mixture of bovids, and ovi-caprids (it was not possible to make positive identifications of the latter on the amount of bone present), originating from the following periods: Napatan (1000-700BC), Meroitic (AD50-300), Early Post Meroitic (AD300-400), Post Meroitic (AD400-550), Christian (AD550-1500) and Ottoman (AD1500-1812). Carbon isotope analysis of individual amino acids from sorghum and barley excavated from Qasr Ibrim and modern barley were also undertaken. Carbon isotope analyses of the $\text{C}_{16:0}$ and $\text{C}_{18:0}$ fatty acid components of these bones have previously been undertaken in this laboratory by Copley (2001). Using the findings from both Chapters 4 and 5, the results obtained from the $\delta^{13}\text{C}$ analysis of individual bone amino acids are used to predict the $\delta^{13}\text{C}$ values of bone components and dietary macronutrients. The wider applicability of the models developed in Chapter 5 are tested by comparing the predicted and measured collagen and apatite $\delta^{13}\text{C}$ values, whilst the predicted dietary macronutrient $\delta^{13}\text{C}$ values are used to interpret differences in feeding practices of ovi-caprids and bovids and how the diets of these animals changed over time.

In order to obtain a more detailed picture of how the animals on Qasr Ibrim were raised, the results from the individual amino acids will be integrated with the results from the stable carbon isotope analyses of the fatty acids to investigate how the animals diets changed over the course of their lifetimes.

6.2 Qasr Ibrim and previous work

Ancient Nubia encompassed an area from just south of Aswan in Egypt to the White and Blue Niles in Sudan. Since Qasr Ibrim is located in Lower Nubia, in the north of the region, the site experiences desert conditions and is essentially

rainless. Qasr Ibrim was originally situated on a cliff top promontory that overlooked the eastern side of the River Nile; however, since the building of the Aswan High Dam, much of the area has been flooded. Due to its geographical position Qasr Ibrim has survived the flooding and is now an island in Lake Nasser. It is an important archaeological site not only because it represents the only major Nubian site exposed above water in Egypt, but also because the arid environment results in the organic materials at the site being amongst the best preserved anywhere in the world. Qasr Ibrim was occupied for nearly three thousand years, (the main archaeological periods are listed above), and due to the excellent preservation conditions, excavations are providing an unusually detailed archaeobotanical record. The following information regarding the agricultural crops of Qasr Ibrim is taken from Rowley-Conwy (1989). During the Napatan period hulled barley (*Hordeum vulgare*), a C₃ plant, was the most common cereal in use. There is also evidence for emmer wheat (*Triticum dicoccum*), another C₃ plant, although this was of lesser importance. Common millet (*Panicum miliaceum*), a C₄ plant was also present along with wild sorghum (C₄) of unknown origin. At the start of the Meroitic, cultivated sorghum (*Sorghum bicolor*) appears for the first time and rapidly increases to become a major crop, rivalled only by barley. Towards the end of the Meroitic, the wheats *Triticum durum* and *T. aestivum* are found but do not achieve major importance. During the Post-meroitic periods, pearl millet is found and during the Christian and Ottoman periods sorghum was in abundance and C₄ crops predominated.

Little is known about animal husbandry in Nubia, as studies in the region have not concentrated on zooarchaeological remains; however, it is likely that in lower Nubia ovi-caprids would have predominated, with lesser numbers of bovids (Copley, 2001). Evidence from the Classical writer Strabo tells us that during the Meroitic period, domestic animals in Nubia were small and consisted of sheep, goats and cattle (Strabo in *Geography* 17.2[1-2]). As with Nubia, the zooarchaeological remains at Qasr Ibrim have not been as intensely studied as the botanical remains. It is likely that sheep and goats predominated, although juvenile cattle bones were the most frequently found faunal remains in context with a temple on site. The age range of these bones may be indicative of a mixed meat/milk economy (Copley, 2001).

Compound-specific stable carbon isotope analysis has already been undertaken on the bones analysed here. $C_{16:0}$ and $C_{18:0}$ fatty acid $\delta^{13}C$ values were obtained as part of a wider investigation of the environmental materials at Qasr Ibrim. The results from the analysis of these bones gave information on the isotopic signature of the whole diet of the animals (Copley, 2001). It was found that for bovids, whilst there was a predominantly C_3 signal during the Napatan period there was an increase in the importance of C_4 forages and fodders up to and during the Christian period corresponding to a reduction of C_3 plant consumption after the Napatan period. The $\delta^{13}C$ values of the $C_{16:0}$ and $C_{18:0}$ fatty acids of the ovi-caprids suggested they had diets that comprised predominantly of C_3 or mixed C_3/C_4 plants across all time periods.

6.3 Results and discussion

6.3.1 Results of non-isotopic analysis

Collagen was extracted from the animal bones as described in Section 2.6. giving an average yield of 10.5% w/w (Table 6.1). Elemental analysis of all the purified collagens gave average C:N ratios of 3.0 ± 0.1 (Table 6.1), indicating that it is very well preserved, values between 2.9 and 3.6 being taken to indicate that there is little, if any, contamination or alteration of the collagen in archaeological samples. Individual amino acids were obtained from the collagen by hydrolysis and derivatised to their trifluoroacetyl isopropyl esters as described in Sections 2.7 and 2.9. Finally, apatite was obtained from the samples as described in Section 2.8 with an average yield of 10.2% w/w (Table 6.1). Figure 6.1 shows a partial gas chromatogram of the individual amino acids from the bone collagen of one of the bovids, where it can be seen that eleven amino acids were successfully separated; this distribution is typical for all bones analysed. Figure 6.2 compares the relative abundances of the amino acids in a typical collagen sample with the known amino acid composition of mammalian collagen (Vaughan, 1970); the close agreement between the distributions provides further evidence that the collagens from Qasr Ibrim are very well preserved.

Table 6.1. Yields of collagen and apatite obtained from animal bones from Qasr Ibrim and C:N ratio of extracted collagen. (Nap = Napatan, Mer = Meroitic, EPM = Early Post Meroitic, PM = Post Meroitic, Chr = Christian, Otto = Ottoman, U = unidentified).

Sample code	Period	% yield (w/w)		
		collagen	apatite	C:N ratio
ovi-caprid				
17048-2	Nap	11.1	8.8	3.0
12513-1	Nap	5.5	17.1	3.1
17035	Nap	11.5	8.6	3.2
17042-2	Nap	12.9	6.1	3.2
17052-2	Nap	5.0	14.4	3.3
17042-1	Nap	11.6	9.3	3.1
18013-1	Mer	11.6	5	3.0
10377	EPM	12.9	10.3	3.0
10110-1	PM	13.3	nd	3.0
10478	PM	12.1	10.5	3.0
10063	PM	14.3	8.4	3.0
10216-3	PM	14.9	4.0	3.0
10216-2	PM	6.6	13.7	3.0
10203(36)	Chr	14.4	10.9	3.0
B1-12	Chr	14.2	6.8	2.9
10045	Otto	9.9	10.5	2.9
14133	Otto	9.7	7.2	3.0
bovid				
17048-1	Nap	9.3	3.5	3.0
10384	EPM	9.4	22.0	3.0
B56	Chr	5.8	16.3	3.0
Ib82 11.7	Chr	10.1	9.2	3.0
B55	Chr	7.6	11.9	3.0
B27	Chr	9.5	16.0	2.9
B35	Chr	9.2	13.4	3.0
10048-L	Otto	14.5	12.4	2.9
10048-R	Otto	12.7	12.1	2.9
10822	U	13.4	14.6	2.9

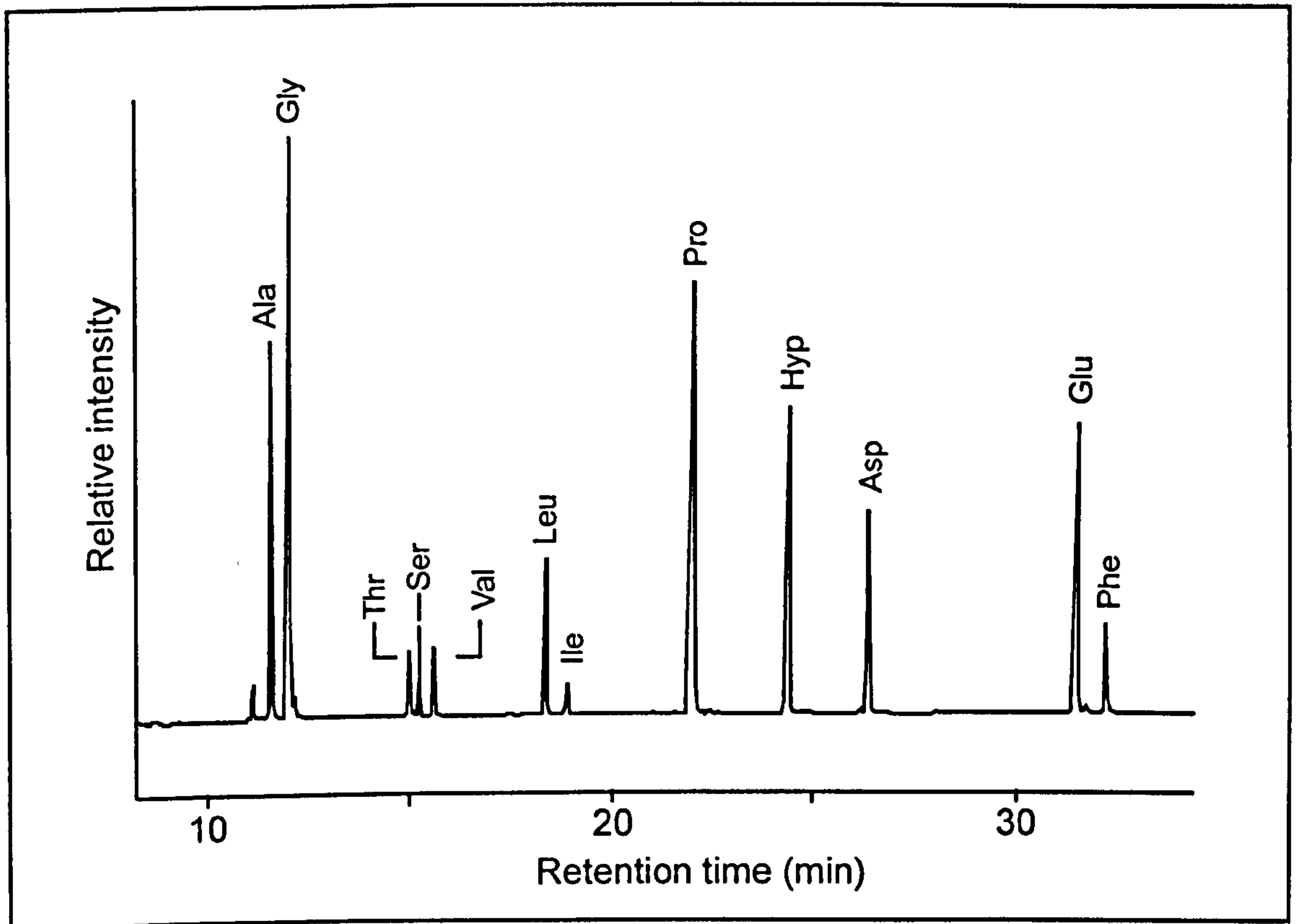


Figure 6.1. Typical partial gas chromatogram of individual amino acids from the bone collagen of a bovid from Qasr Ibrim (sample code 10048_L).

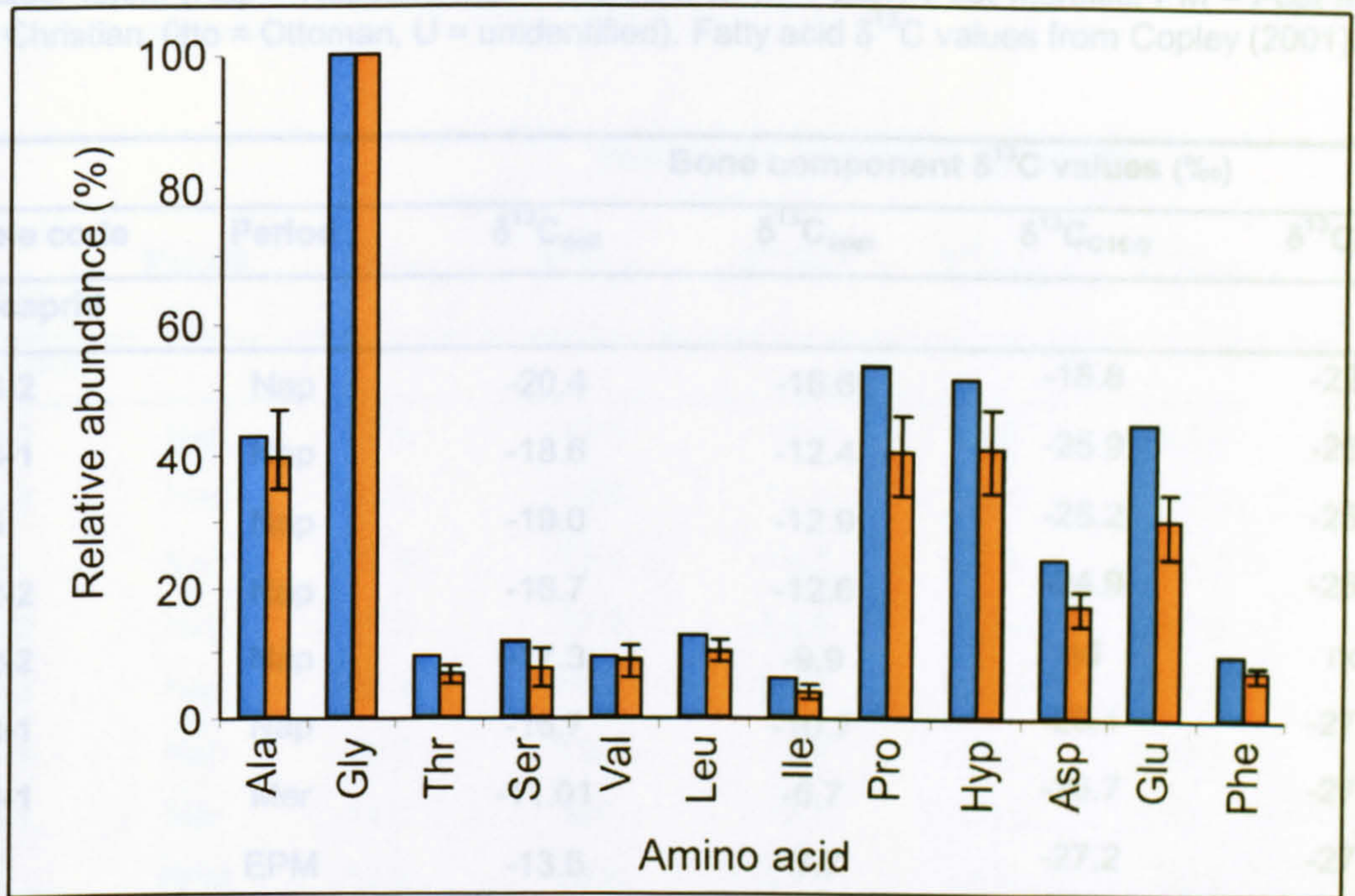


Figure 6.2. Histogram comparing the average relative abundances of amino acids from animal bone collagen samples from Qasr Ibrim (orange), with known abundances based on amino acids in mammalian collagen (blue) (Vaughan, 1970). Bars indicate the lowest and highest relative abundance measured for each amino acid.

6.3.2 Results of carbon isotopic analysis

$\delta^{13}\text{C}$ values for bone collagen, apatite and fatty acids are presented in Table 6.2. The individual amino acid $\delta^{13}\text{C}$ values from the bone collagen, which can be used to predict bone and dietary component $\delta^{13}\text{C}$ values, are presented in Table 6.3. The results of the carbon isotope analysis of individual amino acids from ancient and modern barley are shown in Figure 6.3. It can be seen that the absolute $\delta^{13}\text{C}$ values for modern and ancient barley, with the exception of proline, are identical within experimental error (note that no $\delta^{13}\text{C}$ value was obtained for threonine in modern barley). This suggests that the $\delta^{13}\text{C}$ values of the amino acids in ancient barley have not been altered by degradation during burial. This is an example of how individual amino acid isotopic analyses can be used to assess the degree of

Table 6.2. Bone collagen, apatite, C_{16:0} and C_{18:0} fatty acid $\delta^{13}\text{C}$ values obtained from animal bones from Qasr Ibrim. (Nap = Napatan, Mer = Meroitic, EPM = Early Post Meroitic, PM = Post Meroitic, Chr = Christian, Otto = Ottoman, U = unidentified). Fatty acid $\delta^{13}\text{C}$ values from Copley (2001).

Bone component $\delta^{13}\text{C}$ values (‰)					
Sample code	Period	$\delta^{13}\text{C}_{\text{coll}}$	$\delta^{13}\text{C}_{\text{apat}}$	$\delta^{13}\text{C}_{\text{C}_{16:0}}$	$\delta^{13}\text{C}_{\text{C}_{18:0}}$
ovi-caprid					
17048-2	Nap	-20.4	-16.6	-18.8	-22.9
12513-1	Nap	-18.6	-12.4	-25.9	-26.9
17035	Nap	-19.0	-12.9	-26.2	-25.9
17042-2	Nap	-16.7	-12.6	-24.9	-26.5
17052-2	Nap	-17.3	-9.9	nd	nd
17042-1	Nap	-16.7	-10.7	-26.1	-27.5
18013-1	Mer	-11.01	-6.7	-26.7	-27.9
10377	EPM	-13.6	-7.7	-27.2	-27.9
10110-1	PM	-17.3	nd	-23.6	-24.0
10478	PM	-14.0	-8.2	-25.0	-24.5
10063	PM	-11.7	-6.2	-21.4	-23.3
10216-3	PM	-11.5	-6.2	-23.0	-22.9
10216-2	PM	-11.5	-5.1	-21.3	-20.9
10203(36)	Chr	-18.9	-13.0	-27.0	-26.8
B1-12	Chr	-13.4	-8.1	-23.6	-24.0
10045	Otto	-18.1	-11.9	-26.0	-25.9
14133	Otto	-10.2	-6.2	-20.8	-21.4
bovid					
17048-1	Nap	-11.7	-7.9	-27.2	-28.2
10384	EPM	-11.1	-4.5	-19.5	-20.7
B56	Chr	-11.6	-8.6	-14.7	-16.4
Ib82 11.7	Chr	-13.3	-8.7	-20.0	-21.0
B55	Chr	-9.6	1.0	-18.9	-22.0
B27	Chr	-8.6	0.2	-15.2	-18.2
B35	Chr	-8.8	-2.3	-20.2	-21.3
10048-L	Otto	-10.4	-2.1	-21.7	-23.5
10048-R	Otto	-10.3	-3.9	-21.7	-22.9
10822	U	-13.2	-7.0	-17.8	-20.2

Table 6.3. Individual amino acid $\delta^{13}\text{C}$ values obtained from animal bones from Qasr Ibrim. (Nap = Napatan, Mer = Meroitic, EPM = Early Post Meroitic, PM = Post Meroitic, Chr = Christian, Otto = Ottoman, U = unidentified.)

Bone component $\delta^{13}\text{C}$ values (‰)							
Sample code	Period	$\delta^{13}\text{C}_{\text{ala}}$	$\delta^{13}\text{C}_{\text{gly}}$	$\delta^{13}\text{C}_{\text{thr}}$	$\delta^{13}\text{C}_{\text{ser}}$	$\delta^{13}\text{C}_{\text{val}}$	$\delta^{13}\text{C}_{\text{leu}}$
ovi-caprid							
17048-2	Nap	-27.4	-13.6	-16.9	-8.8	-23.5	-30.2
12513-1	Nap	-23.2	-19.9	-17.6	-14.7	-23.3	-30.9
17035	Nap	-25.6	-13.3	-15.0	-7.5	-20.2	-29.1
17042-2	Nap	-24.2	-17.2	-24.6	-12.4	-17.3	-30.5
17052-2	Nap	-26.3	-16.7	-18.6	-14.3	-25.1	-33.4
17042-1	Nap	-18.8	-13.4	-18.1	-11.3	-22.5	-29.5
18013-1	Mer	-14.0	-8.6	-18.1	-13.6	-19.2	-21.8
10377	EPM	-17.9	-14.6	-14.6	-8.9	-19.3	-24.8
10110-1	PM	-20.5	-12.6	-15.1	-6.7	-18.0	-22.8
10478	PM	-19.2	-17.2	-16.4	-11.9	-22.8	-29.1
10063	PM	-15.1	-7.8	-9.5	-5.2	-15.3	-22.2
10216-3	PM	-15.9	-13.5	-10.9	-5.7	-17.1	-22.9
10216-2	PM	-24.9	-12.0	-15.2	-9.0	-19.7	-25.9
10203(36)	Chr	-22.5	-15.4	-20.9	-15.8	-24.3	-29.5
B1-12	Chr	-19.0	-11.5	-11.4	-7.2	-17.5	-24.5
10045	Otto	-22.3	-9.0	-6.9	-3.6	-14.6	-22.9
14133	Otto	-17.8	-18.3	-20.3	-13.9	-26.4	-31.5
bovid							
17048-1	Nap	-18.3	-11.3	-11.6	-9.5	-16.7	-23.1
10384	EPM	-14.3	-11.4	-12.2	-9.7	-19.3	-23.6
B56	Chr	-20.9	-11.2	-12.5	-7.0	-13.0	-20.5
Ib82 11.7	Chr	-16.3	-6.1	-10.3	-5.2	-15.8	-22.1
B55	Chr	-13.9	-7.7	-9.8	-6.1	-15.8	-22.0
B27	Chr	-13.2	-14.1	-15.7	-12.0	-21.4	-28.3
B35	Chr	-12.4	-10.9	-12.4	-6.8	-19.1	-25.7
10048-L	Otto	-15.0	-14.0	-10.4	-8.4	-16.0	-23.5
10048-R	Otto	-17.3	-13.3	-9.5	-10.4	-16.7	-23.0
10822	U	-15.2	-13.6	-13.2	-11.9	-19.6	-25.1

Table 6.3. cont. Individual amino acid $\delta^{13}\text{C}$ values obtained from animal bones from Qasr Ibrim. (Nap = Napatan, Mer = Meroitic, EPM = Early Post Meroitic, PM = Post Meroitic, Chr = Christian, Otto = Ottoman, U = unidentified.)

Bone component $\delta^{13}\text{C}$ values (‰)							
Sample code	Period	$\delta^{13}\text{C}_{\text{ile}}$	$\delta^{13}\text{C}_{\text{pro}}$	$\delta^{13}\text{C}_{\text{hyp}}$	$\delta^{13}\text{C}_{\text{asp}}$	$\delta^{13}\text{C}_{\text{glu}}$	$\delta^{13}\text{C}_{\text{phe}}$
ovi-caprid							
17048-2	Nap	-24.9	-14.2	-24.4	-21.5	-16.5	-29.7
12513-1	Nap	-27.2	-14.5	-22.0	-20.0	-13.3	-27.9
17035	Nap	-23.6	-12.5	-22.4	-19.5	-14.5	-28.5
17042-2	Nap	-27.6	-13.2	-21.1	-19.2	-12.3	-26.6
17052-2	Nap	-29.5	-16.6	-20.1	-17.1	-11.5	-27.3
17042-1	Nap	-23.2	-12.1	-17.8	-16.1	-10.3	-26.8
18013-1	Mer	-18.3	-7.0	-14.0	-15.3	-5.3	-23.5
10377	EPM	-21.3	-9.4	-17.5	-15.2	-7.9	-26.1
10110-1	PM	-19.3	-7.5	-21.3	-19.4	-13.9	-28.3
10478	PM	-27.1	-13.5	-17.6	-14.7	-7.7	-26.5
10063	PM	-17.5	-6.1	-16.1	-14.2	-5.9	-25.1
10216-3	PM	-19.2	-7.4	-15.1	-14.7	-5.4	-24.6
10216-2	PM	-19.7	-9.6	-14.6	-12.8	-4.7	-23.9
10203(36)	Chr	-23.1	-13.9	-21.9	-21.6	-14.7	-28.7
B1-12	Chr	-20.9	-8.7	-16.5	-12.7	-5.9	-25.8
10045	Otto	-16.1	-5.7	-22.3	-19.7	-13.2	-27.8
14133	Otto	-24.6	-14.6	-14.1	-12.6	-3.6	-23.5
bovid							
17048-1	Nap	-19.2	-6.9	-14.5	-14.6	-5.5	-24.4
10384	EPM	-17.4	-6.3	-14.1	-13.8	-5.5	-24.1
B56	Chr	-20.2	-4.5	-19.4	-17.6	-11.2	-28.5
Ib82 11.7	Chr	-19.2	-4.2	-16.9	-10.6	-7.4	-26.0
B55	Chr	-19.6	-5.5	-12.8	-9.6	-2.5	-23.7
B27	Chr	-23.6	-12.1	-12.3	-10.2	-1.5	-23.5
B35	Chr	-23.5	-9.4	-11.9	-9.5	-0.7	-23.4
10048-L	Otto	-20.4	-6.5	-13.4	-11.6	-2.9	-24.2
10048-R	Otto	-19.1	-6.7	-14.0	-11.9	-4.2	-23.9
10822	U	-22.3	-10.0	-16.5	-16.5	-8.6	-26.2

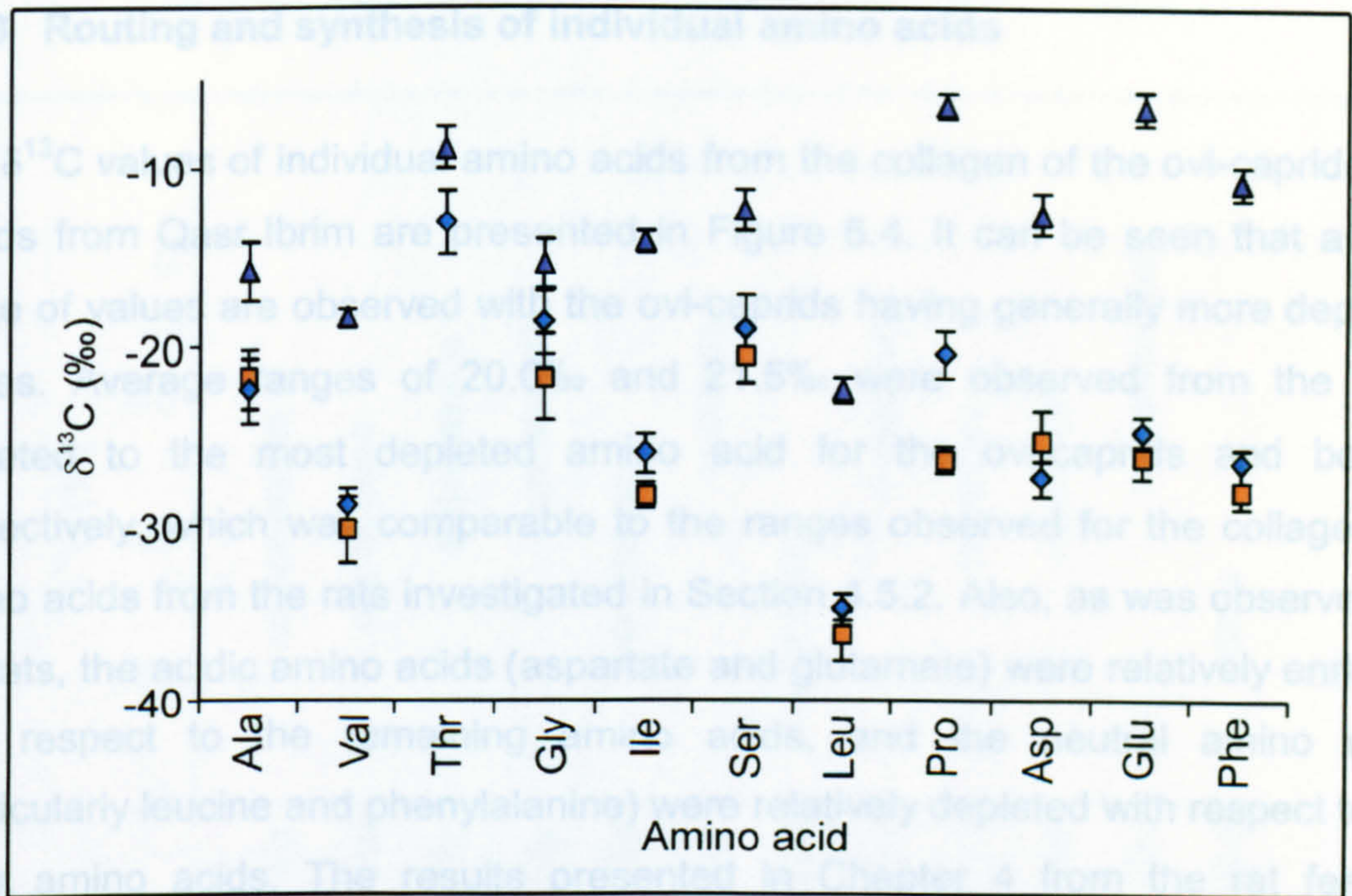


Figure 6.3. Graph showing the $\delta^{13}\text{C}$ values and associated errors of individual amino acids from ancient barley (blue diamonds), modern barley (orange squares) and ancient sorghum (purple triangles).

preservation of archaeological remains (Hare and Estep, 1983). By analogy, we suggest that the ancient sorghum has also been unaffected by degradation. The range of $\delta^{13}\text{C}$ values seen for the different amino acids of ancient barley is somewhat larger than that observed for the ancient sorghum, i.e. 21.6‰ compared to 16.0‰. The amino acids in the ancient sorghum are consistently enriched in ^{13}C compared to the same amino acid in the ancient barley, as would be expected for a C_4 plant. There is, however, a wide range of differences ($\Delta^{13}\text{C}_{\text{sorghum-barley}}$) with the extreme values being seen for threonine (+3.2‰) and glutamate (18.1‰); mean $\Delta^{13}\text{C}_{\text{sorghum-barley}}$ is $10.6\text{‰} \pm 4.9\text{‰}$. There are some similarities in the pattern of $\delta^{13}\text{C}$ values observed, for example leucine has the most depleted value in both barley and sorghum. Given the complexity of plant physiology it is not unexpected that two different species fractionate carbon to slightly different extents during the biosynthesis of amino acids.

6.3.3 Routing and synthesis of individual amino acids

The $\delta^{13}\text{C}$ values of individual amino acids from the collagen of the ovi-caprids and bovids from Qasr Ibrim are presented in Figure 6.4. It can be seen that a wide range of values are observed with the ovi-caprids having generally more depleted values. Average ranges of 20.0‰ and 21.5‰ were observed from the least depleted to the most depleted amino acid for the ovi-caprids and bovids, respectively, which was comparable to the ranges observed for the collagenous amino acids from the rats investigated in Section 4.5.2. Also, as was observed for the rats, the acidic amino acids (aspartate and glutamate) were relatively enriched with respect to the remaining amino acids, and the neutral amino acids (particularly leucine and phenylalanine) were relatively depleted with respect to the other amino acids. The results presented in Chapter 4 from the rat feeding experiments showed that the isotopic signature of different amino acids in bone collagen is determined by the isotopic composition of those macronutrients that provide their carbon. Essential amino acids must be provided directly by the diet and accordingly very little difference was seen between the $\delta^{13}\text{C}$ values of essential amino acids in the diet and the corresponding amino acid in the bone collagen of the consumer. For example, this was observed for phenylalanine, where an average fractionation of 1.3‰ was seen, which is within experimental error. This routing from dietary protein to bone collagen means that the isotopic composition of phenylalanine in the bone collagen of the animals from Qasr Ibrim could be used as a proxy for the isotopic composition of the dietary protein. Alanine is a non-essential amino acid; therefore it can either be incorporated from alanine in the diet or synthesised *de novo*, almost directly from carbohydrates in the diet. In Chapter 4 it was seen that the majority of alanine in bone collagen was synthesised *de novo* from dietary carbohydrates rather than being routed directly from alanine in the diet. Therefore, the isotopic composition of alanine in the bone collagen of the animals from Qasr Ibrim could be used as a proxy for the isotopic composition of the carbohydrate being consumed. The $\delta^{13}\text{C}$ values of phenylalanine and alanine from the bone collagen of the animals from Qasr Ibrim are shown in Figure 6.5.

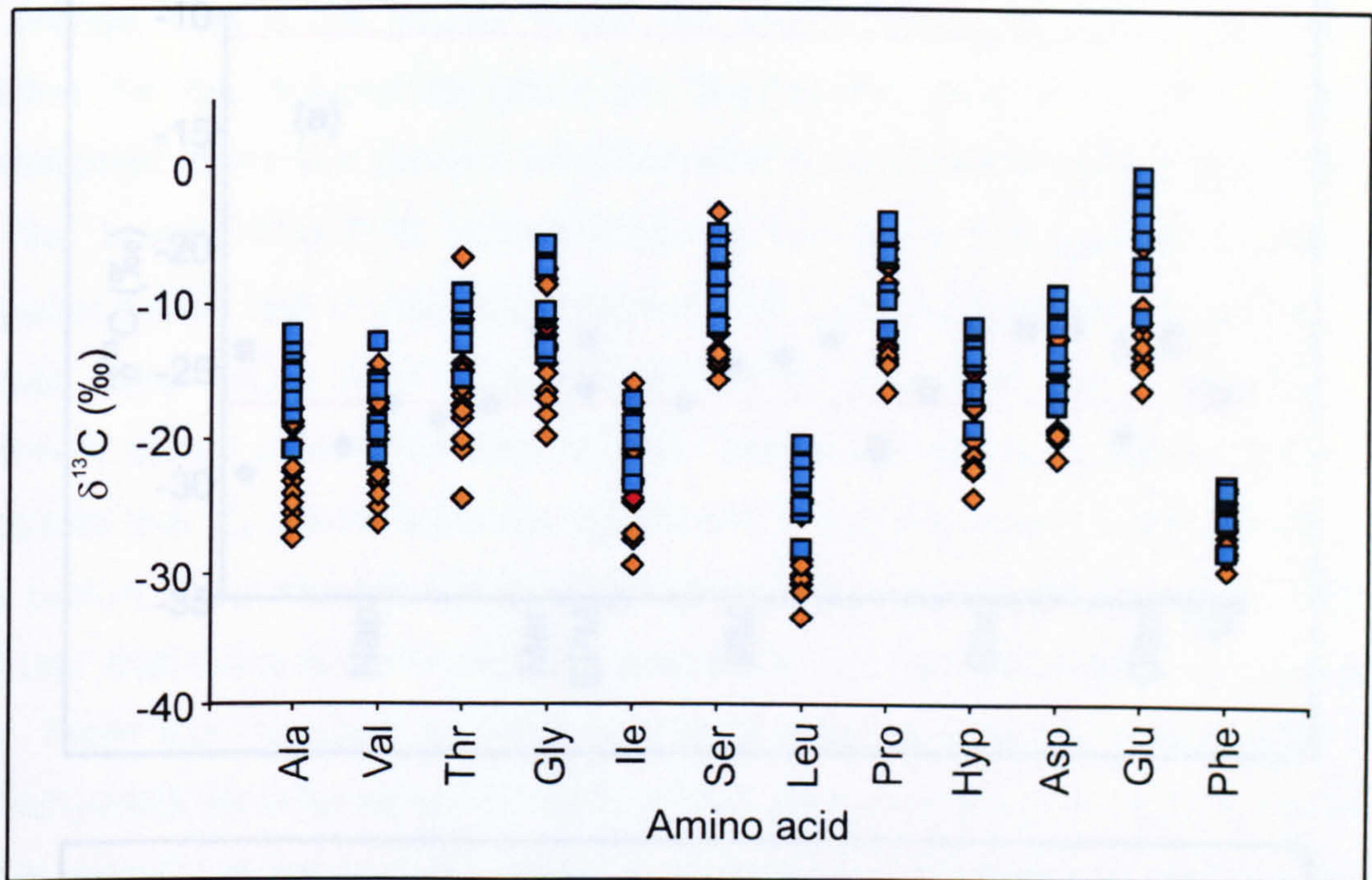


Figure 6.4. Graph showing the $\delta^{13}\text{C}$ values of individual amino acids from bone collagen of ovi-caprids (orange diamonds) and bovids (blue squares) from Qasr Ibrim.

The comparison of collagen phenylalanine $\delta^{13}\text{C}$ values with sorghum and barley phenylalanine isotope values indicates that there is no significant difference in the values observed for ovi-caprids and bovids over time. Also all the collagen phenylalanine $\delta^{13}\text{C}$ values are within ca. 2.5‰ of the value obtained for phenylalanine in barley. This suggests that from the Napatan period through to the Ottoman period, both the ovi-caprids and bovids were obtaining their protein from C_3 sources. This does not mean that they were not also consuming C_4 plants, such as sorghum. Differences in the digestibility of the protein component of different fodders may result in the isotopic composition of the bone collagen being biased towards certain dietary components.

Figure 6.5(b) shows that the $\delta^{13}\text{C}$ value of alanine in bone collagen is much more variable than that of phenylalanine. The $\delta^{13}\text{C}$ values range from -27.4‰ to -14‰ for the ovi-caprids and -20.9‰ to -12.4‰ for the bovids. This encompasses the

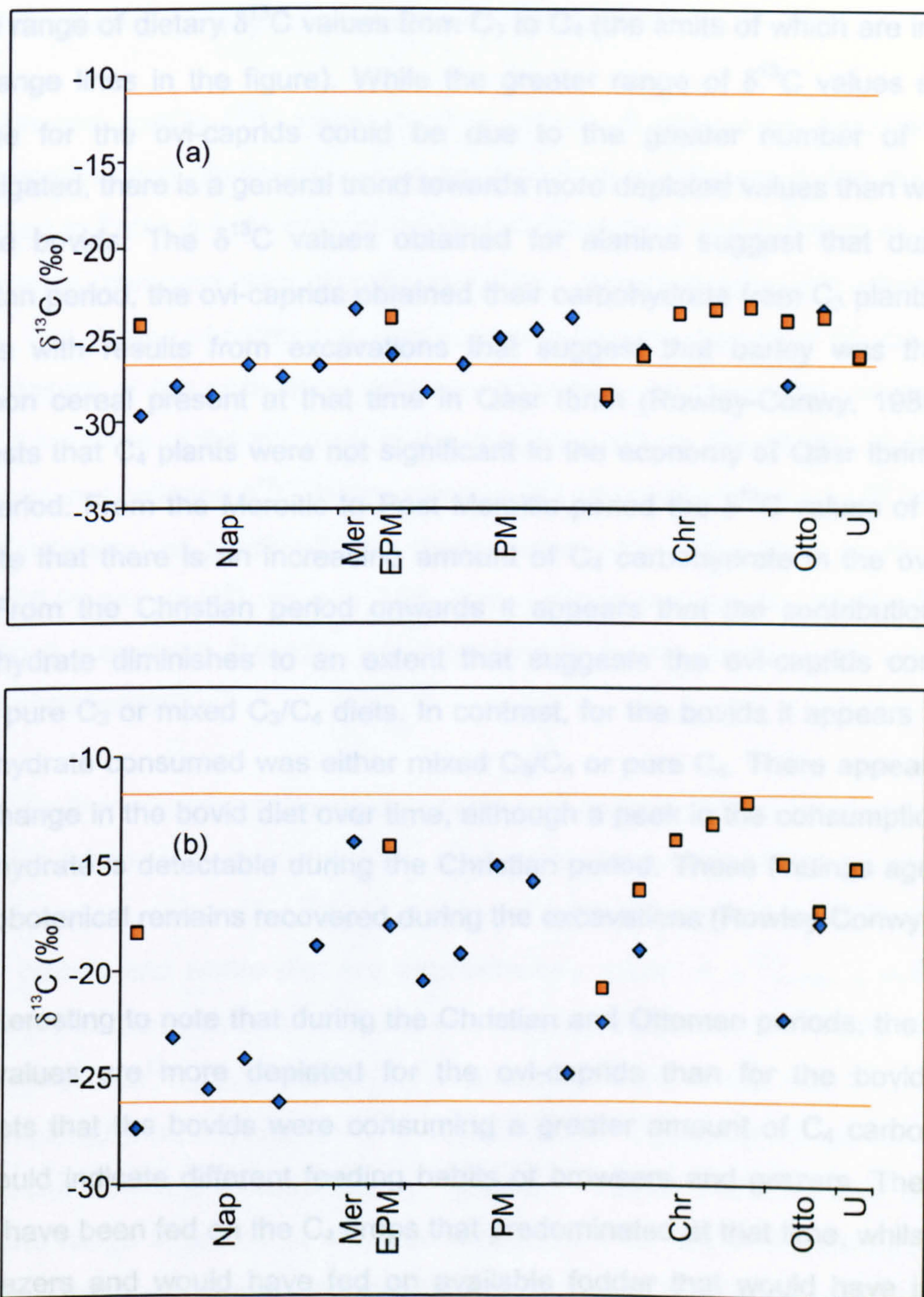


Figure 6.5. Plots showing the $\delta^{13}\text{C}$ values of (a) phenylalanine and (b) alanine from bone collagen of animals from Qasr Ibrim. Ovi-caprids are represented by blue diamonds and bovids by orange squares. In (a) the upper orange line shows the $\delta^{13}\text{C}$ value of phenylalanine in ancient sorghum, whilst the lower line shows the $\delta^{13}\text{C}$ values of phenylalanine in ancient barley. In (b) the upper and lower orange lines are average bulk $\delta^{13}\text{C}$ values of C_4 and C_3 plants, respectively (O'Leary, 1981; Smith and Epstein, 1971).

whole range of dietary $\delta^{13}\text{C}$ values from C_3 to C_4 (the limits of which are indicated by orange lines in the figure). While the greater range of $\delta^{13}\text{C}$ values seen for alanine for the ovi-caprids could be due to the greater number of animals investigated, there is a general trend towards more depleted values than was seen for the bovids. The $\delta^{13}\text{C}$ values obtained for alanine suggest that during the Napatan period, the ovi-caprids obtained their carbohydrate from C_3 plants, which agrees with results from excavations that suggest that barley was the most common cereal present at that time in Qasr Ibrim (Rowley-Conwy, 1989). This suggests that C_4 plants were not significant to the economy of Qasr Ibrim during this period. From the Meroitic to Post Meroitic period the $\delta^{13}\text{C}$ values of alanine indicate that there is an increasing amount of C_4 carbohydrate in the ovi-caprid diet. From the Christian period onwards it appears that the contribution of C_4 carbohydrate diminishes to an extent that suggests the ovi-caprids consumed either pure C_3 or mixed C_3/C_4 diets. In contrast, for the bovids it appears that the carbohydrate consumed was either mixed C_3/C_4 or pure C_4 . There appears to be little change in the bovid diet over time, although a peak in the consumption of C_4 carbohydrate is detectable during the Christian period. These findings agree with palaeobotanical remains recovered during the excavations (Rowley-Conwy, 1989).

It is interesting to note that during the Christian and Ottoman periods, the alanine $\delta^{13}\text{C}$ values are more depleted for the ovi-caprids than for the bovids. This suggests that the bovids were consuming a greater amount of C_4 carbohydrate and could indicate different feeding habits of browsers and grazers. The bovids would have been fed on the C_4 crops that predominated at that time, whilst sheep are grazers and would have fed on available fodder that would have included significant C_3 components. Although C_3 plants were the dominant cultivars during the Napatan period, wild sorghum (of unknown race) did occur in the vicinity of Qasr Ibrim, which would contribute, to the mixed C_3/C_4 signal seen for the bovid from the Napatan period.

6.3.4 Predicting dietary macronutrient $\delta^{13}\text{C}$ values

Collagen and apatite $\delta^{13}\text{C}$ values for the various animals were predicted using hydroxyproline and glutamate values as described in Chapter 5; the results are presented in Table 6.4. As shown in Figure 6.6 the predicted collagen and apatite $\delta^{13}\text{C}$ values compare very closely with their experimentally determined $\delta^{13}\text{C}$ values. The degree of correlation was assessed through the use of R^2 values; R^2_1 is a measure of the correlation between predicted and measured values, whilst R^2_2 is a measure of the accuracy of the predicted values. Correlation of predicted and measured collagen $\delta^{13}\text{C}$ values gave an R^2_1 value of 0.96 and an R^2_2 value of 0.97. Correlation of predicted and measured apatite $\delta^{13}\text{C}$ values gave an R^2_1 value of 0.90 and an R^2_2 value of 0.94. This confirms that the models developed in Chapter 5 based on the rats are transferable to the bovids and ovi-caprids investigated herein.

It is known that the spacing between apatite and collagen $\delta^{13}\text{C}$ values can provide qualitative information concerning the relationship between protein and whole diet $\delta^{13}\text{C}$ values (Jim, 2000). A $\Delta^{13}\text{C}_{\text{apat-coll}}$ value of 5.1 indicates that the $\delta^{13}\text{C}$ values of dietary protein and whole diet are approximately equal. A $\Delta^{13}\text{C}_{\text{apat-coll}}$ value >6.1 indicates that the protein $\delta^{13}\text{C}$ value is more depleted than the whole diet $\delta^{13}\text{C}$ value, whilst a $\Delta^{13}\text{C}_{\text{apat-coll}}$ value <4.1 indicates that the whole diet $\delta^{13}\text{C}$ value is more depleted than the protein $\delta^{13}\text{C}$ value. The $\Delta^{13}\text{C}_{\text{apat-coll}}$ spacings for the ovi-caprids and bovids are presented in Figure 6.7. Values that fall either above or below the range indicated by the dashed purple lines are considered to have a $\Delta^{13}\text{C}_{\text{apat-coll}}$ value significantly different from 5.1. From Figure 6.7(a) it can be seen that the bones from the earlier periods fall within the range centred around $\Delta^{13}\text{C}_{\text{apat-coll}} = 5.1$, which indicates that protein and whole diet $\delta^{13}\text{C}$ values were similar during the period ca. 1000 BC to AD 400. While the same general trend was observed for the bovids (Figure 6.7b), it was not possible to say whether this extended through the Post Meroitic period due to the lack of finds. In the later periods, both the ovi-caprids and bovids generally display $\Delta^{13}\text{C}_{\text{apat-coll}}$ values significantly higher than 5.1, indicating that the dietary protein was more depleted in ^{13}C than whole diet.

Table 6.4. Bone and dietary component $\delta^{13}\text{C}$ values for Qasr Ibrim animal bones predicted from individual amino acid $\delta^{13}\text{C}$ values using the rat model developed in Chapter 5.

Predicted bone and dietary component $\delta^{13}\text{C}$ values (‰)					
Sample code	$\delta^{13}\text{C}_{\text{coll}}$	$\delta^{13}\text{C}_{\text{apat}}$	$\delta^{13}\text{C}_{\text{wdiet(long)}}$	$\delta^{13}\text{C}_{\text{prot}}$	$\delta^{13}\text{C}_{\text{energy}}$
ovi-caprid					
17048-2	-21.4	-16.0	-26.0	-27.7	-24.9
12513-1	-19.2	-13.2	-23.0	-25.8	-22.3
17035	-19.5	-14.3	-24.1	-25.8	-23.3
17042-2	-18.3	-12.4	-22.1	-25.0	-20.9
17052-2	-17.4	-11.7	-21.4	-23.9	-20.4
17042-1	-15.2	-10.6	-20.2	-21.0	-20.0
18013-1	-11.7	-6.3	-15.6	-18.0	-15.2
10377	-15.0	-8.5	-18.0	-22.0	-16.8
10110-1	-18.5	-13.8	-23.6	-24.4	-23.1
10478	-15.1	-8.4	-17.8	-22.2	-16.5
10063	-13.6	-6.8	-16.1	-20.9	-14.8
10216-3	-12.7	-6.4	-15.7	-19.6	-14.7
10216-2	-12.2	-5.7	-15.0	-19.3	-14.0
10203(36)	-19.1	-14.5	-24.3	-24.9	-23.8
B1-12	-14.0	-6.8	-16.1	-21.5	-14.6
10045	-19.5	-13.2	-22.9	-26.4	-21.5
14133	-11.8	-4.8	-14.0	-19.1	-12.7
bovid					
17048-1	-12.1	-6.4	-15.8	-18.7	-15.2
10384	-11.8	-6.4	-15.8	-18.0	-15.4
B56	-16.7	-11.4	-21.1	-23.0	-20.4
lb82 11.7	-14.4	-8.1	-17.5	-21.3	-16.5
B55	-10.6	-3.8	-13.0	-17.7	-11.9
B27	-10.1	-3.0	-12.0	-17.5	-10.8
B35	-9.7	-2.3	-11.3	-17.4	-9.9
10048-L	-11.1	-4.2	-13.4	-18.4	-12.2
10048-R	-11.7	-5.3	-14.5	-18.6	-13.6
10822	-14.0	-9.1	-18.7	-20.0	-18.4

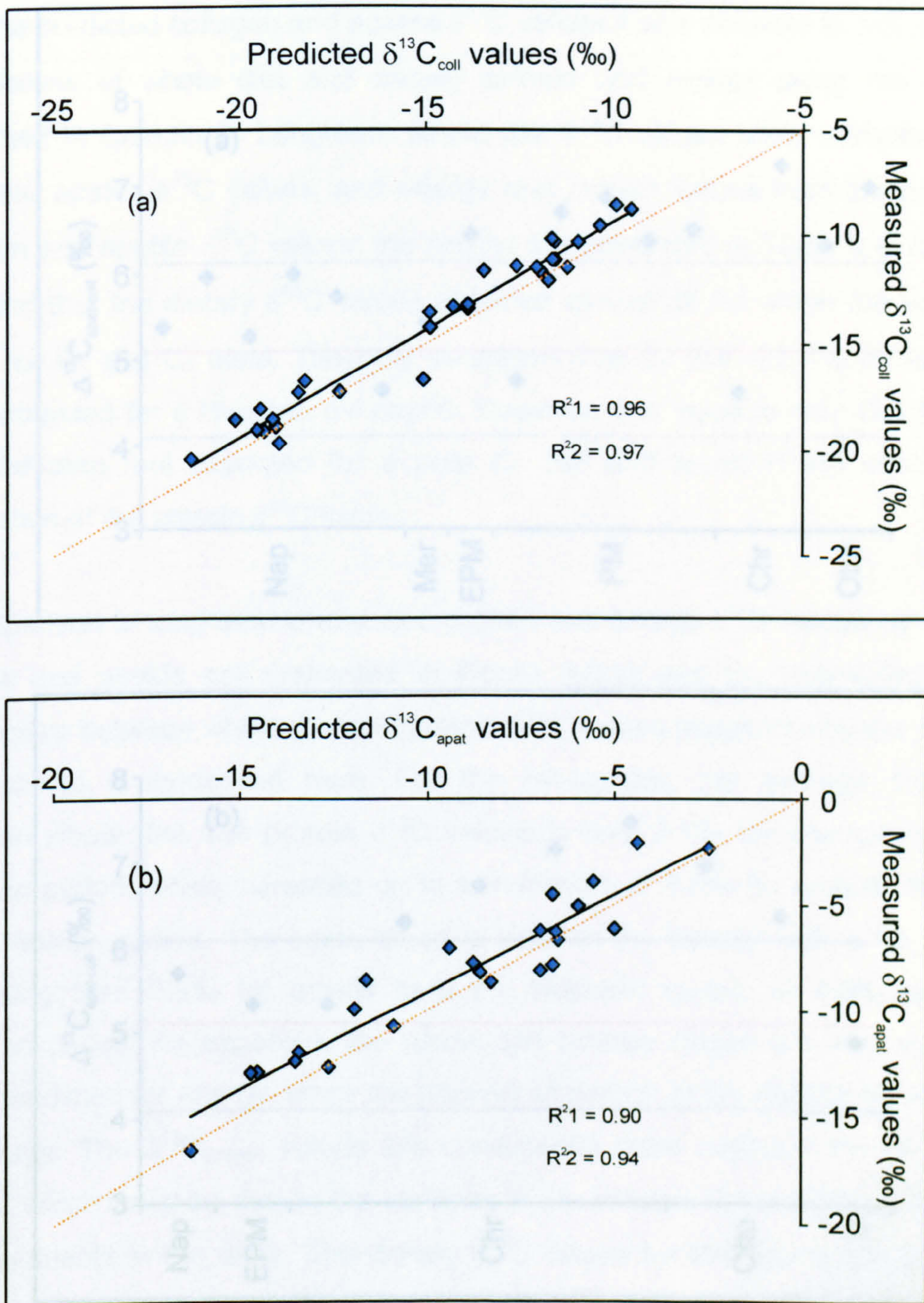


Figure 6.6. Comparison of experimentally determined (a) collagen and (b) apatite $\delta^{13}\text{C}$ values from Qasr Ibrim animal bones with those predicted by the individual amino acid rat model developed in Chapter 5.

$\delta^{13}\text{C}_{\text{apatite}} = \delta^{13}\text{C}_{\text{collagen}}$ (Jim, 2000).

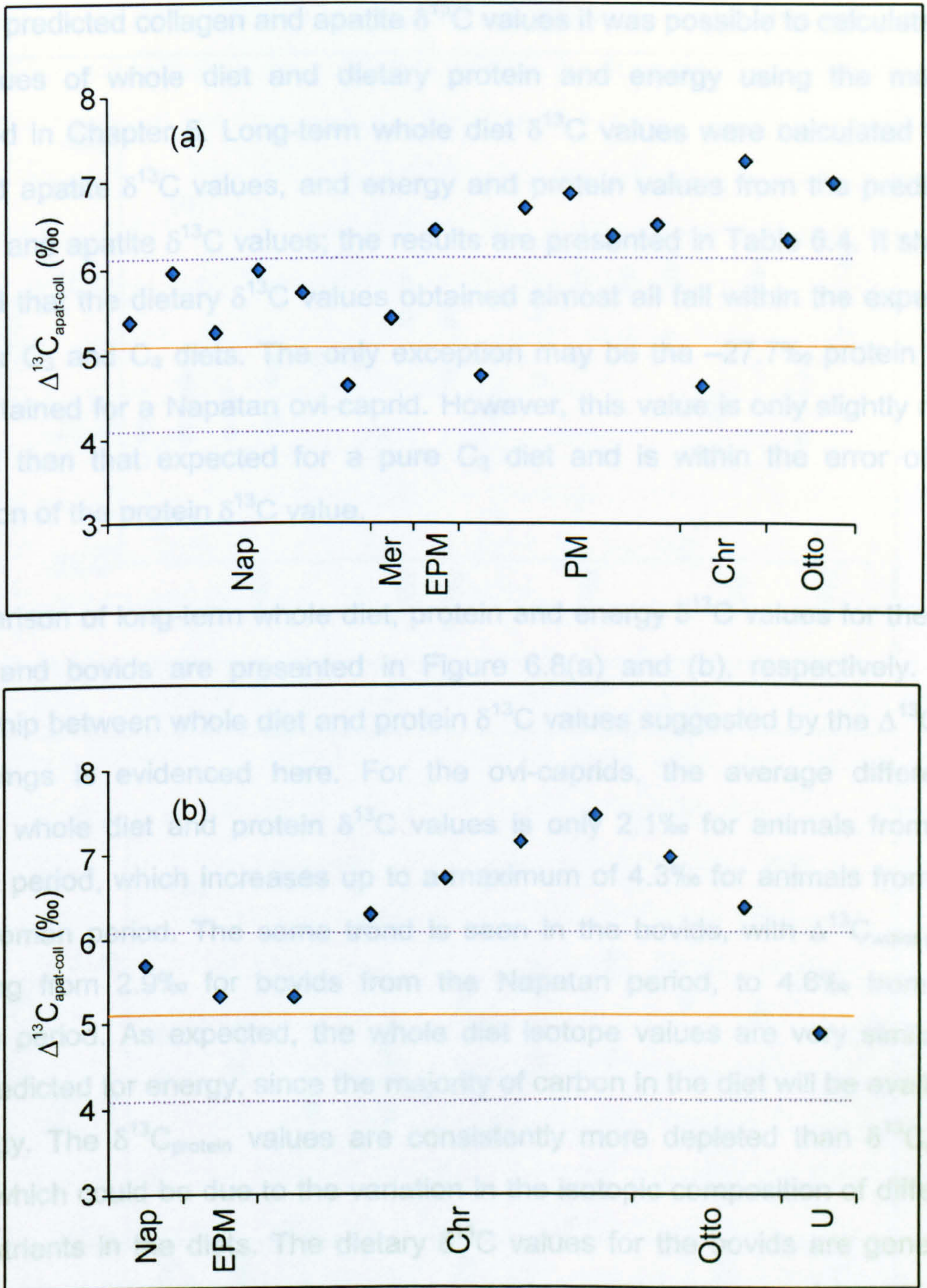


Figure 6.7. $\Delta^{13}\text{C}_{\text{apat-coll}}$ spacings for the Qasr Ibrim samples for (a) ovi-caprids and (b) bovids. Nap = Napatan; Mer = Meroitic; EPM = Early Post Meroitic; PM = Post Meroitic; Chr = Christian; Otto = Ottoman and U = unidentified. Dashed purple lines indicate the upper and lower limits where $\delta^{13}\text{C}_{\text{protein}} \approx \delta^{13}\text{C}_{\text{whole diet}}$ (Jim, 2000).

With the predicted collagen and apatite $\delta^{13}\text{C}$ values it was possible to calculate the $\delta^{13}\text{C}$ values of whole diet and dietary protein and energy using the models presented in Chapter 5. Long-term whole diet $\delta^{13}\text{C}$ values were calculated from predicted apatite $\delta^{13}\text{C}$ values, and energy and protein values from the predicted collagen and apatite $\delta^{13}\text{C}$ values; the results are presented in Table 6.4. It should be noted that the dietary $\delta^{13}\text{C}$ values obtained almost all fall within the expected range for C_3 and C_4 diets. The only exception may be the -27.7‰ protein $\delta^{13}\text{C}$ value obtained for a Napatan ovi-caprid. However, this value is only slightly more depleted than that expected for a pure C_3 diet and is within the error of the calculation of the protein $\delta^{13}\text{C}$ value.

A comparison of long-term whole diet, protein and energy $\delta^{13}\text{C}$ values for the ovi-caprids and bovids are presented in Figure 6.8(a) and (b), respectively. The relationship between whole diet and protein $\delta^{13}\text{C}$ values suggested by the $\Delta^{13}\text{C}_{\text{apat-coll}}$ spacings is evidenced here. For the ovi-caprids, the average difference between whole diet and protein $\delta^{13}\text{C}$ values is only 2.1‰ for animals from the Napatan period, which increases up to a maximum of 4.3‰ for animals from the later Ottoman period. The same trend is seen in the bovids, with $\Delta^{13}\text{C}_{\text{wdiet-protein}}$ increasing from 2.9‰ for bovids from the Napatan period, to 4.6‰ from the Ottoman period. As expected, the whole diet isotope values are very similar to those predicted for energy, since the majority of carbon in the diet will be available as energy. The $\delta^{13}\text{C}_{\text{protein}}$ values are consistently more depleted than $\delta^{13}\text{C}_{\text{energy}}$ values, which could be due to the variation in the isotopic composition of different macronutrients in the diets. The dietary $\delta^{13}\text{C}$ values for the bovids are generally less depleted than those of the ovi-caprids, which may be indicative of the different feeding patterns between ovi-caprids and bovids, especially during the later periods.

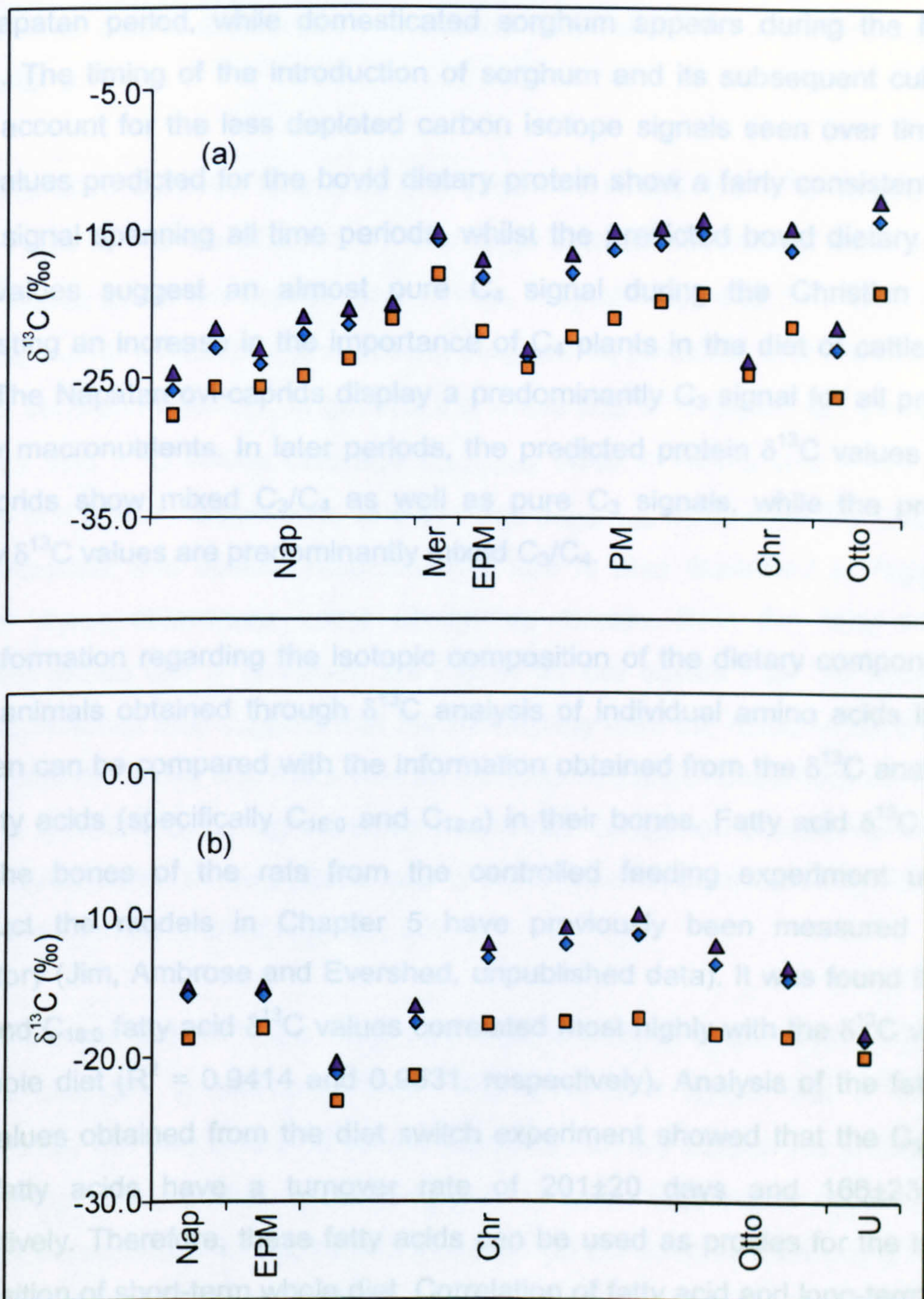


Figure 6.8. Predicted dietary $\delta^{13}\text{C}$ values for the Qasr Ibrim animals for (a) ovi-caprids and (b) bovids. Dietary $\delta^{13}\text{C}_{\text{protein}}$ values are indicated by the orange squares, $\delta^{13}\text{C}_{\text{energy}}$ values by purple triangles and $\delta^{13}\text{C}_{\text{wdiet}}$ by blue diamonds. Nap = Napatan; Mer = Meroitic; EPM = Early Post Meroitic; PM = Post Meroitic; Chr = Christian; Otto = Ottman and U = unidentified.

Excavations have shown that barley was the most common cereal found during the Napatan period, while domesticated sorghum appears during the Meroitic period. The timing of the introduction of sorghum and its subsequent cultivation could account for the less depleted carbon isotope signals seen over time. The $\delta^{13}\text{C}$ values predicted for the bovid dietary protein show a fairly consistent mixed C_3/C_4 signal spanning all time periods, whilst the predicted bovid dietary energy $\delta^{13}\text{C}$ values suggest an almost pure C_4 signal during the Christian period, suggesting an increase in the importance of C_4 plants in the diet of cattle at this time. The Napatan ovi-caprids display a predominantly C_3 signal for all predicted dietary macronutrients. In later periods, the predicted protein $\delta^{13}\text{C}$ values for the ovi-caprids show mixed C_3/C_4 as well as pure C_3 signals, while the predicted energy $\delta^{13}\text{C}$ values are predominantly mixed C_3/C_4 .

The information regarding the isotopic composition of the dietary components of these animals obtained through $\delta^{13}\text{C}$ analysis of individual amino acids in bone collagen can be compared with the information obtained from the $\delta^{13}\text{C}$ analysis of the fatty acids (specifically $\text{C}_{16:0}$ and $\text{C}_{18:0}$) in their bones. Fatty acid $\delta^{13}\text{C}$ values from the bones of the rats from the controlled feeding experiment used to construct the models in Chapter 5 have previously been measured in our laboratory (Jim, Ambrose and Evershed, unpublished data). It was found that the $\text{C}_{16:0}$ and $\text{C}_{18:0}$ fatty acid $\delta^{13}\text{C}$ values correlated most highly with the $\delta^{13}\text{C}$ value of the whole diet ($R^2 = 0.9414$ and 0.9531 , respectively). Analysis of the fatty acid $\delta^{13}\text{C}$ values obtained from the diet switch experiment showed that the $\text{C}_{16:0}$ and $\text{C}_{18:0}$ fatty acids have a turnover rate of 201 ± 20 days and 166 ± 23 days, respectively. Therefore, these fatty acids can be used as proxies for the isotopic composition of short-term whole diet. Correlation of fatty acid and long-term whole diet $\delta^{13}\text{C}$ values predicted from bone collagen aspartate $\delta^{13}\text{C}$ values gave R^2 values of 0.17 for $\text{C}_{16:0}$ and predicted whole diet and 0.19 for $\text{C}_{18:0}$ and predicted whole diet. The absolute differences between the fatty acid and predicted long-term whole diet $\delta^{13}\text{C}$ values are presented in Table 6.5.

This discrepancy is evidence of how the differences in turnover times of bone components lead to differences in predicted whole diet $\delta^{13}\text{C}$ values as suggested in chapter 5.

The difference between fatty acid and predicted whole diet $\delta^{13}\text{C}$ values ranges from -7.2‰ to $+12.4\text{‰}$ (Table 6.5). The large standard deviations (± 4.3 and ± 5.2 for $\Delta^{13}\text{C}_{\text{wdiet-C16:0}}$ for ovi-caprids and bovids, respectively, and ± 3.8 and ± 5.1 for $\Delta^{13}\text{C}_{\text{wdiet-C18:0}}$ for ovi-caprids and bovids, respectively) indicate that the differences are not constant; however, in general the whole diet $\delta^{13}\text{C}$ values are greater than the fatty acid $\delta^{13}\text{C}$ values (average $\Delta_{\text{wdiet-C16:0}}$ value = $+4.6\text{‰}$ and 4.4‰ for ovi-caprids and bovids, respectively and average $\Delta_{\text{wdiet-C18:0}}$ value = $+5.3\text{‰}$ and $+6.1\text{‰}$ for ovi-caprids and bovids, respectively). This is also illustrated in Figure 6.9. Despite these differences some similarities remain. Both the fatty acid and predicted whole diet $\delta^{13}\text{C}$ values are higher for the bovids than the ovi-caprids. Both approaches also suggest that the ovi-caprids from the Napatan period had a predominantly C_3 diet and there was an increase in the C_4 component over time to produce a mixed C_3/C_4 signal, while the bovids consumed predominantly C_3 or mixed C_3/C_4 diets, although there was a trend towards predominantly C_4 signals during the Christian period (Copley, 2001).

The difference between the fatty acid and predicted whole diet $\delta^{13}\text{C}$ values indicate changes in diet over time. The short-term whole diet $\delta^{13}\text{C}$ values illustrated by the fatty acid $\delta^{13}\text{C}$ values suggests that the diets of the animals were more isotopically depleted immediately prior to death than the average long-term diet they consumed. This appears to indicate that the animals were being fattened up on C_3 fodders prior to slaughter.

Table 6.5. Differences between fatty acid and long-term whole diet $\delta^{13}\text{C}$ values obtained from animal bones from Qasr Ibrim. Fatty acid $\delta^{13}\text{C}$ values from Copley, 2001.

Sample code	$\Delta_{\text{diet-C18:0}}$ (‰)	$\Delta_{\text{diet-C18:0}}$ (‰)
ovi-caprid		
17048-2	-7.2	-3.1
12513-1	2.9	3.9
17035	2.1	1.8
17042-2	2.8	4.4
17042-1		
18013-1	5.9	7.3
10377	11.1	12.3
10110-1	9.2	9.9
10478	0	0.4
10063	7.2	6.7
10216-3	5.3	7.2
10216-2	7.3	7.2
10203(36)	6.3	5.9
B1-12	2.7	2.5
10045	7.5	7.9
14133	3.1	3
average	4.6 ±4.3	5.3 ±3.8
bovid		
17048-1	11.4	12.4
10384	3.7	4.9
B56	-6.4	-4.7
lb82 11.7	2.5	3.5
B55	5.9	9
B27	3.2	6.2
B35	8.9	10
10048-L	8.3	10.1
10048-R	7.2	8.4
10822	-0.9	1.5
average	4.4 ±5.2	6.1 ±5.1

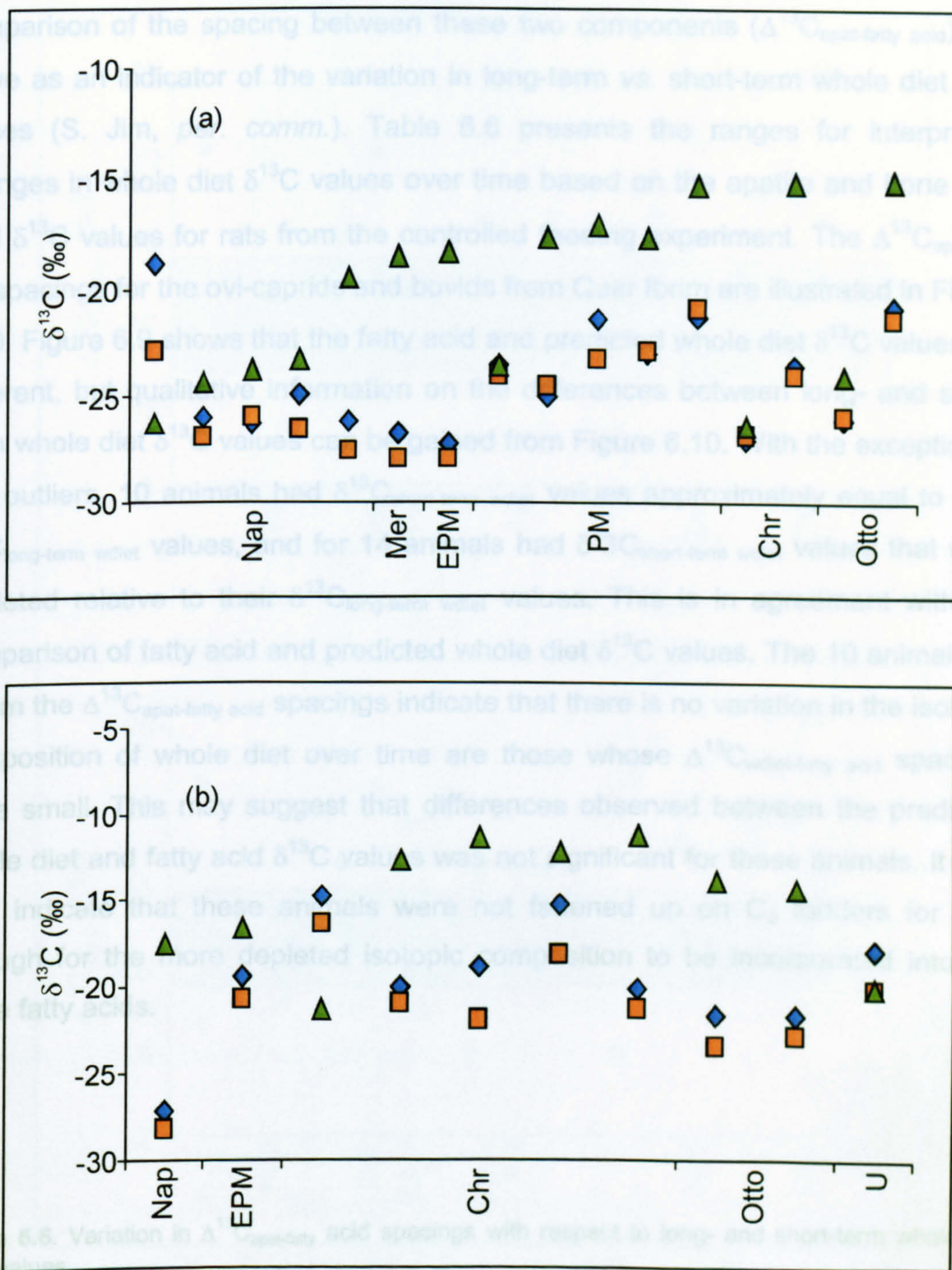


Figure 6.9. Comparison of C_{16:0} and C_{18:0} fatty acids with predicted long-term whole diet $\delta^{13}\text{C}$ values for the Qasr Ibrim samples for (a) ovi-caprids and (b) bovinds. C_{16:0} fatty acid $\delta^{13}\text{C}$ values are indicated by blue diamonds, C_{18:0} fatty acid $\delta^{13}\text{C}$ values by orange squares and predicted whole diet $\delta^{13}\text{C}$ values by green triangles. Nap = Napatan; Mer = Meroitic; EPM = Early Post Meroitic; PM = Post Meroitic; Chr = Christian; Otto = Ottoman and U = unidentified.

Since apatite and bone fatty acids reflect the same dietary isotopic signature, comparison of the spacing between these two components ($\Delta^{13}\text{C}_{\text{apat-fatty acid}}$), will serve as an indicator of the variation in long-term vs. short-term whole diet $\delta^{13}\text{C}$ values (S. Jim, *per. comm.*). Table 6.6 presents the ranges for interpreting changes in whole diet $\delta^{13}\text{C}$ values over time based on the apatite and bone fatty acid $\delta^{13}\text{C}$ values for rats from the controlled feeding experiment. The $\Delta^{13}\text{C}_{\text{apat-fatty acid}}$ spacings for the ovi-caprids and bovids from Qasr Ibrim are illustrated in Figure 6.10. Figure 6.9 shows that the fatty acid and predicted whole diet $\delta^{13}\text{C}$ values are different, but qualitative information on the differences between long- and short-term whole diet $\delta^{13}\text{C}$ values can be gained from Figure 6.10. With the exception of two outliers, 10 animals had $\delta^{13}\text{C}_{\text{short-term wdiet}}$ values approximately equal to their $\delta^{13}\text{C}_{\text{long-term wdiet}}$ values, and for 14 animals had $\delta^{13}\text{C}_{\text{short-term wdiet}}$ values that were depleted relative to their $\delta^{13}\text{C}_{\text{long-term wdiet}}$ values. This is in agreement with the comparison of fatty acid and predicted whole diet $\delta^{13}\text{C}$ values. The 10 animals for whom the $\Delta^{13}\text{C}_{\text{apat-fatty acid}}$ spacings indicate that there is no variation in the isotopic composition of whole diet over time are those whose $\Delta^{13}\text{C}_{\text{wdiet-fatty acid}}$ spacings were small. This may suggest that differences observed between the predicted whole diet and fatty acid $\delta^{13}\text{C}$ values was not significant for these animals. It may also indicate that these animals were not fattened up on C_3 fodders for long enough for the more depleted isotopic composition to be incorporated into the bone fatty acids.

Table 6.6. Variation in $\Delta^{13}\text{C}_{\text{apat-fatty acid}}$ spacings with respect to long- and short-term whole diet $\delta^{13}\text{C}$ values.

$\Delta^{13}\text{C}_{\text{apat-fatty acid}}$ spacing	Isotopic relationship between long- and short-term whole diet $\delta^{13}\text{C}$ values (‰)		
	$\delta^{13}\text{C}_{\text{short}} \approx \delta^{13}\text{C}_{\text{long}}$	$\delta^{13}\text{C}_{\text{short}} > \delta^{13}\text{C}_{\text{long}}$	$\delta^{13}\text{C}_{\text{short}} < \delta^{13}\text{C}_{\text{long}}$
$\Delta^{13}\text{C}_{\text{apat-C16:0}}$ (‰)	7 to 14	< 7	> 14
$\Delta^{13}\text{C}_{\text{apat-C18:0}}$ (‰)	9 to 15	< 9	> 15

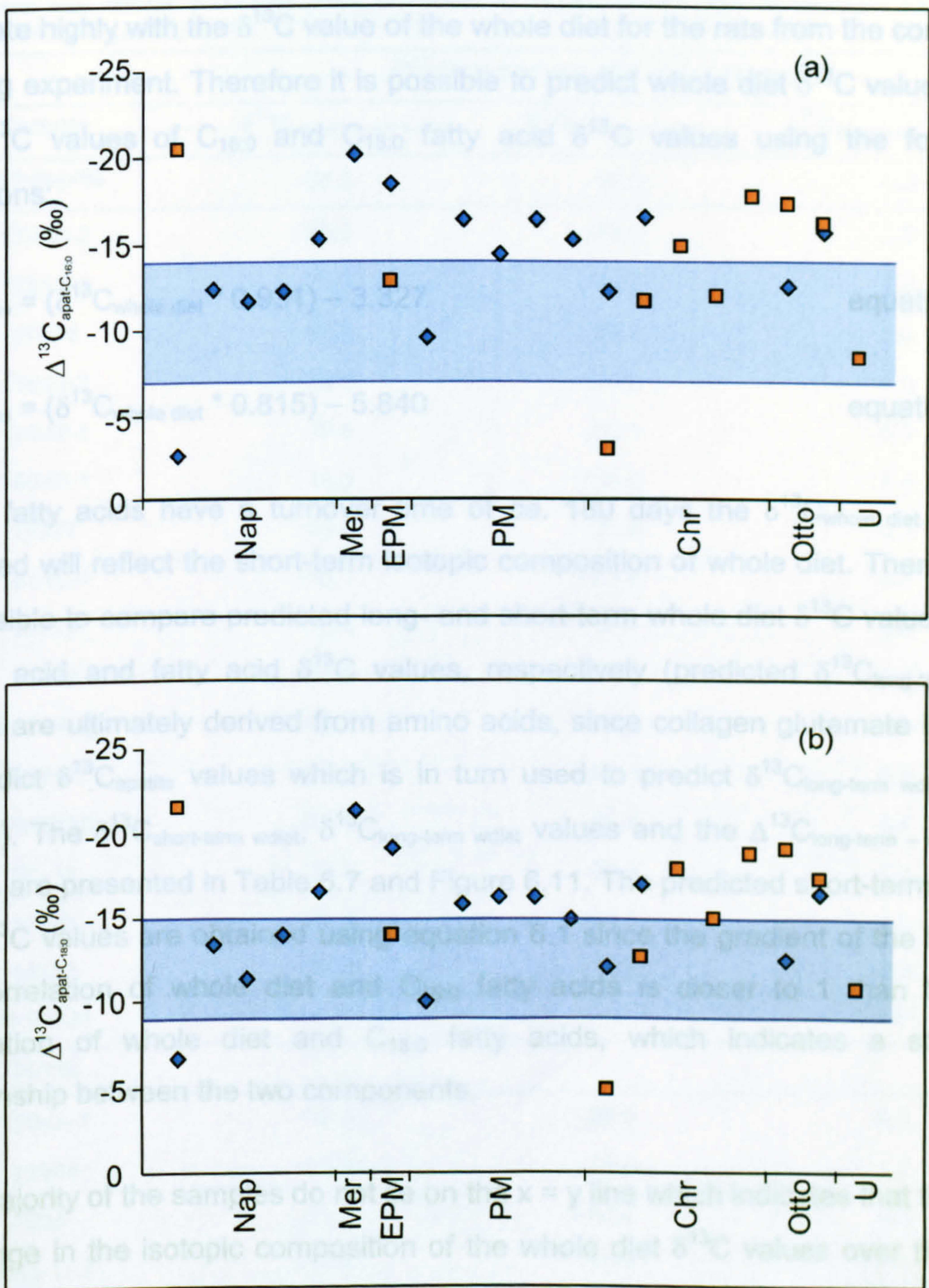


Figure 6.10. $\Delta^{13}\text{C}_{\text{apat-fatty acid}}$ spacings for the Qasr Ibrim samples for (a) $\text{C}_{16:0}$ fatty acid $\delta^{13}\text{C}$ values and (b) $\text{C}_{18:0}$ fatty acid $\delta^{13}\text{C}$ values. Ovi-caprids are indicated by blue diamonds and bovids by orange squares. The shaded area indicates where $\delta^{13}\text{C}_{\text{short-term wdiet}} \approx \delta^{13}\text{C}_{\text{long-term wdiet}}$.

As already mentioned, C_{16:0} and C_{18:0} bone fatty acid $\delta^{13}\text{C}$ values were found to correlate highly with the $\delta^{13}\text{C}$ value of the whole diet for the rats from the controlled feeding experiment. Therefore it is possible to predict whole diet $\delta^{13}\text{C}$ values from the $\delta^{13}\text{C}$ values of C_{16:0} and C_{18:0} fatty acid $\delta^{13}\text{C}$ values using the following equations:

$$\delta^{13}\text{C}_{\text{C}_{16:0}} = (\delta^{13}\text{C}_{\text{whole diet}} * 0.931) - 3.327 \quad \text{equation 6.1}$$

$$\delta^{13}\text{C}_{\text{C}_{18:0}} = (\delta^{13}\text{C}_{\text{whole diet}} * 0.815) - 5.840 \quad \text{equation 6.2}$$

Since fatty acids have a turnover time of ca. 180 days the $\delta^{13}\text{C}_{\text{whole diet}}$ values obtained will reflect the short-term isotopic composition of whole diet. Therefore it is possible to compare predicted long- and short-term whole diet $\delta^{13}\text{C}$ values from amino acid and fatty acid $\delta^{13}\text{C}$ values, respectively (predicted $\delta^{13}\text{C}_{\text{long-term wdiet}}$ values are ultimately derived from amino acids, since collagen glutamate is used to predict $\delta^{13}\text{C}_{\text{apatite}}$ values which is in turn used to predict $\delta^{13}\text{C}_{\text{long-term wdiet}}$ $\delta^{13}\text{C}$ values). The $\delta^{13}\text{C}_{\text{short-term wdiet}}$, $\delta^{13}\text{C}_{\text{long-term wdiet}}$ values and the $\Delta^{13}\text{C}_{\text{long-term} - \text{short-term}}$ values are presented in Table 6.7 and Figure 6.11. The predicted short-term whole diet $\delta^{13}\text{C}$ values are obtained using equation 6.1 since the gradient of the line for the correlation of whole diet and C_{16:0} fatty acids is closer to 1 than for the correlation of whole diet and C_{18:0} fatty acids, which indicates a stronger relationship between the two components.

The majority of the samples do not lie on the $x = y$ line which indicates that there is a change in the isotopic composition of the whole diet $\delta^{13}\text{C}$ values over time for these samples. An average enrichment of 2.5‰ and 2.0‰ is observed for the $\delta^{13}\text{C}_{\text{long-term wdiet}}$ values for the ovi-caprids and bovids, respectively. This is further evidence that these animals were fed on ^{13}C -depleted fodder prior to death, which could indicate fattening up with C₃ plants prior to slaughter.

Table 6.7. Predicted long-term and short-term whole diet $\delta^{13}\text{C}$ values for Qasr Ibrim animal bones. $\delta^{13}\text{C}_{\text{long-term wdiet}}$ values predicted from predicted $\delta^{13}\text{C}_{\text{apatite}}$ values and $\delta^{13}\text{C}_{\text{short-term wdiet}}$ values predicted from $\text{C}_{16.0}$ fatty acid $\delta^{13}\text{C}$ values.

Predicted whole diet $\delta^{13}\text{C}$ values (‰)			
Sample	$\delta^{13}\text{C}_{\text{long-term wdiet}}$	$\delta^{13}\text{C}_{\text{short-term wdiet}}$	$\Delta^{13}\text{C}_{\text{long-term} - \text{short-term}}$
ovi-caprid	-26.3	-16.6	-9.6
17048-2	-23.3	-24.2	1.0
12513-1	-24.4	-24.6	0.2
17035	-22.3	-23.2	0.8
17042-2	-20.5	-24.5	4.0
17042-1	-15.8	-25.1	9.3
18013-1	-18.3	-25.6	7.4
10377	-23.8	-21.8	-2.1
10110-1	-18.1	-23.3	5.2
10478	-16.4	-19.4	3.0
10063	-15.9	-21.1	5.2
10216-3	-15.3	-19.3	4.0
10216-2	-24.6	-25.4	0.8
10203(36)	-16.4	-21.8	5.4
B1-12	-23.2	-24.4	1.2
10045	-14.3	-18.8	4.5
14133	-26.3	-16.6	-9.6
average			2.5 ±4.4
bovid			
17048-1	-16.0	-25.6	9.6
10384	-16.0	-17.4	1.3
B56	-21.3	-12.2	-9.1
lb82 11.7	-17.8	-17.9	0.1
B55	-13.2	-16.7	3.5
B27	-12.3	-12.8	0.4
B35	-11.6	-18.1	6.6
10048-L	-13.6	-19.7	6.1
10048-R	-14.8	-19.7	4.9
10822	-18.9	-15.5	-3.4
average			2.0 ±5.4

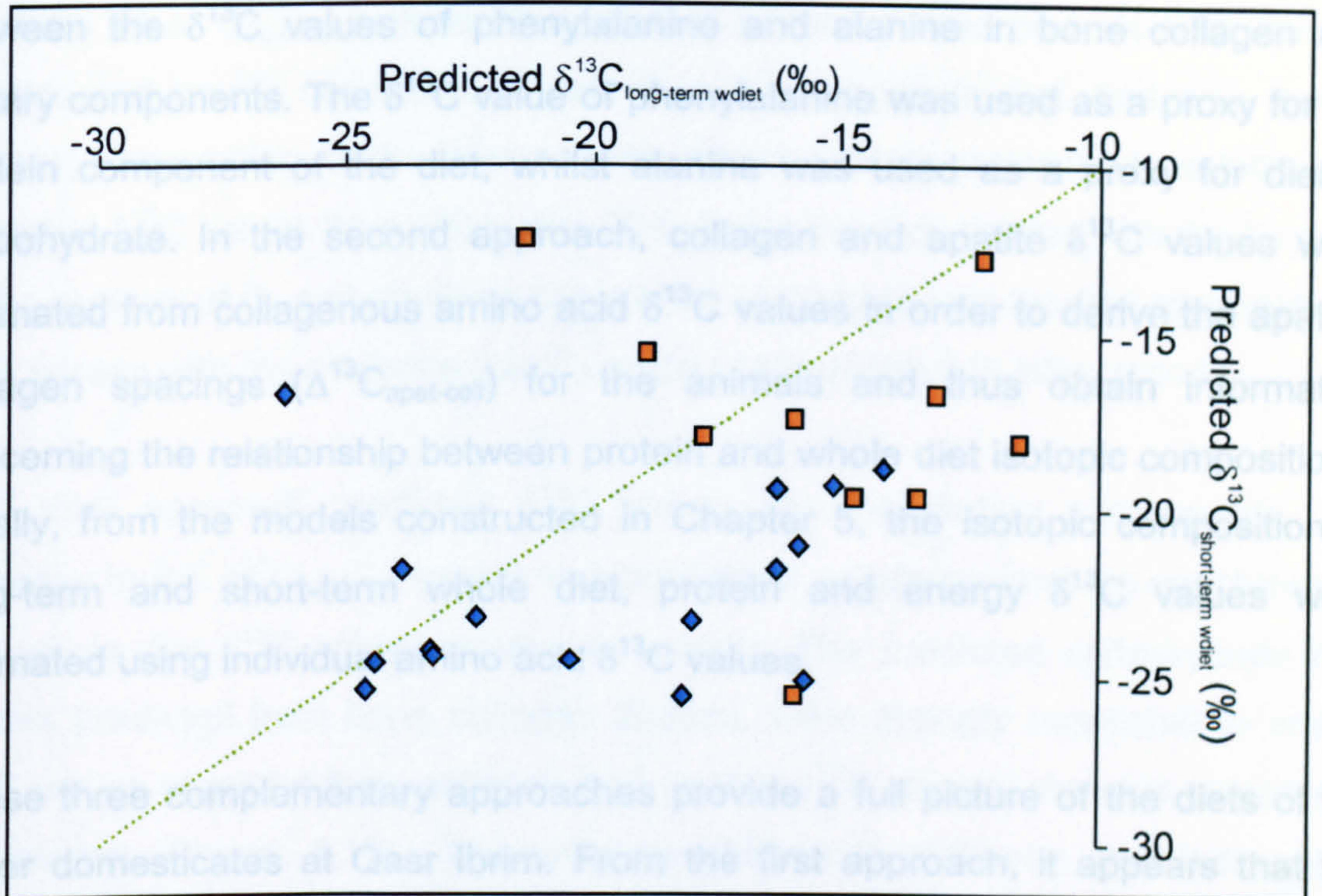


Figure 6.11. Comparison of predicted short-term whole diet $\delta^{13}\text{C}$ values, obtained from $\text{C}_{16:0}$ fatty acid $\delta^{13}\text{C}$ values with predicted long-term whole diet $\delta^{13}\text{C}$ values obtained from predicted apatite $\delta^{13}\text{C}$ values for the Qasr Ibrim samples. Ovi-caprids are indicated by blue diamonds and bovids by orange squares. The dashed green line is where $x=y$.

6.4 Summary

This chapter has shown the wealth of information regarding dietary isotopic compositions that can be provided from the stable carbon isotope analysis of individual amino acids from bone collagen. Although the interpretations were based on models built from data from a controlled rat feeding experiment, these models have provided archaeologically meaningful predictions of the isotopic compositions of the dietary macronutrients of major domesticates at Qasr Ibrim over a 2000 year time period.

Three complementary multi-proxy approaches were used to obtain dietary information for the ovi-caprids and bovids. The first utilised the relationship

between the $\delta^{13}\text{C}$ values of phenylalanine and alanine in bone collagen and dietary components. The $\delta^{13}\text{C}$ value of phenylalanine was used as a proxy for the protein component of the diet, whilst alanine was used as a proxy for dietary carbohydrate. In the second approach, collagen and apatite $\delta^{13}\text{C}$ values were estimated from collagenous amino acid $\delta^{13}\text{C}$ values in order to derive the apatite-collagen spacings ($\Delta^{13}\text{C}_{\text{apat-coll}}$) for the animals and thus obtain information concerning the relationship between protein and whole diet isotopic compositions. Finally, from the models constructed in Chapter 5, the isotopic composition of long-term and short-term whole diet, protein and energy $\delta^{13}\text{C}$ values were estimated using individual amino acid $\delta^{13}\text{C}$ values.

These three complementary approaches provide a full picture of the diets of the major domesticates at Qasr Ibrim. From the first approach, it appears that the protein source for all the animals across all time periods was constant, although the $\delta^{13}\text{C}$ values of the dietary protein for the ovi-caprids were somewhat lower than those of the bovids. This does not necessarily indicate that no C_4 dietary protein was consumed, it may be that the C_3 dietary protein was more digestible than the C_4 dietary protein. The $\delta^{13}\text{C}$ value of the energy component of the diet was much more variable. The ovi-caprids showed either a pure C_3 or mixed C_3/C_4 signal during the Napatan period, which is consistent with the archaeobotanical evidence that barley was the most common cereal found, but common millet and wild sorghum were also present. In later periods the ovi-caprids showed an increasing proportion of C_4 carbohydrate in the diet, which agrees with the evidence that from the Meroitic periods onwards, the percentage of C_4 crops increased until they were predominant during the Christian and Ottoman periods. For the bovids, the earliest animals exhibited a mixed C_3/C_4 signal, which became pure C_4 during the Christian period, which is also consistent with the archaeobotanical evidence. In later time periods, the energy signal was more depleted in ^{13}C for the ovi-caprids than the bovids. This could be indicative of the different feeding behaviours of the two groups of domesticates. Sheep are grazers and would have fed on any available fodder, including millet, sorghum, wheat and barley, whilst bovids would have been fed on fodder derived from the C_4 crops that predominated in these periods.

Analysis of $\Delta^{13}\text{C}_{\text{apat-coll}}$ values showed that in earlier time periods both the ovi-caprids and bovids consumed protein that, like the whole diet, had a C_3 carbon isotopic composition. In the later periods, dietary protein appeared to exhibit more depleted $\delta^{13}\text{C}$ values than whole diet. This latter trend correlates with the increase in the amount of C_4 carbohydrate consumed as deduced via the first approach and also agrees with the evidence that C_4 crops predominated in later periods.

The third approach predicted $\delta^{13}\text{C}$ values for the dietary components. The increase in the $\Delta^{13}\text{C}_{\text{apat-coll}}$ values was confirmed as arising from an enrichment in the whole diet $\delta^{13}\text{C}$ values relative to protein. The predicted carbohydrate $\delta^{13}\text{C}$ values predicted from bone collagen alanine, were strongly correlated to energy $\delta^{13}\text{C}$ values obtained from collagen and apatite $\delta^{13}\text{C}$ values, shows a remarkable correlation (Figure 6.12). The average difference between the two values ($\Delta^{13}\text{C}_{\text{alanine-energy}}$) for the ovi-caprids is 1.6‰ and for the bovids just 0.8‰, which is well within experimental error. This provides further evidence for the majority of alanine in bone collagen being biosynthesised from carbohydrates in the diet.

The comparison of collagen phenylalanine and predicted dietary protein $\delta^{13}\text{C}$ values is shown in Figure 6.13. Although the absolute values for each animal are different, there is a strong correlation between the predicted dietary protein $\delta^{13}\text{C}$ values and collagen phenylalanine $\delta^{13}\text{C}$ values ($R^2 = 0.88$ for the ovi-caprids and 0.94 for the bovids). Identical values would not be expected; although phenylalanine is an essential amino acid and must be provided by the dietary protein, its isotopic composition in bone collagen will reflect the isotopic composition of the phenylalanine in the dietary protein and not the isotopic composition of the total dietary protein. However, the high degree of correlation is indicative of a constant relationship between protein phenylalanine $\delta^{13}\text{C}$ values and the bulk dietary protein $\delta^{13}\text{C}$ values of which it is a component. It also indicates that as expected there is a relationship between the $\delta^{13}\text{C}$ value of phenylalanine in bone collagen and the $\delta^{13}\text{C}$ value of the dietary protein from which it was supplied. It can also be seen that mean differences ($\Delta^{13}\text{C}_{\text{protein-phe}}$) are different for the ovi-caprids and bovids (+4.1‰ \pm 1.3 and 6.1‰ \pm 0.5 for the ovi-

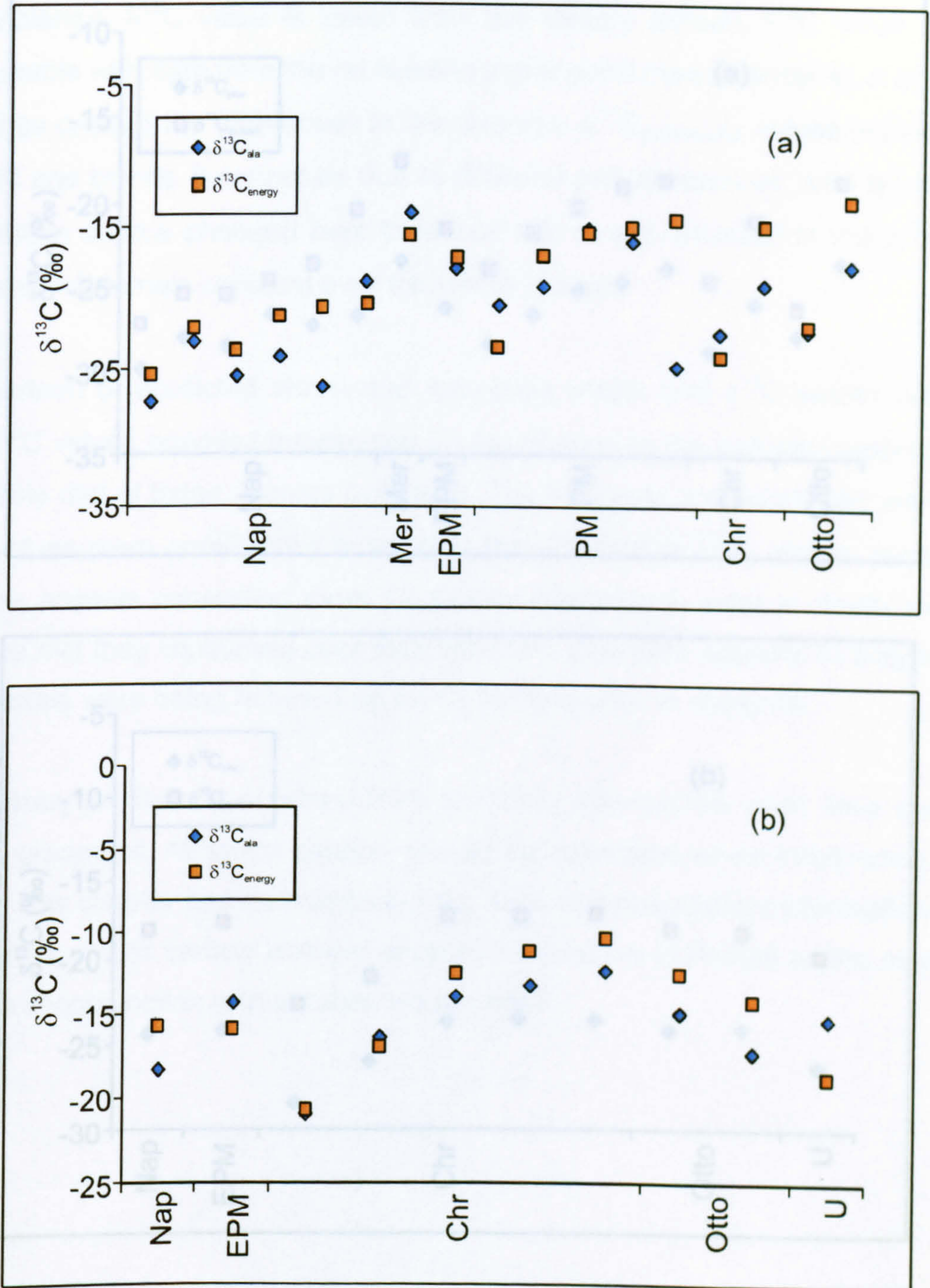


Figure 6.12. Comparison of bone collagen alanine and predicted dietary energy $\delta^{13}\text{C}$ values for (a) ovi-caprids and (b) bovids.

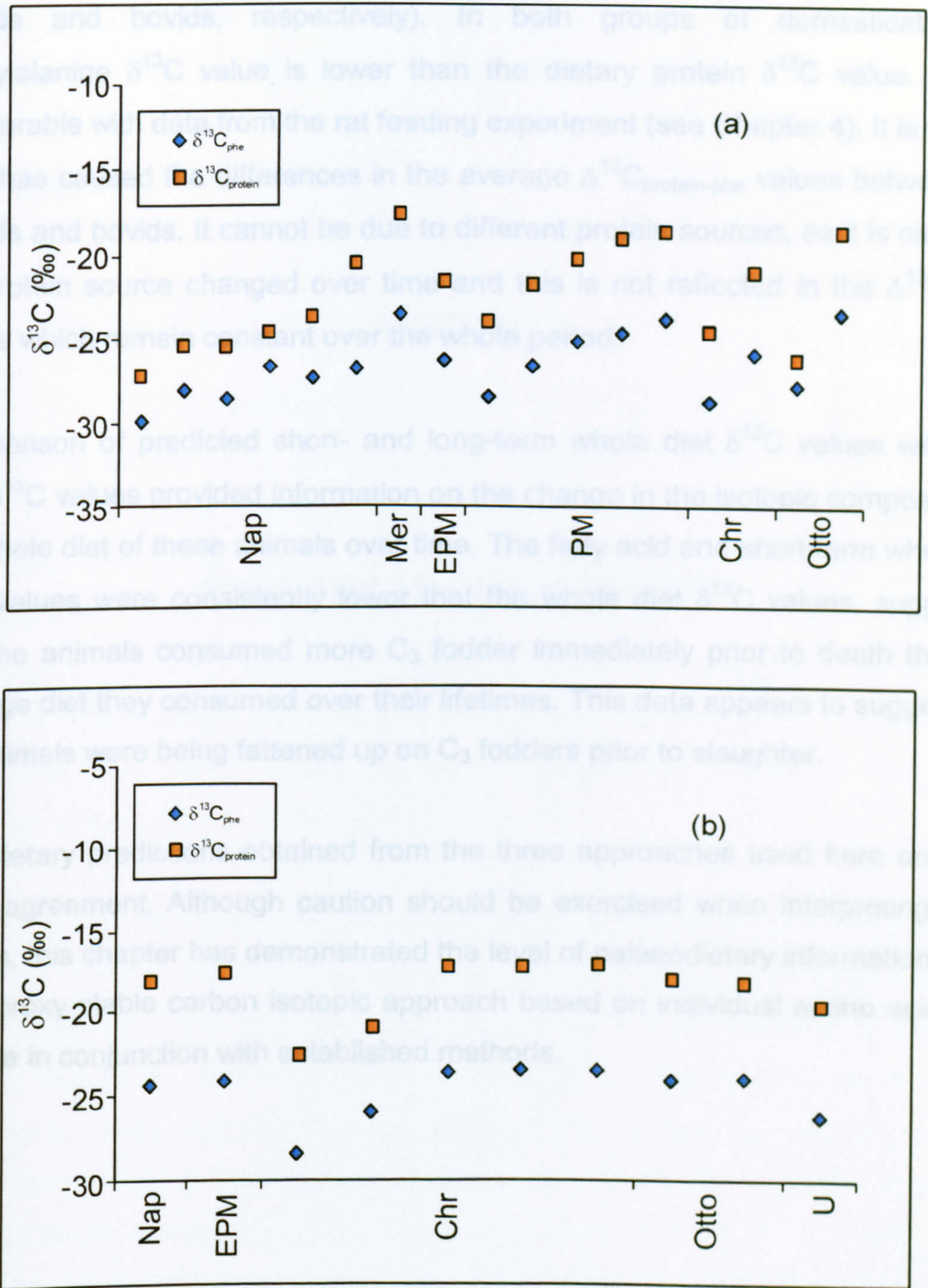


Figure 6.13. Comparison of bone collagen phenylalanine and predicted dietary protein $\delta^{13}\text{C}$ values for (a) ovi-caprids and (b) bovids.

caprids and bovids, respectively). In both groups of domesticates the phenylalanine $\delta^{13}\text{C}$ value is lower than the dietary protein $\delta^{13}\text{C}$ value. This is comparable with data from the rat feeding experiment (see Chapter 4). It is unclear what has caused the differences in the average $\Delta^{13}\text{C}_{\text{protein-phe}}$ values between ovi-caprids and bovids. It cannot be due to different protein sources, as it is clear that the protein source changed over time and this is not reflected in the $\Delta^{13}\text{C}_{\text{prot-phe}}$ values which remain constant over the whole period.

Comparison of predicted short- and long-term whole diet $\delta^{13}\text{C}$ values with fatty acid $\delta^{13}\text{C}$ values provided information on the change in the isotopic composition of the whole diet of these animals over time. The fatty acid and short-term whole diet $\delta^{13}\text{C}$ values were consistently lower than the whole diet $\delta^{13}\text{C}$ values, suggesting that the animals consumed more C_3 fodder immediately prior to death than the average diet they consumed over their lifetimes. This data appears to suggest that the animals were being fattened up on C_3 fodders prior to slaughter.

The dietary predictions obtained from the three approaches used here are all in close agreement. Although caution should be exercised when interpreting these results, this chapter has demonstrated the level of palaeodietary information that a multi-proxy stable carbon isotopic approach based on individual amino acids can provide in conjunction with established methods.

CHAPTER 7

SUMMARY AND FUTURE WORK

Chapter 7 Summary and future work

7.1 Summary

7.1.1 Summary of aims and objectives

The aim of the work presented herein was to investigate the synthesis and routing of amino acids from the diet into bone collagen and thus establish how the determination of $\delta^{13}\text{C}$ values of collagenous amino acids could enhance the information gained from palaeodietary reconstruction. In order to achieve this aim, it was first necessary to undertake developmental work on the techniques applied to measure the $\delta^{13}\text{C}$ values of individual amino acids from bone collagen. Authentic amino acids were used to investigate the effects of hydrolysis and derivatisation on the $\delta^{13}\text{C}$ values of those amino acids and also to assess the precision of the analysis.

To investigate the routing and synthesis of amino acids in bone collagen, the individual amino acids from the bone collagen of rats raised on controlled diets were measured. The $\delta^{13}\text{C}$ values of individual amino acids in the protein components of the diets were also obtained; the $\delta^{13}\text{C}$ values of the bulk dietary components were available from a previous investigation (Ambrose and Norr, 1993). From this information it was possible to elucidate which amino acids had been provided directly from the protein component of the diet and which amino acids had incorporated the isotopic composition of other dietary macronutrients. These results provided insights into the factors that influence the $\delta^{13}\text{C}$ values of bone collagen.

From these results, in conjunction with previously measured $\delta^{13}\text{C}$ values for bone cholesterol, collagen and apatite for the same animals (Ambrose and Norr, 1993; Jim, 2000), a quantitative model was constructed. This model exploited the linear relationship between the $\delta^{13}\text{C}$ values of collagenous amino acids and other bone

components in order to allow the prediction of dietary macronutrient $\delta^{13}\text{C}$ values. The wider applicability of the model was tested by application to $\delta^{13}\text{C}$ values of amino acids obtained from a controlled pig feeding experiment (Mark Howland, unpublished). The accuracy of the model was also tested and applied to collagen and apatite purified from faunal remains from Qasr Ibrim, Egypt. Furthermore, the palaeodietary information obtained from the $\delta^{13}\text{C}$ analysis of individual amino acids from the bone collagen of these animals was compared with previous interpretations based on the $\delta^{13}\text{C}$ analysis of $\text{C}_{16:0}$ and $\text{C}_{18:0}$ fatty acids.

7.1.2 Summary of results and conclusions

In Chapter 3, the analysis of authentic amino acids was undertaken to investigate likely sources of error in the analytical protocol employed in the determination of $\delta^{13}\text{C}$ values of individual amino acids in proteins. The choice of derivative for amino acid analysis was discussed and the TFA/IP derivatives were shown to provide excellent chromatography for authentic amino acids and those isolated from diets and consumer bone collagen. The need for a reduction reactor in the GC/C/IRMS configuration when analysing the $\delta^{13}\text{C}$ values of amino acids was confirmed via the use of pre-derivatised amino acid standards. The use of these pre-derivatised amino acids as co-injected standards during isotopic analysis was shown to be vital in the run-by-run evaluation of reactor performance. Authentic amino acids were used to calculate the correction factors required throughout the thesis accounting for both carbon added during the overall derivatisation of amino acids and a kinetic isotope effect (KIE) during the acetylation step (Rieley, 1994). Since the kinetic isotope effect occurred due to a non-quantitative reaction it was possible that the amount of analyte being derivatised could affect the expression of the KIE. This was investigated by derivatising varying amounts of alanine ranging from 10 μg to 2000 μg and determining the $\delta^{13}\text{C}$ values. The standard deviation of the results obtained was $\pm 0.2\text{‰}$ which is within machine precision ($\pm 0.3\text{‰}$), therefore showing that amount of analyte did not affect the expression of the KIE over the range that would be encountered in the analyses performed in this thesis. The errors involved in the $\delta^{13}\text{C}$ analysis of amino acids were also rigorously investigated. Due to the variation in carbon number of the amino acids

and the number of functional groups, errors were calculated individually for each amino acid. Assuming a GC/C/IRMS precision of $\pm 0.3\text{‰}$, errors varied from $\pm 0.7\text{‰}$ for phenylalanine to $\pm 1.5\text{‰}$ for glycine. The effect of hydrolysis of proteins on the isotopic composition of the individual amino acids that comprise them was investigated using authentic polypeptides comprising a single amino acid or defined mixtures of two amino acid residues. It was found that after 24 and 48 h the $\delta^{13}\text{C}$ values of the individual amino acids as determined by GC/C/IRMS were unaffected by the hydrolysis procedure. Shorter hydrolysis times, and thus incomplete hydrolysis of the polypeptides, did result in $\delta^{13}\text{C}$ values of the amino acids that differed from the parent polypeptide indicating that hydrolysis times of no less than 24 h are required for the determination of $\delta^{13}\text{C}$ values of amino acids in proteins.

In Chapter 4 the $\delta^{13}\text{C}$ values of individual amino acids from the bone collagen of rats from a controlled feeding experiment were determined to investigate the routing and synthesis of amino acids in bone collagen. The $\delta^{13}\text{C}$ values of the amino acids in the protein component of the diet were also determined. The $\delta^{13}\text{C}$ values of the dietary macronutrients had been previously measured (Ambrose and Norr, 1993). These animals could be separated into the following four groups: (i) were raised on 20% C_3 or C_4 protein diets that contained C_3 and/or C_4 energy components; (ii) were raised on 20% marine protein diets and C_3 and/or C_4 energy components; (iii) were raised on 70% marine protein diets and C_3 and/or C_4 energy components, and (iv) were subjected to a diet switch, where diets were switched from C_3 dietary macronutrients to C_4 macronutrients and *vice versa*. Twelve amino acids were separated from bone collagen and their relative abundances were found to compare very closely with theoretical abundances of amino acids in mammalian collagen (Vaughan, 1970). Incorporation of the isotopic signal from dietary amino acids to bone collagen amino acids could clearly be seen for rats raised on either pure C_3 or pure C_4 diets and the fractionation from diet amino acids to tissue amino acids was statistically identical for both essential and non-essential amino acids ($\Delta^{13}\text{C}_{\text{collAA-dietAA}}$ values ranged from -2.8‰ to $+5.5\text{‰}$).

However, the $\delta^{13}\text{C}$ values of amino acids from rats raised on diets containing isotopically distinct macronutrients indicated that the isotopic composition of some amino acids reflected the isotopic composition of the energy component of the diet. Specifically, alanine, glycine, serine, aspartate and glutamate, all showed significant incorporation of the dietary energy isotopic signal ($\Delta^{13}\text{C}_{\text{collAA-dietAA}}$ values averaged +11.7‰ and -6.0‰ for C_3 protein/ C_4 energy and C_4 protein/ C_3 energy diets, respectively). The $\Delta^{13}\text{C}_{\text{coll-diet}}$ values did not reflect the incorporation of the energy isotopic signal into collagen, as those amino acids that comprise the majority of collagen incorporated little or none of the energy $\delta^{13}\text{C}$ values. The incorporation of the energy component of the diet into some of the non-essential amino acids could be explained by their biosynthetic pathways; alanine, glycine and serine are formed from glycolytic intermediates and therefore carbohydrates will provide their carbon skeletons whilst aspartate and glutamate are formed from intermediates of the citric acid cycle which implies that carbohydrates, proteins and lipids will contribute to their carbon skeletons. Interestingly, proline showed no evidence of *de novo* synthesis, despite being a non-essential amino acid, indicating that proline in bone collagen is incorporated from proline in the diet. The high protein diets showed increased incorporation of dietary amino acids into bone collagen. The $\Delta^{13}\text{C}_{\text{collAA-dietAA}}$ values for the non-essential amino acids were statistically identical to the essential amino acids indicating lack of incorporation of the energy signal into these amino acids.

The results from the diet-switch experiment showed that some amino acids incorporated more of the isotopic signal of a new diet after 120 days than others. A percentage incorporation was calculated based on endmember $\delta^{13}\text{C}$ values and these results showed that dietary amino acids are incorporated into bone collagen at different rates which is due to the availability of other amino acids for protein synthesis apart from dietary amino acids.

Correlation of collagenous amino acid $\delta^{13}\text{C}$ values with the $\delta^{13}\text{C}$ values of dietary components (Chapter 5) showed that proline correlated highly with dietary protein ($R^2 = 0.92$) confirming the lack of *de novo* synthesis for this amino acid, and glutamate correlated highly with whole diet ($R^2 = 0.94$) reflecting its biosynthesis

from an intermediate of the citric acid cycle. Glycine and serine did not correlate significantly with any dietary components, but similar correlations with dietary amino acid and whole diet indicated contributions to collagen via direct incorporation from the diet and *de novo* synthesis. The $\delta^{13}\text{C}$ values of isoleucine and phenylalanine correlated very highly with their dietary amino acids ($R^2 = 0.94$ and 0.97 , respectively) confirming their status as essential amino acids.

Linear correlations between collagenous amino acid $\delta^{13}\text{C}$ values and the $\delta^{13}\text{C}$ values of bone collagen, cholesterol and apatite were exploited to construct a quantitative model for predicting dietary $\delta^{13}\text{C}$ values. It was found that amino acid $\delta^{13}\text{C}$ values could be used to accurately predict bone collagen and apatite $\delta^{13}\text{C}$ values ($R^2 = 0.91$ and 0.94 , respectively). These predicted values were then used in a previously constructed model to predict diet $\delta^{13}\text{C}$ values (Jim, 2000). However, a combined approach increased the correlation of predicted and measured dietary $\delta^{13}\text{C}$ values. The combination of glutamate and collagen $\delta^{13}\text{C}$ values allowed the prediction of dietary protein $\delta^{13}\text{C}$ values with an R^2 of 0.97 , which was an improvement from the R^2 value of 0.70 obtained when using collagen $\delta^{13}\text{C}$ values alone (Jim, 2000) and also does not require the use of apatite $\delta^{13}\text{C}$ values. These models were applied to data from pigs from a controlled feeding experiment. It was seen that individual amino acids accurately predicted the collagen and long- and short-term whole diet $\delta^{13}\text{C}$ values. Inaccuracies in predicting dietary protein and energy $\delta^{13}\text{C}$ values were encountered. There was some uncertainty in the actual $\delta^{13}\text{C}$ protein value due to the need to estimate the isotopic contribution of protein from wheat and maize in the diet, however, a difference of only 1.6‰ between predicted and measured values was observed. The difference between predicted and measured $\delta^{13}\text{C}_{\text{energy}}$ values was 4.4‰ , but the R^2 value of 0.89 indicated that a systematic difference between the pig and rat feeding experiments was causing the predicted values to be consistently more enriched than measured values.

In Chapter 6 the model was then applied to $\delta^{13}\text{C}$ values of bone components from animals from an archaeological site, Qasr Ibrim, Egypt to investigate the changes in the animals diets over time possibly as a result of changing animal husbandry practices. Predicted bone collagen and apatite $\delta^{13}\text{C}$ values correlated highly with

the values predicted from amino acid $\delta^{13}\text{C}$ values ($R^2 = 0.96$ and 0.90 , respectively). The predicted dietary $\delta^{13}\text{C}$ values indicated that the isotopic composition of the energy component of the diet varied greatly over time. The ovi-caprids showed either a pure C_3 or mixed C_3/C_4 signal during the Napatan period, which was consistent with the archaeobotanical evidence that barley was the most common cereal found, but common millet and wild sorghum were also present. In later periods, the amount of C_4 carbohydrate in diet increased which correlates with the increase in the percentage of C_4 crops (Rowley-Conwy, 1989). The isotopic composition of the carbohydrate being consumed by the bovids was very similar to that observed for the ovi-caprids, however in later time periods the ovi-caprids had more depleted signals which may be indicative of different feeding behaviours. Ovi-caprids are grazers and would have fed on any available fodder, which would have included millet, sorghum, wheat and barley. Bovids would have been fed on fodder derived from the C_4 crops that predominated in these periods.

Comparison of the short-term whole diet and long-term whole diet $\delta^{13}\text{C}$ values indicated that there was a difference in the isotopic composition of these animals diets over time. The majority of short-term whole diet $\delta^{13}\text{C}$ values were depleted with respect to the long-term values. This suggested that the animals may have been fed on more isotopically depleted fodders prior to death, which could indicate fattening up with C_3 plants (e.g. barley and wheat) prior to slaughter.

Hence, it has been shown that the $\delta^{13}\text{C}$ analysis of individual amino acids in bone collagen can provide detailed information on the input of dietary macronutrients into bone collagen. Individual amino acids can be used to predict dietary $\delta^{13}\text{C}$ values and in conjunction with other bone components can provide a high degree of palaeodietary information.

7.2 Future work

To advance the use of the $\delta^{13}\text{C}$ analysis of individual amino acids in bone collagen for palaeodietary reconstruction, it will be necessary to apply the models

developed herein to human archaeological studies. Further studies of routing and synthesis of amino acids in collagen via controlled feeding experiments would also be advantageous. The findings presented in this thesis were obtained from rats raised on diets containing only one protein source; when the models were applied to data from pigs raised on diets which contained whole natural ingredients, it raised some interesting questions as to which sources of protein were supplying which amino acids and, hence, influencing the isotopic composition of the bone collagen (see Section 5.3.3). Controlled feeding experiments with isotopically distinct sources of protein would enable further investigation of the source of the carbon skeletons of amino acids. Some proteins may be more digestible than others and hence be preferentially routed in to bone collagen. An understanding of these factors would provide greater insights into the information which both bulk collagen and individual amino acid $\delta^{13}\text{C}$ values can provide for palaeodietary reconstruction. This is particularly important for the analysis of ancient human diets as these will most likely have consisted of protein obtained from meat and plants. The analysis of the $\delta^{13}\text{C}$ values of collagenous amino acids from high and low protein diets may give further indications about how animals route macronutrient carbon to their tissues. An understanding of these and other factors is necessary in order to provide meaningful interpretations of isotopic signals from archaeological populations.

The development of the $\delta^{15}\text{N}$ analysis of individual amino acids in bone collagen would also advance the field of palaeodietary reconstruction. Currently little work has been undertaken on the $\delta^{15}\text{N}$ values, partly due to the small amount of nitrogen in amino acids compared with carbon, which demands larger sample sizes and also because of instrumental difficulties involved in obtaining $\delta^{15}\text{N}$ values (Brand *et al.*, 1994). However, nitrogen isotope fractionations in food webs are larger than those of carbon (DeNiro and Epstein, 1981) and therefore could be applied to distinguishing carnivory and herbivory (Schoeninger and DeNiro, 1984). Enriched $\delta^{15}\text{N}$ values have been observed for bulk collagen of drought-stressed animals (Ambrose, 1991), individual amino acid analyses could isolate the source of this enrichment. These analyses would also allow further investigation of the metabolism of organic nitrogen. It is already known that nitrogen isotope

abundances in individual amino acids appear to be related to kinetic isotope effects associated with transamination reactions during synthesis (Macko *et al.*, 1986), but there is still much that is not understood.

Stable isotopes have been used to study human and animal metabolism for approximately 60 years. The earliest work in this area was undertaken by Schoenheimer during the 1930s. Until shortly before this time the components of body tissues were regarded as being structurally and metabolically inert. The first *in vivo* ^{15}N -labelled amino acid tracer study was conducted in order to determine if either dietary glycine or glycine supplied by body tissues was used for the formation of hippuric acid (Rittenberg and Schoenheimer, 1939). This was the beginning of a field of work which changed the fundamental understanding of mammalian protein and amino acid metabolism and many of the principles established then remain true today. The advent of GC/C/IRMS allows the detection of tracer compounds and metabolic products at several orders of magnitude lower isotopic enrichment than has hitherto been possible by means of conventional organic mass spectrometry (Brenna *et al.*, 1997). Hence, stable isotope labelled tracers can be used to study new aspects of turnover and synthesis rates of proteins, such as collagen, and also to investigate the isotope effects associated with metabolism and biosynthesis with previously unattainable sensitivities and specificities. Tracer studies could also be utilised to research the factors that affect *de novo* synthesis of amino acids, what makes an amino acid essential, non-essential or conditionally essential and to assess the requirements of an amino acid vs. the synthetic capacity of the body. These factors could be influenced by such things as dietary composition and the physical state of the body (e.g. rapid growth, starvation) (Young and El-Khoury, 1995). The stable isotope analysis of amino acids using GC/C/IRMS is still at a relatively early stage of development and this research area is set to grow as our understanding of its applications increases and instrumental techniques continue to advance.

REFERENCES

- Abelson P. H. and Hoering T. C. (1961)** Carbon isotope fractionation in formation of amino acids by photosynthetic organisms. *Proceedings of the National Academy of Sciences USA* 47(5), 623-632.
- Adams R. F. (1974)** Determination of amino acid profiles in biological samples by gas chromatography. *Journal of Chromatography* 95, 189-212.
- Ambrose S. H. and DeNiro M. J. (1986)** Reconstruction of african human diet using bone collagen carbon and nitrogen isotope ratios. *Nature* 319, 321-324.
- Ambrose S. H. (1990)** Preparation and characterization of bone and tooth collagen for isotopic analysis. *Journal of Archaeological Science* 17, 431-451.
- Ambrose S. H. (1991)** Effects of diet, climate and physiology on nitrogen isotope abundances in terrestrial food webs. *Journal of Archaeological Science* 18, 293-317.
- Ambrose S. H. (1993)** Isotopic analysis of palaeodiets: methodological and interpretive considerations. In *Investigations of ancient human tissue* (ed. M. K. Sandford), pp. 59-130. Gordon and Breach Scientific Publishers
- Ambrose S. H. and Norr L. (1993)** Experimental evidence for the relationship of the carbon isotope ratios of whole diet and dietary protein to those of bone collagen and carbonate. In *Prehistoric Human Bone: Archaeology at the Molecular Level* (ed. J. B. Lambert and G. Grupe), pp. 1-38. Springer-Verlag.
- Ambrose S. H., Butler B. M., Hanson D. B., Hunter-Anderson R. L., and Krueger H. W. (1997)** Stable isotopic analysis of human diet in the Marianas archipelago, Western Pacific. *American Journal of Physical Anthropology* 104(3), 343-361.
- Barrie A., Bricout J., and Koziat J. (1984)** Gas chromatography stable isotope ratio analysis at natural abundance levels. *Biomedical Mass Spectrometry* 11, 583-588.
- Bender D. A. (1997)** *Introduction to nutrition and metabolism*. Taylor and Francis.
- Benyon S. (1998)** Protein metabolism. In *Metabolism and Nutrition* (ed. D. Horton-Szar), pp. 77-98. Mosby.
- Bier D. M. (1989)** Intrinsically difficult problems: the kinetics of body proteins and amino acids in man. *Diabetes - metabolism reviews* 5(2), 111-132.

- Boutton T. W. (1991)** Stable carbon isotope ratios of natural materials: II. atmospheric, terrestrial, marine and freshwater environments. In *Carbon Isotope Techniques* (ed. T. W. Boutton), pp. 173-185. Academic Press.
- Brand W. A., Tegtmeier A. R., and Hilkert, A. (1994)** Compound-specific isotope analysis: extending toward $^{15}\text{N}/^{14}\text{N}$ and $^{18}\text{O}/^{16}\text{O}$. *Organic Geochemistry* 21(6/7), 585-594.
- Brand W. A. (1996)** High precision isotope ratio monitoring techniques in mass spectrometry. *Journal of Mass Spectrometry* 31(3), 225-235.
- Brenna J. T., Corso T. N., Tobias H. J., and Caimi R. J. (1997)** High-precision continuous-flow isotope ratio mass spectrometry. *Mass Spectrometry Reviews* 16, 227-258.
- Bull I. D., Simpson I. A., van Bergen P. F., and Evershed R. P. (1999)** Muck 'n' molecules: organic geochemical methods for detecting ancient manuring. *Antiquity* 73, 86-96.
- Chisholm B. S., Nelson D. E., and Schwarcz H. P. (1982)** Stable-carbon isotope ratios as a measure of marine versus terrestrial protein in ancient diets. *Science* 216(4550), 1131-1132.
- Copley M. (2001)** Chemical investigations of pottery and palaeoenvironmental material from Qasr Ibrim, Egypt, University of Bristol.
- Copley M. S., Rose P. J., Clapham A., Edwards D. N., Horton M. C., and Evershed R. P. (2001a)** Detection of palm fruit lipids in archaeological pottery from Qasr Ibrim, Egyptian Nubia. *Proceedings of the royal society of London series B - Biological sciences* 268, 593-597.
- Copley M. S., Rose P. J., Clapham A., Edwards D. N., Horton M. C., and Evershed R. P. (2001b)** Processing palm fruits in the Nile Valley - Biomolecular evidence from Qasr Ibrim. *Antiquity* 75, 538-542.
- Craig H. (1957)** Isotopic standards for carbon and oxygen and correction factors for mass spectrometric analysis of carbon dioxide. *Geochimica et Cosmochimica Acta* 12, 133-149.
- Demmelmaier H. and Schmidt H.-L. (1993)** Precise $\delta^{13}\text{C}$ -determination in the range of natural abundance on amino acids from protein hydrolysates by gas chromatography - isotope ratio mass spectrometry. *Isotopenpraxis* 29, 237-250.
- DeNiro M. J. (1985)** Postmortem preservation and alteration of *in vivo* bone collagen isotope ratios in relation to palaeodietary reconstruction. *Nature* 317, 806-809.
- DeNiro M. J. and Epstein S. (1977)** Mechanisms of carbon isotope fractionation associated with lipid synthesis. *Science* 197, 261-263.

- DeNiro M. J. and Epstein S. (1978)** Influence of diet on the distribution of carbon isotopes in animals. *Geochimica et Cosmochimica Acta* **42**, 495-506.
- DeNiro M. J. and Epstein S. (1981)** Influence of diet on the distribution of nitrogen isotopes in animals. *Geochimica et Cosmochimica Acta* **45**, 341-351.
- DeNiro M. J. and Schoeninger M. J. (1983)** Stable carbon and nitrogen isotope ratios of bone collagen: Variations within individuals, between sexes, and within populations raised on monotonous diets. *Journal of Archaeological Science* **10**, 199-203.
- Docherty D., Jones V., and Evershed R. P. (2001)** Practical and theoretical considerations in the gas chromatography/combustion/isotope ratio mass spectrometry $\delta^{13}\text{C}$ analysis of small polyfunctional molecules. *Rapid Communications in Mass Spectrometry* **15**, 730-738.
- Dudd S. N. and Evershed R. P. (1998)** Direct demonstrations of milk as an element of archaeological economies. *Science* **282**, 1478-1480.
- Dudd S. N., Evershed R. P., and Gibson A. M. (1999)** Evidence for varying patterns of exploitation of animal products in different prehistoric pottery traditions based on lipids preserved in surface and absorbed residues. *Journal of Archaeological Science* **26**, 1473-1482.
- Engel M. H., Macko S. A., and Silfer J. A. (1990)** Carbon isotope composition of individual amino acids in the Murchison meteorite. *Nature* **348**(6296), 47-49.
- Evershed R. P., Dudd S. N., Charters S., Mottram H., Stott A. W., Raven A., van Bergen P. F., and Bland H. A. (1999)** Lipids as carriers of anthropogenic signals from prehistory. *Philosophical Transactions of the Royal Society of London, Series B* **354**, 19-31.
- Evershed R. P., Turner-Walker G., Hedges R. E. M., Tuross N., and Leyden A. (1995)** Preliminary results for the analysis of lipids in ancient bone. *Journal of Archaeological Science* **22**, 277-290.
- Fantle M. S., Dittel A. I., Schwalm S. M., Epifanio C. E., and Fogel M. L. (1999)** A food web analysis of the juvenile blue crab, *Callinectes sapidus*, using stable isotopes in whole animals and individual amino acids. *Oecologia* **120**(3), 416-426.
- Farquhar G. D., Ehleringer J. R., and Hubick K. T. (1989)** Carbon isotope discrimination and photosynthesis. *Annual Review of Plant Physiology and Plant Molecular Biology* **40**, 503-537.
- Fogel M. L., Tuross N., Johnson B. J., and Miller G. H. (1997)** Biogeochemical record of ancient humans. *Organic Geochemistry* **27**, 275-287.

- Fortier G., Tenaschuk D., and MacKenzie S. L. (1986)** Capillary gas chromatography micro-assay for pyroglutamic, glutamic and aspartic acids, and glutamine and asparagine. *Journal of Chromatography* **361**, 253-261.
- Farquhar G. D., Ehleringer J. R., and Hubick K. T. (1989)** Carbon isotope discrimination and photosynthesis. *Annual Review of Plant Physiology and Plant Molecular Biology* **40**, 503-537.
- Freedman P. A., Gillyon E. C. P., and Jumeau E. J. (1988)** Design and application of a new instrument for gc-isotope ratio ms. *American Laboratory* **20**(6), 114.
- Freeman K. H., Hayes J. M., Trendel J. M., and Albrecht P. (1990)** Evidence from carbon isotope measurements for diverse origins of sedimentary hydrocarbons. *Nature* **343**, 254-256.
- Garten C. T. J. (1993)** Variation in foliar ^{15}N abundance and the availability of soil nitrogen on Walker Branch watershed. *Ecology* **74**, 2098-2113.
- Gillon J. S., Borland A. M., Harwood, K. G., Roberts A., Broadmeadow M. S. J., and Griffiths H. (1998)** Carbon isotope discrimination in terrestrial plants: carboxylations and decarboxylations. In *Stable Isotopes* (ed. H. Griffiths), pp. 111-131. BIOS Scientific Publishers, Oxford.
- Gleixner G. and Schmidt H.-L. (1997)** Carbon isotope effects on the fructose-1-6-bisphosphate aldolase reaction, origin for non-statistical ^{13}C distributions in carbohydrates. *Journal of Biological Chemistry* **272**, 5382-5387.
- Habfast K. (1991)** The methodology and instrumentation of GC/C/IRMS, pp. 1-8. Finnigan MAT.
- Hare P. E. and Estep M. L. F. (1983)** Carbon and nitrogen isotopic composition of amino acids in modern and fossil collagens. *Carnegie Institution Washington Yearbook* **82**, 410-414.
- Hare P. E., Fogel M. L., Stafford T. W., Jr, Mitchell A. D., and Hoering T. C. (1991)** The isotopic composition of carbon and nitrogen in individual amino acids isolated from modern and fossil proteins. *Journal of Archaeological Science* **18**, 277-292.
- Herring G. M. (1972)** The organic matrix of bone. In *The biochemistry and physiology of bone* (ed. G. H. Bourne), pp. 127-189. Academic Press.
- Ho T.-Y. (1967)** The amino acids of bone and dentine collagen in Pleistocene mammals. *Biochimica et Biophysica Acta* **133**, 568-573.
- Hofmann D., Jung K., Segschneider H.-J., Gehre M., and Schuurmann G. (1995)** $^{15}\text{N}/^{14}\text{N}$ analysis of amino acids with GC-C-IRMS - methodological investigation and ecotoxicological applications. *Isotopes in Environmental Health Studies* **31**, 367-375.

- Husek P. (1995)** Simultaneous profile analysis of plasma amino and organic-acids by capillary gas chromatography. *Journal of Chromatography* **669**, 352-357.
- Jim S. (2000)** The development of bone cholesterol $\delta^{13}\text{C}$ values as a new source of palaeodietary information: Models of its use in conjunction with bone collagen and apatite $\delta^{13}\text{C}$ values, University of Bristol.
- Johnson B. J., Fogel M. L., and Miller G. H. (1993)** Paleoecological reconstructions in southern Egypt based on the stable carbon and nitrogen isotopes in the organic fraction and stable carbon isotopes in individual amino acids of fossil ostrich eggshell. *Chemical Geology* **107**, 493-497.
- Johnson B. J., Fogel M. L., and Miller G. H. (1998)** Stable isotopes in modern ostrich eggshell: A calibration for paleoenvironmental applications in semi-arid regions of southern Africa. *Geochimica et Cosmochimica Acta* **62(14)**, 2451-2461.
- Katzenberg M. A., Schwarcz H. P., Knyf M., and Melbye F. J. (1995)** Stable isotope evidence for maize horticulture and palaeodiet in southern Ontario, Canada. *American Antiquity* **60(2)**, 335-350.
- Koch P. L., Fogel M. L., and Tuross N. (1994)** Tracing the diets of fossil animals using stable isotopes. In *Stable isotopes in ecology and environmental science* (ed. K. Lajtha and R. H. Michener), pp. 63-92. Blackwell Scientific Publishers.
- Koch P. L., Tuross N., and Fogel M. L. (1997)** The effects of sample treatment and diagenesis on the isotopic integrity of carbonate in biogenic hydroxylapatite. *Journal of Archaeological Science* **24(5)**, 417-429.
- Koletzko B., Sauerwald T., and Demmelair H. (1997)** Safety of stable isotope use. *European Journal of Paediatrics* **156**, S12-S17.
- Krueger H. W. and Sullivan C. H. (1984)** Models for carbon isotope fractionation between diet and bone. In *Stable isotopes in human nutrition*, Vol. 258 (ed. J. S. Turnlund and P. E. Johnson), pp. 205-220. American Chemical Society.
- Krueger H. W. (1991)** Exchange of carbon with biological apatite. *Journal of Archaeological Science* **18**, 355-361.
- Leblond C. P. and Weinstock M. (1976)** A comparative study of bone and dentin formation. In *The biochemistry and physiology of bone* (ed. G. H. Bourne), pp. 517-562. Academic Press.
- Lee-Thorp J. A., Sealy J. C., and van der Merwe N. J. (1989)** Stable carbon isotope ratio differences between bone-collagen and bone apatite, and their relationship to diet. *Journal of Archaeological Science* **16(6)**, 585-599.

- Lee-Thorp J. A. and van der Merwe N. J. (1991)** Aspects of the chemistry of modern and fossil biological apatites. *Journal of Archaeological Science* **18**, 343-354.
- Leimer K. R., Rice R. H. and Gehrke C. W. (1977)** Complete mass spectra of N-trifluoroacetyl-*n*-butyl esters of amino acids. *Journal of Chromatography* **141**, 121-144.
- Libby W. F., Berger R., Mead J. F., G.V. A., and Ross J. F. (1964)** Replacement rates for human tissue from atmospheric radiocarbon. *Science* **146**, 1170-1172.
- Macko S. A., Estep M. L. F., Hare P. E., and Hoering T. C. (1983)** Stable nitrogen and carbon isotopic composition of individual amino acids isolated from cultured microorganisms. *Carnegie Institution Washington Yearbook* **82**, 404-410.
- Macko S. A., Fogel Estep M. L. Engel M. H., and Hare P. E. (1986)** Kinetic fractionation of stable nitrogen isotopes during amino acid transamination. *Geochimica et Cosmochimica Acta* **50**, 2143-2146.
- Macko S. A., Fogel (Estep) M. L., Hare P. E., and Hoering T. C. (1987)** Isotopic fractionation of nitrogen and carbon in the synthesis of amino acids by microorganisms. *Chemical Geology (Isotope Geoscience Section)* **65**, 79-92.
- Macko S. A. (1994)** Compound-specific approaches using stable isotopes. In *Methods in Ecology, Stable Isotopes in Ecology and Environmental Science* (ed. K. Lajtha and R. Michener), pp. 241-247. Blackwell Scientific Publications.
- Matthews D. E. and Hayes J. M. (1978)** Isotope-ratio-monitoring gas chromatography-mass spectrometry. *Analytical Chemistry* **50**, 1465-1473.
- Mays S. A. (1997)** Carbon stable isotope ratios in Mediaeval and later human skeletons from Northern England. *Journal of Archaeological Science* **24**, 561-567.
- McKinney A. R., McCrea J. M., Epstein S., Allen H. A., and Urey H. C. (1950)** Improvements in mass spectrometry for the measurement of small differences in isotope abundance ratios. *Revue of Scientific Instruments* **21**, 724-730.
- Medina R., and Schmidt H. -L. (1982)** Nitrogen isotope ratio variations in biological matter, indicator for metabolic correlations? In *Stable Isotopes* (ed. H. -L. Schmidt, H. Forstel, and K. Heinzinger), pp. 465-473. Elsevier Scientific Publishing Company.
- Meier-Augenstein W. (1997)** The chromatographic side of isotope ratio mass spectrometry: Pitfalls and answers. *LC-GC International* **15**(3), 244-252.

- Meier-Augenstein W. (1999)** Use of gas chromatography-combustion-isotope ratio mass spectrometry in nutrition and metabolic research. *Current Opinions in Clinical Nutrition and Metabolic Care* 2(6), 465-70.
- Meier-Augenstein W. (1999)** Applied gas chromatography coupled to isotope ratio mass spectrometry. *Journal of Chromatography a* 842(1-2), 351-371.
- Merritt D. A. and Hayes J. M. (1994)** Nitrogen isotopic analyses by isotope-ratio-monitoring gas chromatography mass spectrometry. *Journal of the American Society for Mass Spectrometry* 5, 387-397.
- Merritt D. A., Freeman K. H., Ricci M. P., Studley S. A., and Hayes J. M. (1995)** Performance and optimization of a combustion interface for isotope ratio monitoring gas chromatography mass spectrometry. *Analytical Chemistry* 67(14), 2461-2473.
- Metges C. C., Petzke K.-J., and Hennig U. (1996)** Gas chromatography/combustion/isotope ratio mass spectrometric comparison of N-acetyl- and N-pivaloyl amino acid esters to measure ^{15}N isotopic abundances in physiological samples: A pilot study on amino acid synthesis in the upper gastro-intestinal tract of minipigs. *Journal of Mass Spectrometry* 31, 367-376.
- Metges C. C. and Daenzer M. (2000)** ^{13}C gas chromatography-combustion isotope ratio mass spectrometry analysis of N-pivaloyl amino acid esters of tissue and plasma samples. *Analytical Biochemistry* 278(2), 156-64.
- Montigon F., J. B. J., and Fay L. B. (2001)** Determination of ^{13}C - and ^{15}N -enrichment of glutamine by gas chromatography/mass spectrometry and gas chromatography/combustion/isotope ratio mass spectrometry after N(O,S)-ethoxycarbonyl ethyl ester derivatisation. *Rapid Communications in Mass Spectrometry* 15, 116-123.
- Moss C. W. and Lambert M. A. (1971)** Gas-liquid chromatography of twenty protein amino acids on a single column. *Journal of Chromatography* 60, 134-136.
- Nier A. O. (1947)** A mass spectrometer for isotope and gas analysis. *Revue of Scientific Instruments* 18, 398-411.
- O'Leary M. H. (1981)** Carbon isotope fractionation in plants. *Phytochemistry* 20(4), 553-567.
- Owens N. J. P. (1987)** Natural variations in ^{15}N in the marine environment. *Advances in Marine Biology* 24, 389-450.
- Parker P. L. (1964)** The biogeochemistry of the stable isotopes of carbon in a marine bay. *Geochimica et Cosmochimica Acta* 28, 1155-1164.

- Parkington J. E. (1972)** Seasonal mobility in the Late Stone Age. *African Studies* 1, 223-243.
- Parkington J. E. (1976)** Coastal settlement between the mouths of the Berg and Olifants Rivers, Cape Province. *South African Archaeological Bulletin* 31, 127-140.
- Parkington J. E. (1977)** Soaqua: Hunter-fisher-gatherers of the Olifants River valley, western Cape. *South African Archaeological Bulletin* 32, 150-157.
- Parkington L. (1991)** Approaches to dietary reconstruction in the Western Cape: are you what you have eaten? *Journal of Archaeological Science* 18, 331-342.
- Pelaez M. V., Bayon M. M., Alonso J. I. G., and Sanz-Medel A. (2000)** A comparison of different derivatisation approaches for the determination of selenomethionine by GC-ICP-MS. *Journal of Analytical Atomic Spectrometry* 15, 1217-1222.
- Preston T., and Barrie A. (1991)** Recent progress in continuous flow isotope ratio mass spectrometry. *International Laboratory (September 1991)*, 31-34.
- Ricci M. P., Merritt D. A., Freeman K. H., and Hayes J. M. (1994)** Acquisition and processing of data for isotope-ratio-monitoring mass spectrometry. *Organic Geochemistry* (21)6/7, 561-571.
- Richards M. P., Pettitt P. B., Trinkaus E., Smith F. H., Paunovic M., and Karavanic I. (2000)** Neanderthal diet and Vindija and Neanderthal predation: The evidence from stable isotopes. *Proceedings of the National Academy of Science USA* 97(13), 7663-7666.
- Rieley G., Collier R. J., Jones D. M., Eglinton G., Eakin P. A., and Fallick A. E. (1991)** Sources of sedimentary lipids deduced from stable carbon isotope analyses of individual compounds. *Nature* 353, 425-427
- Rieley G. (1994)** Derivatisation of organic compounds prior to gas-chromatographic combustion-isotope ratio mass-spectrometric analysis - identification of isotope fractionation processes. *Analyst* 119(5), 915-919.
- Rittenberg D., and Schoenheimer R. (1939)** Studies in protein metabolism VI. Hippuric acid formation studied with the aid of the nitrogen isotope. *Journal of Biological Chemistry* 127, 329-331.
- Rowley-Conwy P. (1989)** Nubia AD 0-550 and the "Islamic" agricultural revolution: Preliminary botanical evidence from Qasr Ibrim, Egyptian Nubia. *Archeologie du Nil Moyen* 3, 131-138.
- Santrock J., Studley S. A., and Hayes J. M. (1985)** Isotopic analyses based on the mass spectrum of CO₂. *Analytical Chemistry* 57, 1444-1448.

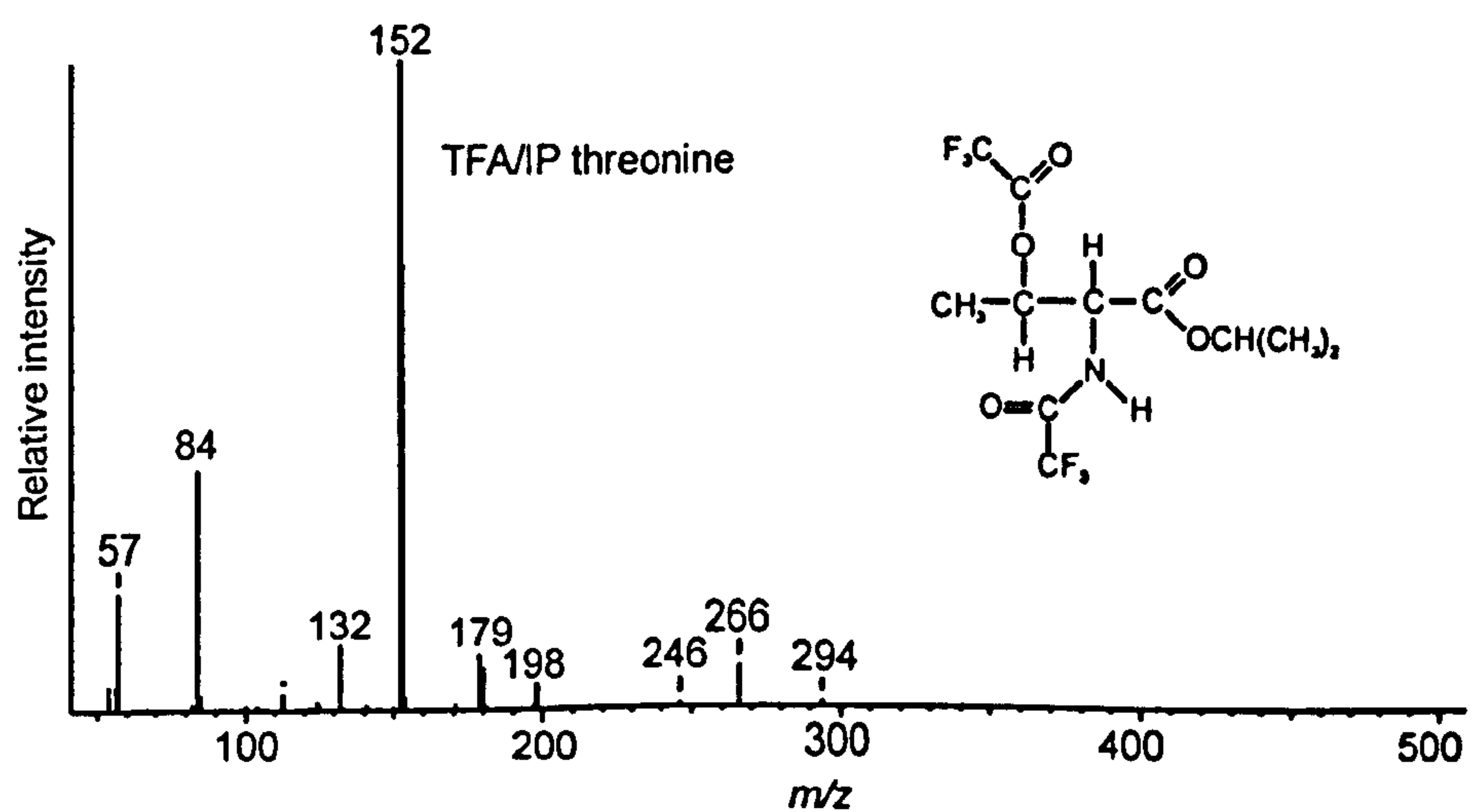
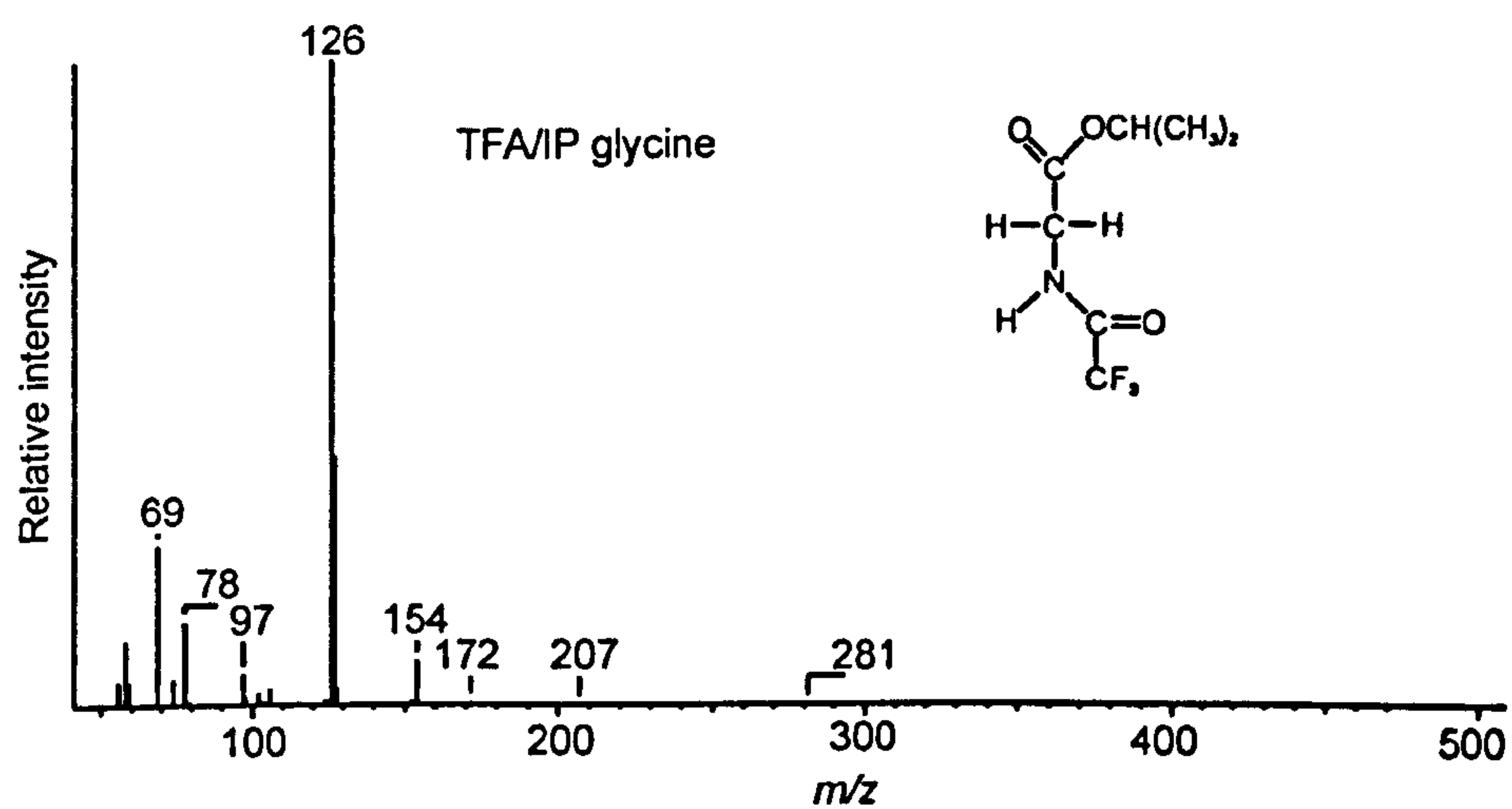
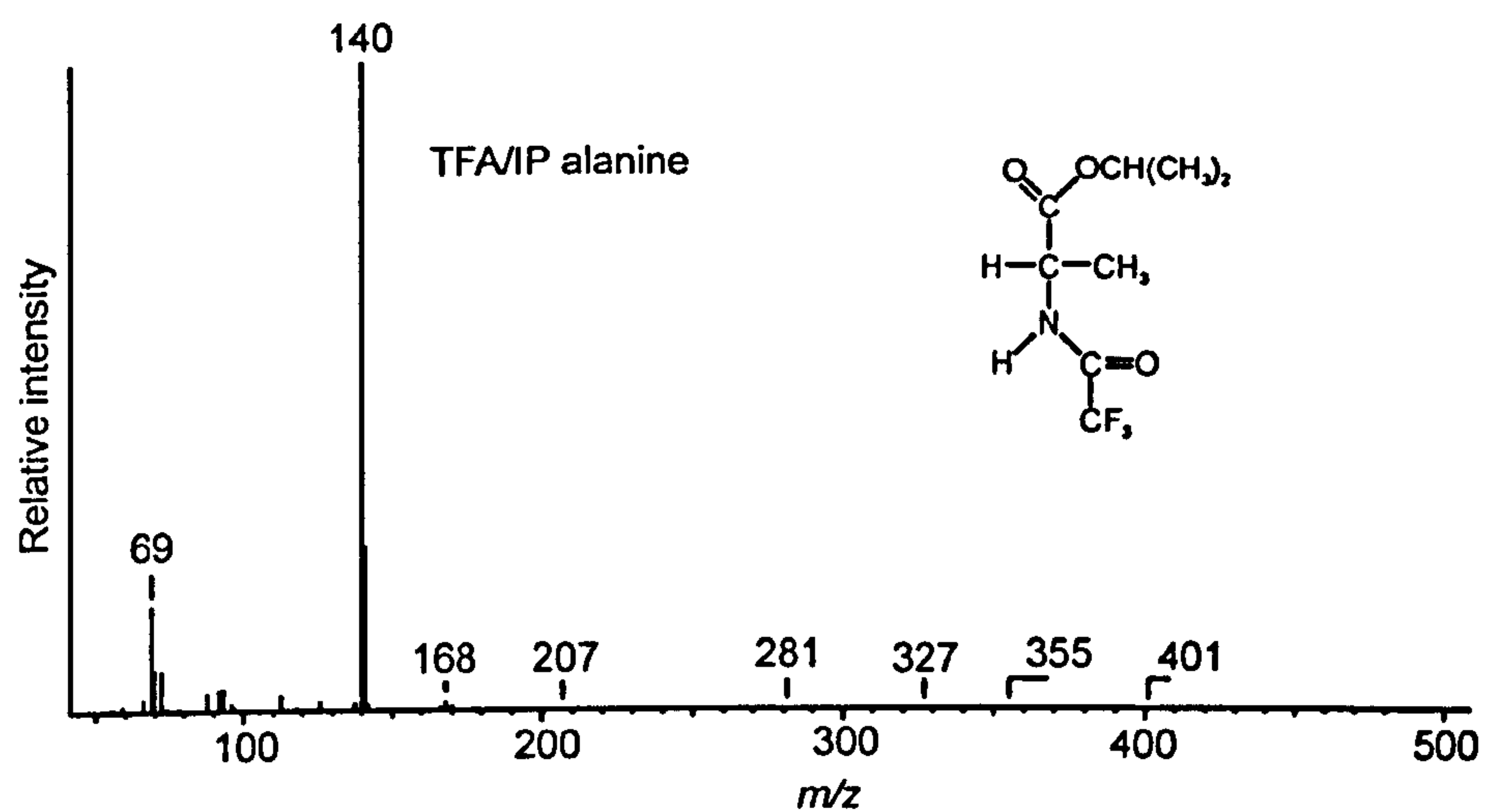
- Schmidt H., L and Gleixner G. (1998)** Carbon isotope effects on key reactions in plant metabolism and ^{13}C patterns in natural compounds. In *Stable isotopes* (ed. H. Griffiths, D. Robinson, and P. van Gardingen), pp. 13-25. BIOS Scientific Publishers.
- Schoeninger M. J. and DeNiro M. J. (1982)** Carbon isotope ratios of apatite from fossil bone cannot be used to reconstruct diets of animals. *Nature* 297, 577-578.
- Schoeninger M. J. and DeNiro M. J. (1983)** Carbon isotope ratios of bone apatite and animal diet reconstruction - reply. *Nature* 301, 178-178.
- Schoeninger M. J. and DeNiro M. J. (1984)** Nitrogen and carbon isotopic composition of bone collagen from marine and terrestrial animals. *Geochimica et Cosmochimica Acta* 48(4), 625-639.
- Schwarcz H. P. (1991)** Some theoretical aspects of isotope paleodiet studies. *Journal of Archaeological Science* 18(3), 261-275.
- Schwarcz H. P. and Schoeninger M. J. (1991)** Stable isotopic analyses in human nutritional ecology. *Yearbook of Physical Anthropology* 34, 283-321.
- Schwenk W. F., Berg P. J., Beaufriere B., Miles J. M., and Haymond M. W. (1984)** Use of *t*-butyldimethylsilylation in the gas chromatographic/mass spectrometric analysis of physiological compounds found in plasma using electron-impact ionization. *Analytical Biochemistry* 141, 101-109.
- Sealy J. and van der Merwe N. J. (1985)** Isotope assessment of holocene human diets in the southwestern Cape, South Africa. *Nature* 315, 138-140.
- Sealy J. C. and van der Merwe N. J. (1986)** Isotope assessment and seasonal-mobility hypothesis in the southwestern Cape of South Africa. *Current Anthropology* 27, 135-150.
- Sealy J. C. and van der Merwe N. J. (1988)** Social, spatial and chronological patterning in marine food use as determined by $\delta^{13}\text{C}$ measurements of Holocene human skeletons from the southwestern Cape, South Africa. *World Archaeology* 20, 87-102.
- Silfer J. A., Engel M. H., Macko S. A., and Jumeau E. J. (1991)** Stable carbon isotope analysis of amino acid enantiomers by conventional isotope ratio mass spectrometry and combined gas chromatography/ isotope ratio mass spectrometry. *Analytical Chemistry* 63, 370-374.
- Silfer J. A., Qian Y., Macko S. A., and Engel M. H. (1994)** Stable carbon isotope compositions of individual amino acid enantiomers in mollusc shell by GC/C/IRMS. *Organic Geochemistry* 21, 603-610.

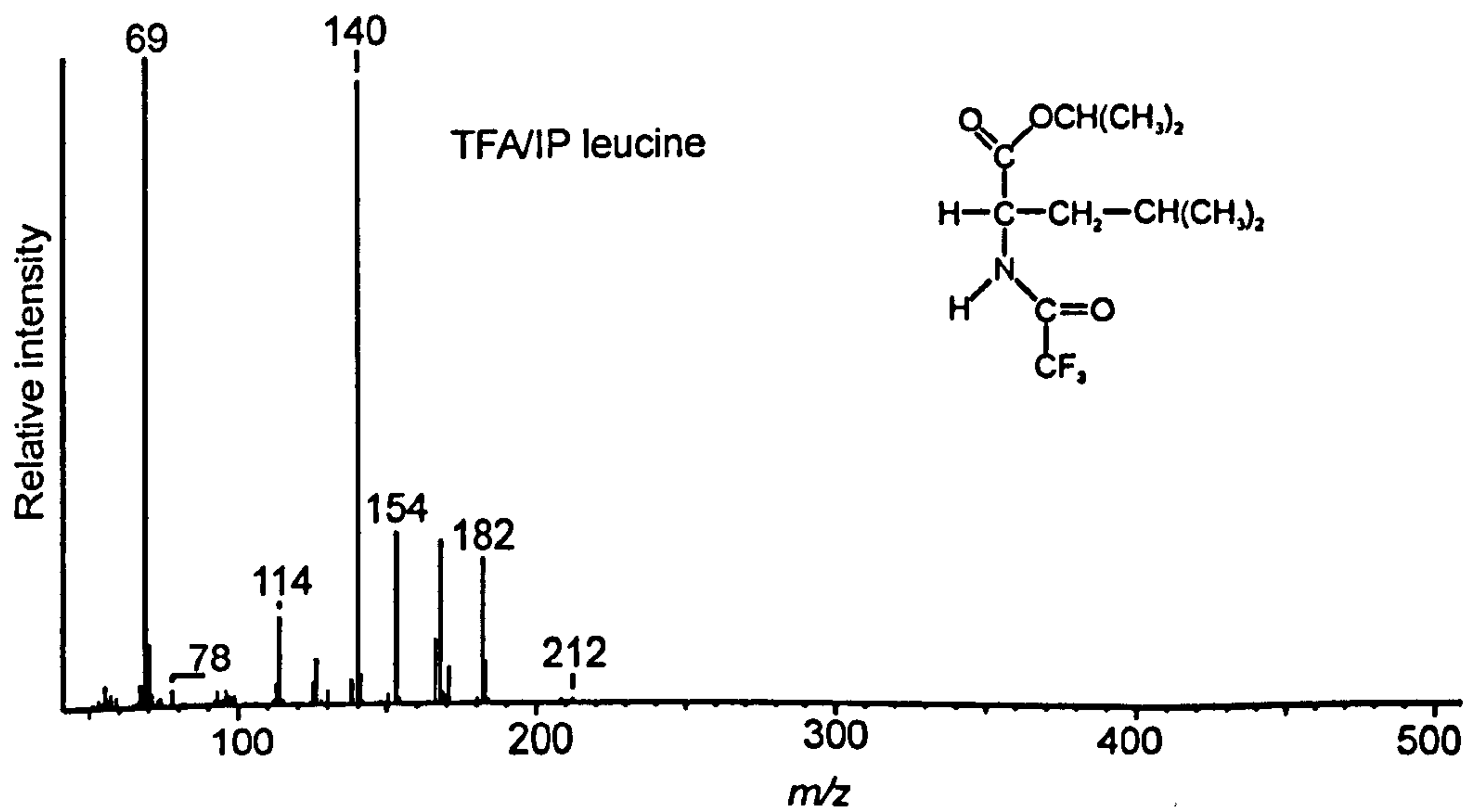
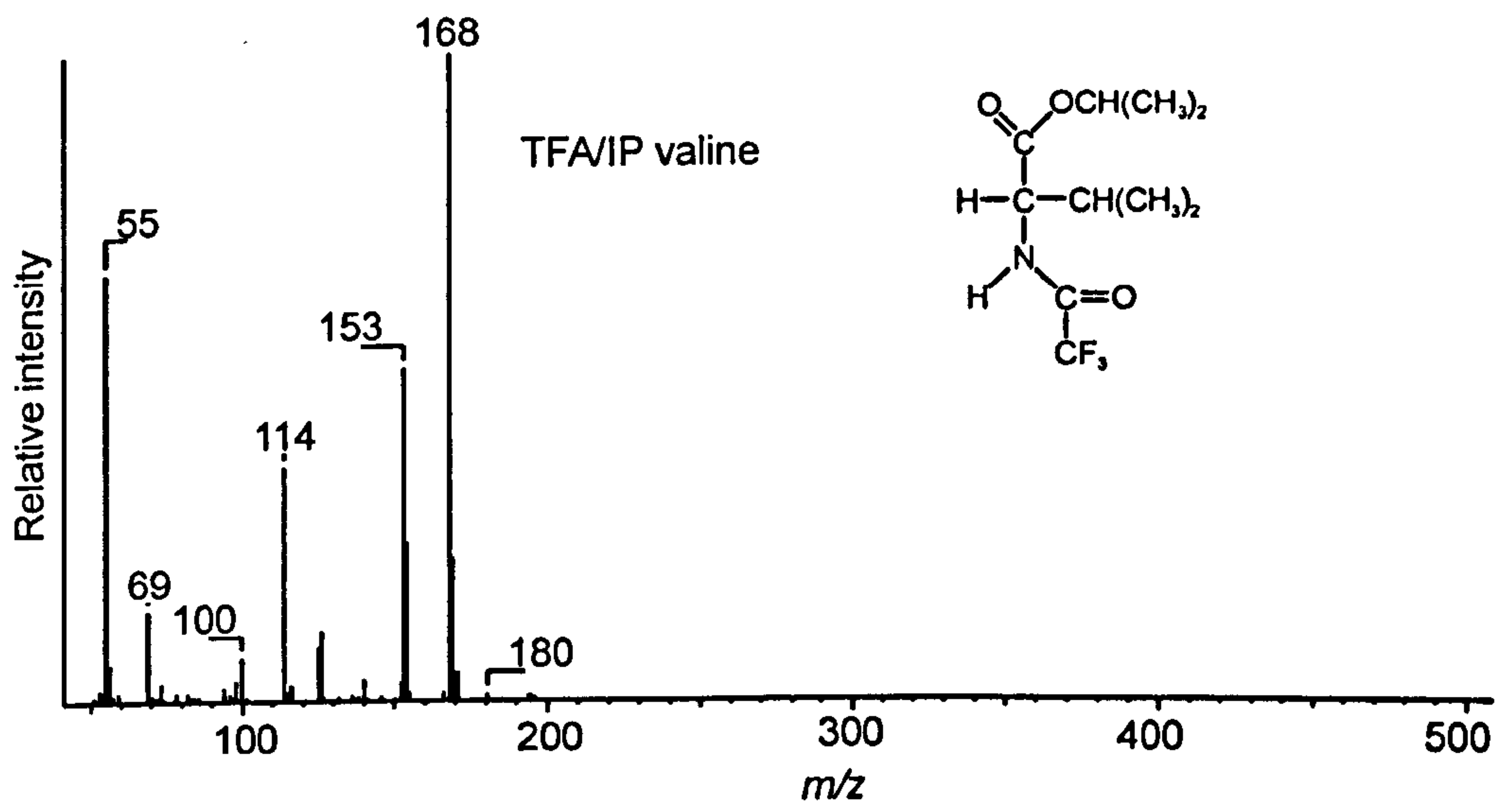
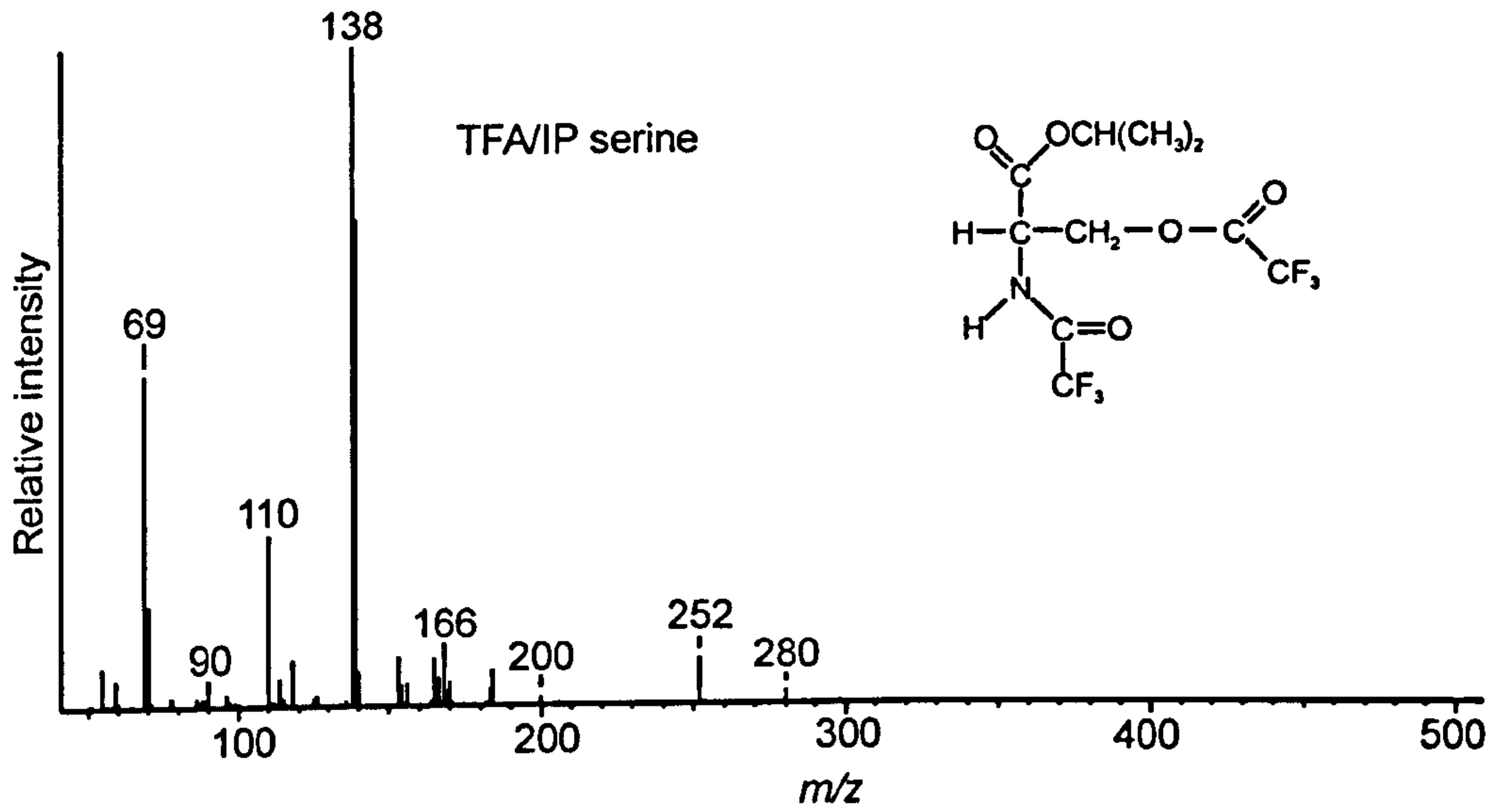
- Simpson I. A., Bol R., Dockrill S. J., Petzke K.-E., and Evershed R. P. (1997) Compound-specific $\delta^{15}\text{N}$ amino acid signals in palaeosols as indicators of early land use: A preliminary study. *Archaeological Prospection* 4, 147-152.
- Smith B. N. and Epstein S. (1971) Two categories of $^{13}\text{C}/^{12}\text{C}$ ratios for higher plants. *Plant Physiology* 47, 380-384.
- Stenhouse M. J. and Baxter M. S. (1979) The uptake of bomb ^{14}C in humans. In *Radiocarbon dating* (ed. R. Berger and H. E. Suess), pp. 324-341. University of California Press.
- Stott A. W., Davies E., and Evershed R. P. (1997) Monitoring the routing of dietary and biosynthesised lipids through compound-specific stable isotope ($\delta^{13}\text{C}$) measurements at natural abundances. *Naturwissenschaften* 84, 82-86.
- Stott A. W., Evershed R. P., Jim S., Jones V., Rogers J. M., Tuross N., and Ambrose S. H. (1999) Cholesterol as a new source of palaeodietary information: experimental approaches and archaeological applications. *Journal of Archaeological Science* 26, 705-716.
- Sullivan C. H. and Krueger H. W. (1983) Carbon isotope ratios of bone apatite and animal diet reconstruction. *Nature* 301, 177-177.
- Teaford M. F. and Walker A. C. (1984) Quantitative differences in dental microwear between primate species with different diets and a comment on the presumed diet of Sivapithecus. *American Journal of Physical Anthropology* 64, 191-200.
- Teaford M. F. (1988) A review of dental microwear and diet in modern mammals. *Scanning Microscopy* 2, 1149-1166.
- Tieszen L. L., Boutton T. W., Tesdahl K. G., and Slade N. A. (1983) Fractionation and turnover of stable carbon isotopes in animal tissues - implications for $\delta^{13}\text{C}$ analysis of diet. *Oecologia* 57(1-2), 32-37.
- Tieszen L. L. (1991) Natural Variations in the Carbon Isotope Values of Plants - Implications For Archaeology, Ecology, and Paleoecology. *Journal of Archaeological Science* 18(3), 227-248.
- Tieszen L. L. and Fagre T. (1993a) Carbon isotopic variability in modern and archaeological maize. *Journal of archaeological science* 20, 25-40.
- Tieszen L. L. and Fagre T. (1993b) Effect of diet quality and composition on the isotopic composition of respiratory CO_2 , bone collagen, bioapatite and soft tissues. In *Prehistoric Human Bone: Archaeology at the Molecular Level* (ed. J. B. Lambert and G. Grupe), pp. 121-155. Springer-Verlag.
- Tissot S., Normand S., Guilly R., Pachiaudi C., Beylot M., Laville M., Chen R., Mornex R., and Riou J. P. (1990) Use of a new gas chromatograph

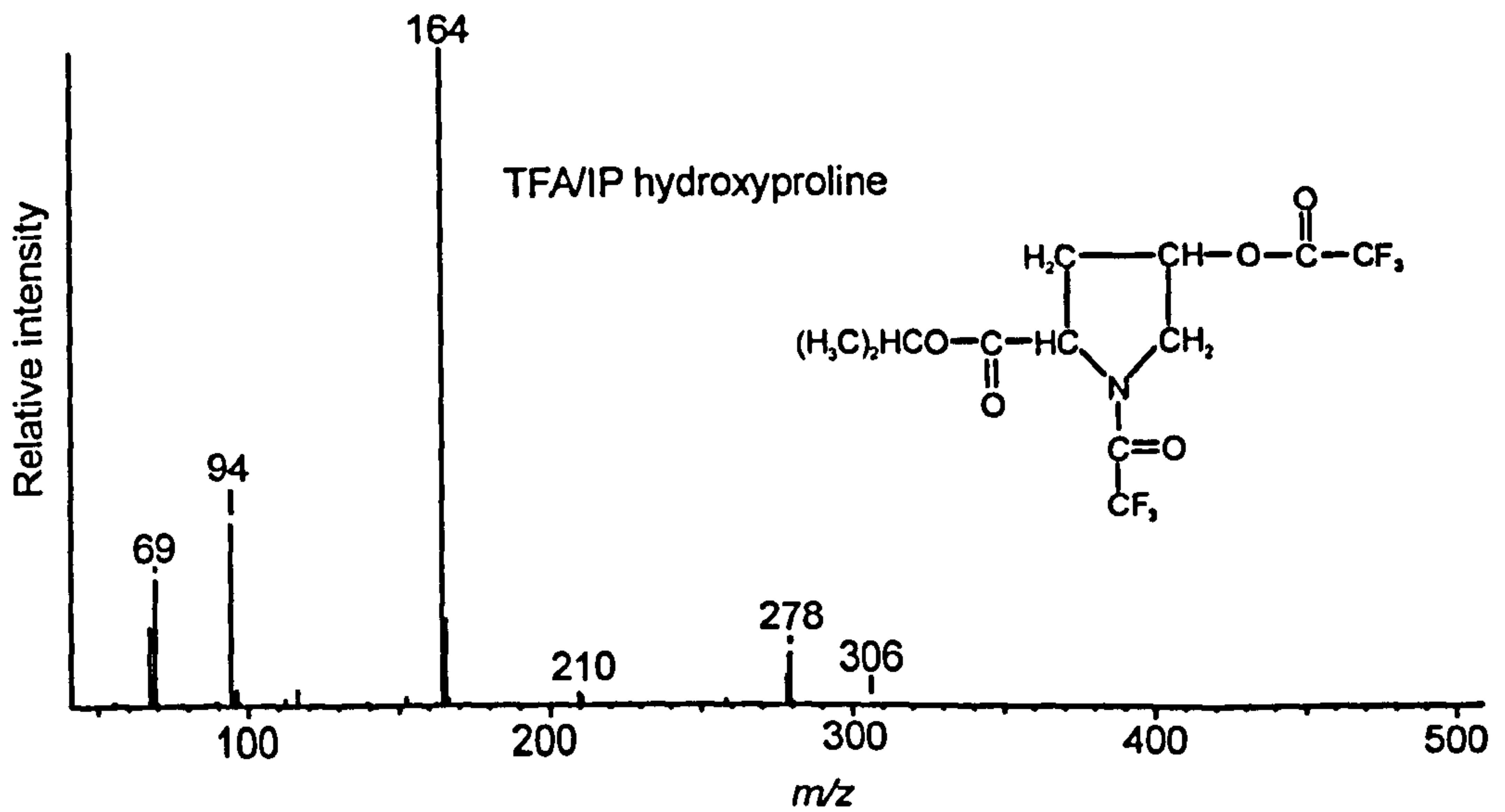
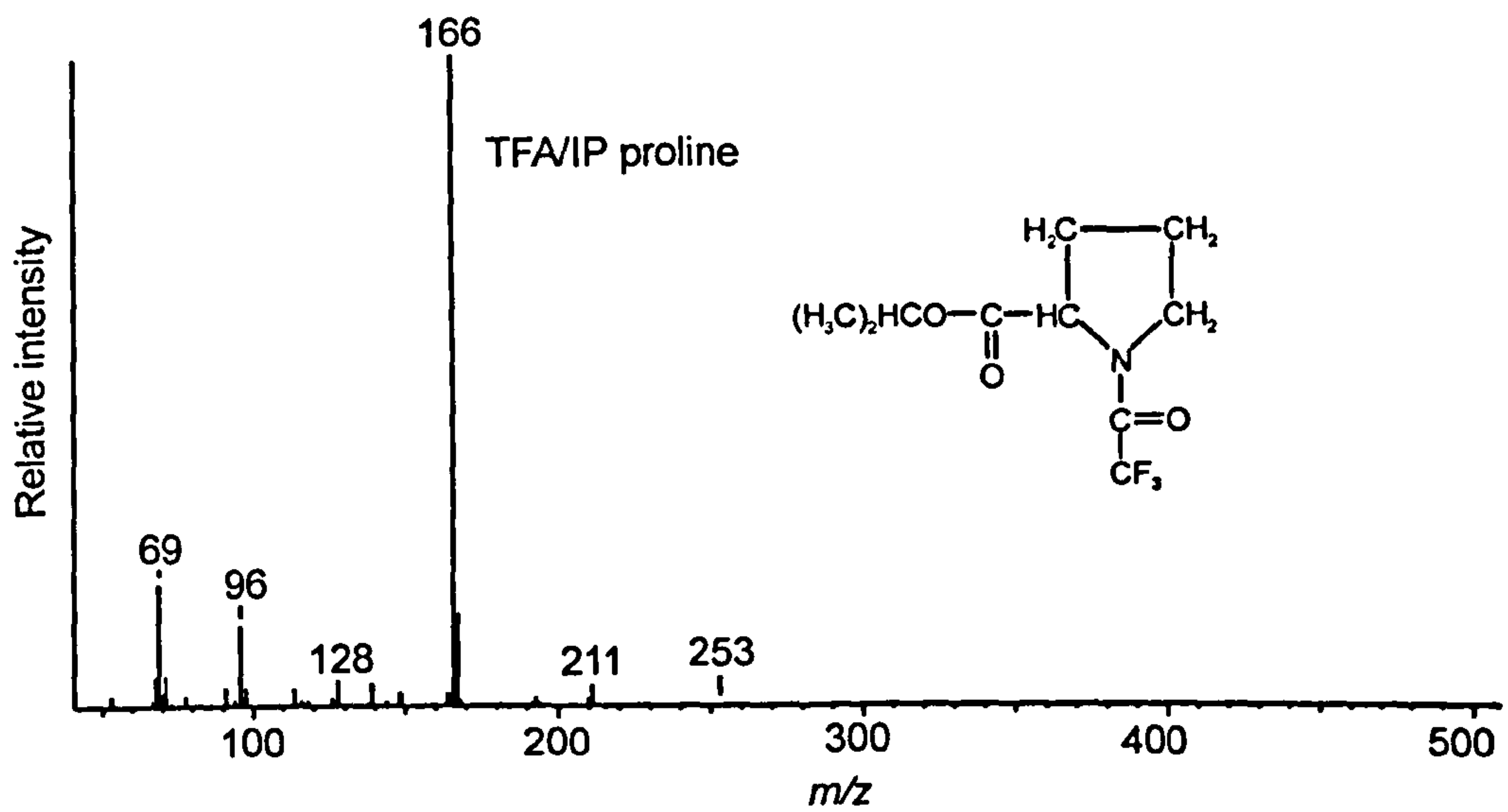
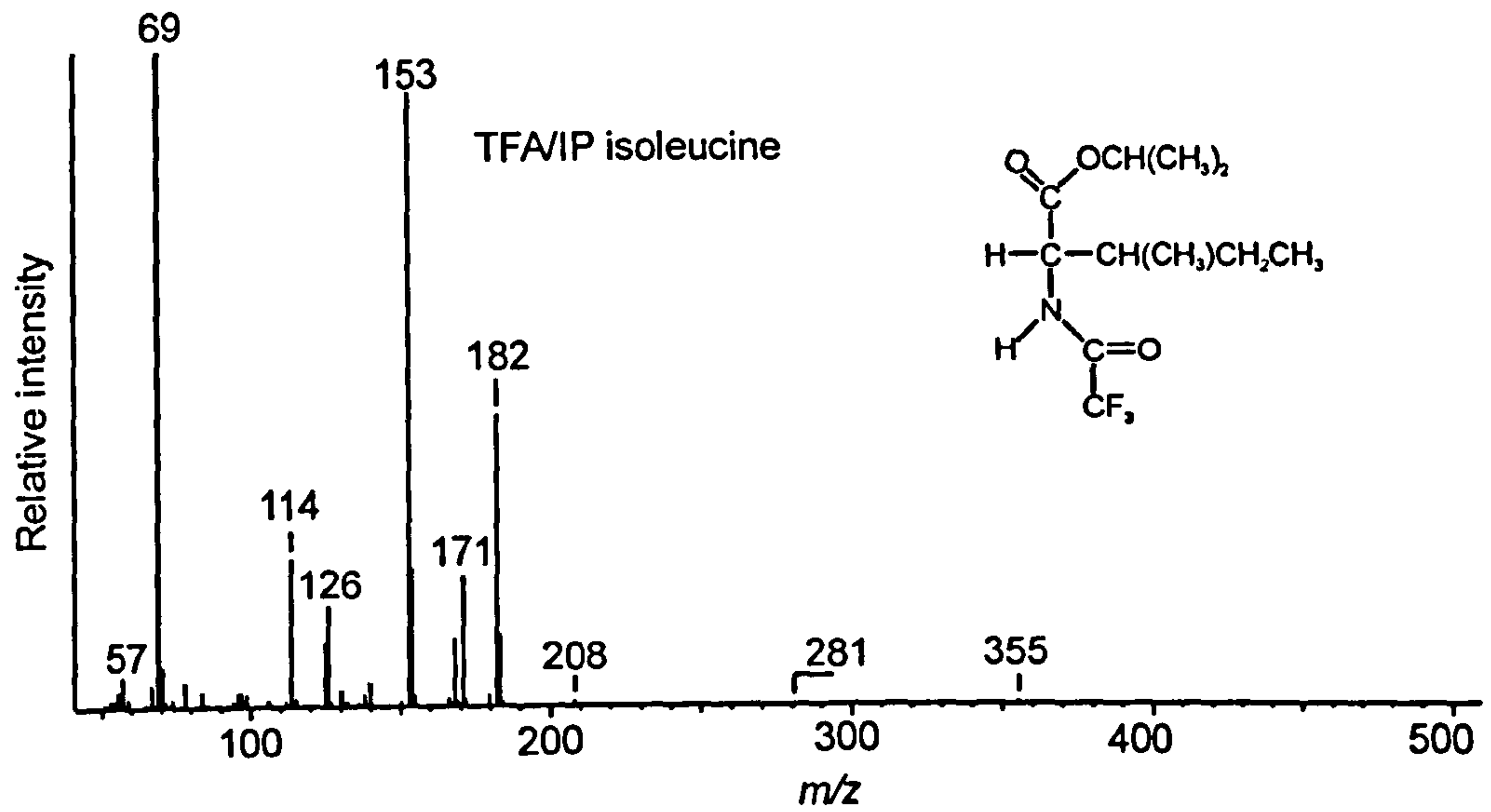
- isotope ratio mass spectrometer to trace exogenous ^{13}C labelled glucose at very low levels of enrichment in man. *Diabetologia* **33**, 449-456.
- Tuross N., Fogel M. L., and Hare P. E. (1988)** Variability in the preservation of the isotopic composition of collagen from fossil bone. *Geochimica et Cosmochimica Acta* **52**, 929-935.
- Tuross N., Behrensmeyer A. K., Eanes E. D., Fisher L. W., and Hare P. E. (1989)** Molecular preservation and crystallographic alterations in a weathering sequence of wildbeest bones. *Applied Geochemistry* **4**, 261-270.
- Tuross N., and Fogel M. L. (1994)** Stable isotope analysis and subsistence patterns at the Sully site. In *Skeletal Biology in the Great Plains* (ed. D. W. Owsley and R. L. Jantz), pp. 283-289. Smithsonian Institution Press.
- Udenfriend S. (1966)** Formation of hydroxyproline in collagen. *Science* **152**, 1335-1340.
- van der Merwe N. J., Vogel, J. C. (1978)** ^{13}C content of human collagen as a measure of prehistoric diet in woodland North America. *Nature* **276**, 815-816.
- van der Merwe N. J. (1982)** Carbon isotopes, photosynthesis and archaeology. *American Scientist* **70**, 596-606.
- van der Merwe N. J. and Medina E. (1991)** The canopy effect, carbon isotope ratios and foodwebs in Amazonia. *Journal of Archaeological Science* **18**, 249-259.
- Vaughan J. M. (1970)** *Physiology of bone*. Oxford University Press.
- Vogel J. C. (1978a)** Isotopic assessment of the dietary habits of ungulates. *South African Journal of Science* **74**, 298-301.
- Vogel J. C. (1978b)** Recycling of carbon in a forest environment. *Oecologia Plantarum* **13**, 89-94.
- Vogel J. C. (1982)** Isotopic evidence for the past climates and vegetation of South Africa. *Bothalia, Pretoria* **14**, 391-394.
- Vogel J. C., Fuls A., and Ellis R. P. (1978)** The geographical distribution of Kranz species in southern Africa. *South African Journal of Science* **75**, 209-215.
- Vogel J. C. and van der Merwe N. J. (1977)** Isotopic evidence for early maize cultivation in New York state. *American Antiquity* **42(2)**, 238-242.
- Welte D. H. (1968)** Determination of $^{13}\text{C}/^{12}\text{C}$ isotope ratios of individual higher *n*-paraffins from different petroleums. In *Advances in Organic Geochemistry* (ed. P.A. Schenck and I. Havenaar), pp. 269-277. Pergamon.

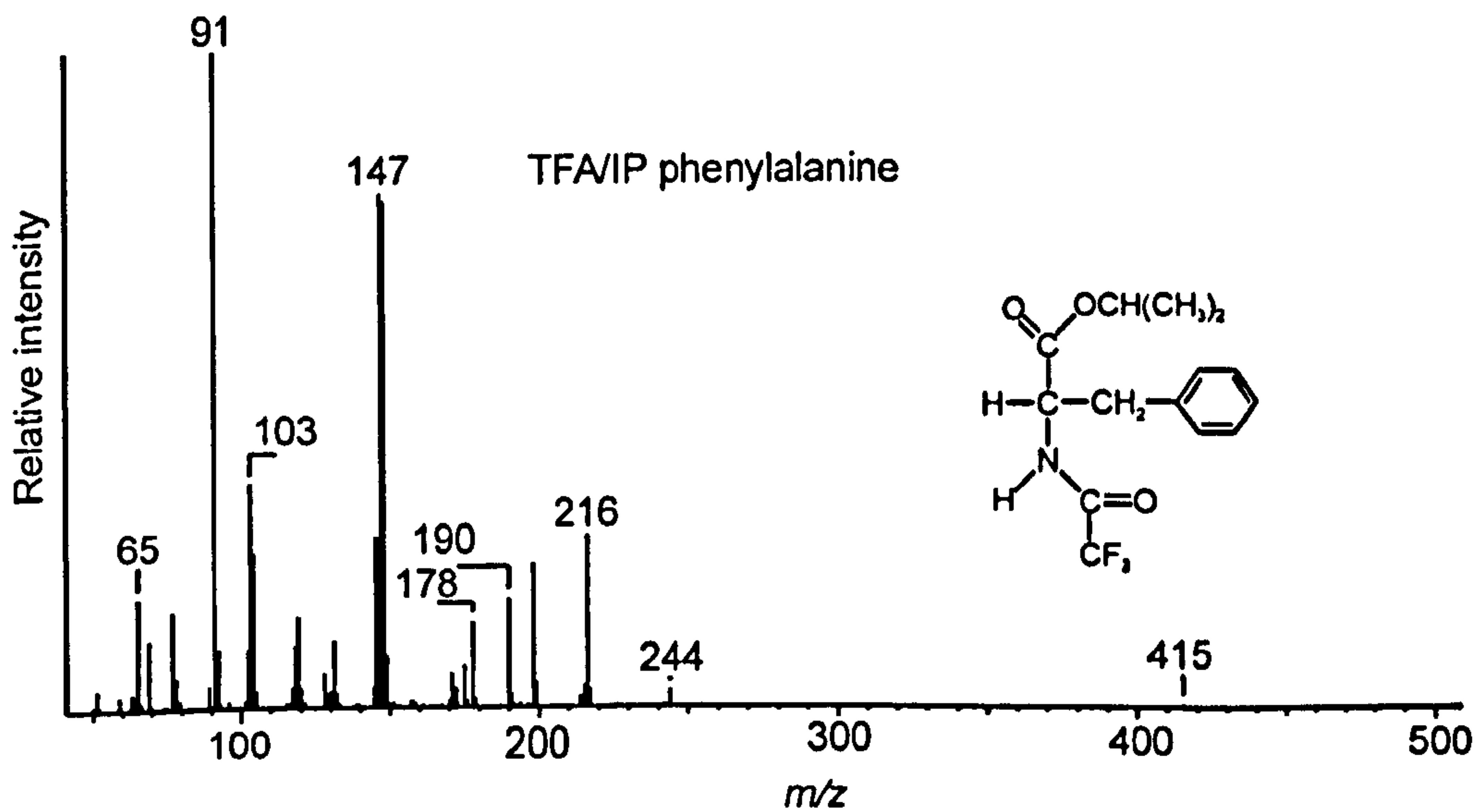
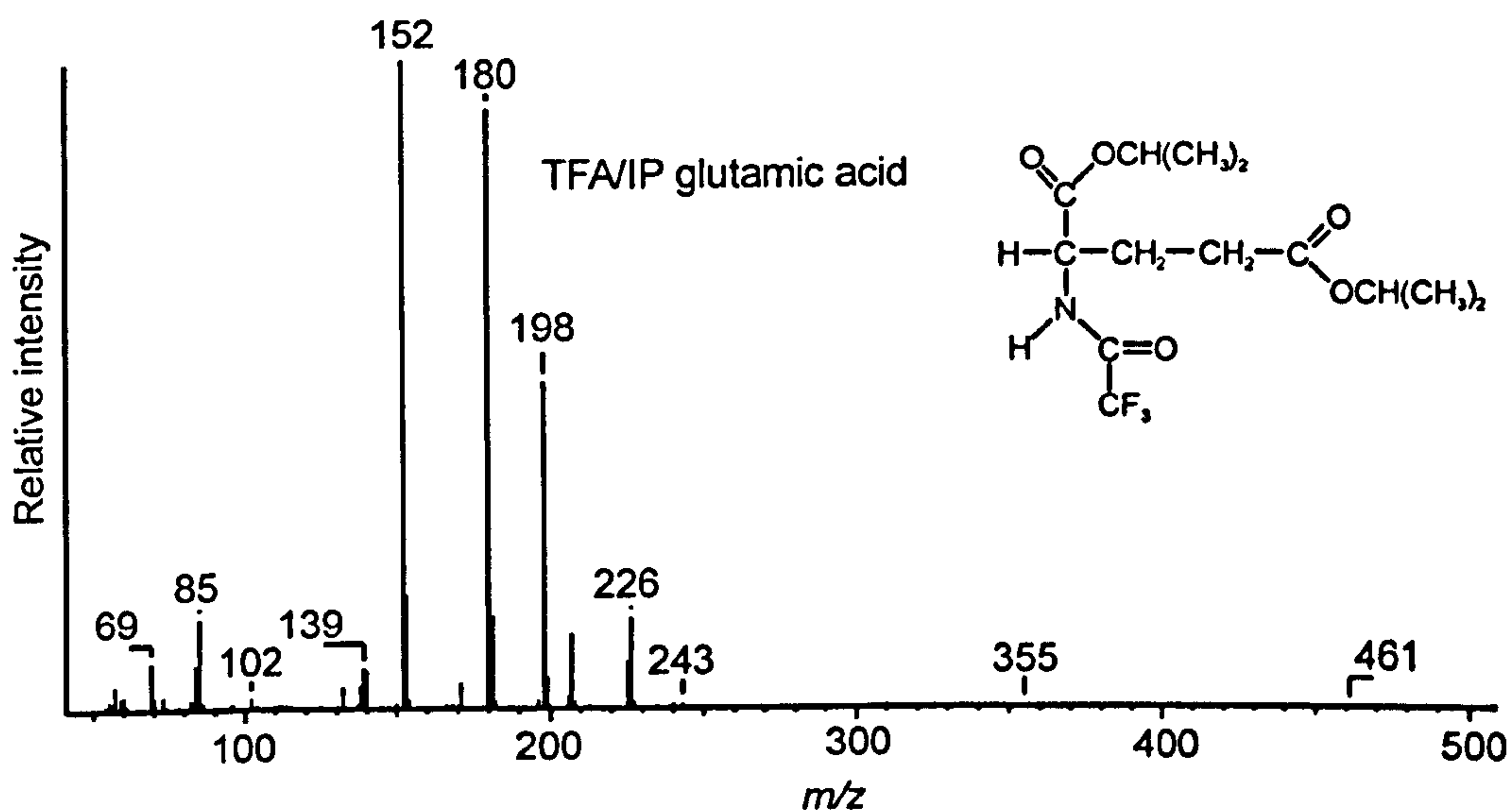
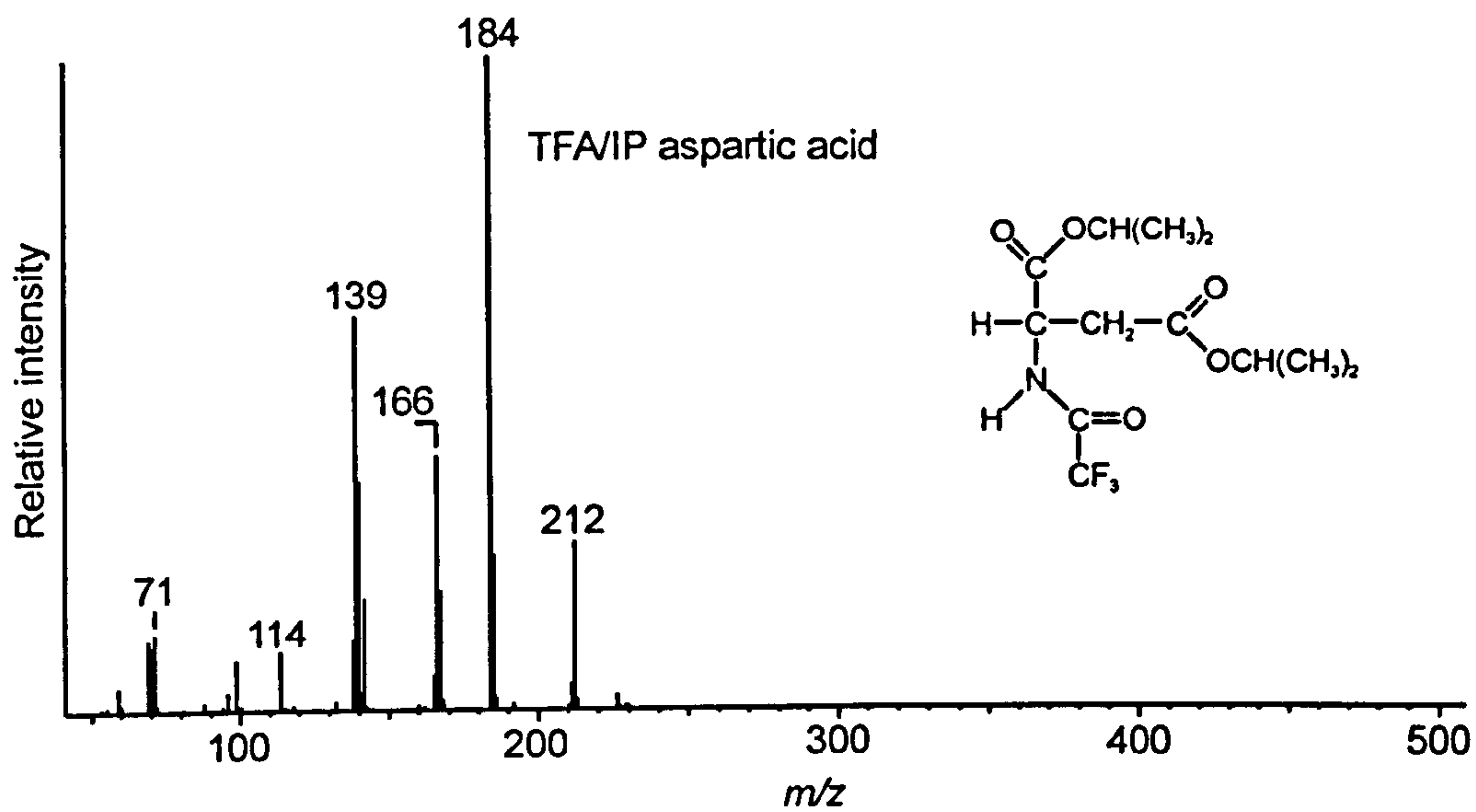
- Woodbury S. E., Evershed R. P., Rossell J. B., Griffith R. E., and Farnell P. (1995)** Detection of vegetable oil adulteration using GC/C/IRMS. *Analytical Chemistry* **67**, 2685-2690
- Young R. V. and El-Khoury A. E. (1985)** The notion of the nutritional essentiality of amino acids, revisited, with a note on the indispensable amino acid requirements in adults. In *Amino acid metabolism and therapy in health and nutritional disease* (ed. L. A. Cynober), pp. 191-233. CRC Press.

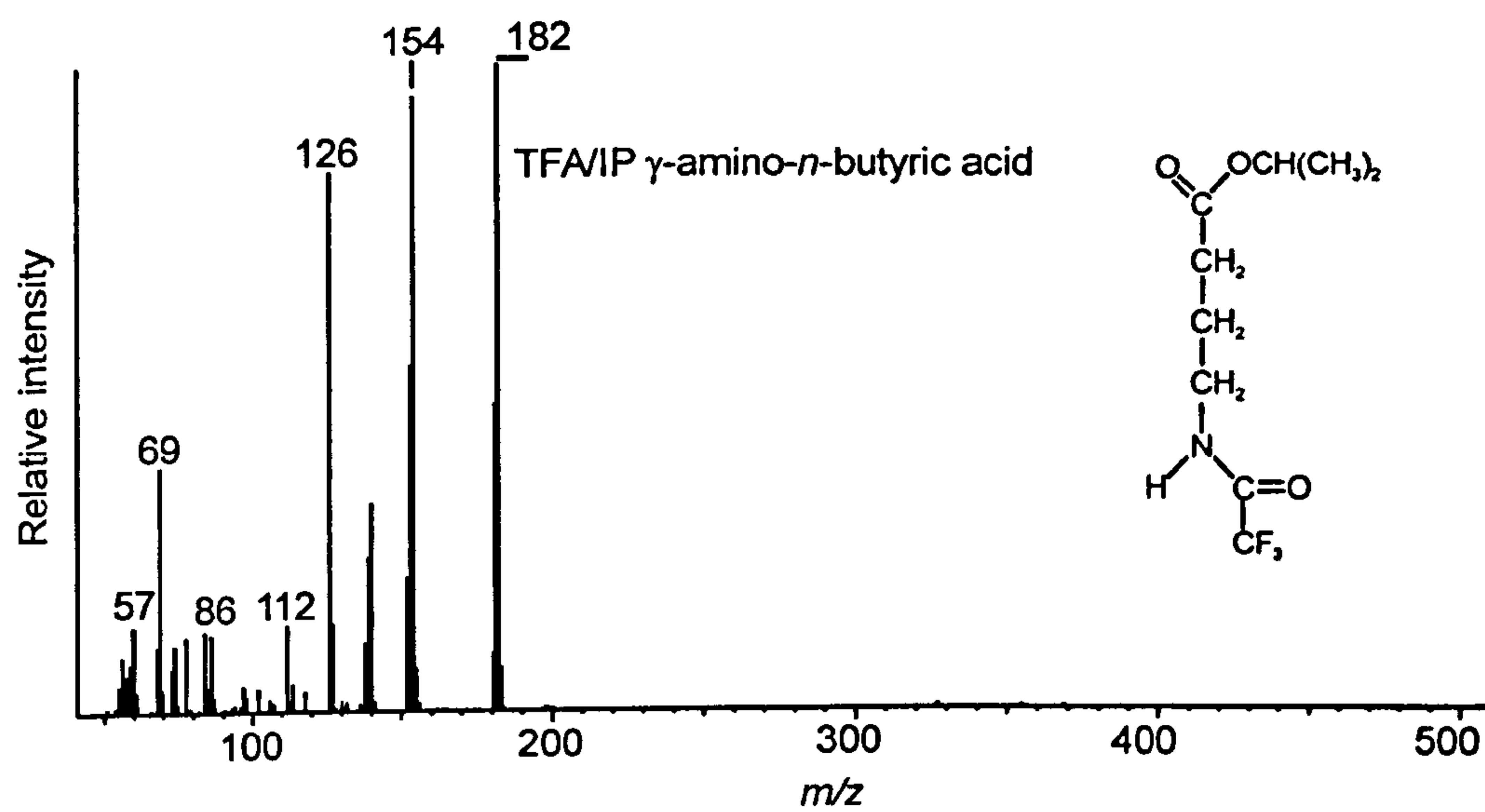
APPENDIX 1. Mass spectra of trifluoroacetyl isopropyl amino acid derivatives











APPENDIX 2 Results of linear regression analysis of carbon isotope data from the rat feeding experiment. x and y are variables from the equation of the line $y = mx + c$. R² values are listed in descending order for each amino acid.

ALANINE

y	x	R2
wd-prot	prot-energy	0.999406
wd-dAA	energy-dAA	0.997213
wd-coll	energy-coll	0.99659
wd-dAA	dAA-apat	0.996249
energy-dAA	dAA-apat	0.994609
wd-energy	prot-energy	0.993942
prot-energy	prot-apat	0.993781
wd-prot	prot-apat	0.992558
prot-energy	energy-coll	0.992351
wd-prot	energy-coll	0.991697
wdiet	apat	0.991158
prot-apat	energy-coll	0.989833
wd-energy	prot-apat	0.989776
wd-prot	wd-energy	0.989576
wd-energy	energy-coll	0.986545
wd_dAA	dAA-bchol	0.983142
wd-prot	wd-coll	0.982662
wd-tAA	apat-tAA	0.982072
wd-coll	prot-energy	0.981449
wd-coll	prot-apat	0.979781
wd-coll	coll-apat	0.979589
prot-tAA	coll-tAA	0.979531
dAA_apat	dAA-bchol	0.97757
energy-coll	coll-apat	0.977135
prot-apat	coll-apat	0.974515
energy_dAA	dAA-bchol	0.97274
wd_coll	prot-bchol	0.971964
wd_prot	prot-bchol	0.970917
energy_coll	prot-bchol	0.970856
wd-energy	wd-coll	0.969794
wd-dAA	dAA-coll	0.96775
prot_energy	prot-bchol	0.967527
energy-dAA	energy-coll	0.964557
wd-coll	energy-dAA	0.964188
dAA_coll	dAA-bchol	0.963008
dAA-coll	dAA-apat	0.960221
prot_apat	prot-bchol	0.959541
prot-tAA	dAA-tAA	0.959012
wd-prot	energy-dAA	0.958988
prot-energy	energy-dAA	0.957658
apat_tAA	tAA-bchol	0.95721
prot-energy	prot-coll	0.956842
wd-prot	energy-apat	0.956592

x	y	R2
wd-prot	prot-coll	0.956425
prot-energy	energy-apat	0.9555
wd_tAA	tAA-bchol	0.955367
prot-energy	coll-apat	0.954841
wdiet	energy	0.953469
wd-prot	coll-apat	0.953163
wd-energy	coll-apat	0.952603
wd-energy	prot-coll	0.950567
energy-dAA	dAA-coll	0.950384
wd-coll	dAA-apat	0.949625
wd_energy	prot-bchol	0.949091
energy	apat	0.948456
wd-dAA	wd-coll	0.948282
prot-apat	energy-dAA	0.947807
energy-coll	dAA-apat	0.946712
wd-energy	energy-dAA	0.945822
wd-dAA	energy-coll	0.944991
wd_energy	ener-bchol	0.944965
wd-energy	energy-apat	0.944435
prot-coll	prot-apat	0.942397
energy_dAA	prot-bchol	0.940272
energy-coll	energy-apat	0.938642
wd-prot	wd-dAA	0.937603
coll-apat	prot-bchol	0.937314
prot-coll	energy-apat	0.93673
dAA-tAA	coll-tAA	0.936688
wd-dAA	prot-energy	0.935038
wd-prot	dAA-apat	0.93499
prot-energy	dAA-apat	0.933631
prot_energy	ener-bchol	0.932696
prot_tAA	ener-bchol	0.93241
prot-apat	dAA-apat	0.931603
energy-dAA	coll-apat	0.9302
prot_apat	ener-bchol	0.929681
energy_apat	prot-bchol	0.929646
dAA-apat	coll-apat	0.929069
prot_coll	ener-bchol	0.928068
wd_prot	ener-bchol	0.926553
wd-coll	energy-apat	0.926188
energy-dAA	energy-apat	0.9253
wd-dAA	prot-apat	0.924089
wd_dAA	prot-bchol	0.92401
wd-energy	dAA-apat	0.921894

x	y	R2
prot-bchol	coll-bchol	0.920705
coll-bchol	prot-bchol	0.920705
wd-energy	wd-dAA	0.91947
dAA_apat	prot-bchol	0.918946
wd_bchol	ener-bchol	0.918447
energy-bchol	wd-bchol	0.918447
wd_coll	dAA-bchol	0.917889
prot-bchol	dAA-bchol	0.917603
dAA-bchol	prot-bchol	0.917603
prot-apat	energy-apat	0.917412
w diet	bchol	0.9158
prot-coll	energy-coll	0.914444
wd-dAA	coll-apat	0.911065
energy_coll	ener-bchol	0.910498
wd-dAA	energy-apat	0.906965
energy_coll	dAA-bchol	0.90607
dAA_tAA	ener-bchol	0.902311
prot_coll	prot-bchol	0.900982

GLYCINE

x	y	R2
wd-prot	prot-energy	0.999406
wd-dAA	dAA-apat	0.99711
wd-coll	energy-coll	0.99659
wd-energy	prot-energy	0.993942
prot-energy	prot-apat	0.993781
wd-prot	prot-apat	0.992558
prot-energy	energy-coll	0.992351
wd-prot	energy-coll	0.991697
wd-dAA	energy-dAA	0.991272
wdiet	apat	0.991158
prot-apat	energy-coll	0.989833
wd-energy	prot-apat	0.989776
wd-prot	wd-energy	0.989576
energy-dAA	dAA-apat	0.988663
wd-energy	energy-coll	0.986545
wd-prot	wd-coll	0.982662
wd-coll	prot-energy	0.981449
dAA_coll	dAA-bchol	0.979818
wd-coll	prot-apat	0.979781
wd-coll	coll-apat	0.979589
wd_dAA	dAA-bchol	0.978188
wd-tAA	apat-tAA	0.977949
energy-coll	coll-apat	0.977135
dAA_apat	dAA-bchol	0.975798
prot-apat	coll-apat	0.974515
wd_coll	prot-bchol	0.971964
wd_prot	prot-bchol	0.970917
energy_coll	prot-bchol	0.970856
wd-energy	wd-coll	0.969794
prot_energy	prot-bchol	0.967527
prot_apat	prot-bchol	0.959541
prot-energy	prot-coll	0.956842
wd-prot	energy-apat	0.956592
wd-prot	prot-coll	0.956425
prot-energy	energy-apat	0.9555
prot-energy	coll-apat	0.954841
wdiet	energy	0.953469
wd-prot	coll-apat	0.953163
wd-energy	coll-apat	0.952603
wd-energy	prot-coll	0.950567
wd_energy	prot-bchol	0.949091
energy	apat	0.948456
energy_dAA	dAA-bchol	0.946799
wd_energy	energy-bchol	0.944965
wd-energy	energy-apat	0.944435
prot-coll	prot-apat	0.942397
wd-dAA	dAA-coll	0.939557
energy-coll	energy-apat	0.938642

x	y	R2
coll-apat	prot-bchol	0.937314
prot-coll	energy-apat	0.93673
energy_dAA	coll-bchol	0.936691
dAA-coll	dAA-apat	0.934263
prot_energy	energy-bchol	0.932696
prot_apat	energy-bchol	0.929681
energy_apat	prot-bchol	0.929646
wd-tAA	energy-tAA	0.929005
prot_coll	energy-bchol	0.928068
wd_prot	energy-bchol	0.926553
wd-coll	energy-apat	0.926188
dAA_apat	coll-bchol	0.921021
prot-bchol	coll-bchol	0.920705
coll-bchol	prot-bchol	0.920705
wd_bchol	energy-bchol	0.918447
energy-bchol	wd-bchol	0.918447
prot-apat	energy-apat	0.917412
wd_dAA	coll-bchol	0.91645
wdiet	bchol	0.9158
prot-coll	energy-coll	0.914444
energy-tAA	apat-tAA	0.910613
energy_coll	energy-bchol	0.910498
wd-coll	energy-dAA	0.90336
prot_coll	prot-bchol	0.900982

THREONINE

x	y	R2
wd-prot	prot-energy	0.999406
wd-coll	energy-coll	0.99659
wd-dAA	energy-dAA	0.995701
wd-dAA	dAA-apat	0.994467
wd-energy	prot-energy	0.993942
prot-energy	prot-apat	0.993781
wd-tAA	apat-tAA	0.992689
wd-prot	prot-apat	0.992558
prot-energy	energy-coll	0.992351
wd-prot	energy-coll	0.991697
wdiet	apat	0.991158
prot-apat	energy-coll	0.989833
wd-energy	prot-apat	0.989776
wd-prot	wd-energy	0.989576
wd-energy	energy-coll	0.986545
wd-tAA	energy-tAA	0.986282
energy-dAA	dAA-apat	0.984922
wd_dAA	dAA-bchol	0.983003
wd-prot	wd-coll	0.982662
wd-coll	prot-energy	0.981449
dAA_apat	dAA-bchol	0.981357
wd-coll	prot-apat	0.979781
wd-coll	coll-apat	0.979589
energy-coll	coll-apat	0.977135
prot-apat	coll-apat	0.974515
energy_dAA	dAA-bchol	0.973459
wd_coll	prot-bchol	0.971964
wd_prot	prot-bchol	0.970917
energy_coll	prot-bchol	0.970856
wd-energy	wd-coll	0.969794
energy-tAA	apat-tAA	0.968541
prot_energy	prot-bchol	0.967527
apat_tAA	taa-bchol	0.963187
wd_tAA	taa-bchol	0.960742
prot_apat	prot-bchol	0.959541
prot-energy	prot-coll	0.956842
wd-prot	energy-apat	0.956592
wd-prot	prot-coll	0.956425
prot-energy	energy-apat	0.9555
prot-energy	coll-apat	0.954841
wdiet	energy	0.953469
wd-prot	coll-apat	0.953163
wd-energy	coll-apat	0.952603
wd-energy	prot-coll	0.950567
wd_energy	prot-bchol	0.949091
energy	apat	0.948456
wd_energy	energy-bchol	0.944965
wd-energy	energy-apat	0.944435

x	y	R2
prot-coll	prot-apat	0.942397
energy-coll	energy-apat	0.938642
coll-apat	prot-bchol	0.937314
prot-coll	energy-apat	0.93673
wd-energy	energy-dAA	0.934117
prot_energy	energy-bchol	0.932696
prot_apat	energy-bchol	0.929681
energy_apat	prot-bchol	0.929646
prot_coll	energy-bchol	0.928068
wd_prot	energy-bchol	0.926553
wd-coll	energy-apat	0.926188
prot-apat	energy-dAA	0.921946
energy-tAA	coll-apat	0.921412
prot-bchol	coll-bchol	0.920705
coll-bchol	prot-bchol	0.920705
wd_bchol	energy-bchol	0.918447
energy-bchol	wd-bchol	0.918447
energy-dAA	energy-coll	0.917857
prot-apat	energy-apat	0.917412
energy-dAA	coll-apat	0.916388
energy_tAA	taa-bchol	0.915817
w diet	b chol	0.9158
prot-coll	energy-coll	0.914444
prot-energy	energy-dAA	0.91187
energy_coll	energy-bchol	0.910498
energy_dAA	energy-bchol	0.910122
dAA-coll	dAA-apat	0.908354
wd-prot	energy-dAA	0.902698
prot_coll	prot-bchol	0.900982
wd-coll	energy-dAA	0.900421

SERINE

x	y	R2
wd-prot	prot-energy	0.999406
wd-coll	energy-coll	0.99659
wd-energy	prot-energy	0.993942
prot-energy	prot-apat	0.993781
wd-dAA	dAA-apat	0.993304
wd-prot	prot-apat	0.992558
prot-energy	energy-coll	0.992351
wd-prot	energy-coll	0.991697
wdiet	apat	0.991158
prot-apat	energy-coll	0.989833
wd-energy	prot-apat	0.989776
wd-prot	wd-energy	0.989576
wd-energy	energy-coll	0.986545
wd-dAA	energy-dAA	0.984515
wd-prot	wd-coll	0.982662
wd-coll	prot-energy	0.981449
wd-coll	prot-apat	0.979781
wd-coll	coll-apat	0.979589
energy-coll	coll-apat	0.977135
energy-dAA	dAA-apat	0.976719
prot-apat	coll-apat	0.974515
wd_coll	prot-bchol	0.971964
wd_prot	prot-bchol	0.970917
energy_coll	prot-bchol	0.970856
wd-energy	wd-coll	0.969794
wd-tAA	apat-tAA	0.968115
prot_energy	prot-bchol	0.967527
prot_apat	prot-bchol	0.959541
prot-energy	prot-coll	0.956842
wd-prot	energy-apat	0.956592
wd-prot	prot-coll	0.956425
prot-energy	energy-apat	0.9555
prot-energy	coll-apat	0.954841
wdiet	energy	0.953469
wd-prot	coll-apat	0.953163
wd-energy	coll-apat	0.952603
wd_dAA	dAA-bchol	0.951581
wd-energy	prot-coll	0.950567
wd_energy	prot-bchol	0.949091
energy	apat	0.948456
dAA_apat	dAA-bchol	0.947027
wd_energy	energy-bchol	0.944965
wd-energy	energy-apat	0.944435
prot-coll	prot-apat	0.942397
energy-coll	energy-apat	0.938642
coll-apat	prot-bchol	0.937314
prot-coll	energy-apat	0.93673
prot_energy	energy-bchol	0.932696

x	y	R2
prot_apat	energy-bchol	0.929681
energy_apat	prot-bchol	0.929646
prot_coll	energy-bchol	0.928068
wd_prot	energy-bchol	0.926553
wd-coll	energy-apat	0.926188
prot-bchol	coll-bchol	0.920705
coll-bchol	prot-bchol	0.920705
wd_bchol	energy-bchol	0.918447
energy-bchol	wd-bchol	0.918447
prot-apat	energy-apat	0.917412
wdiet	bchol	0.9158
wd-coll	energy-dAA	0.91481
prot-coll	energy-coll	0.914444
energy_coll	energy-bchol	0.910498
energy_dAA	coll-bchol	0.901884
prot_coll	prot-bchol	0.900982

VALINE

x	y	R2
wd-prot	prot-energy	0.999406
wd-coll	energy-coll	0.99659
wd-energy	prot-energy	0.993942
prot-energy	prot-apat	0.993781
wd-prot	prot-apat	0.992558
prot-energy	energy-coll	0.992351
wd-dAA	dAA-apat	0.992232
wd-prot	energy-coll	0.991697
wdiet	apat	0.991158
wd-dAA	energy-dAA	0.990078
prot-apat	energy-coll	0.989833
wd-energy	prot-apat	0.989776
wd-prot	wd-energy	0.989576
wd-tAA	apat-tAA	0.988989
wd-tAA	energy-tAA	0.987289
wd-energy	energy-coll	0.986545
wd-prot	wd-coll	0.982662
wd-coll	prot-energy	0.981449
energy-dAA	dAA-apat	0.97984
wd-coll	prot-apat	0.979781
wd-coll	coll-apat	0.979589
energy-coll	coll-apat	0.977135
prot-apat	coll-apat	0.974515
wd-coll	energy-dAA	0.974332
wd_coll	prot-bchol	0.971964
wd_prot	prot-bchol	0.970917
energy_coll	prot-bchol	0.970856
wd-energy	wd-coll	0.969794
prot_energy	prot-bchol	0.967527
energy-tAA	apat-tAA	0.963452
energy-dAA	coll-apat	0.960702
prot_apat	prot-bchol	0.959541
prot-energy	prot-coll	0.956842
wd-prot	energy-apat	0.956592
wd-prot	prot-coll	0.956425
prot-energy	energy-apat	0.9555
energy-dAA	energy-coll	0.954902
prot-energy	coll-apat	0.954841
wdiet	energy	0.953469
wd-prot	coll-apat	0.953163
wd-energy	coll-apat	0.952603
wd_dAA	dAA-bchol	0.952079
wd-energy	prot-coll	0.950567
wd_energy	prot-bchol	0.949091
energy	apat	0.948456
apat_tAA	taa-bchol	0.947451
dAA_apat	dAA-bchol	0.947253
wd_tAA	taa-bchol	0.945151

x	y	R2
wd_energy	energy-bchol	0.944965
wd-energy	energy-apat	0.944435
dAA-bchol	coll-bchol	0.943285
coll-bchol	dAA-bchol	0.943285
prot-coll	prot-apat	0.942397
dAA_coll	dAA-bchol	0.941811
energy_dAA	prot-bchol	0.94066
energy-coll	energy-apat	0.938642
coll-apat	prot-bchol	0.937314
prot-coll	energy-apat	0.93673
wd-dAA	wd-coll	0.934642
prot_energy	energy-bchol	0.932696
dAA-apat	coll-apat	0.930529
wd_dAA	coll-bchol	0.929901
prot_apat	energy-bchol	0.929681
energy_apat	prot-bchol	0.929646
prot_coll	energy-bchol	0.928068
wd_prot	energy-bchol	0.926553
wd-coll	energy-apat	0.926188
energy_dAA	coll-bchol	0.92589
wd-prot	energy-dAA	0.923579
prot-apat	energy-dAA	0.923291
wd-dAA	coll-apat	0.922678
prot-bchol	coll-bchol	0.920705
coll-bchol	prot-bchol	0.920705
prot-energy	energy-dAA	0.919195
wd_bchol	energy-bchol	0.918447
energy-bchol	wd-bchol	0.918447
wd-coll	dAA-apat	0.918276
prot-apat	energy-apat	0.917412
w diet	b chol	0.9158
dAA_apat	coll-bchol	0.914675
prot-coll	energy-coll	0.914444
prot-apat	energy-tAA	0.911567
energy_coll	energy-bchol	0.910498
energy_dAA	dAA-bchol	0.909785
energy_tAA	taa-bchol	0.90579
wd-dAA	energy-coll	0.905089
prot_coll	prot-bchol	0.900982

LEUCINE

x	y	R2
wd-prot	prot-energy	0.999406
wd-dAA	energy-dAA	0.999213
wd-coll	energy-coll	0.99659
prot-apat	energy-dAA	0.995331
wd-tAA	energy-tAA	0.994317
prot-energy	energy-dAA	0.994097
energy-dAA	energy-coll	0.994001
wd-energy	prot-energy	0.993942
wd-dAA	prot-apat	0.993873
prot-energy	prot-apat	0.993781
wd-dAA	energy-coll	0.993157
wd-prot	prot-apat	0.992558
prot-energy	energy-coll	0.992351
wd-energy	energy-dAA	0.992306
wd-prot	energy-dAA	0.992181
wd-dAA	dAA-apat	0.991833
wd-prot	energy-coll	0.991697
wdiet	apat	0.991158
wd-dAA	prot-energy	0.990915
energy-dAA	dAA-apat	0.989978
prot-apat	energy-coll	0.989833
wd-prot	wd-dAA	0.989788
wd-energy	prot-apat	0.989776
wd-prot	wd-energy	0.989576
prot-apat	dAA-apat	0.988809
wd-tAA	apat-tAA	0.988106
wd-energy	wd-dAA	0.98663
wd-energy	energy-coll	0.986545
dAA-apat	coll-apat	0.986466
wd-dAA	wd-coll	0.98632
wd-coll	energy-dAA	0.984728
prot	dAA	0.984601
prot-bchol	dAA-bchol	0.983794
dAA-bchol	prot-bchol	0.983794
wd-prot	wd-coll	0.982662
wd_coll	dAA-bchol	0.981499
wd-coll	prot-energy	0.981449
energy-tAA	apat-tAA	0.981226
wd-coll	prot-apat	0.979781
wd-coll	coll-apat	0.979589
energy-coll	dAA-apat	0.978705
energy_coll	dAA-bchol	0.977308
energy-coll	coll-apat	0.977135
wd-dAA	coll-apat	0.976147
prot-apat	coll-apat	0.974515
wd-energy	dAA-apat	0.974177
energy-dAA	coll-apat	0.972811
prot-energy	dAA-apat	0.972336

x	y	R2
wd_coll	prot-bchol	0.971964
wd-coll	dAA-apat	0.971011
coll-apat	dAA-bchol	0.97099
wd_prot	prot-bchol	0.970917
energy_coll	prot-bchol	0.970856
wd_dAA	dAA-bchol	0.970513
wd-energy	wd-coll	0.969794
wd-prot	dAA-apat	0.969338
energy_dAA	dAA-bchol	0.967753
prot_energy	prot-bchol	0.967527
prot_apat	dAA-bchol	0.965406
dAA-coll	dAA-apat	0.965326
wd_prot	dAA-bchol	0.962486
wd-energy	energy-tAA	0.961804
energy-dAA	dAA-coll	0.961633
dAA_apat	dAA-bchol	0.96145
prot_energy	dAA-bchol	0.961176
wd-dAA	dAA-coll	0.96103
prot_apat	prot-bchol	0.959541
prot-energy	prot-coll	0.956842
wd-prot	energy-apat	0.956592
wd-prot	prot-coll	0.956425
prot-apat	dAA-coll	0.955967
prot-energy	energy-apat	0.9555
energy_dAA	prot-bchol	0.954879
prot-energy	coll-apat	0.954841
wd_tAA	taa-bchol	0.954228
dAA_coll	energy-bchol	0.954175
wd-energy	dAA-coll	0.953757
wd_dAA	prot-bchol	0.953628
wdiet	energy	0.953469
wd-prot	coll-apat	0.953163
wd-energy	coll-apat	0.952603
wd-energy	prot-coll	0.950567
prot-energy	energy-tAA	0.950499
prot-coll	energy-tAA	0.950107
wd_energy	dAA-bchol	0.949374
wd_energy	prot-bchol	0.949091
energy	apat	0.948456
prot-energy	dAA-coll	0.945506
wd_energy	energy-bchol	0.944965
wd-prot	energy-tAA	0.944611
wd-energy	energy-apat	0.944435
prot-apat	energy-tAA	0.943178
prot-coll	prot-apat	0.942397
energy_tAA	taa-bchol	0.9415
wd-prot	dAA-coll	0.940578
apat tAA	taa-bchol	0.939549

x	y	R2
energy-coll	energy-apat	0.938642
energy-dAA	energy-tAA	0.938098
coll-apat	prot-bchol	0.937314
energy_dAA	energy-bchol	0.937039
prot-coll	energy-apat	0.93673
prot-coll	energy-dAA	0.933796
prot_energy	energy-bchol	0.932696
prot-coll	dAA-coll	0.932627
wd_dAA	energy-bchol	0.931469
energy-dAA	energy-apat	0.930543
wd-tAA	prot-coll	0.930489
energy_tAA	energy-bchol	0.929865
prot_apat	energy-bchol	0.929681
energy_apat	prot-bchol	0.929646
dAA_apat	prot-bchol	0.929459
prot_coll	energy-bchol	0.928068
wd-energy	wd-tAA	0.927738
wd-dAA	energy-tAA	0.927542
wd_prot	energy-bchol	0.926553
energy-coll	dAA-coll	0.926428
wd-coll	energy-apat	0.926188
energy-coll	energy-tAA	0.926078
wd-dAA	prot-coll	0.925438
dAA-bchol	coll-bchol	0.924371
coll-bchol	dAA-bchol	0.924371
wd-dAA	energy-apat	0.923104
dAA_apat	energy-bchol	0.922988
prot-bchol	coll-bchol	0.920705
coll-bchol	prot-bchol	0.920705
wd_bchol	energy-bchol	0.918447
energy-bchol	wd-bchol	0.918447
energy-tAA	dAA-coll	0.918104
prot-apat	energy-apat	0.917412
w diet	b chol	0.9158
wd-tAA	prot-energy	0.914721
prot-coll	energy-coll	0.914444
energy-tAA	dAA-apat	0.913659
prot-tAA	dAA-tAA	0.913357
wd-energy	apat-tAA	0.912353
energy-apat	energy-tAA	0.911905
energy_coll	energy-bchol	0.910498
dAA-coll	coll-apat	0.910452
wd-prot	wd-tAA	0.908392
wd-tAA	prot-apat	0.906385
wd_tAA	energy-bchol	0.905105
wd-coll	dAA-coll	0.903457
prot_coll	prot-bchol	0.900982

ISOLEUCINE

x	y	R2
wd-prot	prot-energy	0.999406
wd-coll	energy-coll	0.99659
wd-dAA	energy-dAA	0.996452
wd-tAA	energy-tAA	0.995089
wd-energy	prot-energy	0.993942
prot-energy	prot-apat	0.993781
wd-dAA	dAA-apat	0.993664
wd-tAA	apat-tAA	0.992614
wd-prot	prot-apat	0.992558
prot-energy	energy-coll	0.992351
wd-prot	energy-coll	0.991697
wdiet	apat	0.991158
wd-coll	energy-dAA	0.990765
energy-tAA	apat-tAA	0.990141
prot-apat	energy-coll	0.989833
energy-dAA	dAA-apat	0.989786
wd-energy	prot-apat	0.989776
wd-prot	wd-energy	0.989576
wd-energy	energy-coll	0.986545
energy-dAA	energy-coll	0.985879
wd-prot	wd-coll	0.982662
wd-coll	prot-energy	0.981449
wd-dAA	wd-coll	0.98083
wd-coll	prot-apat	0.979781
wd-coll	coll-apat	0.979589
energy-dAA	energy-tAA	0.977193
energy-coll	coll-apat	0.977135
wd-dAA	apat-tAA	0.976455
dAA-apat	coll-apat	0.976433
wd-prot	energy-dAA	0.976137
prot-apat	energy-dAA	0.974529
prot-apat	coll-apat	0.974515
wd-dAA	energy-tAA	0.973615
prot-energy	energy-dAA	0.973264
energy-dAA	coll-apat	0.972421
wd-coll	dAA-apat	0.972351
wd_coll	prot-bchol	0.971964
energy-dAA	apat-tAA	0.971551
wd_prot	prot-bchol	0.970917
energy_coll	prot-bchol	0.970856
wd_dAA	dAA-bchol	0.970553
wd-coll	energy-tAA	0.970264
wd-dAA	energy-coll	0.969858
wd-energy	wd-coll	0.969794
wd-dAA	dAA-coll	0.969001
prot_energy	prot-bchol	0.967527
dAA-coll	dAA-apat	0.965728
energy-coll	energy-tAA	0.964981

x	y	R2
dAA_apat	dAA-bchol	0.963669
wd-dAA	wd-tAA	0.963074
energy_dAA	prot-bchol	0.962656
wd-dAA	coll-apat	0.96245
energy_tAA	prot-bchol	0.9624
energy-coll	dAA-apat	0.961687
dAA-apat	apat-tAA	0.960907
wd-tAA	energy-dAA	0.960271
prot_apat	prot-bchol	0.959541
wd-prot	energy-tAA	0.959059
dAA_coll	dAA-bchol	0.95884
wd_tAA	tAA-bchol	0.956933
prot-energy	prot-coll	0.956842
wd-coll	apat-tAA	0.956756
wd-prot	wd-dAA	0.956674
wd-prot	energy-apat	0.956592
wd-prot	prot-coll	0.956425
wd-energy	energy-dAA	0.956415
prot-energy	energy-tAA	0.955894
apat_tAA	dAA-bchol	0.955511
prot-energy	energy-apat	0.9555
energy_dAA	dAA-bchol	0.955074
prot-energy	coll-apat	0.954841
wd-dAA	prot-apat	0.954585
prot-apat	dAA-apat	0.954201
wdiet	energy	0.953469
wd-prot	coll-apat	0.953163
wd-energy	coll-apat	0.952603
wd-dAA	prot-energy	0.951821
wd_dAA	prot-bchol	0.951053
wd-energy	prot-coll	0.950567
wd_tAA	prot-bchol	0.950419
coll_tAA	tAA-bchol	0.94975
wd_energy	prot-bchol	0.949091
dAA-bchol	coll-bchol	0.948769
coll-bchol	dAA-bchol	0.948769
energy-dAA	dAA-coll	0.94874
energy	apat	0.948456
tAA-bchol	dAA-bchol	0.948439
dAA-bchol	tAA-bchol	0.948439
wd-coll	wd-tAA	0.947204
dAA-coll	apat-tAA	0.946257
apat_tAA	tAA-bchol	0.946215
energy-tAA	dAA-apat	0.945905
wd_energy	energy-bchol	0.944965
wd-energy	energy-apat	0.944435
prot	dAA	0.944299
energy-coll	apat-tAA	0.944211

x	y	R2
prot-apat	energy-tAA	0.944042
apat_tAA	prot-bchol	0.943848
dAA	tAA	0.943784
wd-prot	dAA-apat	0.942944
prot-coll	prot-apat	0.942397
wd_tAA	dAA-bchol	0.94188
prot-energy	dAA-apat	0.93959
wd-energy	energy-tAA	0.939005
energy-coll	energy-apat	0.938642
prot-bchol	dAA-bchol	0.938636
dAA-bchol	prot-bchol	0.938636
wd_coll	dAA-bchol	0.937536
coll-apat	prot-bchol	0.937314
prot-coll	energy-apat	0.93673
wd-tAA	energy-coll	0.936675
dAA_apat	prot-bchol	0.934562
wd-tAA	dAA-apat	0.932776
prot_energy	energy-bchol	0.932696
wd-tAA	coll-tAA	0.931924
energy_tAA	dAA-bchol	0.931917
prot_apat	energy-bchol	0.929681
energy_apat	prot-bchol	0.929646
energy_tAA	tAA-bchol	0.929388
wd-tAA	dAA-coll	0.929032
wd-prot	wd-tAA	0.928899
wd-energy	wd-dAA	0.928898
prot_coll	energy-bchol	0.928068
wd_prot	energy-bchol	0.926553
wd-coll	energy-apat	0.926188
wd-prot	apat-tAA	0.925796
energy-tAA	dAA-coll	0.92417
wd-tAA	prot-energy	0.923829
tAA-bchol	coll-bchol	0.923682
coll-bchol	tAA-bchol	0.923682
prot-apat	apat-tAA	0.923242
prot-energy	apat-tAA	0.922356
coll-apat	apat-tAA	0.921941
wd-energy	dAA-apat	0.921489
prot-bchol	coll-bchol	0.920705
coll-bchol	prot-bchol	0.920705
wd_bchol	energy-bchol	0.918447
energy-bchol	wd-bchol	0.918447
coll-apat	dAA-bchol	0.917766
prot-apat	energy-apat	0.917412
wdiet	bchol	0.9158
prot-coll	energy-coll	0.914444
energy_coll	dAA-bchol	0.913982
energy-tAA	coll-apat	0.913791
energy-apat	energy-tAA	0.912479

x	y	R2
energy-dAA	energy-apat	0.910894
energy_coll	energy-bchol	0.910498
wd-tAA	prot-apat	0.910357
tAA-bchol	prot-bchol	0.907654
prot-bchol	tAA-bchol	0.907654
coll-tAA	apat-tAA	0.906577
wd-energy	apat-tAA	0.90485
wd-coll	dAA-coll	0.903489
wd-energy	wd-tAA	0.901234
prot_coll	prot-bchol	0.900982

PROLINE

x	y	R2
wd-prot	prot-energy	0.999406
wd-tAA	energy-tAA	0.998124
wd-coll	energy-coll	0.99659
wd-dAA	energy-dAA	0.995505
wd-energy	prot-energy	0.993942
prot-energy	prot-apat	0.993781
wd-prot	prot-apat	0.992558
wd-dAA	dAA-apat	0.992467
prot-energy	energy-coll	0.992351
wd-prot	energy-coll	0.991697
wdiet	apat	0.991158
prot-apat	energy-tAA	0.991073
energy-coll	energy-tAA	0.99089
energy-dAA	dAA-apat	0.990714
prot-apat	energy-coll	0.989833
wd-energy	prot-apat	0.989776
wd-prot	wd-energy	0.989576
wd-tAA	apat-tAA	0.98896
prot-energy	energy-tAA	0.988756
wd-coll	energy-dAA	0.987398
wd-prot	energy-tAA	0.987082
wd-energy	energy-coll	0.986545
wd-energy	energy-tAA	0.986235
wd-tAA	energy-coll	0.98559
energy-tAA	apat-tAA	0.985045
wd-tAA	prot-apat	0.984647
energy-dAA	energy-coll	0.9835
wd-coll	energy-tAA	0.983135
wd-prot	wd-coll	0.982662
coll-apat	apat-tAA	0.981865
wd-coll	prot-energy	0.981449
wd-coll	wd-tAA	0.98122
wd-prot	energy-dAA	0.980654
wd-tAA	prot-energy	0.979965
energy_dAA	prot-bchol	0.979922
wd-coll	prot-apat	0.979781
wd-coll	coll-apat	0.979589
wd-prot	wd-tAA	0.97929
wd-coll	dAA-apat	0.97776
energy-coll	coll-apat	0.977135
prot-energy	energy-dAA	0.976604
prot-apat	apat-tAA	0.974926
wd-dAA	wd-coll	0.974609
prot-apat	coll-apat	0.974515
wd-energy	wd-tAA	0.974326
wd-tAA	coll-apat	0.973554
energy-tAA	coll-apat	0.972833
wd_coll	prot-bchol	0.971964

x	y	R2
wd_dAA	prot-bchol	0.971531
wd_prot	prot-bchol	0.970917
energy_coll	prot-bchol	0.970856
wd-energy	wd-coll	0.969794
prot-apat	energy-dAA	0.969137
energy-coll	dAA-apat	0.967593
prot_energy	prot-bchol	0.967527
dAA_apat	prot-bchol	0.966249
energy-coll	apat-tAA	0.965122
wd-dAA	energy-coll	0.964213
prot-bchol	taa-bchol	0.963761
tAA-bchol	prot-bchol	0.963761
dAA-apat	coll-apat	0.961982
dAA-bchol	coll-bchol	0.961003
coll-bchol	dAA-bchol	0.961003
wd-coll	apat-tAA	0.959851
wd-prot	wd-dAA	0.959566
prot_apat	prot-bchol	0.959541
energy-dAA	energy-tAA	0.959465
wd_dAA	dAA-bchol	0.957781
wd_coll	taa-bchol	0.957297
prot-energy	prot-coll	0.956842
wd-prot	dAA-apat	0.956809
wd-prot	energy-apat	0.956592
wd-prot	prot-coll	0.956425
prot-apat	dAA-apat	0.956398
wd-energy	apat-tAA	0.956054
wd-energy	energy-dAA	0.956014
prot-energy	energy-apat	0.9555
wd_tAA	taa-bchol	0.955402
prot-energy	coll-apat	0.954841
prot-energy	apat-tAA	0.954681
wd-tAA	energy-dAA	0.954053
wdiet	energy	0.953469
wd-prot	coll-apat	0.953163
wd-dAA	prot-energy	0.95295
wd-energy	coll-apat	0.952603
energy-dAA	coll-apat	0.952559
energy_tAA	prot-bchol	0.952011
wd-prot	apat-tAA	0.951874
prot-energy	dAA-apat	0.951764
wd-energy	prot-coll	0.950567
coll-apat	taa-bchol	0.950158
wd_energy	prot-bchol	0.949091
energy	apat	0.948456
energy_tAA	taa-bchol	0.947937
energy_coll	taa-bchol	0.94783
dAA_coll	dAA-bchol	0.947721

x	y	R2
dAA_apat	dAA-bchol	0.946986
wd_tAA	prot-bchol	0.946456
wd_energy	energy-bchol	0.944965
wd-dAA	prot-apat	0.94459
wd-energy	energy-apat	0.944435
apat_tAA	taa-bchol	0.944265
prot-coll	prot-apat	0.942397
energy-tAA	dAA-apat	0.941218
wd-tAA	dAA-apat	0.939463
energy-coll	energy-apat	0.938642
coll-apat	prot-bchol	0.937314
prot-bchol	dAA-bchol	0.937175
dAA-bchol	prot-bchol	0.937175
energy-dAA	energy-apat	0.936805
prot-coll	energy-apat	0.93673
dAA_apat	taa-bchol	0.935432
coll-bchol	taa-bchol	0.934977
tAA-bchol	coll-bchol	0.934977
wd-dAA	coll-apat	0.934798
energy_dAA	taa-bchol	0.934646
energy_dAA	dAA-bchol	0.934528
wd-dAA	energy-tAA	0.933188
prot_energy	energy-bchol	0.932696
prot_apat	taa-bchol	0.931573
wd-dAA	dAA-coll	0.931492
wd-dAA	wd-tAA	0.929903
prot_apat	energy-bchol	0.929681
energy_apat	prot-bchol	0.929646
energy_tAA	energy-bchol	0.928783
prot	dAA	0.928751
wd-energy	dAA-apat	0.928235
prot_coll	energy-bchol	0.928068
wd_prot	taa-bchol	0.927296
wd_prot	energy-bchol	0.926553
wd-coll	energy-apat	0.926188
wd_dAA	taa-bchol	0.925033
prot_energy	taa-bchol	0.924968
wd-energy	wd-dAA	0.92448
prot-coll	energy-tAA	0.923656
energy-apat	energy-tAA	0.92273
energy-dAA	apat-tAA	0.922188
dAA-apat	apat-tAA	0.921028
prot-bchol	coll-bchol	0.920705
coll-bchol	prot-bchol	0.920705
prot	tAA	0.920145
wd_bchol	energy-bchol	0.918447
energy-bchol	wd-bchol	0.918447
prot-apat	energy-apat	0.917412
wd-dAA	energy-apat	0.916942

x	y	R2
wd_tAA	energy-bchol	0.916396
w diet	b chol	0.9158
apat_tAA	prot-bchol	0.914973
prot-coll	energy-coll	0.914444
wd-tAA	energy-apat	0.908381
dAA-coll	dAA-apat	0.907747
wd-tAA	prot-coll	0.90742
prot-coll	energy-dAA	0.901371
energy-dAA	dAA-coll	0.900057

HYDROXYPROLINE

x	y	R2
wd-prot	prot-energy	0.999406
wd-coll	energy-coll	0.99659
wd-energy	prot-energy	0.993942
prot-energy	prot-apat	0.993781
wd-prot	prot-apat	0.992558
prot-energy	energy-coll	0.992351
wd-tAA	energy-tAA	0.992183
wd-prot	energy-coll	0.991697
wdiet	apat	0.991158
prot-apat	energy-coll	0.989833
wd-energy	prot-apat	0.989776
wd-prot	wd-energy	0.989576
wd-energy	energy-coll	0.986545
wd-tAA	apat-tAA	0.984898
wd-prot	wd-coll	0.982662
wd-coll	energy-tAA	0.982235
wd-coll	prot-energy	0.981449
wd-coll	prot-apat	0.979781
wd-coll	coll-apat	0.979589
energy-coll	energy-tAA	0.978902
energy-coll	coll-apat	0.977135
energy-tAA	apat-tAA	0.975206
prot-apat	coll-apat	0.974515
wd_coll	prot-bchol	0.971964
wd_prot	prot-bchol	0.970917
energy_coll	prot-bchol	0.970856
wd-energy	wd-coll	0.969794
energy_tAA	prot-bchol	0.969253
prot_energy	prot-bchol	0.967527
prot-apat	energy-tAA	0.966188
wd-prot	energy-tAA	0.964925
prot-energy	energy-tAA	0.963594
wd-coll	wd-tAA	0.962023
coll-apat	apat-tAA	0.959806
prot_apat	prot-bchol	0.959541
energy-tAA	coll-apat	0.959044
prot-energy	prot-coll	0.956842
wd_tAA	prot-bchol	0.95664
wd-prot	energy-apat	0.956592
wd-prot	prot-coll	0.956425
prot-energy	energy-apat	0.9555
prot-energy	coll-apat	0.954841
wdiet	energy	0.953469
wd-prot	coll-apat	0.953163
wd-energy	coll-apat	0.952603
wd-energy	prot-coll	0.950567
wd-tAA	energy-coll	0.949583
wd-energy	energy-tAA	0.949455

x	y	R2
wd_energy	prot-bchol	0.949091
energy	apat	0.948456
wd_energy	energy-bchol	0.944965
wd-energy	energy-apat	0.944435
prot-coll	prot-apat	0.942397
wd-coll	apat-tAA	0.941618
wd-tAA	coll-apat	0.94073
energy-coll	energy-apat	0.938642
coll-apat	prot-bchol	0.937314
prot-coll	energy-apat	0.93673
prot_energy	energy-bchol	0.932696
wd-tAA	prot-apat	0.931513
wd-prot	wd-tAA	0.929852
prot_apat	energy-bchol	0.929681
energy_apat	prot-bchol	0.929646
energy-coll	apat-tAA	0.929039
prot_coll	energy-bchol	0.928068
wd_prot	energy-bchol	0.926553
wd-coll	energy-apat	0.926188
wd-tAA	prot-energy	0.925876
prot-apat	apat-tAA	0.92249
apat_tAA	prot-bchol	0.920708
prot-bchol	coll-bchol	0.920705
coll-bchol	prot-bchol	0.920705
wd_bchol	energy-bchol	0.918447
energy-bchol	wd-bchol	0.918447
prot-apat	energy-apat	0.917412
w diet	b chol	0.9158
prot-coll	energy-coll	0.914444
coll	tAA	0.911048
energy_coll	energy-bchol	0.910498
wd_tAA	taa-bchol	0.906361
wd-energy	wd-tAA	0.903842
prot_coll	prot-bchol	0.900982

ASPARTATE

x	y	R2
wd-prot	prot-energy	0.999406
wd-coll	energy-coll	0.99659
wd-dAA	energy-dAA	0.995301
wd-energy	prot-energy	0.993942
prot-energy	prot-apat	0.993781
wd-prot	prot-apat	0.992558
prot-energy	energy-coll	0.992351
wd-prot	energy-coll	0.991697
wd-dAA	dAA-apat	0.991644
wdiet	apat	0.991158
prot-apat	energy-coll	0.989833
wd-energy	prot-apat	0.989776
wd-prot	wd-energy	0.989576
wd-energy	energy-coll	0.986545
energy-dAA	dAA-apat	0.985766
wd-prot	wd-coll	0.982662
wd-coll	prot-energy	0.981449
wd-coll	prot-apat	0.979781
wd-coll	coll-apat	0.979589
energy-coll	coll-apat	0.977135
prot-apat	coll-apat	0.974515
wd_dAA	dAA-bchol	0.972891
wd_coll	prot-bchol	0.971964
wd_prot	prot-bchol	0.970917
energy_coll	prot-bchol	0.970856
wd-energy	wd-coll	0.969794
prot_energy	prot-bchol	0.967527
energy_dAA	dAA-bchol	0.96471
dAA_apat	dAA-bchol	0.962466
prot_apat	prot-bchol	0.959541
prot-energy	prot-coll	0.956842
wd-prot	energy-apat	0.956592
wd-prot	prot-coll	0.956425
prot-energy	energy-apat	0.9555
wd-energy	energy-dAA	0.955389
prot-coll	energy-dAA	0.955139
prot-energy	coll-apat	0.954841
wdiet	energy	0.953469
wd-prot	coll-apat	0.953163
wd-energy	coll-apat	0.952603
prot-energy	energy-dAA	0.95246
wd-energy	prot-coll	0.950567
prot_tAA	prot-bchol	0.949874
wd-prot	energy-dAA	0.949172
wd_energy	prot-bchol	0.949091
prot-apat	energy-dAA	0.948674
energy	apat	0.948456
dAA_tAA	dAA-bchol	0.948076

x	y	R2
tAA	bchol	0.94799
wd_energy	energy-bchol	0.944965
wd-energy	energy-apat	0.944435
prot-coll	prot-apat	0.942397
energy-coll	energy-apat	0.938642
wd-dAA	prot-coll	0.93822
coll-apat	prot-bchol	0.937314
prot-coll	energy-apat	0.93673
energy_dAA	energy-bchol	0.93471
prot_energy	energy-bchol	0.932696
prot_apat	energy-bchol	0.929681
energy_apat	prot-bchol	0.929646
prot_coll	energy-bchol	0.928068
energy-dAA	dAA-tAA	0.926765
energy-dAA	energy-coll	0.926713
wd_prot	energy-bchol	0.926553
wd-tAA	apat-tAA	0.926354
wd-coll	energy-apat	0.926188
energy_tAA	energy-bchol	0.926106
wd-energy	wd-dAA	0.922872
wd-dAA	prot-energy	0.920977
prot-bchol	coll-bchol	0.920705
coll-bchol	prot-bchol	0.920705
wd-dAA	dAA-tAA	0.919359
wd_bchol	energy-bchol	0.918447
energy-bchol	wd-bchol	0.918447
wd-prot	wd-dAA	0.91809
prot-apat	energy-apat	0.917412
wd-dAA	prot-apat	0.917383
wd-coll	prot-tAA	0.916939
wdiet	bchol	0.9158
prot-coll	energy-coll	0.914444
wd_dAA	energy-bchol	0.913429
prot-coll	dAA-apat	0.913009
prot-apat	dAA-apat	0.911799
energy_coll	energy-bchol	0.910498
wd-energy	dAA-apat	0.910413
prot-tAA	energy-coll	0.908538
energy-dAA	energy-tAA	0.906512
dAA_apat	energy-bchol	0.906136
energy-dAA	energy-apat	0.90448
wd-dAA	energy-tAA	0.903261
wd-coll	energy-dAA	0.903079
dAA-apat	dAA-tAA	0.902463
prot-energy	dAA-apat	0.902358
energy-tAA	dAA-apat	0.901231
prot_coll	prot-bchol	0.900982

GLUTAMATE

x	y	R2
wd-prot	prot-energy	0.999406
wd-coll	energy-coll	0.99659
wd-dAA	energy-dAA	0.996257
wd-energy	prot-energy	0.993942
prot-energy	prot-apat	0.993781
wd-dAA	dAA-apat	0.992942
wd-prot	prot-apat	0.992558
prot-energy	energy-coll	0.992351
wd-prot	energy-coll	0.991697
wdiet	apat	0.991158
prot-apat	energy-coll	0.989833
wd-energy	prot-apat	0.989776
wd-prot	wd-energy	0.989576
wd-energy	energy-coll	0.986545
energy-dAA	dAA-apat	0.984779
prot-tAA	coll-tAA	0.983109
wd-prot	wd-coll	0.982662
wd-coll	prot-energy	0.981449
wd-coll	prot-apat	0.979781
wd-coll	coll-apat	0.979589
energy-coll	coll-apat	0.977135
wd_dAA	dAA-bchol	0.976107
prot-apat	coll-apat	0.974515
wd_coll	prot-bchol	0.971964
dAA_apat	dAA-bchol	0.971933
wd_prot	prot-bchol	0.970917
energy_coll	prot-bchol	0.970856
wd-energy	wd-coll	0.969794
prot_energy	prot-bchol	0.967527
energy_dAA	dAA-bchol	0.966832
energy-dAA	dAA-tAA	0.960445
prot_apat	prot-bchol	0.959541
wd-dAA	dAA-tAA	0.957993
prot-coll	prot-tAA	0.957202
prot-energy	prot-coll	0.956842
wd-prot	energy-apat	0.956592
wd-prot	prot-coll	0.956425
wd-energy	energy-dAA	0.955854
prot-energy	energy-apat	0.9555
prot-energy	coll-apat	0.954841
prot-energy	prot-tAA	0.954033
wdiet	energy	0.953469
wd-prot	coll-apat	0.953163
wd-energy	prot-tAA	0.952965
wd-energy	coll-apat	0.952603
wd-prot	prot-tAA	0.95199
prot-apat	energy-dAA	0.950737
wd-energy	prot-coll	0.950567

x	y	R2
wd_energy	prot-bchol	0.949091
energy	apat	0.948456
dAA-apat	dAA-tAA	0.945066
wd_energy	energy-bchol	0.944965
wd-energy	energy-apat	0.944435
prot-energy	energy-dAA	0.944242
wdiet	tAA	0.942936
prot-coll	prot-apat	0.942397
prot-tAA	energy-apat	0.939001
energy-coll	energy-apat	0.938642
wd-prot	energy-dAA	0.938273
prot-apat	prot-tAA	0.93775
coll-apat	prot-bchol	0.937314
apat	tAA	0.936838
prot-coll	energy-apat	0.93673
energy-dAA	energy-coll	0.936668
prot_energy	energy-bchol	0.932696
prot_apat	energy-bchol	0.929681
energy_apat	prot-bchol	0.929646
prot_coll	energy-bchol	0.928068
prot-tAA	energy-coll	0.928042
wd-energy	wd-dAA	0.927354
wd_prot	energy-bchol	0.926553
wd-coll	energy-apat	0.926188
prot_tAA	energy-bchol	0.92508
wd-dAA	prot-apat	0.923757
energy-dAA	coll-apat	0.92089
prot-bchol	coll-bchol	0.920705
coll-bchol	prot-bchol	0.920705
wd_bchol	energy-bchol	0.918447
energy-bchol	wd-bchol	0.918447
energy_dAA	energy-bchol	0.918014
wd-coll	energy-dAA	0.917594
prot-apat	energy-apat	0.917412
w diet	b chol	0.9158
prot-coll	energy-coll	0.914444
wd-dAA	prot-energy	0.914383
wd-energy	dAA-tAA	0.914209
dAA_tAA	energy-bchol	0.913398
wd-energy	coll-tAA	0.912836
prot-energy	coll-tAA	0.910659
energy_coll	energy-bchol	0.910498
dAA_tAA	dAA-bchol	0.908197
wd-prot	wd-dAA	0.908069
wd-prot	coll-tAA	0.90771
wd-dAA	energy-coll	0.906889
wd-coll	prot-tAA	0.906234
prot-tAA	dAA-tAA	0.906138

<u>x</u>	<u>y</u>	<u>R2</u>
prot-apat	dAA-apat	0.904567
prot-coll	energy-dAA	0.904309
wd-energy	dAA-apat	0.901987
prot_coll	prot-bchol	0.900982

PHENYLALANINE

x	y	R2
wd-prot	prot-energy	0.999406
wd-tAA	apat-tAA	0.996863
wd-coll	energy-coll	0.99659
wd-tAA	energy-tAA	0.994235
wd-energy	prot-energy	0.993942
prot-energy	prot-apat	0.993781
wd-prot	prot-apat	0.992558
prot-energy	energy-coll	0.992351
wd-dAA	energy-dAA	0.992058
wd-prot	energy-coll	0.991697
wd-dAA	dAA-apat	0.991697
wdiet	apat	0.991158
prot-apat	energy-coll	0.989833
wd-energy	prot-apat	0.989776
wd-prot	wd-energy	0.989576
energy-dAA	energy-tAA	0.98698
wd-energy	energy-coll	0.986545
apat_tAA	tAA-bchol	0.985297
energy-tAA	apat-tAA	0.985146
wd_tAA	tAA-bchol	0.982767
wd-prot	wd-coll	0.982662
wd-coll	prot-energy	0.981449
wd-dAA	apat-tAA	0.980066
wd-coll	prot-apat	0.979781
wd-coll	coll-apat	0.979589
dAA_apat	dAA-bchol	0.97919
wd-dAA	wd-tAA	0.978875
wd_dAA	dAA-bchol	0.977903
wd-tAA	energy-dAA	0.977807
dAA-apat	apat-tAA	0.977393
energy-coll	coll-apat	0.977135
wd-dAA	energy-tAA	0.975724
prot-apat	coll-apat	0.974515
energy-dAA	dAA-apat	0.973141
apat_tAA	dAA-bchol	0.972122
wd_coll	prot-bchol	0.971964
energy-dAA	apat-tAA	0.971344
energy_tAA	tAA-bchol	0.971181
wd_prot	prot-bchol	0.970917
energy_coll	prot-bchol	0.970856
wd-energy	wd-coll	0.969794
tAA-bchol	dAA-bchol	0.968952
dAA-bchol	tAA-bchol	0.968952
wd-tAA	dAA-apat	0.968919
prot_energy	prot-bchol	0.967527
dAA	tAA	0.965879
energy_dAA	dAA-bchol	0.964086
wd_tAA	dAA-bchol	0.962959

x	y	R2
prot_apat	prot-bchol	0.959541
energy-tAA	dAA-apat	0.958985
prot-energy	prot-coll	0.956842
wd-prot	energy-apat	0.956592
wd-prot	prot-coll	0.956425
prot-energy	energy-apat	0.9555
prot-energy	coll-apat	0.954841
wdiet	energy	0.953469
energy_tAA	dAA-bchol	0.953424
wd-prot	coll-apat	0.953163
wd-energy	coll-apat	0.952603
wd-energy	prot-coll	0.950567
wd_energy	prot-bchol	0.949091
energy	apat	0.948456
wd_dAA	tAA-bchol	0.947581
wd_energy	energy-bchol	0.944965
wd-energy	energy-apat	0.944435
dAA_apat	tAA-bchol	0.944065
energy_dAA	tAA-bchol	0.943206
prot-coll	prot-apat	0.942397
energy-coll	energy-apat	0.938642
coll-apat	prot-bchol	0.937314
prot-coll	energy-apat	0.93673
prot_energy	energy-bchol	0.932696
prot_apat	energy-bchol	0.929681
energy_apat	prot-bchol	0.929646
prot_coll	energy-bchol	0.928068
wd_prot	energy-bchol	0.926553
wd-coll	energy-apat	0.926188
energy_dAA	energy-bchol	0.925657
prot-bchol	coll-bchol	0.920705
coll-bchol	prot-bchol	0.920705
wd_bchol	energy-bchol	0.918447
energy-bchol	wd-bchol	0.918447
wd-energy	energy-tAA	0.91801
prot-apat	energy-apat	0.917412
wd-energy	energy-dAA	0.916969
wdiet	bchol	0.9158
prot-coll	energy-coll	0.914444
prot-apat	energy-tAA	0.912485
energy_tAA	energy-bchol	0.911663
energy_coll	energy-bchol	0.910498
prot-apat	energy-dAA	0.909236
energy-tAA	coll-apat	0.9056
prot_coll	prot-bchol	0.900982

Appendix 3. Pig individual amino acid, collagen and bone cholesterol $\delta^{13}\text{C}$ values (unpublished data). Individual amino acid and cholesterol $\delta^{13}\text{C}$ values obtained in our laboratory by Mar Howland and Lorna Corr, respectively. Collagen $\delta^{13}\text{C}$ values were measured at Harvard University.

Bone component	Isotopic composition (‰)					
	253 (diet 1)	254 (diet 1)	280 (diet 2)	247 (diet 3)	248 (diet 3)	266 (diet 4)
Ala	-9.2	-8.5	-9.9	-20.4	-21.4	-17.5
Gly	-10.3	-7.9	-10.9	-13.5	-13.5	-13.8
Thr	-4.5	-12.2	-10.7	-12.2	-11.6	-10.4
Ser	3.9	-2.0	-0.9	-10.5	-9.6	-6.2
Val	-24.9	-21.9	-27.0	-26.2	-24.1	-25.0
Leu	-23.9	-25.7	-25.5	-27.2	-27.9	-28.1
Ile	-18.2	-18.9	-21.1	-22.8	-23	-21.0
Pro	-15.9	-13.0	-13.3	-18	-18.7	-15.6
Hyp	-14.8	-13.2	-14.2	-18.2	-18.4	-18.8
Asp	-9.8	-10.6	-11.4	-19.1	-18.3	-18.8
Glu	1.0	1.9	-4.7	-10.7	-10.7	-9.0
Phe	-18.4	-20.8	-21.8	-24.4	-23.4	-22.1
Coll	-12.2	-12.2	-13.9	-18.6	-18.5	-16.6
Bchol	-16.7	-17.6	-18.9	-24.5	-26.1	-22.3

Isotopic composition (‰)						
Bone component	267 (diet 4)	268 (diet 4)	269 (diet 4)	257 (diet 5)	258 (diet 5)	255 (diet 6)
Ala	-16.3	-18.0	-17.2	-15.1	-14.2	-10.9
Gly	-11.5	-14.9	-11.8	-9.1	-9.1	-7.9
Thr	-9.1	-5.4	-7.0	-6.5	-8.9	-10.2
Ser	-3.9	-3.3	-6.1	-4.4	-3.1	-2.0
Val	-27.1	-25.0	-23.0	-22.6	-25.2	-28.4
Leu	-26.7	-27.8	-26.7	-26.4	-27.1	-25.8
Ile	-20.1	-21.3	-21.7	-22.4	-24.7	-19.4
Pro	-16.9	-18.9	-16.0	-15.5	-15.1	-13.0
Hyp	-17.0	-18.0	-16.2	-15.8	-15.4	-16.2
Asp	-15.4	-17.7	-16.0	-15.0	-15.2	-11.2
Glu	-9.5	-10.4	-8.2	-3.7	-3.9	-4.3
Phe	-23.9	-22.7	-24.8	-24.3	-24.1	-23.6
Coll	-16.7	-16.2	-16.5	-14.7	-14.7	-12.9
Bchol	-23.3	-22.7	-23.0	-21.4	-21.4	-20.3

Isotopic composition (‰)						
Bone component	251 (diet 7)	252 (diet 7)	274 (diet 9)	279 (diet 9)	278 (diet 10)	238 (diet 11)
Ala	-9.6	-10.7	-13.8	-14.1	-8.3	-19.4
Gly	-6.6	-6.9	-14.2	-9.3	-8.3	-13.0
Thr	-5.3	-10.7	-15.2	-22.5	-9.5	-12.1
Ser	1.4	-2.5	-2.7	-8.1	0.2	-8.1
Val	-23.7	-25.4	-29.7	-30.6	-22.3	-26.0
Leu	-23.3	-24.4	-29.1	-29.4	-22.5	-28.2
Ile	-20.0	-17.8	-23.8	-22.2	-16.0	-22.5
Pro	-13.0	-12.6	-17.9	-16.4	-10.0	-17.9
Hyp	-12.4	-12.3	-18.2	-17.1	-11.3	-17.6
Asp	-11.5	-9.9	11.7	-15.5	-9.2	-17.4
Glu	-0.9	0.1	-6.9	-3.3	-6.1	-9.2
Phe	-24.9	-21.8	-23.8	-28.5	-22.6	-26.5
Coll	-11.7	-11.8	-17.1	-16.0	-11.5	-17.8
Bchol	-16.2	-16.7	-20.6	-19.4		-23.2

Isotopic composition (‰)						
Bone component	239 (diet 11)	240 (diet 12)	241 (diet 12)	242 (diet 12)	243 (diet 12)	244 (diet 12)
Ala	-18.3	-13.6	-12.3	-9.2	-12.3	-11.1
Gly	-15.3	-13.0	-7.9	-7.4	-7.1	-9.4
Thr	-14.6	-4.7	-4.9	-10.5	-10.7	-7.6
Ser	-4.7	-1.4	-2.8	-0.4	-3.8	-1.2
Val	-26.9	-26.2	-23.7	-21.4	-23.1	-26.3
Leu	-28.5	-25.7	-23.1	-25.9	-24.6	-24.6
Ile	-26.5	-18.9	-20.9	-26.8	-18.8	-19.3
Pro	-18.3	-13.4	-14.6	-15.4	-13.1	-14.0
Hyp	-18.0	-16.3	-14.3	-16.3	-13.6	-14.7
Asp	-17.4	-11.7	-11.6	-13.6	-12.0	-11.9
Glu	-9.7	-2.3	-3.6	-2.4	-2.5	-2.5
Phe	-24.4	-18.9	-22.6	-20.9	-23.2	-22.7
Coll	-17.2	-13.4	-13.4	-14.5	-13.3	-13.0
Bchol	-25.8	-17.4	-18.4	-20.0	-17.6	-18.8

Bone component	Isotopic composition (‰)			
	245 (diet 12)	246 (diet 12)	277 (diet 13)	276 (diet 14)
Ala	-12.8	-12.6	-17.2	-15.6
Gly	-8.9	-10.9	-12.2	-11.4
Thr	-10.2	-9.3	-11.3	-14.8
Ser	-4.0	-5.9	-4.0	-5.2
Val	-23.2	-27.5	-23.5	-25.3
Leu	-24.3	-24.1	-26.6	-26.1
Ile	-21.3	-20.0	-20.5	-18.9
Pro	-14.2	-13.8	-17.3	-16.7
Hyp	-14.0	-14.2	-16.5	-14.4
Asp	-12.9	-11.4	-15.7	-13.7
Glu	-0.9	-1.4	-8.2	-7.0
Phe	-22.6	-22.4	-20.9	-22.1
Coll	-13.0	-13.3	-15.3	-14.1
Bchol	-18.9	-19.3		

Appendix 3. Pig individual amino acid, collagen and bone cholesterol $\delta^{13}\text{C}$ values (unpublished data). Individual amino acid and cholesterol $\delta^{13}\text{C}$ values obtained in our laboratory by Mark Howland and Lorna Corr, respectively. Collagen $\delta^{13}\text{C}$ values were measured at Harvard University.

Isotopic composition (‰)						
Bone component	253 (diet 1)	254 (diet 1)	280 (diet 2)	247 (diet 3)	248 (diet 3)	266 (diet 4)
Ala	-9.2	-8.5	-9.9	-20.4	-21.4	-17.5
Gly	-10.3	-7.9	-10.9	-13.5	-13.5	-13.8
Thr	-4.5	-12.2	-10.7	-12.2	-11.6	-10.4
Ser	3.9	-2.0	-0.9	-10.5	-9.6	-6.2
Val	-24.9	-21.9	-27.0	-26.2	-24.1	-25.0
Leu	-23.9	-25.7	-25.5	-27.2	-27.9	-28.1
Ile	-18.2	-18.9	-21.1	-22.8	-23	-21.0
Pro	-15.9	-13.0	-13.3	-18	-18.7	-15.6
Hyp	-14.8	-13.2	-14.2	-18.2	-18.4	-18.8
Asp	-9.8	-10.6	-11.4	-19.1	-18.3	-18.8
Glu	1.0	1.9	-4.7	-10.7	-10.7	-9.0
Phe	-18.4	-20.8	-21.8	-24.4	-23.4	-22.1
Coll	-12.2	-12.2	-13.9	-18.6	-18.5	-16.6
Bchol	-16.7	-17.6	-18.9	-24.5	-26.1	-22.3

Isotopic composition (‰)						
Bone component	267 (diet 4)	268 (diet 4)	269 (diet 4)	257 (diet 5)	258 (diet 5)	255 (diet 6)
Ala	-16.3	-18.0	-17.2	-15.1	-14.2	-10.9
Gly	-11.5	-14.9	-11.8	-9.1	-9.1	-7.9
Thr	-9.1	-5.4	-7.0	-6.5	-8.9	-10.2
Ser	-3.9	-3.3	-6.1	-4.4	-3.1	-2.0
Val	-27.1	-25.0	-23.0	-22.6	-25.2	-28.4
Leu	-26.7	-27.8	-26.7	-26.4	-27.1	-25.8
Ile	-20.1	-21.3	-21.7	-22.4	-24.7	-19.4
Pro	-16.9	-18.9	-16.0	-15.5	-15.1	-13.0
Hyp	-17.0	-18.0	-16.2	-15.8	-15.4	-16.2
Asp	-15.4	-17.7	-16.0	-15.0	-15.2	-11.2
Glu	-9.5	-10.4	-8.2	-3.7	-3.9	-4.3
Phe	-23.9	-22.7	-24.8	-24.3	-24.1	-23.6
Coll	-16.7	-16.2	-16.5	-14.7	-14.7	-12.9
Bchol	-23.3	-22.7	-23.0	-21.4	-21.4	-20.3

Isotopic composition (‰)						
Bone component	251 (diet 7)	252 (diet 7)	274 (diet 9)	279 (diet 9)	278 (diet 10)	238 (diet 11)
Ala	-9.6	-10.7	-13.8	-14.1	-8.3	-19.4
Gly	-6.6	-6.9	-14.2	-9.3	-8.3	-13.0
Thr	-5.3	-10.7	-15.2	-22.5	-9.5	-12.1
Ser	1.4	-2.5	-2.7	-8.1	0.2	-8.1
Val	-23.7	-25.4	-29.7	-30.6	-22.3	-26.0
Leu	-23.3	-24.4	-29.1	-29.4	-22.5	-28.2
Ile	-20.0	-17.8	-23.8	-22.2	-16.0	-22.5
Pro	-13.0	-12.6	-17.9	-16.4	-10.0	-17.9
Hyp	-12.4	-12.3	-18.2	-17.1	-11.3	-17.6
Asp	-11.5	-9.9	11.7	-15.5	-9.2	-17.4
Glu	-0.9	0.1	-6.9	-3.3	-6.1	-9.2
Phe	-24.9	-21.8	-23.8	-28.5	-22.6	-26.5
Coll	-11.7	-11.8	-17.1	-16.0	-11.5	-17.8
Bchol	-16.2	-16.7	-20.6	-19.4		-23.2

Isotopic composition (‰)						
Bone component	239 (diet 11)	240 (diet 12)	241 (diet 12)	242 (diet 12)	243 (diet 12)	244 (diet 12)
Ala	-18.3	-13.6	-12.3	-9.2	-12.3	-11.1
Gly	-15.3	-13.0	-7.9	-7.4	-7.1	-9.4
Thr	-14.6	-4.7	-4.9	-10.5	-10.7	-7.6
Ser	-4.7	-1.4	-2.8	-0.4	-3.8	-1.2
Val	-26.9	-26.2	-23.7	-21.4	-23.1	-26.3
Leu	-28.5	-25.7	-23.1	-25.9	-24.6	-24.6
Ile	-26.5	-18.9	-20.9	-26.8	-18.8	-19.3
Pro	-18.3	-13.4	-14.6	-15.4	-13.1	-14.0
Hyp	-18.0	-16.3	-14.3	-16.3	-13.6	-14.7
Asp	-17.4	-11.7	-11.6	-13.6	-12.0	-11.9
Glu	-9.7	-2.3	-3.6	-2.4	-2.5	-2.5
Phe	-24.4	-18.9	-22.6	-20.9	-23.2	-22.7
Coll	-17.2	-13.4	-13.4	-14.5	-13.3	-13.0
Bchol	-25.8	-17.4	-18.4	-20.0	-17.6	-18.8

Isotopic composition (‰)				
Bone component	245 (diet 12)	246 (diet 12)	277 (diet 13)	276 (diet 14)
Ala	-12.8	-12.6	-17.2	-15.6
Gly	-8.9	-10.9	-12.2	-11.4
Thr	-10.2	-9.3	-11.3	-14.8
Ser	-4.0	-5.9	-4.0	-5.2
Val	-23.2	-27.5	-23.5	-25.3
Leu	-24.3	-24.1	-26.6	-26.1
Ile	-21.3	-20.0	-20.5	-18.9
Pro	-14.2	-13.8	-17.3	-16.7
Hyp	-14.0	-14.2	-16.5	-14.4
Asp	-12.9	-11.4	-15.7	-13.7
Glu	-0.9	-1.4	-8.2	-7.0
Phe	-22.6	-22.4	-20.9	-22.1
Coll	-13.0	-13.3	-15.3	-14.1
Bchol	-18.9	-19.3		

10

